Oncolytic Vaccinia Virus for the Treatment of Liver Cancer

Rajiv Vipool Dave

Submitted in accordance with the requirements for the degree of

Doctor of Medicine

The University of Leeds

Faculty of Medicine and Health

School of Medicine

February 2014

The candidate confirms that the work submitted is his own, except where work which had formed part of jointly authored publications has been included. The contribution of the candidate and other authors to this work has been explicitly indicated below. The candidate confirms that appropriate credit has been given within the thesis where reference has been made to the work of others.

Viral warfare! Front-line defence and arming the immune system against cancer using oncolytic vaccinia and other viruses. Dave R, Jebar A, Jennings V, Adair R, West E, Errington-Mais F, Toogood G, Melcher A. *Surgeon*. 2014 Feb 4. epub ahead of print. doi: 10.1016/j.surge.2014.01.001.

The published work above is based on chapter 1, 'Introduction,' and is a review article which does not contain any results from this thesis. The co-authors have been involved in the identification of publications for review for the paper, and for format adjustment and review of the manuscript prior to submission.

Assertion of moral rights:

The right of Rajiv Vipool Dave to be identified as Author of this work has been asserted by him in accordance with the Copyright, Designs and Patents Act 1988.

Acknowledgements

I wish to thank Professor Alan Melcher and Mr Giles Toogood for giving me the opportunity to carry out this research. I wish to acknowledge the support provided by Dr Fiona Errington-Mais, Dr Emma West and Miss Karen Scott in teaching me the laboratory techniques required to complete my research. I wish to acknowledge the support provided by the consultant team at St James' University hospital and the theatre staff in assisting with sample provision, and my wife Dr Farnaz Dave for her moral support.

Abstract

Aims: Current treatment of colorectal cancer (CRC) liver metastases has a success rate of 50% 5-year survival, and recurrence rates of 50%. There is therefore still a need for a novel treatment modality. We aimed to examine the ability of JX-594 to preferentially replicate in and kill CRLM *in vitro* and *ex vivo*, and induce immune-mediated tumour cytotoxicity by activation of natural killer (NK) cells.

Methods: The Wyeth strain of vaccinia virus has been genetically manipulated to encode for granulocyte macrophage colony stimulating factor (JX-594-GM-CSF-fLuc) and green fluorescent protein (JX-594-GM-CSF-GFP) in the disrupted thymidine kinase locus. Viability assays and Enzyme Linked Immunoabsorbent Assay (ELISA) was used to confirm tumour cell killing and production of inflammatory cytokines when CRC cell lines were infected with JX-594. Viral replication *in vitro* was investigated by plaque assay and using an *ex vivo* 'tissue core' method. Induction of the innate immune response was measured by upregulation of activatory markers on virus-treated-NK cells and monocytes by flow cytometry and anti-tumour cytotoxicity by chromium release.

Results: JX-594 can directly lyse CRC cell lines, with greater lysis and replication (up to 250-fold) in cells with upregulated surface EGFR. JX-594 treatment resulted in substantial expression of GM-CSF and induction of inflammatory cytokines within the tumour microenvironment, and inhibition of anti-inflammatory and pro-angiogenic cytokines. *Ex vivo* infection of CRLM with JX-594-GFP-GM-CSF resulted in tumour-specific GFP and GM-CSF expression. Treatment of NK cells with JX-594-GM-CSF led to activation, degranulation and increased cytotoxicity

against CRC cell targets. This was dependent on the presence of $CD14^{+ve}$ monocytes, which acquired an antigen-presenting phenotype ($CD86^{+ve}CD11c^{+ve}ClassIIDR^{+ve}$).

Conclusions: JX-594 holds promise as a novel treatment modality for disseminated CRC. Direct tumour-specific lysis and transgene expression and the induction of tumour-specific innate immunity means that it may provide a two-pronged attack against tumour cells whilst sparing normal tissue.

Table of Contents

List of Tables

List of Figures

Chapter 1

Introduction

1 Introduction

1.1 Cancer: Impact, tumourigenesis and interaction with the immune system

1.1.1 Cancer: Impact of the disease

Cancer is defined as a disease in which abnormal cells divide uncontrollably and spread. In the UK in 2009, there were 156,090 deaths from cancer. 28% of all deaths in the UK in 2007-2009 were due to cancer, which was higher than both coronary heart disease (by 69,000 deaths) and stroke (by 104,000 deaths) [1].

1.1.2 Liver cancer

1.1.2.1 Colorectal liver metastasis

Colorectal cancer (CRC) is the third most common cancer in England; 13.6% of all registered cancer diagnoses in men and 11% in women, and 16,000 people die from colorectal cancer in the United Kingdom (UK) annually [2]. World-wide, an estimated 1.24 million new cases of colorectal carcinoma were diagnosed in 2008 [3]. About 65% of all patients with CRC develop distant metastasis, the liver being the most common site (40%). Liver resection is the only modality shown to convincingly cure colorectal liver metastasis (CRLM), although newer ablative treatments are showing promise. Currently, due to newer surgical techniques [4] and imaging modalities and the introduction of more effective cytotoxic chemotherapy agents, the accepted 5-year survival rate is 50% [5] [6]. Although surgery remains the mainstay of potentially curative therapy, the role of systemic neo-adjuvant chemotherapy is increasing, with 5-fluorouracil (5-FU) plus leucovorin (LV) in combination with irinotecan (FOLFIRI) or oxaliplatin (FOLFOX) reported to facilitate resection rates of 9%-40% in initially unresectable disease [7]. A targeted

antibody with additional immunomodulatory properties, Cetuximab, is undergoing a major randomised trial in the UK. Cetuximab is a chimeric (mouse/human) monoclonal antibody that functions as an epidermal growth factor receptor (EGFR) inhibitor, in patients with Kirsten rat sarcoma (*Kras*) wild-type disease. The New EPOC trial (ISRCTN: 22944367) is a neo-adjuvant trial investigating the survival benefit of the addition of Cetuximab to standard chemotherapy regimes.

1.1.2.2 Primary liver cancer (Hepatocellular carcinoma- HCC)

HCC is within the top twenty most common cancers in the UK (18th). In 2009, 3,960 people in the UK were diagnosed with liver cancer and in 2010 there were 3,789 deaths from HCC. Almost two-thirds of cases of liver cancer occur in men [8]. Therapeutic options available include liver transplantation, surgical resection and local ablative therapies, but the prognosis of HCC remains poor due to high tumor recurrence rates. 50-80% of HCC express alpha-feto protein (AFP), and it is used as a marker for tumour diagnosis and follow-up.

1.1.3 Mutation and tumourigenesis

Cancer-causing agents can be broadly categorized into: oncogenic viruses, chemicals, and radiation. Oncogenic DNA viruses including Human Papilloma Virus (HPV), Epstein-Barr Virus (EBV), and Hepatitis B Virus (HBV) can integrate their DNA into the genome of the host, replicating and producing proteins that enable the virus to hijack the DNA synthesis machinery of the host cell. Two of these viral genes, E6 and E7, have the ability to act as oncogenes, and their encoded proteins can bind to two important tumour suppressor genes, p53 and retinoblastoma (*RB*) [9]. Only one human retrovirus, the human T-cell leukemia virus type I (HTLV-I), is linked to a human tumour (T-cell leukemia/lymphoma). Carcinogenic chemicals (mutagens) such as nitrogen mustard, benzoyl chloride, polycyclic aromatic

hydrocarbons etc. can target proto-oncogenes and tumour suppressor genes. Radiation with Ultraviolet-B (UV-B) rays have been linked to basal-cell carcinoma, squamous-cell carcinoma, and malignant melanoma of the skin. Ionising radiation has also been linked with tumourigenesis. Dramatic evidence of this has been seen in the consequences of atomic explosions in Japan at Hiroshima and Nagasaki in 1945.

During tumourigenesis, the cell becomes damaged due to a variety of mechanisms. These genetic and epigenetic changes participate in oncogenic intracellular pathways that promote proliferation and dissemination. Hanahan and Weinberg described classic hallmarks of cancer; self-sufficiency in growth signals, insensitivity to anti-growth signals, evading apoptosis, limitless replication potential, sustained angiogenesis, tissue invasion and metastasis [10, 11]. Several other hallmarks have been described; genetic instability, evasion of cell senescence, epigenetic alterations of cancer related-genes, RNA interference alterations in the expression of cancer related-genes, changes in glucose and glutamine metabolism, participation of cancer stem cells in cellular proliferation, stromal cell participation in the tumour's micro-environment, and changes in antigenic presentation and immunosuppression due to cytokines in the tumour's micro-environment [12].

1.1.4 Cancer and the immune system

1.1.4.1 The immune system

The immune system serves to defend against infection, and consists of two fundamentally different arms. The innate response, which is the 'first line defence' against invading pathogens, is generally a non-specific response, and results in 'inflammation' at the site of the pathogen regulated by a system of cytokines, prostaglandins, leukotrienes and complement proteins. The cellular component of the innate immune system comprises phagocytes (macrophages, neutrophils, and dendritic cells), cells that release inflammatory mediators (mast cells, eosinophils, basophils), natural killer (NK) cells, NK-T cells and γδT cells [13]. NK cells contain cytotoxic granules contained in lysosymes that express perforin, which when binding to surface of tumour cells, make them permeable to the contained cytotoxic granules. NK cells are discussed in more detail in chapter 5.

The adaptive (or acquired) immune response comes into play following an initial innate response, and creates immunological memory, leading to an enhanced response to subsequent encounters with that same pathogenic antigen. This process forms the basis of vaccination, whereby a low volume pathogenic trigger can lead to long lasting immunity. Cells of the adaptive immune response are specialised leukocytes, called lymphocytes. Derived from the hematopoietic stem cells in the bone marrow, the B cells (humoral response) and thymus-derived T cells (cell-mediated response) are the major types of lymphocyte. T cells are antigen-specific and proliferate in response to presentation of an antigen to the surface receptors of these cells by antigen-presenting cells (APC) such as dendritic cells (DC). This process occurs in secondary lymphoid tissue such as the lymph nodes and spleen [14].

1.1.4.2 Immune cell 'crosstalk'

A symbiotic relationship between NK cells and DCs has been demonstrated in recent years, both in the periphery and in lymphoid organs. Myeloid DCs support innate immunity by promoting the production of cytokines and enhancing the cytotoxicity of NK cells. In reply, NK cells also play immunoregulatory 'helper' functions and activate DCs, enhancing their ability to produce pro-inflammatory cytokines. NK cells also play a key role in polarizing a T helper (Th1) i.e. cytotoxic T lymphocyte (CTL), rather than antibody (Th2) response [15].

1.1.4.3 Tumour associated antigens

Many studies have demonstrated that cancer sera contain antibodies, which react with a unique group of autologous cellular antigens generally known as tumour-associated antigens (TAAs). TAAs can be classified into 1) products of mutated oncogenes and tumor suppressor genes and 2) products of other mutated genes (e.g. oncogenic viral antigens, overexpressed/aberrantly expressed cellular proteins, oncofetal antigens and altered cell surface glycolipids and glycoproteins). By definition, these have to be produced by the tumour and not by the normal tissue. TAAs not only function as candidates for diagnostic tests, but also act as potential new targets for therapeutic intervention [16].

1.1.4.4 Tumour associated antigens in colorectal cancer

In CRC, the most commonly identified TAA is Carcino-embryogenic antigen (CEA). Gold and Freedman [17] demonstrated the presence of antibodies to a component present in colonic cancer tumour when rabbits were immunised with an extract of the tumour. This was not observed in normal adult colon, but was present in the human gastrointestinal tract during embryogenesis, hence the term 'Carcino-

embryogenic antigen.' This is a complex glycoprotein that is found in 50-80% of CRCs, and is used clinically for diagnosis and follow-up, but as it is not expressed in the early stages, its application in screening is limited.

Using a TAA mini-array system, Liu *et al*. have identified several other TAAs in early CRC, including Imp1, p62, Koc, p53 and c-myc. Titres were significantly higher in sera of CRC patients versus healthy donors. Despite the high specificity, their clinical application may be hindered by poor sensitivity [18]. Babel *et al*. identified five further immunoreactive antigens in sera from patients with CRC; PIM1, MAPKAPK3, STK4, SRC, and FGFR4. Increased expression of these antigens was confirmed in CRC cell lines and colonic mucosa [19].

Vascular Endothelial Growth Factor (VEGF) is involved in the growth and development of colorectal cancer. VEGF is expressed at higher levels in tumors than in distant mucosa [20] and is correlated with poor prognosis [21]. Although not classically regarded as a TAA, anti-VEGF therapy (Avastin; bevacizumab) has played a role in the treatment of CRC [22]. Similarly, EGFR inhibitors such as cetuximab and panitumumab have recently shown activity in patients with CRLM whose tumors have wild-type *Kras* [23].

1.1.4.5 Tumour associated antigens in hepatocellular carcinoma

Several vaccination strategies based on AFP as a TAA have been investigated for HCC immunotherapy. AFP-specific vaccination can significantly impair the growth of an autochthonous HCC [24]. In two conducted clinical trials, AFP-specific CTLs have been detected in blood after AFP peptide administration, however, this has not been correlated with an objective clinical response [25]. More recently,

vaccination using a Modified Vaccinia virus Ankara (MVA) which expressed membrane-bound AFP, induced a $CD8^+$ T-cell response and elicited the production of AFP-specific antibodies. This was more effective than the secreted and intracellular versions of the AFP, hence concluding that the system of TAA delivery as a membrane-bound antigen induced a more effective response [26].

1.1.4.6 The danger hypothesis

Although the classical hypothesis of antigenic recognition of 'self' versus 'non-self' is well established, there are a number of phenomena which cannot be explained by this hypothesis. Matzinger proposed that "danger" signals are crucial to the generation of an effective immune response. This danger signal may be represented by pathogens, including viruses, and therefore oncolytic virotherapy might provide a potent immunological trigger; not only by releasing TAAs by tumour lysis, but also through a 'danger signal' [27].

A range of danger signals has been proposed. Interestingly, Zhang *et al*. described the recognition of mitochondria as bacterial pathogens by the immune system; explained by the theory that these organelles are in fact 'evolutionised' bacteria. Thus, once released from the cell in abnormal conditions, they can initiate a 'danger' response [28]. Mitochondria exemplify an inherent characteristic of a danger signal as they are not present extra-cellularly in normal physiological conditions. These intracellular danger signals are described as damage-associated molecular patterns (DAMPs) and they include other molecules such as adenosine tri-phosphate (ATP), nucleic acids, heat shock proteins (eg Hsp70), HMGB-1, S100 calcium binding proteins, and the cytokine Interleukin (IL)- 1a.

Alternatively, danger signals may be pathogen-associated molecular patterns (PAMPs). These molecules are associated with pathogens, that are recognized by cells of the innate immune system by Toll-like receptors (TLRs) and other pattern recognition receptors (PRRs) such as helicase RIG-I. Both TLRs and helicase RIG-I are the major PRRs implicated in response to viral PAMPs. Bacterial Lipopolysaccharide (LPS), is a prime example of a PAMP; it is an endotoxin found on the cell membrane of a bacterium, recognised by TLR 4 [29].

1.1.4.7 The immunesurveillance hypothesis

A theory proposed by Burnet in 1957 [30], hypothesised that immune cells constantly surveyed host tissue and could identify and destroy abnormal cells due to recognition of abnormal antigens on their cell surface. Sceptics argued that the immune system would fail to recognise tumours due to antigenic similarity, and that tumours may still develop in immune-competent individuals. The immunosurveillance hypothesis was further challenged by the observation of a lack of increased tumour incidence in nude, athymic mice [31]. However, new studies in the 1990s explained this phenomenon by the demonstration of increased development of malignancy in NK-cell deficient mice [31-33]. Further studies have shown that deficiencies in Interferon (IFN)-γ and perforin increased susceptibility to both chemically induced and spontaneous tumours [34].

1.1.4.8 The immuoediting hypothesis

It eventually became recognised that immunosurveillance represents only part of the anti-tumour immunological response, hence the emergence of the ‘Immuoediting Hypothesis.’ Cancer immunoediting is a process consisting of three phases; ‘Elimination’ (cancer immunosurveillance), ‘Equilibrium’ and ‘Escape’. The concept of elimination is similar to the classical theories of immunosurveillance,

initiated by a danger signal from the tumour, as described above [27]. Equilibrium is a period of 'status quo' whereby some surviving tumour cells at the end of the elimination phase go into a period of dormancy, which may be quite protracted [33]. This is exemplified by the demonstration of transmission of cancer from organ donors thought to be tumour-free for many years at the time of donation [35]. At this stage, the tumour cells could eventually be eradicated by the immune system, may remain permanently in the dormant phase, or undergo continued transformation and enter the 'Escape' phase. These escaping tumours represent naturally selected tumour variants that are less immunogenic.

1.1.4.9 Evasion of the immune system

The development of tumours may be seen as a failure of immunosurveillance; the continued mutagenic process in even the most immunogenic tumours may eventually overcome the immune system's capacity. However, not all tumour cells are immunogenic, and thus do not initiate an immune response. This can be explained by several mechanisms. For example, there may be abnormal or disordered expression of cell surface proteins; the process of major histocompatibility class (MHC) I downregulation by tumours (which can reduce sensitivity to cytotoxic T cell-mediated lysis [36]); impaired binding of perforin [37]; and the downregulation of cytotoxic pathways such as the Fas and TRAIL (tumour necrosis factor-related apoptosis-inducing ligand), both of which have been implicated in cancer immune-therapy [38]. Tumour-derived Fas-ligand (FasL) may lead to the active killing of Fas-sensitive tumour-infiltrating lymphocytes (TILs) and metastatic colorectal cancer shows high levels of FasL expression [39, 40]. The evasion of innate attack by NK cells may be mediated by an increase of NK ligands in the tumour microenvironment. It has been observed in a wide variety of tumours that NKG2D-mediated (an activatory receptor on NK cells) tumour

immunosurveillance may be subverted the release of NKG2D ligands (NKG2DL) by the tumour [41].

Another factor may be the solid nature of the tumour which may circumvent detection by T lymphocytes. It was observed in a sarcoma model that a single-cell suspension injected subcutaneously induced a strong cytotoxic T-Lymphocyte response, however the same tumour transferred as a solid fragment did not [42].

It must also be recognised that tumour cells arise from a body's own tissue, and hence express 'self' antigens to which T-cells are tolerised, either centrally (in the thymus) or peripherally . Evidence suggests that the mechanisms of tolerance, by which the body prevents autoimmune disease, may lead to reduced anti-tumour immunity [43].

1.1.4.10 Immunodeficiency

An interesting demonstration of the protective role of the immune system lies in patients with immunodeficiency. Whether due to the acquired immune deficiency syndrome (AIDS) or iatrogenic immunosuppression in the immunosuppressed transplant patient, there is a higher incidence of virus-associated cancer (Burkitt's lymphoma; EBV), skin (Squamous-cell and Basal-cell carcinoma) and other cancers [44, 45].

1.1.4.11 Inflammation and cancer; "wounds that do not heal"

Infection with a pathogen triggers an acute inflammatory response, which is mediated by the complement cascade, triggering the release of histamine and thus increased vascular permeability. Coupled with the up-regulation of adhesion

molecules on vascular endothelium and inflammatory mediators such as prostaglandins, leukotrienes and chemokines, inflammatory cells are recruited into the infected tissue. Injury, trauma or infection can initiate a systemic inflammatory response syndrome (SIRS).

A paradox exists when discussing the role of inflammation in tumorigenesis. Virchow first observed the presence of leukocytes within tumours in the 19th century [46]. It is now accepted that an inflammatory microenvironment is an essential component of all tumours and that many somatic mutations leading to cancer are caused by chronic disease (obesity), pathogens (e.g. Helicobacter Pylori) and chemicals (e.g. tobacco) which can promote chronic inflammation. Once the tumour has developed, certain oncogenes can induce a pro-inflammatory tumour environment by expression of tumour-promoting chemokines and cytokines. In the case of HCC, IL-6 has been found to be a critical tumour-promoting cytokine [47]. As the tumour grows beyond its nutrient supply, the resulting necrosis can influence further pro-inflammatory mediators [46]. Dvorak *et al*. thus described tumours as ‘wounds that do not heal’ [48].

Inflammation may serve to influence the host immune response. During chemotherapy, the ensuing inflammation due to induced necrotic death of cancer cells can lead to the production of DAMPs and can stimulate antigen presentation by tumour-infiltrating dendritic cells, which collectively can stimulate an anti-tumour response [46]. However, chemotherapy-induced anti-tumour immunity is only seen with certain agents (e.g. Oxaliplatin) [49]. Modulating this inflammatory response may be used to augment conventional chemotherapy [50].

1.1.4.12 Cancer immunotherapy

The first report of cancer immunotherapy was William Coley's description of using a bacterial infection to treat sarcomas in the 1890s, which he termed 'Coley's toxin' [51]. His vaccine consisted of a combination of *Streptococcus Pyogenes* and *Serratia Marcescens* [52]. Coley asserted that induction of a fever was key to the success of his treatment, and in subsequent years it was demonstrated that fever is accompanied by enhanced leucocyte proliferation, maturation, and activation [53]. The description of microbial preparations used by William Coley has led to modern-day therapies, and the Bacillus Calmette-Guerin (BCG) vaccine is a well-established treatment used successfully in the treatment of superficial bladder cancer [54]. Although BCG therapy is not meant to induce a fever, but to cause a local cytokine storm with repeated administrations.

The essence of cancer immunotherapy is the recruitment of the host's immune system to identify and kill tumour cells, leading to a long-term memory response, preventing future recurrence. Immunotherapy strategies include antitumor monoclonal antibodies, cancer vaccines, adoptive transfer of *ex vivo* activated T cells and NK cells, and administration of antibodies or recombinant proteins that either co-stimulate immune cells or block immune inhibitory pathways. Unlike conventional cancer therapies, most immunotherapies are active and dynamic, capable of inducing immune memory [55].

The potential use of OV to stimulate anti-tumour immunity is an interesting strategy as they have a direct cytotoxic effect along with the ability to activate host immunity, by exposure of TAA, induction of danger signals, and eventual recognition by immune effecter cells. Antitumoural immune responses may dictate the long-term therapeutic success of cancer treatment.

1.2 Oncolytic Viruses

1.2.1 The evolution of oncolytic viruses

Cancer therapy prior to the early twentieth century had only one modality, surgery, which only evolved following the advent of anaesthesia in 1846. Radiotherapy eventually contributed, once Roentgen discovered X-rays in 1895 [56]. Chemotherapy gained prominence after the introduction of aminopterin, a folic acid antagonist, by Farber *et al* [57]. Despite these advancements, we are still to find an absolute cure. The need for oncolytic viruses stems from the requirement for a novel mechanism of action that would not be cross-resistant with established therapy and would be effective in apoptosis-blocked cells. The first approval of an oncolytic virus was in November 2005, granted by Chinese regulators, for H101, a genetically modified adenovirus [58]. Prior to this, viruses had been pursued as anti-tumour therapy for a hundred years, however enthusiasm diminished, but has recently been revived over the past two decades [59].

Biochemical analysis of viruses only progressed after the invention of the plaque assay in 1917, and it was only towards the end of the 20th century that viruses were employed for cancer therapy. Evolution has armed viruses with the ability to infect, replicate within and eventually lyse cells and consequently spread through tissues. Since the 1800s, there have been reports of transient cancer remissions following an episode of viral illness [59], and this led to further interest in the use of viruses as potential therapeutic agents [60]. In 1896, Dock described remission of “myelogenous leukaemia” after what was described as influenza infection – although this was years before the discovery that influenza was a virally-mediated disease [61]. In 1949, a clinical trial was undertaken in which 22 patients with Hodgkin’s disease were given sera and tissue samples from patients infected with the hepatitis virus [62]. In the UK, glandular fever serum was used for treatment of

acute leukaemia [63]. In 1974, Asada *et al*. used non-attenuated mumps virus in Japan to treat eighteen different types of tumour via various routes; intravenous, oral, per-rectal, topical and nasal inhalation [64]. This was perhaps a significant trial as 37 of 90 patients had complete tumour regression following therapy.

Harnessing these viral characteristics/mechanisms for therapeutic potential was faced with one major challenge however; harm to normal cells alongside tumour cell destruction. Oncolytic viruses (OV) have the ability to specifically infect cancer cells and replicate within them. They can subsequently lyse these cells and spread to adjacent cancer [65-69]. They can also be targeted to cancer cells with activated genetic pathways and/or loss of tumour suppressor function [70]. OVs can induce activation of tumour-specific immune effector cells and be “armed” by expression of therapeutic transgene products [71]. These characteristics can be used to bypass some of the limitations of non-replicating viral therapeutics.

Reovirus, for example, is a first-generation oncolytic virus, and has been extensively tested in clinical trials. Although it is safe and selective for cancer, little therapeutic potency has yet been observed in humans either through an intratumoural (IT) or intravenous (IV) delivery. With the limitations of OV such as reovirus, new therapeutic agents with better anticancer properties, delivery and systemic spread are required. Poxviruses, such as vaccinia, were selected and armed with a gene encoding granulocyte-macrophage colony-stimulating factor (GM-CSF), to stimulate anti-tumoural immunity. Preclinical [72-75] and clinical [76, 77] testing has shown these agents to be tumour selective and have a high degree of systemic efficacy.

1.2.2 Where did it all start: Smallpox

The Poxviridae family is an enveloped double-stranded DNA virus, of which the orthopoxvirus subfamily includes vaccinia [78]. This family of viruses has notorious and impressive ancestry: the eradication of smallpox [79]. Anecdotes of inoculation against smallpox in China date back to the late 10th century. The procedure, infection with a variola virus, was widely practiced by the 16th century, during the Ming Dynasty [80]. In 1796 Dr Edward Jenner, in Berkeley, Gloucestershire, discovered that inoculating a person with material from a cowpox lesion could induce immunity to smallpox. Cowpox is a poxvirus in the same family as variola. He called this material ‘vaccine’, from the Latin root word vacca, (cow). This was a safer procedure than the Chinese method of variolation, which involved a risk of smallpox transmission. Vaccination was soon practiced all over the world. During the 19th century, the cowpox virus used for smallpox vaccination was replaced by vaccinia virus [81]. In 1922, it was discovered that the smallpox vaccine could inhibit the growth of tumours in mice and rats [59].

1.3 Vaccinia Virus

1.3.1 Viral structure, replication and life cycle

Vaccinia is an enveloped, brick-shaped virion, which measures 250nm by 200nm, and has a 192-kb double-stranded DNA genome encoding over 200 polypeptides, of which approximately half are incorporated into virus particles. The unique characteristic of poxviruses is that the entire life cycle (transcription, genome replication, and virus assembly), occurs in the cytoplasm of the host cell. The large viral genome encodes for virtually all the enzymes required for these processes. The virus attaches to glycosaminoglycans (GAGs) on the host cell wall, and can either undergo membrane fusion or macropinocytosis. Membrane fusion leads to the release of the virus core into the cytoplasm. In some occasions, the fusion of the viral and host cell membranes triggers endocytosis and vesicular transport. Maturation of the transporting endosome eventually leads to fusion between endosome and virus membrane [82]. In the ‘early phase’ of replication, which begins 30 minutes post infection, early genes are transcribed in the cytoplasm by viral RNA polymerase. The viral core is completely uncoated by the time early expression ends, and the viral dsDNA is now free in the cytoplasm of the host cell. Approximately 100 minutes post-infection, the ‘intermediate phase’ genes are expressed, which initiate genomic DNA replication. In the ‘late phase’, which occurs 140 min to 48 hours post-infection, all structural viral proteins are translated, and assembly of viral progeny begins with the first virion, the intracellular mature virus (IMV).

Vaccinia virus produces four distinct virions throughout its life cycle; intracellular mature virus (IMV) (see figure 1-1), intracellular enveloped virus (IEV), cell-associated enveloped virus (CEV) and extracellular enveloped virus (EEV) (see figure 1-2). Each virion has a different role in the viral life cycle. The IMV is the first

to be assembled, and is the abundant form of the virus. As the name suggests, it is retained intra-cellularly until lysis. It is covered in a surface membrane that displays surface tubules or surface filaments. IMV is a stable virion, which is capable of infective transmission between hosts. IEV is formed from the IMV virion by acquiring two additional membranes via wrapping in Golgi-derived cisternae. IEV is an intermediate to the CEV/EEV. Fusion of the outermost IEV membrane with the plasma membrane results in the formation of the CEV. This remains attached to the outside of the cell. EEV is formed from CEV that have been released from the cell. CEV induce the formation of actin tails that drive the virion away from the cell surface (see figure 1-3). It is these two virions that are responsible for spread of a poxvirus infection in culture and in infected animals [83, 84].

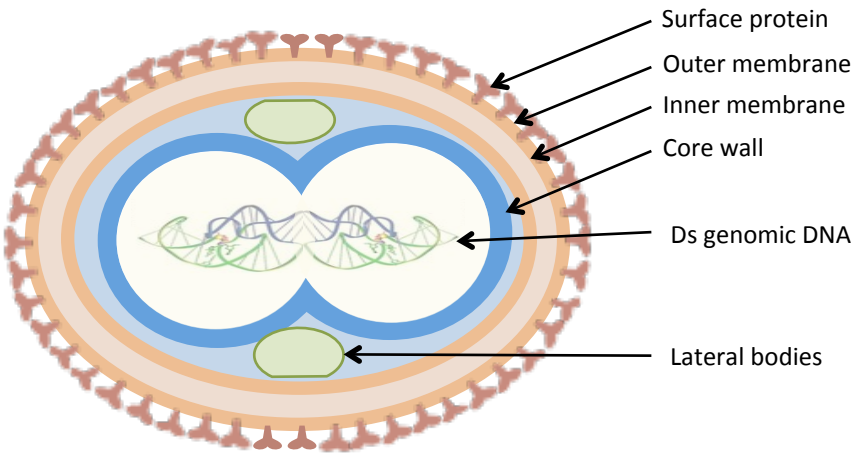

Figure 1-1 Vaccinia structure: Intracellular Mature Virus

The Intracellular Mature Virus (IMV) is the first viral particle to be assembled, and the most abundant form of the virus. It in covered in a surface membrane that displays surface proteins. This form of the virus is now capable of transmission between hosts. Ds; double stranded.

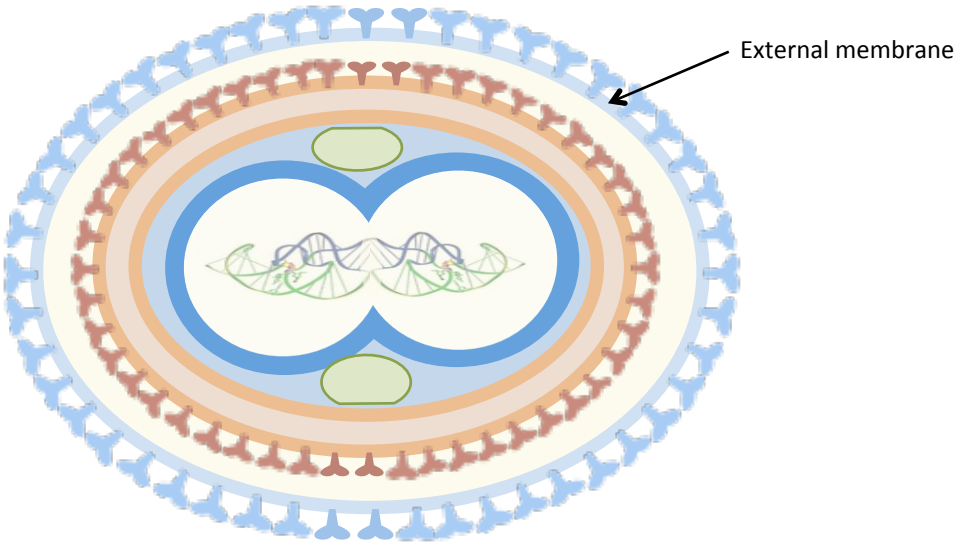

Figure 1-2 Vaccinia structure: Extracellular Enveloped Virus

Extracellular Enveloped virus (EEV) is formed by gaining additional membranes as the IMV wraps in Golgi-derived cisternae, and then fuses with the plasma membrane, forming first the Cellular Enveloped virus (CEV) which then dissociates to form the EEV.

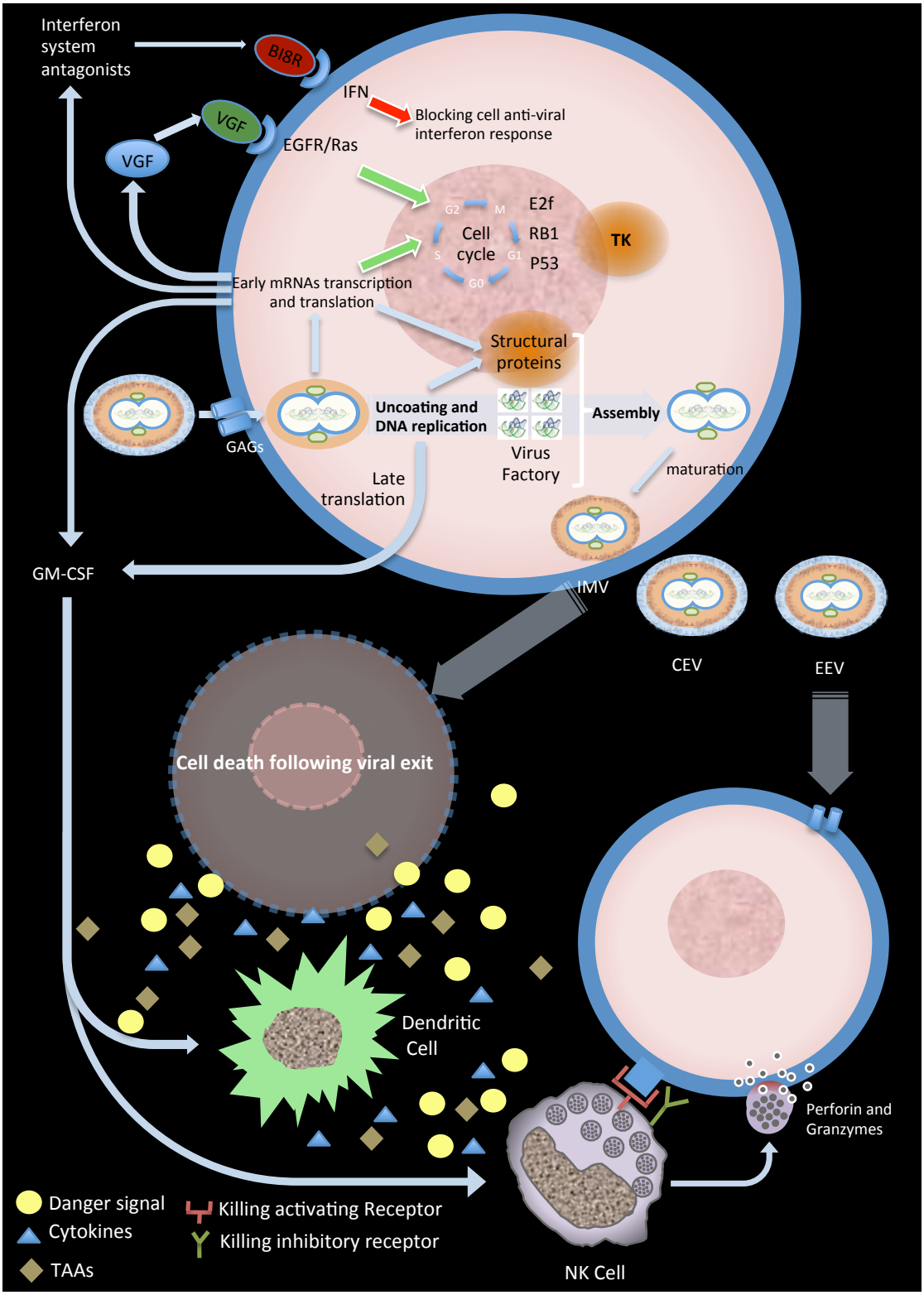

Figure 1-3 Vaccinia replication and activation of the immune system

Vaccinia enters a tumour cell by binding onto surface receptors (GAGs). Tumour cells have an activated EGF pathway, and have high levels of Thymidine kinase (TK) which supports viral replication. Early proteins can inactivate the host cell's anti-viral interferon response and provide further signals to the EGFR. Following formation of viral progeny, the cell is lysed and virus particles are released, and can infect nearby cells. The lysis of the cell releases pro-inflammatory cytokines, tumour associated antigens and danger signals- this, coupled with the GM-CSF production from engineered forms of the virus (JX-594), can lead to recruitment of immune effector cells and further immune-mediated tumour cell lysis.

1.3.2 Why does vaccinia work?

Vaccinia and other poxviruses present an ideal platform for development as oncolytic agents. They are able to replicate and lyse cells rapidly, with the first viral particles secreted within 8 hours of infection [85]. Poxviruses have a broad tumour tropism. 'Tropism' refers to the way in which different viruses/pathogens have evolved to preferentially target specific host species, or specific cell types within those species. They infect cells through several membrane fusion pathways [86, 87] and inherently target tumour cells, as the cancer cell infrastructure is similar to that of virally infected host cells; blocked apoptotic pathways, deregulated cell cycle control and immune evasion [88]. Furthermore, most human cancers show activation of the epidermal growth factor (EGF) – Ras signalling pathway, which has been associated with vaccinia replication and spread [89]. Vaccinia also produces an EGF homologue, called Vaccinia Growth Factor (VGF) that is produced during the early phase of viral replication, which can bind EGFR, thereby priming the cell for enhanced viral proliferation [90] [91]. Wali *et al*. demonstrated that vaccinia decreases the number of cells in G_1 and increases the number of cells in the S and G_2M phases of the cell cycle. They also showed that vaccinia can regulate altered expression of p53 and p27 proteins, which can influence the cell cycle. P53 was found to initially up-regulate and then down-regulate in response to vaccinia infection [92].

Once within the cell, replication takes place in mini-nuclear structures in the cytoplasm, and hence vaccinia does not integrate into the host DNA, and some forms have the ability to envelope themselves in host cell-derived proteins [93]. Therefore, each virus particle is capable of infecting a tumour cell and generate progeny capable of spreading to other cells, remaining largely undetected as they move through the tumour microenvironment or bloodstream, achieving higher levels

of viral delivery [74, 94]. Viral therapy can employ a variety of targeting mechanisms; therefore different tumour phenotypic properties can be targeted with different viral strains [95]. Furthermore, vaccinia viruses are able to accommodate large quantities of foreign DNA [96], allowing for insertion of various genes resulting in different mechanisms of anti-tumour therapy. The vaccinia genome expresses several genes, including anti-apoptotic and immunomodulatory genes, and deletion of several individual, or a combination, of these genes can improve efficacy of the virus [97, 98] and recruit the immune system; recombinant vaccinia containing certain co-stimulatory molecules (B7-1/ICAM-1/LFA-3) can induce CD4+ and CD8+ T-cell hyperstimulation [99].

Vaccinia has been shown, in preclinical and clinical models, to induce vascular collapse within tumours. This phenomenon is mediated by neutrophil infiltration into the tumour, induced by chemokines and cytokines, which eventually results in intravascular thrombosis and avascular necrosis. Vaccinia strains are also capable of infecting tumour-associated endothelial cells, destroying these cells and leading to vascular collapse [100] [101]. On the other hand, Weibel *et al*. [102] showed extensive malignant-cell specific necrosis, whilst the vasculature remained functional and infection-free, using breast tumour xenografts in nude mice, following 6 weeks of recombinant vaccinia (GLV-1h658) infection. However, viral colonization did result in hyper-permeability of the tumour vasculature, and there was an increase in the expression of genes involved in endothelial cell/leukocyte interactions, which would result in peri-vascular inflammation. This was confirmed by immunohistochemical analysis which showed infiltration of MHCII positive cells into infected tumours, which was not observed in immunosuppressed mice, which still showed similar levels of tumour necrosis and enhanced viral spreading.

1.3.3 JX-594

A new therapeutic class of oncolytic poxvirus has recently been developed that combines targeted and armed approaches for treating cancer. Developed from the Wyeth strain, JX-594 is a targeted and transgene-armed oncolytic poxvirus. It has been modified by the insertion of *human GM-CSF* and *LacZ* genes (encoding for β-gal) into the viral *TK* gene (see figure 1-4) [72, 103, 104]. JX-594 is designed to selectively replicate in, and destroy, cancer cells with cell-cycle abnormalities and epidermal growth factor receptor (EGFR)-ras pathway activation [89]. Direct oncolysis plus granulocyte-macrophage colony-stimulating factor (GM-CSF) expression also stimulates shutdown of tumour vasculature and antitumoral immunity [77].

Recently, JX-594 has shown promise as an i.v.-delivered, targeted virotherapeutic. Using an immunocompetent liver tumour rabbit model (with reproducible time-dependant metastases) and a carcinogen-induced rat tumour model, Kim *et al*. showed complete response against both the intrahepatic tumours and the pulmonary metastases. Tumor-specific virus replication and gene expression, systemically detectable levels of hGM-CSF, and tumor-infiltrating CTLs were also demonstrated [72].

1.3.4 Deletion of thymidine kinase

Thymidine kinase (TK) is an E2F- responsive gene and drives JX-594 replication in cancer cells that have cell cycle abnormalities. The deletion of the *TK* gene means that viral replication is reliant on cellular TK expression, which is expressed in abundance in the majority of cancers [105]. The *TK* disruption is also important in the context of viral toxicity. The TK-deletion virus is less likely to infect healthy

organs and nervous tissue, and is quickly cleared from these, but replicates efficiently in tumour tissue [103].

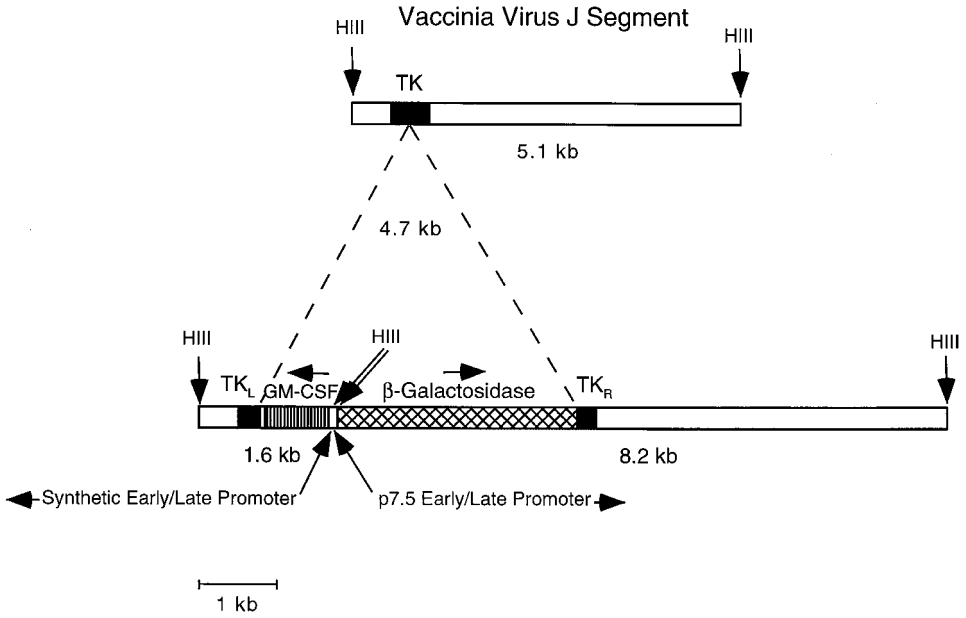

Figure 1-4 Schematic of the generation of JX-594, with the insertion of the *GM-CSF* and *LacZ* genes into the *TK* gene.

The top fragment represents the 5.1-kb "J" fragment, where the TK gene resides. Homologous recombination into the *TK* gene using the pSC65 vector, into which the *GM-CSF* gene has been inserted, disrupts the *TK* gene. The *LacZ* gene, encoding for β-galactodase, is inserted as well. Figure from Mastrangelo *et al [106].* In the virus strains used in experiments in this work, the β-Galactodase expression is substituted by either fLuc or GFP.

1.3.5 Double-deleted vaccinia virus

Vaccinia-growth factor (VGF) is an epidermal growth factor (EGF)-like glycoprotein encoded by vaccinia, consisting of 77 amino-acids. VGF is expressed in the early phase of the virus replicative cycle and is secreted into the extra-cellular environment. VGF is reported to be important as a mitogen, to stimulate the growth of vaccinia-infected cells and support viral replication [107, 108]. Deletion of the *TK* gene or *VGF* genes significantly decreases pathogenecity compared with wild-type (WT) virus, with decreased viral replication in resting cells [109, 110]. McCart *et al*. reported the construction of a vaccinia virus with deletion of both the *TK* and *VGF* portion of the genome - vvDD (figure 1-5) [73]. They theorised that the combined effect of both deletions would mean that replication would occur only in actively dividing cells (those that have high TK, and those that do not require VGF-stimulation to divide), thus improving tumour selectivity. In resting murine NIH3T3 cells, *in vitro* infection with vvDD yielded reduced viral recovery compared to WT, TK^{-ve} or VGF^{-ve}, whereas similar viral recovery was seen in actively dividing cells. In an *in vivo* mouse model, intra-peritoneal vvDD was safer than WT, TK^{-ve} or VGF^{-ve} strains, with significantly less virus recovered from brain, but more in bone-marrow (though not statistically significant). A similar amount was recovered from tumour, and vvDD-injected mice lived for longer (>100 days) than the WT (6 days), TK^{-ve} (17 days) or VGF^{-ve} (29 days) group.

Lun *et al*. have used a vvDD in combination with rapamycin and cyclophosphamide to treat malignant gliomas *in vitro* and *in vivo*. Systemic delivery targeted solitary and multifocal intracranial tumors and prolonged survival of immunocompetent rats. Viral replication was enhanced by combination therapy with rapamycin or cyclophosphamide and further prolonged survival [111].

Currently, a phase I dose-escalation trial of a vvDD administered by IT or IV injection is currently in progress, but not recruiting (ClinicalTrials.gov Identifier: NCT00574977).

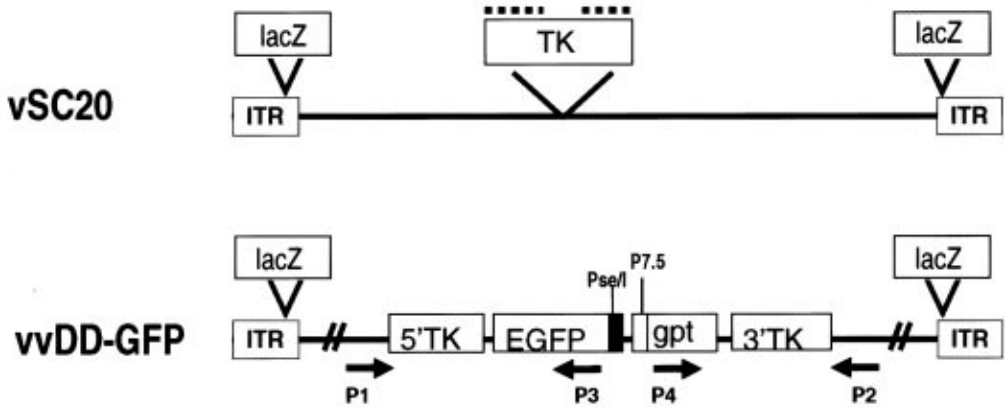

Figure 1-5. The double deletion vaccinia virus (vvDD).

The *TK* locus of parenteral vaccinia (vSC20) is disrupted by insertion of *eGFP* which is under the control of a synthetic early/late promoter (Pse/l). The *VGF* sites within Inverted terminal repeats (ITR) are disrupted by insertion of the LacZ gene. Adapted from McCart *et al [73]*.

1.3.6 Histone deacetylase inhibitors (HDACi)

HDACi decrease interferon production, and can dampen cellular innate immune responses. MacTavish *et al*. used Trichostatin A (TSA, a HDACi) in combination with vvDD *in vitro,* in murine 4T1 breast cancer cells, and demonstrated enhanced vvDD-associated GFP expression. Similarly, in a syngeneic lung metastasis mouse model injected intravenously with melanoma cells, followed by intraperitoneal TSA and/or intravenous vvDD, they demonstrated a further therapeutic benefit of the dual therapy when compared to either TSA or vvDD alone .

1.3.7 Pro-inflammatory cytokines

The vaccinia genetic backbone can be easily manipulated to 'arm' the virus with pro-inflammatory cytokines. This presents a platform for targeted inflammation at the site of the tumour, without causing a generalised systemic response. One of the most effective demonstrations of this was in athymic mice bearing a human tumour which were injected with the Copenhagen vaccinia strain which harboured cDNA for IL-6. Infective vaccinia particles were found to efficiently infect tumour cells, sparing liver, spleen, brain and bone marrow, with detectable IL-6 in the serum. Similarly, in euthymic mice, vaccinia expressing IL-2 reduced growth rate of 50% of tumours and complete rejection in 17% [112]. Concurrently, it was found that organs such as liver, spleen, brain and bone marrow showed barely detectable levels or no signs at all of virus infection.

Li *et al*. in Pittsburgh, hypothesized that combinations of immunotherapy and oncolytic viral therapy may be used to produce improved anticancer effects. To demonstrate this, they used a vvDD backbone to create vvCCL5, which expresses a murine chemokine CCL5 (RANTES; regulated upon activation, normal T-cell expressed and secreted). They used a mouse model, which had subcutaneously

implanted MC38 (murine, colonic adenocarcinoma). When compared to vvDD, vvCCL5 showed increased persistence and enhanced therapeutic effect, and was also found to be more actively cleared from normal tissue. The therapeutic effect also correlated with increased immune cell infiltration into the tumour [113].

1.3.8 JX-963

In 2007, Thorne *et al*. [74] described the design of a new systemically effective virotherapeutic (JX-963). Using the Western Reserve (WR) strain of vaccinia, a highly potent poxvirus strain, they engineered a vvDD that expressed human GM-CSF. Significant cancer selectivity of JX-963 was demonstrated *in vitro* in human tumor cell lines, *in vivo* in tumor-bearing rabbits, and in primary human surgical samples *ex vivo*. JX-963 was compared with vvDD to assess the potential of GM-CSF expression, and with JX-594, to compare the WR strain versus the Wyeth strain backbone. They showed that at 1 x 10^9 pfu, there were significant antitumor effects, and inhibition of the outgrowth of microscopic lung metastases, compared to vvDD and JX-594. There was also an increased amount of blood GM-CSF in the JX-963 treated model, which indicated increased replication of the WR strain backbone.

More recently (2010), the JX-963 strain of vaccinia has been investigated by Lee *et al,* using an immunocompetent, orthotopic and spontaneously metastasizing rabbit liver cancer model [114]. Antitumoral efficacy against primary and metastatic tumour foci was evaluated by serial chest and abdominal computerised tomography (CT) scanning, and there was significant reduction in primary tumour mass, and liver and lung metastases. Replication of virus was observed in all tumour tissue, despite rising neutralizing antibodies to JX-963 from day 5-18. Following intravenous administration of JX-963, GM-CSF was detected in tumour-burdened

rabbits, but not in controls, indicting that viral replication and GM-CSF production was tumour-specific. GM-CSF production at 24 hours was also higher for JX-963 as compared to vvDD. Splenocytes were isolated before and after injection of JX-963, which confirmed a significant increase in tumour-targeting CTLs. A significant improvement in median survival was also observed, along with prevention of weight loss, and no significant organ toxicity was noted.

1.3.9 B18R protein and the development of JX-795

Interferons (IFNs) are a class of cytokine that are important in the host antiviral response, and play a major role in the treatment of hepatitis C. IFNs are so-named as they 'interfere' with viral replication within cells and allow communication between cells to trigger the immune system to eradicate pathogens and tumours. Thus, the IFN antiviral defence mechanism presents a barrier to OV therapy. OV-related cancer selectivity is partly due to IFN-mediated inhibition of viral replication in normal tissues, whereas replication and oncolysis proceeds unhindered in tumour cells with defects in IFN responses. Vaccinia has evolved to expresses a protein, B18R, which acts as a 'decoy' receptor to bind type I IFNs (see figure 1-3), preventing binding onto the cell-surface which would initiate the host protein kinase-R (PKR) mediated anti-viral response. B18R deletion increases the median lethal dose (LD50) of vaccinia by 3-logs [98] and integration of B18R into a Herpes simplex virus (HSV) has been shown to improve replication and enhance killing ability against otherwise resistant cell lines [115].

Kirn *et al*. hypothesised that IFN expression from vaccinia would increase anti-cancer effects, and reduce toxicity to normal tissue with intact interferon pathways. In order to do this, using a WR backbone, the *B18R* locus was disrupted, and murine IFNβ was cloned for expression from the 7.5 early/late promoter in a similar

fashion to GM-CSF expression from JX-594. This virus was termed JX-795. This WR B18R deletion mutant demonstrated IFN-dependent cancer selectivity and efficacy *in vitro*, and tumour targeting and efficacy in mouse models *in vivo*, which was further enhanced by the addition of IFNβ [116].

1.3.10 Suicide genes to direct chemotherapy

Bacterial and yeast cytosine deaminase (CDase) have been well characterised as an enzyme–prodrug system that converts 5-fluorocytosine (5-FC; a non-toxic anti-fungal agent) to its highly toxic derivate 5-fluorouracil (5-FU), which is a chemotherapeutic agent capable of inhibiting DNA and RNA synthesis and interfering with DNA repair. Using a vaccinia virus carrying the bacterial and yeast CDase genes, directed expression of CDase enzyme in tumours has been achieved [117, 118]. Follope *et al*. used a *TK*-deleted vaccinia virus (Copenhagen strain) that expressed the fusion suicide gene *FCU1* (vvDD-FCU1). Intratumoral inoculation of this virus, along with IV prodrug 5-FC, resulted in statistically significant reductions in the growth of subcutaneous human colon cancer in nude mice compared with control 5-FU alone. They also demonstrated a reduction in tumour volume in nude mice bearing orthotopic liver metastasis of a human colon cancer, following intravenous delivery of VV-FCU1 and 5-FC. [119].

1.3.11 Oncolysate: active specific immunotherapy

In 1992, Scoggin *et al*. observed antitumor effects with vaccinia virus infected tumor cell lysate in animal models, and therefore established a adjuvant immunotherapeutic clinical trial in patients with melanoma using vaccinia virus infected melanoma oncolysate (VMO). Preliminary clinical trials showed minimal side effects and moderate responses. Postimmune sera contained melanoma-specific antibodies. In August 1985, a Phase II clinical trial was initiated and 19 of

39 patients with stage II disease had a disease-free mean survival time of 24.6 months (which was statistically significant compared with historical controls) [120].

This eventually resulted in a randomized, double-blind, multicenter phase III trial (across 11 centers), initiated in June 1988. 217 patients with stage 3 melanoma were recruited. The VMO was prepared by using 4 tested melanoma cell lines infected with Vaccinia virus. Following incubation, the infected cells were lysed by sonication and the nucleus-free lysate was obtained. This VMO was then injected once a week for 13 weeks and then once every 2 weeks for a total of 12 months, or until recurrence. This trial showed no statistically significant increase in either disease-free interval (DFI) ($p = 0.61$) or overall survival (OS) ($p = 0.79$) of patients treated with VMO ($n = 104$) compared with Vaccinia virus alone ($n = 113$). Although a subset of patients (Male, aged 44-57, with 1-5 nodes) had significant improvement in survival. [121]. It was suggested that the VMO trial may have shown an enhanced efficiency if compared to a no-treatment observation control arm [122].

Published in 2002, another large (N= 675) phase III, unblinded, multicenter trial, conducted by Hersey *et al*. showed a non-significant trend towards overall survival improvement after a vaccinia melanoma cell lysate (VMCL) treatment (intention-to-treat analysis; 59.6% vs 55.1% at 5 years). In this trial, patients with stages IIB and III melanoma received intradermal injections of VMCL over a 2-year period at reducing dose frequency, and were followed up for a median of 8 years [123].

Tanaka *et al*. in 1994 published results of a study of vaccinia colon oncolysate (VCO). In this case, oncolysate was prepared with VV engineered to express interleukin-2 (IL-2) (IL-2VCO) in combination with recombinant IFNα. This was

studied in a syngeneic murine CC-36 colon hepatic metastasis model. This showed an improvement in survival compared with controls, consistent with a reduction in hepatic metastases (mean liver weight), and induction of cytolytic T-cell activity. It was suggested IL-2VV could be used as a substitute for recombinant IL-2 in cytokine-augmented active specific immunotherapy [124].

1.3.12 GLONC-1 virus

Another strain of vaccinia has been used as a backbone to construct an OV; the Lister strain from the Institute of Viral preparations (LIVP). The OV, termed GLV-1h68 carries a *Renilla* luciferase-green fluorescent protein (GFP) fusion cassette at the F14.5L locus, and the *TK* locus (*J2R*) is disrupted by insertion of a β-galactosidase cassette. Robust GLV-1h68 transgene expression was found following infection of four human sarcoma cell lines with >80% cytotoxicity at an multiplicity of infection (MOI) of 5. In a human sarcoma cell-line xenograft model in mice, IT injection of GLV-1h68 resulted in localised viral-luciferase activity, with no spread to adjacent normal tissue. There was near-complete tumour regression over a 28-day period without observed cytotoxicity [125]. A similar virus, GLV-1h153 was found to infect, replicate in, and kill triple-negative breast cancer cell-lines *in vitro*. In an *in vivo* orthotopic murine model with reliable metastases from a mammary fat pad xenograft, IT and IV injection both resulted in a 90% reduction in tumour volume compared to control mice, and all harvested tumours and metastases showed no evidence of residual malignant metastatic cells [126].

1.4 Clinical trials with JX-594

Table 1.1 summarises all human clinical trials performed to date using JX-594 therapy in multiple tumours.

1.4.1 Metastatic prostate cancer

It has been previously shown that prostate-specific antigen (PSA)-specific CTLs could be generated that lyse PSA-expressing prostate cancer cells [127]. Vaccinia has been used as a potential vector for presentation of the PSA antigen and thereby inducing specific cellular immunity.

In 2002, Gulley *et al*. conducted a phase I trial of recombinant vaccinia prostate specific antigen (rV-PSA) in 42 patients with advanced metastatic prostate cancer. Vaccinia virus containing the gene for PSA was delivered by two routes: dermal scarification and subcutaneous injection, given three times, at 4-week intervals. Results showed no significant treatment-related toxicity apart from local reaction at the injection site. There was an increase in the proportion of PSA-specific T cells, and these were shown to lyse tumour cells *in vitro*. They did not demonstrate any objective tumour response. They postulated that this was due to a combination of the advanced nature of the disease in the patient population (and thus impaired immune functional status) and relative lack of potency of this vaccine regimen required for an immune response [128].

Similar results were seen in a study by Alren *et al*. in 2007. In this study a recombinant vaccinia virus with transgenes for PSA and a triad of co-stimulatory molecules (B7.1, ICAM-1, and LFA-3) was utilised as a priming vaccine. This was followed by a boost vaccination with a recombinant fowlpox virus. Some grade 2

toxicity was seen with higher doses. Viable vaccinia was seen using plaque assay at the site swab of 1 of 4 patients analyzed, and PSA-specific immune responses were seen in 4 of 6 patients [129]. In 2010, Kantoff *et al*. performed a randomized, controlled, and blinded phase II trial of the same treatment strategy in 122 patients (therapy: control; 82:40). They found that progression-free survival was similar in both treatment and control arms, but at three years, overall survival was longer by a median of 8.5 months in the treatment group [130].

Most recently, a vaccine based on a modified vaccinia Ankara virus combined with the oncofetal antigen 5T4 has been developed (TroVax), which has been used for the treatment of castration-resistant prostate cancer. The 5T4 TAA is highly expressed in a large number of carcinomas, including prostate cancer, but rarely in healthy tissue. Disease progression was monitored by PSA measurements every 4 weeks and CT and bone scans every 8 weeks. All 24 patients mounted a significant 5T4-specific immune response. All patients experienced disease progression, and 1 year follow-up, 16 patients remained alive. There were no objective clinical responses on CT or bone scans [131].

1.4.2 Colorectal cancer

Similarly, TroVax has been used in colorectal cancer, which was the first trial of TroVax. This dose-escalation study showed that TroVax was safe and well-tolerated [132]. In 2012, a phase IIa trial of neo-adjuvant IV and IT JX-594 injection in patients with colorectal liver cancer trial was terminated early due to logistic concerns rather than adverse events. Currently, JX-594 is being investigated in a phase I/IIa dose-escalation trial, administered by multiple IV infusions (ClinicalTrials.gov Identifier:NCT01469611) or multiple IV infusions followed by IT

boosts, in combination with Irinotecan (ClinicalTrials.gov Identifier: NCT01394939) in patients with metastatic, refractory colorectal carcinoma .

1.4.3 Melanoma

Several early-phase and proof-of-concept clinical trials in humans have been performed. In 1999, a phase I, dose escalation pilot JX-594 trial conducted by Mastrangelo *et al*., investigated IT therapy in cutaneous melanoma. Seven patients with surgically incurable and metastatic cutaneous melanoma received twice-weekly IT injections of escalating doses for 6 weeks. Immunological responses and virus-derived GM-CSF were seen in all patients. There was tumour response at the site of the injection in 5 patients, of which 4 had regression in non-injected dermal lesions. Importantly, JX-594 was safe, and the maximum-tolerated dose (MTD) was not reached [106]. In 2011, Hwang *et al*. described a mechanistic proof-of-concept trial in 10 patients with previously treated metastatic melanoma. JX-594 was delivered intratumourally, and β-Galactosidase (a different trnasgene) was expressed in tumour, in all patients, and an increase in GM-CSF-responsive white cell subsets was also seen. Despite the presence of neutralising antibodies (NAb) against JX-594 after initial treatment, replication was also observed in non-injected tumours. Using the Response Evaluation Criteria in Solid Tumours (RECIST) criteria, stable disease was demonstrated in all 5 evaluated patients, and 3 patients had stable disease in non-injected tumours. JX-594 was well tolerated, and all patients reported only grade 1 or 2 toxicity, with grade 3 toxicity in 1 patient only (anaemia) [133].

1.4.4 Primary and secondary liver tumours

In South Korea, a phase I trial by Park *et al.* in 2008 showed that IT injection of JX-594 into primary or metastatic liver tumours was generally well-tolerated and had anti-tumoral effects against several refractory tumours. 14 patients with liver tumour (both primary and metastatic from colorectal, lung and melanoma) were recruited into the trial and injected with varying doses of JX-594 every 3 weeks; $1x10^8$ plaque-forming units (pfu), $3x10^8$ pfu, $1x10^9$ pfu, or $3x10^9$ pfu. An average of 3.4 cycles was given. All patients experienced flu-like symptoms and 4 had dose-related thrombocytopenia, 2 patients had hyperbilirubinaemia. The maximum tolerated dose was $1x10^9$ pfu. In 10 assessed patients, tumour responses were observed in injected and non-injected tumours, and according to RECIST criteria 3 patients had partial response, 6 had stable disease, and 1 had progressive disease.

Heo *et al*. treated three HCC patients who had progressive disease following JX-594 treatment, with sorafenib (a small molecule inhibitor of B-raf and vascular endothelial growth factor receptor). All three patients showed rapid and marked tumour necrosis, and had objective responses according to Choi and Response Evaluation Criteria in Solid Tumors (RECIST) criteria, which occurred as early as 2.5 weeks following sorafenib initiation; comparative responses had not been observed in patients with HCC treated with sorafeib alone in the same unit [134]. These observations clearly pave the way for combination studies using vaccinia or other oncolytic viruses with established small molecule inhibitors as well as standard chemotherapeutic agents.

In a more recent phase II trial in 2013, Heo *et al*. infused low-dose (10^8 pfu) or high-dose (10^9 pfu) JX-594 by image-guided IT injection (3 doses; days 1, 15 and 29) in 30 patients with HCC [135]. Most had had previous locoregional treatment, and

some had progressed despite systemic therapy. This trial was halted due to significant survival in the high-dose group. The intrahepatic mRECIST disease control rate at week 8 was 46% overall with no difference between dose-groups, with objective mRECIST responses and decreased tumor perfusion and contrast enhancement in both injected and noninjected tumors. GM-CSF expression was detectable by day 5 in more than 60% of patients. Induction of antitumoral immunity was demonstrated by assessing antibody-mediated complement-dependent cytotoxicity (CDC) in patients' serum, and 11/16 (69%) patients developed CDC against at least one of four HCC cell lines. Cellular immunity was also demonstrated by the induction of CTLs against vaccinia peptides. Patients' survival was significantly related to dose (median survival of 14.1 months compared to 6.7 months on the high and low dose, respectively).

1.4.5 HBV-associated HCC

In this phase I study (part of the same cohort as Park *et al.* [77]), Liu *et al*. showed that JX-594 demonstrates anti-tumoural, anti-vascular and anti-HBV activities in patients with HCC [76]. Three patients with advanced refractory HBV-associated HCC received 4-8 cycles of intratumoral administration of JX-594. Treatment response was evaluated clinically using CT, positron emission tomography (PET)-CT, and tumour markers (AFP). Treatment was well tolerated in all 3 patients and showed tumour responses based on RECIST and Choi criteria, and two patients showed a reduction in tumour markers. Response in distant metastases was also demonstrated; one patient developed a metastasis in the neck, and following four cycles of intra-tumoural JX-594, there was a 76% decrease in metabolic activity on PET-CT and a 98% reduction in AFP.

JX-594 replication was also demonstrated; initially detectable 15 minutes after the injection and eventually cleared with a half life of 15-30 minutes. Interestingly, JX-594 was detectable once again from days 5-8, despite the development of neutralizing antibodies, suggestive of viral replication. Dissemination to non-injected tumour sites was also demonstrated. GM-CSF was detectable at 3 hours and up to 22 days in one patient. On day 3, consistent with the initiation of viral replication, there was ten-fold increase in white blood cells. At 3 hours, induction of IL-4, IL-6 and IL-10, TNF-α and interferon-γ was observed. There was a sustained reduction in serum VEGF levels in two patients, suggesting tumour vascular disruption.

In addition to the anti-tumour response, there was a reduction in HBV DNA concentrations (70-91%) in all three patients, which rose again once extra-hepatic metastases developed. Interestingly, further successful treatment of the metastases was associated with a further fall in HBV DNA, suggesting that tumour cells are a source of HBV genomes.

1.4.6 Intravenous JX-594 in multiple tumours

A further pivotal early-phase trial by Breitbach *et al*. treated 23 patients (of which 22 were evaluable) with intravenous JX594; lung, colorectal, melanoma, thyroid, pancreatic, ovarian, mesothelioma, leiomyosarcoma and gastric cancers were all targeted. This study showed that JX-594 selectively infects, replicates and expresses transgene products in cancer, but not normal tissue. Disease control was seen in 13 of these patients by RECIST criteria [136].

Virus **Author, Year** **Phase**	**Patient population and modality of viral delivery**	**Outcome and important findings**	**Toxicity**
JX-594 Mastangelo *et al*., October 1999 Phase I dose-escalation trial	N= 7; surgically incurable cutaneous melanoma, re-vacciniated with WT Vaccinia. Intratumoural injection 10^4 - $8x10^7$ pfu/session	2/7 Complete remission (with one patient having remission of un-injected lesions) 3/7 Mixed response 2/7 No response All patients developed an anti-vaccinia humoral response, yet β-Gal transgene expressed in all patients in tumour.	Local inflammation at site of injection Grade 1 flu-like symptoms
JX-594 Park *et al*. June 2008 Phase I dose escalation trial	N= 14; refractory primary (3) or secondary (11) liver tumours, heavily pre-treated Intratumoural 10^8 - $3x10^9$ pfu every 3 weeks. MTD found to be 1 x 10^9 pfu	4/6 patients at MTD had GM-CSF related increase in neutrophil count RECIST criteria; 3/10 Partial response 6/10 Stable disease 1/10 Progressive disease CHOI criteria; 8/14 showed decrease in HU (6/8 > 30% decrease)	14/14 grade 1–3 flu-like symptoms 4/14 transient grade 1–3 dose-related thrombocytopenia. 2/14 Grade 3 hyperbilirubinaemia at max dose (3 $x10^9$ pfu).
JX-594 Lui *et al*., July 2008 (Same cohort as above, Park *et al*.)	N=3, advanced, surgically unresectable hepatitis B virus (HBV) -associated HCC. All failed previous treatment. Intratumoral Inj. 3 $x10^8$ – 3 x 10^9 pfu/cycle	3/3 showed objective response on RECIST criteria, including the extrahepatic disease on N=1/1. N =2/3 had reductions on serum VEGF N=3/3 had significant reductions in HBV DNA Following acute clearance after 15 minutes, a second wave on replication-dependant genomes were detected in serum, despite neutralising antibodies.	Transient flu-like symptoms
JX-594 + Sorafenib Heo *et al*., Jun 2011 Phase II	N=3 HCC, failed response on intratumoural Inj. of JX-594 and subsequent Sorafenib treatment N=1 metastatic RCC, intratumoural JX-595 followed by sunitinib	3/3 had response based on RECIST and CHOI criteria CHOI tumour responses in liver and abomen following JX-594 and complete whole body tumour response after sunitinib by CT.	No liver toxicity

Virus **Author, Year** **Phase**	**Patient Population and modality of viral delivery**	**Outcome and important findings**	**Toxicity**
JX-594 Breitbach *et al*., September 2011 Phase I dose-escalation trial)	23 patients; Lung (NSCLC) (N=5) Colorectal (N=6) Melanoma (N=4) Thyroid (N=1) Pancreatic (N=1) Ovarian (N=2) Mesothelioma (N=1) Leiomyosarcoma (N=1) Gastric (N=1) Intravenous delivery; $1x10^5$ – $3x10^7$ pfu/kg)	Disease Control in: 3/5 3/6 2/4 1/4 0/1 2/2 1/1 1/1 0/1 JX-594 selectively infects, replicates, ,and expresses transgene products in cancer tissue.	Grade 1 and 2 flu-like symptoms only
JX-594 Hwang *et al*., October 2011 Mechanistic proof-of-concept trial	10 patients; previously treated stage IV Melanoma Intratumoural delivery; 10^8 pfu/cycle	β-Gal transgene expressed in all patients in tumour Increase in GM-CSF responsive WCC subsets (60%) Replication seen in non-injected tumour (at day 5) All patients developed NAb titres. RECIST criteria; stable in 5/5 injected tumours and in 3/5 non-injected tumours	Grade 1 flu-like symptoms. Grade 3 in N=1 (anaemia)
JX-594 Heo *et al*., January 2013 Phase II trial	30 patients; 22 had loco-regional treatment and 18 were virally-associated IT delivery; 3 cycles of low-dose (10^8 pfu) or high dose (10^9 pfu)	Intrahepatic mRECIST criteria; 46% overall disease control rate at week 8 Modified Choi response; 62% overall GM-CSF (69% of high-dose patients) and β –Gal antibodies (75% of high-dose patients). Complement-dependent cytotoxicity in 1/16 Survival; 14.1 months in low-dose and 6.7 months in high-dose	Grade 3 in N=5 (low-dose and high-dose) and Grade 4 in N=1 (high-dose)

Table 1-1 Summary of JX-594 trials

Table above summarises the trails published to date investigating the clinical effectiveness of JX-594. NSCLC = non-small cell lung cancer, NAb = neutralising antibody. RECIST = Response Evaluation Criteria in Solid Tumors, MTD = maximum tolerable dose, HU=Hounsfield units, pfu = plaque forming units.

1.5 Other oncolytic viruses

1.5.1 Adenovirus

Adenoviruses were the first class of OV used in clinical trials in humans. Tumour specificity was enhanced via a number of mechanisms, including deletion of viral E1B, which leads to ubiquitinylation of p53, targeting it for degradation, thereby theoretically limiting viral replication to p53 deficient malignant cells. Onyx015 was developed in 1996 and a related virus gained a licence in China for use in combination with chemotherapy for head and neck cancer [65]. However, interest in Onyx015 dissipated thereafter due to the lack of significant therapeutic effect on testing in larger trials. More recently, a tumour-specific replicating adenovirus hTert-Ad (human telomerase reverse transcriptase promoter-regulated adenovirus) was investigated in the treatment of HCC in combination with bortezomib. In a mouse model with subcutaneous HCC implantation, bortezomib and hTert-Ad were found to trigger complementary unfolded protein response (UPR) pathways and negatively interfere with important recovery checkpoints, resulting in enhanced endoplasmic reticulum stress induced apoptosis and improved oncolysis *in vivo* [137].

1.5.2 Newcastle Disease Virus

Newcastle disease virus (NDV) is an avian pathogen, and transmission to humans (for example in poultry processing plants) can cause mild conjunctivitis and influenza-like symptoms, but poses otherwise no major hazard to human health [138]. It displays tumour specific killing due to tumour specific defects in the IFN-mediated antiviral response. It has been investigated *in vivo* and *in vitro* in combination with another OV, reovirus, leading to improved cytotoxicity and simultaneous replication of both viruses [139]. A naturally attenuated, non-engineered NDV, PV701 has been investigated in phase I clinical trials. IV-administration led to flu-like symptoms and fatigue, which was then improved by a

desensitisation regimen [140, 141]. There have been three phase I trials of 114 patients using IV administration of PV701, and in the most recent, out of 19 patients, 6 responses were observed [142].

1.5.3 Vesicular Stomatitis Virus

Vesicular stomatitis virus (VSV) is an enveloped, nonsegmented, negative-strand RNA virus of the Rhabdoviridae family. VSV is a pathogen of livestock, with human crossover being relatively rare and subclinical in presentation. Similar to other OV, VSV replicates in tumour cells due to a defect in the interferon anti-viral response pathway. VSV is a promising OV for clinical use, due to a lack of pre-existing immunity in humans, its small, easily manipulated genome, relative independence of a receptor and cytoplasmic replication (hence no host-cell transformation). A phase I trial is underway [107, 143].

1.5.4 Herpes Simplex Virus

The most clinically advanced oncolytic virus, based on herpes simplex virus 1, is called OncoVEX (now renamed T-Vec), and is an oncolytic HSV encoding GM-CSF to enhance anti-tumour immune responses. In a recently published phase II trial of intra-tumoural injection of OncoVEX in advanced melanoma [144], 13 of 50 patients achieved a radiological response, including 8 with a complete response. OncoVEX is currently undergoing phase III trial testing in melanoma. The first completed phase III clinical trial with an oncolytic virus, using an intratumoural T-Vec treatment in melanoma, has just been reported to have met its primary endpoint of durable response rate.

1.5.5 Measles Virus

Measles Virus (MV) has also been tested in the clinical setting. The Edmonston-Zagreb (MV-Edm) lineage has been used as a live attenuated vaccine [145], and preferentially infects malignant cells, which overexpress a measles virus receptor, CD46. MV-CEA is an engineered strain of MV-Edm, which expresses the soluble biomarker CEA, thus allowing *in vivo* monitoring of viral replication. A phase I trial of MV-CEA has has been completed in recurrent ovarian cancer resistant to paclitaxel and platinum chemotherapy [146]. Five of the 21 patients had significant decreases in CA125 levels, indicating a biochemical response to therapy.

1.5.6 Reovirus

Reovirus (Respiratory Enteric Orphan Virus) has no known clinical syndrome in humans. It is a naturally occurring, ubiquitous virus, and most of the population have been exposed to it in childhood, and hence carry neutralising antibodies. It was thought to infect *Ras*-activated malignant cells due to their inability to mount an RNA-activated protein kinase (PKR) response, although this theory has been challenged. An activated Ras signalling pathway is prevalent in the majority of solid malignancies, including 80-90% of pancreatic cancers, 40-50% of colorectal cancers and 50% of thyroid cancers. Early phase trials of both local and systemic Reolysin® (Oncolytics Biotech Inc) have demonstrated some significant promise in patients with metastatic cancers including those of the pancreas, lung and malignant melanoma. The safety profile of this treatment is excellent and it is generally well tolerated [147]. Reovirus is safe and tumour-specific following intravenous delivery in patients with colorectal liver metastases [148]. In this study, delivery of reovirus to tumour was demonstrated despite the presence of neutralising antibodies (NAb); replication-competent reovirus was recovered from blood cells but not plasma, suggesting that transport by immune cells could protect virus from systemic neutralisation. A phase III trial is currently underway using

Reolysin® in combination with Paclitaxel and Carboplatin in platinum-refractory head and neck cancers (Clinical trials.gov indentifier: NCT01166542).

Our laboratory has considerable experience with reovirus, and hence this is used as a positive control in some of the experiments described in this thesis, in order to understand and measure the response of vaccinia virus.

1.6 Obstacles to oncolytic viral therapy

Vaccinia strains and other pox viruses have been used in various clinical trials for treatment of established cancers [149-151], but their efficacy has been limited. This may be due to several factors; the local immunosuppressive nature of the tumour microenvironment, immune editing (escape of tumour populations that do not express target antigens), failure to cross the endothelial barrier during intravenous delivery, and the host anti-viral response.

Tumours evade the immune system by mechanisms such as down-regulating/modifying various components of the antigen presenting machinery resulting in loss of MHC-I antigen presentation [152], and the induction of immune tolerance via release of soluble immunosuppressive factors, such as transforming growth factor beta (TGF-β), indoleamine 2,3-dioxygenase (IDO), VEGF, IL-10 and prostaglandin E2 (PGE_2). These immunosuppressive cytokines, along with immune-suppressive cell populations present in the tumour microenvironment, can prevent the successful eradication of tumour cells. Therefore, reversing this tumour-induced immune tolerance will be critical to generating effective anti-tumour immunity. OV, as potent viral immune danger signals, have the potential to reverse this suppressive tumour microenvironment, facilitating the generation of an anti-tumour response.

Systemic delivery is the ideal route of administration to allow dissemination of OV to distant metastases. However, even in a previously un-exposed host, there are obstacles to overcome. The delivery of virus to tumour sites may be impeded by the development of NAbs and sequestering by the reticuloendothelial system and complement components. Even once delivery to a tumour site has been achieved, crossing the endothelial barrier to ensure adequate penetration into tumours may be yet another obstacle. Various strategies to overcome these limitations have been investigated; reducing anti-viral responses by immunosuppression, inhibiting viral clearance by coating viruses in antigenically inert polymers, overcoming specific anti-viral immunity by serotype switching, and 'hiding' OVs from NAbs with the use of cell based delivery strategies. Cells that traffic to tumours and that are permissive to viral replication have therefore been utilised as 'Trojan horses' to deliver OV direct to the tumour [153]; these carriers include stem cells (mesenchymal, adipose, neuronal and endothelial cells), immune cells (cytokine-induced killer (CIK) cells, DC, monocytes and T cells) and irradiated tumour cells.

1.7 Aim of study

To investigate the potential oncolytic and immune-stimulatory effects of vaccinia virus on liver cancer by testing; (i) direct tumour lysis, (ii) replication in tumour cell lines and fresh tissue, (iii) immune-stimulatory effects and (iv) development of an *ex vivo* tissue system for a more clinically relevant translational model.

Chapter 2

Materials and Methods

2 Materials and Methods

2.1 Chemicals

All chemicals and reagents were Molecular Biology Grade.

2.2 Cell culture

2.2.1 Cell lines

Colorectal cell lines, purchased from American Type Culture Collection (ATCC), were cryopreserved in 90% foetal calf serum (FCS) supplemented with 10% (*v*/*v*) dimethyl sulphoxide (DMSO) (Fisher Chemical, Loughborough, UK), in liquid nitrogen. CRC cell lines used were ; HCT116, LoVo, SW480 and SW620. The latter two are cell lines were derived from the same patient; SW480 from the primary tumour and SW620 from the metastatic tumour. Other cell lines used include; K562 (human chronic myeloid leukaemia) and Vero (kidney epithelial cells extracted from an African green monkey). See Appendix A for further details of cell lines.

2.2.2 Cell culture method

Cell culture was performed under aseptic conditions in NuAire Class II Microbiological Safety Cabinets (NuAire, Plymouth, USA). Sterility was maintained by laminar flow, and pre- and post-use cleaning with 2% Virkon (Dupont, Suffolk, UK) followed by 70% Ethanol. All cell lines and primary cultures were grown in either Dulbecco's Modified Eagle's Medium (DMEM) or Roswell Park Memorial Institute (RPMI) 1640 (both Gibco, NY, USA), supplemented with 10% (*v/v*) heat inactivated (30 minutes at 56^0C) FCS.

Cell lines were stored in 10% DMSO in 1.2ml cryotubes (Nunc, NY, USA) in liquid nitrogen. Cell recovery from frozen was performed by rapid thawing in a water bath at 37^0C, then dilution with 10x excess fresh media and centrifugation (Eppendorf centrifuge 5810R, 400g, 5 minutes) to harvest cells and remove otherwise toxic DMSO. Maintenance of cell lines was performed in vented plastic tissue culture flasks (Corning Costar, Amsterdam, The Netherlands) ($75cm^2$, $150cm^2$), in a Sanyo CO_2 incubator at 37^0C. Adherent cells are then harvested when near-confluent by washing with phosphate buffered saline (PBS) (Sigma, Dorset, UK) (with or without supplementation with Ethylenediaminetetraacetic acid (EDTA)), followed by Trypsin-EDTA (10x Stock solution (Sigma) diluted 10:1 in Hanks' Buffered Salt Solution (HBSS) (Sigma)). Cells were then harvested in media and centrifuged in a 50ml Falcon tube (Corning), and viable cell counts were obtained using a Nikon Eclipse TS100 microscope, using tryptan blue (Sigma) exclusion and an Improved Neubauer haemocytometer (Weber Scientific, NJ, USA) [154].

2.3 Isolation of peripheral blood mononuclear cells (PBMC) from fresh blood

PBMCs were isolated from fresh whole blood using density gradient separation. Peripheral blood was collected from healthy donors or patients with identified liver pathology in accordance with local guidelines and appropriate precautions. Written, informed consent was obtained from all patients in accordance with local institutional ethics review and approval. Blood was first diluted 2:1 with HBSS and 30 mls then layered over 15 mls Lymphoprep© (Axis Shield, Oslo, Norway) in 50 ml Falcon tubes. Tubes were centrifuged at 800g for 25 minutes at RT with no brake, and the interface PBMC layer collected using a Pasteur pipette (Alpha laboratories Ltd. Hampshire, UK). Cells were washed in 50 ml of HBSS and centrifuged at 400 g

for 10 minutes at RT. Cells were washed again in 50 ml HBSS and pelleted by further centrifugation at 400 g for 5 minutes at RT and supernatant discarded. PBMCs were maintained in culture at $2x10^6$ cells/ml of culture medium (RPMI + 10% FCS) for all future experiments.

2.4 Cell separation of PBMC population using magnetic-activated cell sorting (MACS) bead selection

Fresh PBMCs were isolated from whole blood as described in section 2.3. To separate $CD14^{-ve}$ cells, PBMCs were centrifuged, pelleted and re-suspended in 80 $\mu L/10^7$ cells of MACS buffer (PBS+1% (v/v) FCS+ 2mM EDTA). 30 µL of CD14 Microbeads (Miltenyi Biotec Ltd., Surrey, UK) per 10^7 cells was added and incubated at 4^oC for 15 minutes and then washed in 2 ml MACS buffer. Cells were pelleted by centrifugation and re-suspended in 500 µL MACS buffer, and passed over a MACS LS separation column mounted on a magnetic board (both Miltenyi Biotec Ltd.) and unbound cells ($CD14^{-ve}$) collected by washing with 1 ml MACS buffer (repeated three times). The remaining $CD14^{+ve}$ cells are collected by flushing out the retained cells in the MACS LS column using the supplied plunger, away from the magnetic board. NK cells were isolated in a similar fashion, by incubating first with an NK Cell Biotin-Antibody cocktail at 20 $\mu L/10^7$ cells for 10 minutes at 4^oC and then 40 $\mu L/10^7$ cells of NK Cell Microbead Cocktail for 15 mins at 4^oC (both Miltenyi Biotec Ltd.) and collecting the unbound cells.

2.5 Vaccinia virus (JX-594)

Varying genetically modified strains related to clinical JX-594 were provided by The Centre for Innovative Cancer Research, Ottawa Hospital, Canada, courtesy of John Bell laboratories, Dr. Fabrice Le Boef and Jennerex Therapeutics. These included JX-594-GM-CSF-fLuc (here onwards referred to as 'JX-594-GM-CSF'), JX-594-GM-CSF-eGFP (here onwards referred to as JX-594-GFP) and JX-594-YFP (which does not express GM-CSF). The insertion of the gene encoding for GM-CSF under an early/late promoter has clinical relevance, but along with GFP, can be used as a surrogate marker to make assessments of cellular entry and replication of the virus using flow cytometry, Enzyme-Linked Immunoabsorbent Assay (ELISA) and confocal microscopy (described later in sections 2.7, 2.10 and 2.15 respectively).

2.6 JX-594 infection of cells and tissue

Human CRC cell lines were harvested when near-confluent from tissue culture flasks and 2 x 10^5 cells seeded into a 6-well plate in 3mls of DMEM + 10% FCS. As described later in section 2.13, tissue cores and slices were placed in 'fresh tissue culture medium.' Serial dilutions of JX-594 were prepared in DMEM, and once cells were adherent, JX-594 was added to the culture medium at titres of 0, 0.01, 0.1, 1 and 10 pfu/cell. In the case of tissue cores/sections, a standard dosage of 10^6 and 10^7 pfu of virus was used. Following infection for defined time points, supernatant +/- cells can be collected and stored for later experiments. Cells/Tissue were fixed in 1% paraformaldehyde (PFA) (Adams Healthcare, Leeds, UK) for further processing/experiments.

2.7 Flow Cytometry

2.7.1 Background

Cytometry is a process by which physical and/or chemical characteristics of single cells can be measured. Flow cytometry has evolved to incorporate the use of multiple fluorochromes to effectively identify and isolate subset populations in a mixed-cell sample. Flow cytometers work using four closely related systems. The fluidic system transports cells from a suspension into a stream of a single column of cells through the cytometer into an illumination system, where a laser beam is applied onto each cell in turn. The resulting light scattering and fluorescence from a fluorescently labeled cell is collected, filtered and converted into electrical signals by the optical and electronics system (see figure 2-1). The processing system utilises specialised software to save acquired data and to analyse the resulting information, which is heavily graphically oriented (see figure 5-2). Two standard modalities of graphical representation are used: one-parameter histograms give information of mean fluorescence and distributional statistics and may be superimposed to show a 'shift' in the fluorescence of cells exposed to different treatment conditions; and two-parameter box plots, which are important for identifying cells of interest based on size and density and by expression of cell surface markers. Experience and pattern-recognition are an important part of flow cytometric analysis [155].

2.7.2 Method

PBMCs treated for specified time intervals with virus were harvested into 15 ml Falcon tubes (Corning) and centrifuged at 400g for 5 minutes, supernatant was collected and stored at -80^{0}C for later use. Cells were re-suspended in 200 μL per 1x10^6 cells of FACS buffer (Sterile PBS, 1% FCS, 0.1% Sodium Azide).

Approximately 5 x 10^5 - 1 x 10^6 cells (in 100 – 200 μL) were then transferred into FACS tubes that have been previously loaded with 3 - 10 μL fluorescent antibodies (see table 2.2). Cells were incubated with antibody for 20 minutes in the dark at RT, and subsequently washed with 2mls of FACS buffer and pelleted by centrifugation at 400g for 5 minutes. The excess FACS buffer was decanted and the cells re-suspended in 300 μL of 1% PFA for acquisition and analysis at a later date. Analysis was then performed using a FACSCalibur machine and BD CellQuest© Pro software (v4.0.1) (both Becton-Dickinson, Oxford, UK).

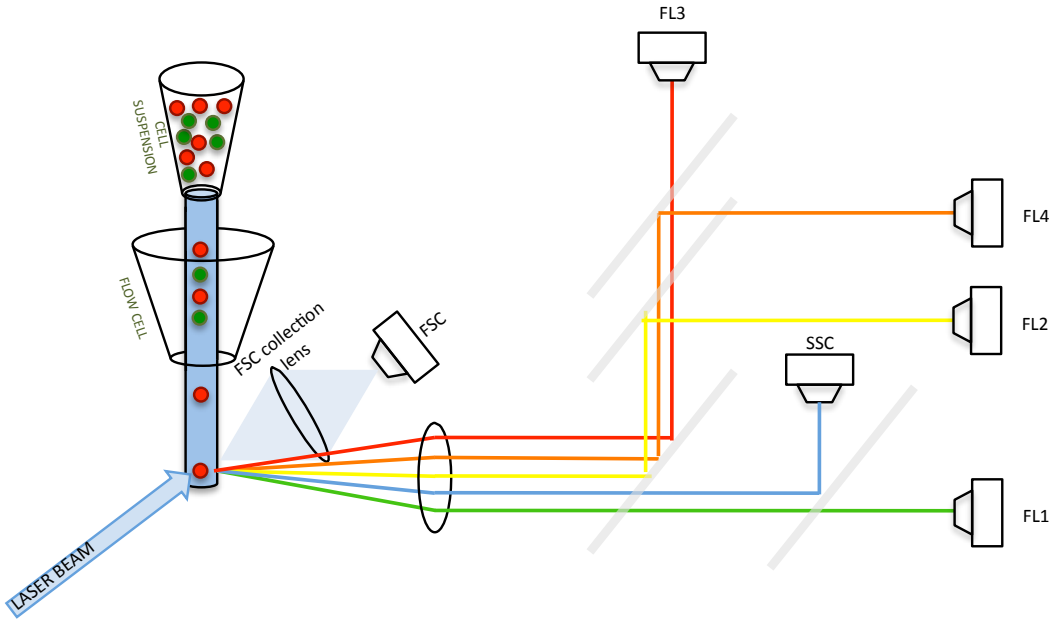

Figure 2-1. Flow cytometry

A mixed population of fluorochrome-labelled cells in suspension is streamlined into a single column of cells in a 'flow cell'. A laser beam (480nm) is applied onto each cell in turn, and its light emitting properties used to determine its physical and chemical properties. Photodiode electrodes ( ) analyse the emitted light and convert it into an electric signal. The identity of each cell can be determined by cell mass (FSC; forward scatter) and cell density (SSC; side scatter). Labelled with fluorescent antibodies, each cell will emit a light signal(s) of a particular wavelength(s). A system of dircroic interference filters will reflect emitted light of a particular wavelength onto a photodiode electrode (FL1=530nm, FL2=585nm, FL3=670nm, FL4=661nm), and this will be acquired and analysed using specialised software.

Target antigen	Significance	Flourochrome	Volume	Source
Isotype Mix	Control	FITC, PE, PerCP	2 µl	Dako Cytomation
CD3	T-cell Marker	PerCP	3 µl	BD Biosciences
CD56	Marker on NK cells and a subset of activated T-cells (NK-T cells)	PE	2 µl	Abd Serotec
CD56		FITC	10 µl	BD Biosciences
CD69	Early Activation marker, and signal-transmitting receptor	PE	5 µl	BD Biosciences
CD69		FITC	10 µl	BD Biosciences
NKG2D	Activation receptor on NK cells and T-cells	PE	3 µl	BD Biosciences
DNAM-1	Activation marker	PE	3 µl	BD Biosciences
NKp30	Natural cytotoxicity receptors, expressed exclusively on NK cells, play a major role in NK-mediated killing	PE	3 µl	BD Biosciences
NKp44		PE	3 µl	BD Biosciences
NKp46		PE	3 µl	BD Biosciences
CD107	Marker of NK/T-cell cytotoxicity due to degranulation	FITC	5 µl	BD Biosciences
CD80	Marker on activated B cells and monocytes. Provides a costimulatory signal for T cell activation and survival.	PE	5 µl	BD Biosciences
CD86	Expressed on antigen-presenting cells that provides a costimulatory signal for T cell activation and survival	PE	5 µl	BD Biosciences
CD11c	expressed in antigen presenting cells (APC: B lymphocytes, dendritic cells, macrophages)	PE	5 µl	BD Biosciences
Class II DR		PE	5 µl	BD Biosciences
CD14	Expressed on monocytes.	FITC	5 µl	BD Biosciences
CEA	Marker of colorectal carcinoma.	FITC	5 µl	BD Biosciences
EGFR	Receptor for epidermal growth factor. Stimulates cell growth and differentiation.	PE	5 µl	BD Biosciences

Table 2-1 Antibodies used for cell-surface phenotyping

2.8 Cell viability

2.8.1 Microculture tetrazolium test (MTT)

2.8.1.1 MTT background

3-(4,5-Dimethylthiazol-2-yl)-2,5-diphenyltetrazolium bromide (MTT), is a yellow tetrazole that is reduced to purple in living cells. A solubilisation solution e.g. DMSO is required to turn the insoluble purple product into a soluble, coloured solution. The absorbance can then be measured at a certain wavelength by a spectrophotometer, hence giving the level of cell viability due to active reductase enzymes [156].

2.8.1.2 MTT method

8×10^3 cells/well were seeded into each well of a 96-well plate (Costar) and incubated overnight at 37^0C to adhere. Serial dilutions of the virus were made and added to each well in triplicate, from 10 pfu/cell to 1×10^{-6} pfu/cell, with an un-infected control, and cells were incubated at 37^0c overnight. At specified time points, 20µL MTT (Sigma) was added to medium for 4 hours at 37^0C and then medium containing dead cells was removed. 150 µL DMSO was added to solubilise the cells and optical density was measured using a Multiskan EX plate reader (Thermo Fisher Scientific, Northumberland, UK) at wavelength 550nm using Ascent software (v 2.6, Thermo Fisher Scientific). The fluorescence output in sample wells was then compared to the un-infected control, and a relative fluorescence was calculated.

2.8.2 Cell viability assessment using a Live/Dead® fluorescent dye kit

The Live/Dead® reactive dye can permeate the compromised membranes of dead cells and react with free amines both on the cell surface and in the interior, resulting in intense fluorescent staining. In viable cells, only the cell-surface amines will react with the dye, resulting in relatively dim staining. Following infection with escalating doses of JX-594 for specified time points in 6-well plates, cells were harvested, washed in PBS and placed in FACS tubes (BD Falcon) and centrifuged at 400g for 5 minutes. 1 µL of Live/Dead fluorescent dye (PE) (Invitrogen, Paisely, UK) was added to the suspended cell pellet for 20 minutes at room temperature (RT). Following a final wash in PBS, and fixation in 1% PFA, acquisition and analysis was then performed using a FACSCalibur machine (Becton-Dickinson, Oxford, UK) using BD CellQuest© Pro software (v4.0.1), with the percentage of dead cells being determined as those that showed higher PE fluorescence.

2.8.3 Intracellular active caspase-3 production

2.8.3.1 Background

Caspase-3 is a member of the Cysteine-aspartic acid protease (Caspase) family. The activation of caspase-3 plays a key role in the execution phase of apoptosis. Caspases exist as inactive proenzymes that undergo proteolytic processing by self-proteolysis and/or cleavage by another protease, to produce two subunits that dimerise to form the active enzyme, active caspase-3.

2.8.3.2 Method

SW480 and SW620 cells were seeded into 6-well plates ($2x10^5$ cells in 3 mls culture medium). Following a 4-hour period to facilitate adherence of the cells, they were treated with 0, 0.1, 1 and 10 pfu/cell JX-594. Similarly, PBMCs were

suspended in culture medium at $2x10^6$/ml in 6-well plates and treated with JX-594 at 0, 0.1 and 1 pfu/cell.

Following treatment over specified time-points, cells were harvested into FACS tubes, pelleted and fixed in 1% PFA. Active caspase-3 production was measured using a PE-conjugated Active Caspase-3 Apoptosis Kit (BD Pharmigen, Oxford, UK). Briefly, fixed cells were incubated for 20 minutes on ice with a Cytofix/Cytoperm™ solution at a volume of 0.5 ml/$1x10^6$ cells. Cells were centrifuged at 400g for 5 minutes at RT to remove excess buffer, washed in the Perm/Wash™ buffer at a volume of 0.5ml/$1x10^6$ cells and pelleted. Cells were incubated with a PE-conjugated Active Caspase-3 antibody diluted in Perm/Wash™ buffer for 30 minutes at RT. Cells were then washed with 1 ml Perm/Wash™ buffer, pelleted, and re-suspended in 500 µL Perm/Wash™ buffer. Cells were analysed immediately using a FACS Calibur flow cytometer (described in section 2.17).

2.9 JX-594 replication

2.9.1 Plaque assay background

In order to determine the quantity of infectious virus particles, a procedure known as a plaque assay may be adopted. This technique was first developed for use in animal virology by Renato Dulbecco in 1952 [157]. 10-fold dilutions of a virus stock are prepared and 0.1ml aliquots are inoculated onto susceptible cell monolayers, and left to incubate. The cells are then covered with an overlay medium; a thick, nutrient-containing medium, that restricts spread of the virus to defined ‘plaques’ and aids to keep the cells stable. The originally infected cells will eventually lyse and release viral progeny, which is restricted to neighbouring cells by the overlay medium. Eventually, each virus particle produces a circular zone of infected/dead

cells; a ‘plaque.’ The plaque eventually becomes large enough to be visible to the naked eye. Surrounding living cells can be stained with a dye (e.g. methylene blue) to provide a contrast. The subsequent titre of a virus stock can be calculated in plaque-forming units (pfu) per ml. Each dilution of virus is plated in duplicate, and only those plates that have between 10 to 100 plaques are counted (for accuracy). The concentration of sample and stock virus used is determined by the formula below;

$$\frac{\#\ \text{plaques}}{d \times V} = \text{pfu/ml}$$

where d = dilution factor and V = volume of diluted virus added to the well

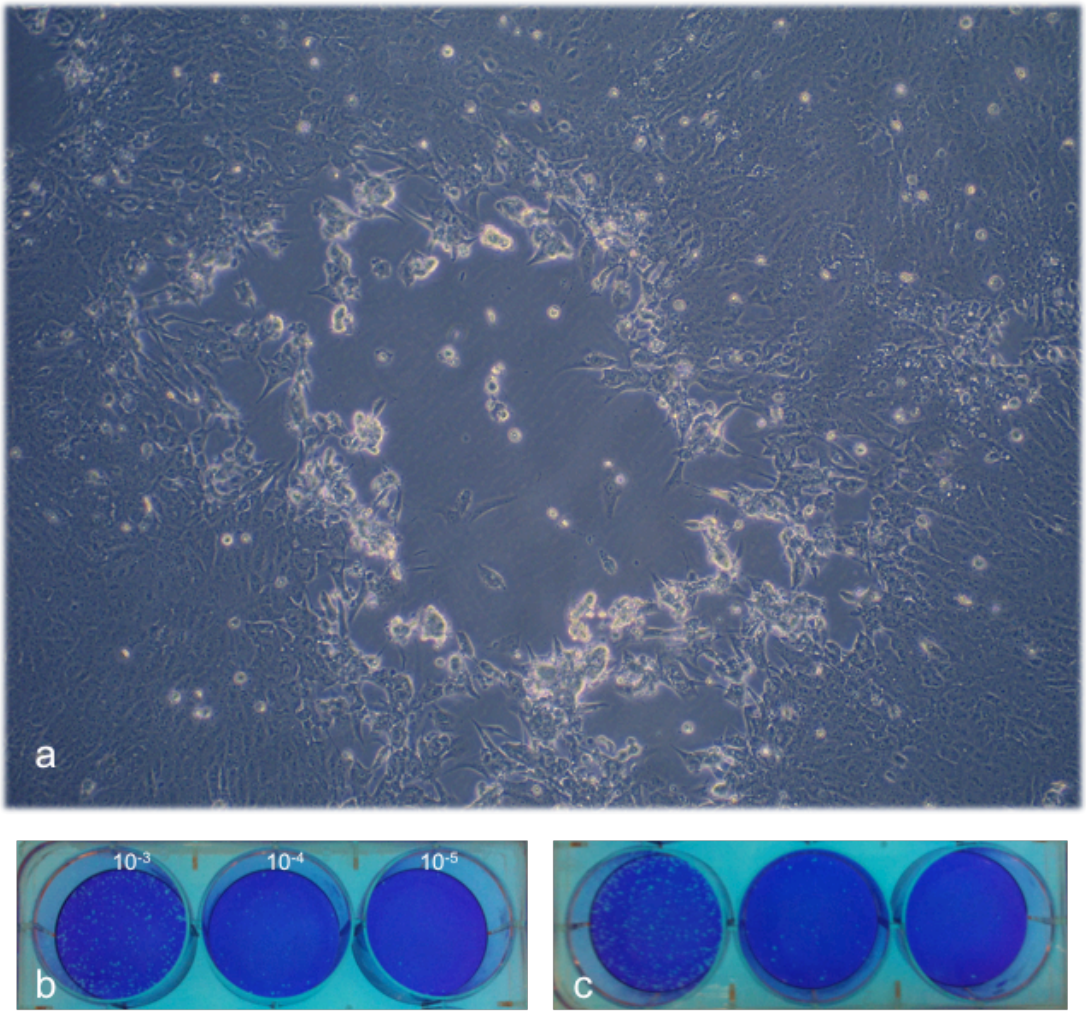

Figure 2-2 Illustration of viral plaques

Figure a) shows a photomicrograph at 40x magnification of a vaccinia viral plaque on Vero cells. There is a central area of cells that have been killed by the virus. The overlay medium restricts each plaque-forming unit to a single plaque, minimising merging of plaques, hence allowing the quantification of the total number of infectious viral plaques. Figures b) and c) show duplicate wells demonstrating viral plaques following serial dilutions on a background of Vero cells dyed with methylene blue, fixed in 1% PFA.

2.9.2 Plaque assay method

2.9.2.1 Sample preparation; CRC cell lines

7.5 x 10^4 cells (SW480 and SW620) were adhered to a 24-well plate in 1 ml of medium at 37^0C for 4 hours. JX-594 was then added to the medium and incubated for various time points at 37^0C. Cells and supernatant were then harvested and subjected to three rounds of freeze-thaw; methanol/dry ice followed by a block-heater at 37^0C (Grant Instruments, Cambridgeshire, UK). These were then stored at -80^0C until required.

2.9.2.2 Sample preparation; PBMCs

PBMCs were cultured at 2x10^6/ml in RPMI + 10% FCS and cell suspension including media harvested and frozen following 24 hour and 48 hour incubation with JX-594 at 0.1 pfu/cell in a 6-well plate. Samples were subjected to three cycles of freeze/thaw prior to plaque assay.

2.9.2.3 Plaque assay

Vero cells, which are susceptible to Vaccinia, were cultured in vented plastic tissue culture flasks (150 cm^2), in a Sanyo CO_2 incubator at 37^0C. Near-confluent cells were harvested and seeded at 2 x 10^5 in 6-well plates in 2ml DMEM + 10% FCS for 4 hours to allow cells to adhere. Samples and reference stock virus sample dilutions were prepared by serial dilutions in DMEM, resulting in logarithmic dilutions ranging from 10^{-2} to 10^{-11}.

Medium was removed from the adherent Vero cells and replaced with 500 µL of serum-free medium and 100 µL of the diluted sample or stock virus (in duplicate wells) and incubated at 37^0C for a further 4 hours. The media containing the

sample/stock virus was then taken off and 2 mls of overlay medium (2:1 ratio of DMEM + 10% FCS and 1.6% (*w/v*) of carboxymethylcellulose (CMC)) was added to each well. Cells were then incubated at 37^0C for 3 days.

Following this incubation, the excess media:CMC solution was removed and the cells were washed with PBS, and fixed with 0.5 ml 1% glutaraldehyde for 10 mins at RT. Following removal of the fixative solution, the cells were stained with 0.5 mls 1% methylene blue (in 50% ETOH) for 3 minutes at RT and washed to remove the excess dye. Plaques were counted using a light box to aide visualisation and the average of duplicate wells was used to calculate viral titre using the formula described above.

2.10 ELISA (Enzyme-Linked Immunoabsorbent Assay)

Flat bottomed 96 well Maxisorp© plates (Nunc) were coated with pre-optimized dilutions of capture antibodies (see table 2-2) diluted in coating buffer (100 mM $NaHCO_3$ in ddH_20) or PBS. These were then wrapped in cling-film and foil and incubated at 4^0C, overnight. Plates were then washed three times with PBS-Tween (0.05% Tween (Sigma) in PBS) using a plate washer (Skan Washer 300, Molecular devices, Berkshire, UK) and 200 µL of blocking solution (PBS + 10% FCS) was then added for 2 hours at RT. Plates were then washed a further 3 times with PBS/Tween. 200 µL of recombinant protein standards (at known concentrations) were added to the top three wells (in triplicate), and serial dilution were made to create a 'standard curve.' In order to prevent drying, the remainder of the wells were filled with 20 µL of medium, and the stored supernatants were thawed and 80 µL added to the remainder of the wells, also in triplicate. This dilution was corrected for in the final algorithm. Following an overnight incubation at 4^0C, plates were washed six times in PBS/Tween and 100 µL of biotinylated detection antibody (see table) were added at appropriate dilutions in blocking solution for 2 hours, at RT. Following another 6 washes with PBS/Tween, 100 µL of Extravidin-alkaline phosphatase conjugate (Sigma), diluted 1:5000 with PBS/Tween was added for 1 hour at room temperature. Plates were then washed again three times with PBS/Tween and three times with ddH_2O. 100 µL of substrate solution was then added (p-nitrophenyl phosphate 1 mg/ml (Sigma) in 0.2 M TRIS Buffer (Sigma)) per well. Plates were left in the dark to develop for 30-180 minutes and placed in a multiskan EX plate reader (Thermo Fisher Scientific) at wavelength 450 nM to determine optical densities. Optical densities for each sample well are converted to a quantity of protein (pg/ml) by extrapolating from the standard curve.

Antibody	Capture	Detection	Standard (top concentration)	Type	Source
GM-CSF	1:500	1:1000	2000 pg/ml	Mouse Anti-human	Mabtech
IL-2	1:250	1:500	5000 pg/ml	Mouse Anti-human	BD Biosciences
IL-6	1:500	1:500	2000 pg/ml	Rat Anti-human	BD Biosciences
IL-8	1:500	1:500	500 pg/ml	Mouse Anti-human	BD Biosciences
IL-10	1:500	1:1000	2000 pg/ml	Rat Anti-human	BD Biosciences
IL-28	1:180	1:180	8000 pg/ml	Mouse Anti-human	R&D Systems
IL-29	1:180	1:180	4000 pg/ml	Mouse Anti-human	R&D Systems
TNFα	1:1000	1:1000	2000 pg/ml	Mouse Anti-human	BD Biosciences
VEGF	1:500	1:250	2000 pg/ml	Mouse Anti-human	R&D Systems
IFNα	1:250	1:500	5000 pg/ml	Mouse Anti-human	Mabtech
IFNγ	1:250	1:500	10,000 pg/ml	Mouse Anti-human	BD Biosciences
RANTES (CCL5)	1:250	1:500	1000 pg/ml	Mouse Anti-human	R&D Systems / Mabtech

Table 2-2 Antibodies and Standards used in ELISA

2.11 Interferon β ELISA

IFNβ production was measured using the *Verikine*™ Human IFN Beta ELISA Kit (PBL Interferon source, NJ, USA). Pre-coated 96-well plates were supplied in the kit and 50 µL of sample supernatants were added in duplicate, along with serial dilutions of recombinant protein standards. Following a 1 hour incubation at RT, plates were washed three times with the supplied Wash Buffer in a trough and 100 µL of the supplied detection antibody (diluted in the Concentrate Diluent) was added and incubated for 1 hour at RT. Following a further three washes in Wash Buffer, 100 µL of diluted Horseradish peroxidase (HRP) was added, incubated for 1 hour and washed again with Wash Buffer. 100 µL of the supplied TMB substrate was added and developed in the dark for 15 minutes, following which 100 µL stop solution was added, and optical densities read using the Multiscan EX plate reader at a wavelength of 405 nm. Optical densities for each sample well are converted to a quantity of protein (pg/ml) by extrapolating from the standard curve.

2.12 Assessment of NK cell activity

2.12.1 NK cell CD107 degranulation assay

Degranulation of NK cells within a mixed PBMC population was determined by cell-surface expression of CD107. PBMCs were isolated and cultured overnight in RPMI + 10% FCS with 0, 0.1 and 1 pfu/cell JX-594. These 'effector cells' were then cultured in FACS tubes at a 10:1 effector:target ratio with SW480, SW620 or K562 'targets' in a total volume of 400 µL at 37^{o}C for 1 hour, along with 5 µL each of anti-CD107a and anti-CD107b FITC antibodies (BD Biosciences). K562 served as a positive control. Following a one-hour incubation, 3 µL of 10 µg/ml Brefeldin A (Sigma) was added and incubation continued at 37^{o}C for a further 4 hours. Cells were washed in FACS buffer and pelleted by centrifugation at 400g for 5 minutes at RT. 3 µL anti-CD3 PerCP and 2 µL anti-CD56 PE antibodies were added to each FACS tube, and incubated at RT for 20 minutes. Cells were pelleted by centrifugation and fixed with 300 µL 1% PFA and stored at 4^{o}C prior to acquisition by flow cytometry.

2.12.2 ^{51}Chromium release assay

The cytotoxicity of NK cells within a mixed PBMC population was analysed using the ^{51}Chromium (^{51}Cr) release assay. PBMCs were isolated and cultured overnight in RPMI + 10% FCS with 0, 0.01, 0.1 and 1 pfu/cell JX-594. SW480 and SW620 tumour target cells were harvested, washed and pelleted by centrifugation and incubated with 100 µL of ^{51}Chromium at 37^{o}C for 1 hour in a 50 ml Falcon tube, taking appropriate radioactive substance handling precautions. Effector cells (PBMCs) with or without overnight pre-treatment with JX-594 were harvested, washed and pelleted and re-suspended in lymphocyte culture medium at 5x10^{6}/ml. 1x10^{6} effector cells (200 µL) were pipetted into the top wells of a 96-well round-bottomed plate (NUNC Thermo Scientific, Roskilde, Denmark) in triplicate, and diluted serially downwards to obtain effector: target ratios of 100:1, 50:1, 25:1 and

12.5:1. Following labelling, target cells were washed three times with 50 ml HBSS and re-suspended in lymphocyte culture medium at $5x10^4$ cells/ml. $5x10^3$ target cells (in 100 µL, making a total of 200 µL in each well) were added to each well. A separate plate containing no effectors was set up with 1% (*v/v*) Triton X in lymphocyte culture medium and media alone to determine maximum and spontaneous ^{51}Cr release respectively. Triton X will lyse the target cells, providing a positive reference point for maximal ^{51}Cr release. The plates were incubated at 37^oC for 4 hours, centrifuged at 400g for 5 minutes at RT and 50 µL of supernatant from each well was transferred into a Luma scintillation plate (Perkin Elmer, Warrington, Cheshire) and left to dry overnight. ^{51}Cr release was determined using a liquid 1450 Microbeta scintillation and luminescence counter (Wallack Betajet System, Perkin Elmer). The results are expressed as percent tumour lysis using the formula:

$$\% \text{ lysis} = \frac{100 \times (\text{sample cpm} - \text{spontaneous cpm})}{(\text{maximum cpm} - \text{spontaneous cpm})}$$

Where cpm = counts per minute as determined by the scintillation and luminescence counter.

2.13 Fresh liver tissue culture

Liver cancer tissue and accompanying normal liver tissue was obtained from freshly resected liver specimens immediately following surgical resection in a sterile environment in the operating theatre. Written, informed consent was obtained in accordance with institutional ethics review and approval. Tissue was placed in 'fresh tissue culture medium' for transfer; DMEM + 10% FCS with 1% Antibiotic Antimycotic Solution (10,000 units Penicillin, 10mg Streptomycin and 25µg Amphoterecin B (Sigma)). Tissue slices were made using a precision-cutting microtone (Leica, VT1000S), using 5x5 mm cubes of tissue embedded in 3% Agar. Slices were immediately placed in 2mls of the above described 'fresh tissue culture medium' in 6-well plates (Costar). Tissue cores were made using a Tru-Cut® biopsy needle (CareFusion, Surrey, UK), resulting in cores of 1mm diameter and 15mm length. In order to facilitate standardisation of tissue conditions, as well as optimal surface area for viral exposure, these 15mm cores were then divided into three 5mm-length cores and placed into three separate wells. Tissue cores were maintained in flat-bottomed 12-well plates (Costar), with 3 cores in each well in 1ml of 'fresh tissue culture medium' for up to 96 hours.

2.13.1 Validation of technique; Alamer blue

In order to ensure that these tissue cores can be used as a true '*ex vivo'* system, it was vital to ensure that the tissue retained steady metabolic activity for the duration of the incubation. AlamarBlue® is a proven indicator of cell viability [158, 159] and uses the natural reducing power of living cells to reduce resazurin (a blue, nontoxic, nonfluorescent cell permeable compound) to a fluorescent molecule, resorufin, which produces a bright red fluorescence. Viable cells continuously convert resazurin to resorufin, thereby generating a quantitative measure of viability.

During tissue processing, separate cores of tissue were obtained for assessment of tissue viability. This assay was initially performed as described in the literature; wells containing three 5 mm cores of tissue in 'fresh tissue culture medium' were set up. At specified time points 25 µL of AlamerBlue® dye (Invitrogen) was added to each well, and left to incubate for 1 hour at 37^{o}C, and 100 µL was pipetted in triplicate into a 96-well Microtitre plate (Greiner Bio One, Stonehouse, UK). The fluorescence from each well was measured using a fluorescence plate reader using 530nm excitation and 590nm emission filters. The same cores were used for the entire duration of the experiment, with fresh media replenished at each time point up to 120 hours.

In the second experimental condition, four wells containing three cores each were set up (once for each time point), with no replenishing of media. This mimicked the experimental conditions applied to all future experiments, and hence was more representative of the viability of the tissue cores following 96 hours of viral treatment.

2.14 Isolation of liver- and tumour- derived mononuclear cells

Freshly resected CRLM tumour and normal liver tissue was obtained from patients undergoing liver resection as detailed in section 2.13. Tissue was placed in a 100mmx20mm petri dish (Corning Inc., NY, USA) and disaggregated manually using a standard disposable surgical scalpel (Swann-Morton, Sheffield, UK), with or without 10 ml of 0.5 mg/ml Collagenase II (Lorne laboratories, Reading, UK). The resulting tissue was then passed through a 70 µm cell strainer (BD Biosciences) and debris removed by washing with 50 ml HBSS and centrifugation at 400 g for 5 minutes at RT. The resulting pellet was then either cultured in 'tissue culture

medium' and treated directly with JX-594-GM-CSF or a further density gradient separation step was performed. In the latter case, the pellet was re-suspended in 30 ml HBSS and layered over 15 ml of Lymphoprep© in a 50 ml Falcon tube and centrifuged at 800g for 25 minutes at RT with no brake. Liver mononuclear cells (LMCs) and tumour mononuclear cells (TMCs) were collected from the interface layer using a Pasteur pipette, washed with HBSS, centrifuged, and cultured at $2x10^6$ cells/ml of culture medium (RPMI + 10% FCS + 1% Antibiotic Antimycotic Solution).

2.15 Confocal laser scanning microscopy (CLSM)

2.15.1 Background

Although a standard fluorescent microscope would suffice to detect the fluorescence emission, the advantage of CLSM is that it enables the acquisition of high-resolution images which can be taken from selected depths within tissue, a process known as 'optical sectioning'. Reconstructed images can be displayed as three-dimensional images and the process of 'Z-stacking' achieves this by taking images at pre-set planes. Hence, fluorescence present at both the surface and within the tissue can be detected at equal intensity.

A laser beam is focussed onto the tissue via an objective lens, and any scattered and reflected laser light (as well as any inherent fluorescent light) is then re-collected by the objective lens. A system of mirrors separates off some portion of light into the detection apparatus, via a filter, which selectively passes fluorescent wavelengths into a photodetection device. Separate images of various fluorescent wavelengths can be achieved and combined (see figure 4-1). In order to provide a focal contrast for CLSM lens, and to provide a demonstration of the tissue

architecture, a nucleic acid stain is used prior to microscopy. 4',6-diamidino-2-phenylindole (DAPI) is a fluorescent stain that binds strongly to A-T rich regions in DNA. In order to ensure penetration of the dye, particularly in live cells, it may be diluted in 0.1% Triton X.

2.15.2 Method

At specified time points following infection of the tissue slices/cores with JX-594-GFP, supernatant was harvested, and the tissue fixed in 1% PFA. Prior to CLSM, nuclear staining was performed with DAPI (Invitrogen); 1% DAPI diluted in 0.1% Triton X (diluted in PBS) at RT for 45 minutes. The stain was washed off with PBS and the tissue re-suspended in 1% PFA. CLSM was preformed using a Nikon A1 Confocal Laser Scanning Microscope (Nikon, Tokyo, Japan). Settings for the lasers (DAPI, FITC) were kept as standard throughout all experiments. DAPI; HV: 110, Offset: -110, FITC; HV: 90, Offset: -17.

2.16 Statistical Analysis

Continuous data is graphically presented as mean + standard deviation (SD). P values were calculated using paired student's t-test with two-tailed distribution and the one-way or two-way Analysis of Variants (ANOVA) test with Bonferroni's multiple comparison *post-hoc* test. $p<0.05$ was regarded as significant. Statistics were performed using Graphpad Prism for Mac (v 5.0b, Graphpad Software, Inc).

Chapter 3

Results: JX-594 can replicate in and kill tumour cells and trigger inflammatory changes in the tumour microenvironment

3 JX-594 can kill tumour cells and trigger inflammatory changes in the tumour microenvironment

3.1 Introduction

The infection of a tumour cell by JX-594 leads to a series of events that eventually results in tumour cell death. The complexity of the viral genome is not fully understood, however several favourable attributes have been demonstrated which result in tumour-specific toxicity, as described in detail in section 1.3. As previously discussed, associated with viral killing is the potential induction of an inflammatory tumour microenvironment, which promotes the recruitment of immune cells and may result in the subsequent induction of anti-tumour memory. This chapter describes studies to investigate the direct cytotoxicity of JX-594 against CRC cell lines, and the induction of a cytokine/chemokine response. Cytokines/chemokines analysed and a summary of their functions are outlined in table 3-1.

Cytokine/ Chemokine	Main Source	Function
IL-6	Th2 T-cells and macrophages	Activation of lymphocytes, differentiation of B cells, stimulating production of acute-phase proteins
IL-8	T-cells and macrophages	Chemotaxis of neutrophils, basophils and T cells
IL-10	Monocytes and lymphocytes	Inhibiting synthesis of pro-inflammatory cytokines, and impairs proliferation of lymphocytes
CCL5	CD8+ T cells	Chemotactic for T cells, eosinophils, and basophils, and recruits leukocytes into inflammatory sites.
VEGF	Rapidly differentiating cells	Stimulates vasculogenesis and angiogenesis
GM-CSF	T-cells, macrophages, NK cells, and B-cells	Promotion of the growth of granulocytes and macrophages
IFNα	Virally infected cells, NK cells, B-cells and T-cells, pDCs (maximal IFNα), macrophages, fibroblasts, endothelial cells, osteoblasts	Resistance to virus, and activation of lymphocytes with NK and T cell phenotype.
IFNβ		Resistance to virus
IL-28	Virally infected cells	Induces an anti-viral state in response to viral particles

Table 3-1 Cytokines/chemokines involved in the inflammatory response

Table shows the cytokines/chemokines involved in the inflammatory response that are studied in this chapter.

3.2 JX-594 infection results in tumour cell death

To investigate the direct lytic potential of JX-594 in an *in vitro* system, the cytotoxicity of JX-594 against tumour cell lines was investigated. The CRC cell lines HCT116, LoVo, SW480 and SW620 were infected with JX-594-GM-CSF, at concentrations of 0, 0.1, 1 and 10 pfu/cell for 24, 48, 72 and 96 hours. At specified time points, cells were harvested and percentage cell viability was determined using MTT and a Live/Dead® discrimination kit. Figure 3-1 illustrates tumour cell viability following JX-594 infection as demonstrated by the MTT assay. All cell lines were susceptible to JX-594 induced death, although a variation in sensitivity was evident, with the HCT116 and SW620 cell lines being more resistant to the lytic effects of the virus than LoVo and SW480. In HCT116 cells, a significant decrease in viability was only evident after 96 hours p.i., and only with 10pfu/cell JX-594. In SW620 cells, significant decrease in viability was evident after 72 hours p.i., and again, only following 10pfu/cell JX-594 treatment. In contrast to HCT116 and SW620 cells, LoVo cells showed a significant reduction in metabolic activity by MTT assay by 48 hours, and following treatment with 10 pfu/cell. By 96 hours of treatment, a reduction in viability was observed with both 1 pfu/cell and 10 pfu/cell treatment. SW480 cells showed similar susceptibility to LoVo cells.

To confirm that loss of metabolic activity was a result of cell death, the Live/Dead® assay was performed (figure 3-2). In HCT116 cells, a significant ($p<0.05$) reduction in viability compared to untreated cells was evident only after 72 hours of treatment, and only with 10pfu/cell JX-594. There was a significant difference in viability of HCT116 cells treated with 1 and 10 pfu/cell JX-594 at 96 hours post-infection (p.i.). In SW620 cells, a similar pattern was observed, with significant reduction in viability following treatment with only 10 pfu/cell JX-594 for at least 72 hours. In contrast to HCT116 and SW620, significant reduction in viability of LoVo cells compared to

untreated control was observed by 72 hours and 96 hours p.i., with both 1 pfu/cell and 10 pfu/cell treatment, with a significant improvement in killing with escalating doses of virus (1 pfu/cell vs 10 pfu/cell). SW480 cells showed similar susceptibility to LoVo cells; following 96 hours of treatment, a reduction in viability was observed with both 1 pfu/cell and 10 pfu/cell JX-594. The cytopathic effect of JX-594 on SW480 and SW620 cells is depicted in photomicrographs in figure 3-3. It is interesting to note that HCT116 and SW620 cell lines were less susceptible to viral killing, and these were observed to grow more rapidly in culture compared to LoVo and SW480 cell lines, as observed by the differing split ratios required when passaging these cells in culture.

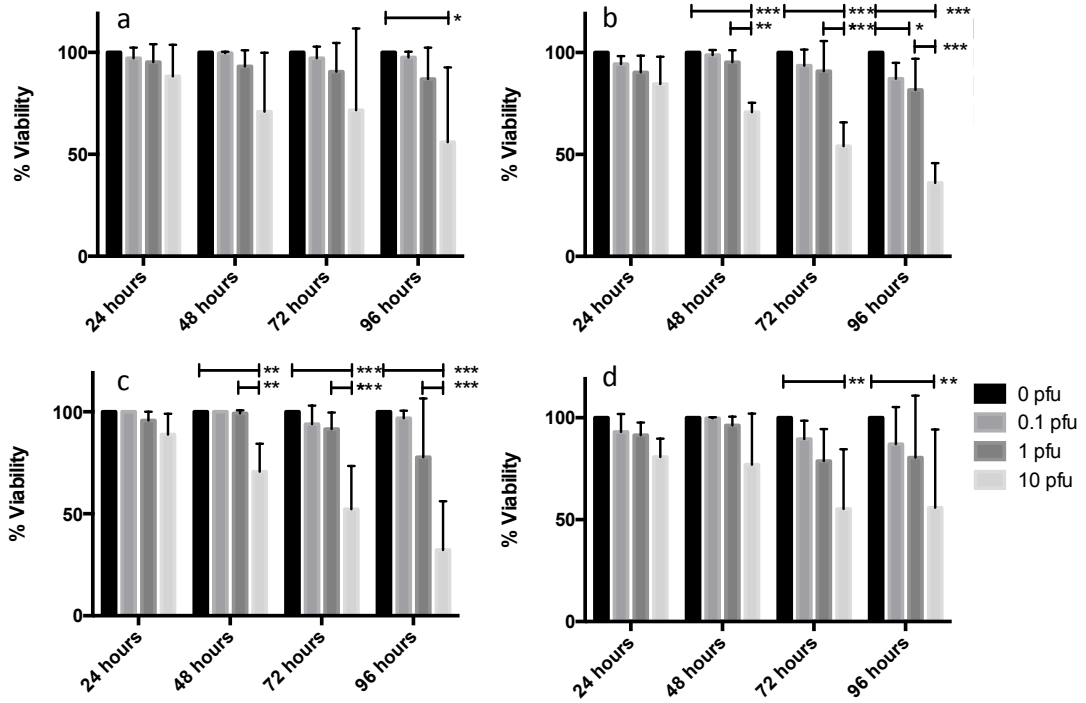

Figure 3-1. Susceptibility of CRC cell lines to JX-594-mediated death by MTT assay

CRC cell lines a) HCT116 b) LoVo, c) SW480 and d) SW620 were seeded at 8 x 10^3 cells per well in a 96-well plate and infected with JX-594 at concentrations of 0, 0.1, 1 and 10 pfu/cell overnight. At appropriate time points post infection, MTT was added for 4 hours and DMSO used to solubilise the cells. Absorbance was measured and % viability was calculated relative to untreated cells. All experiments were performed in triplicate (N=3), and bars show the mean + SD. * indicate significant reduction in viability; *p<0.05, ** p<0.01, ***p<0.001.

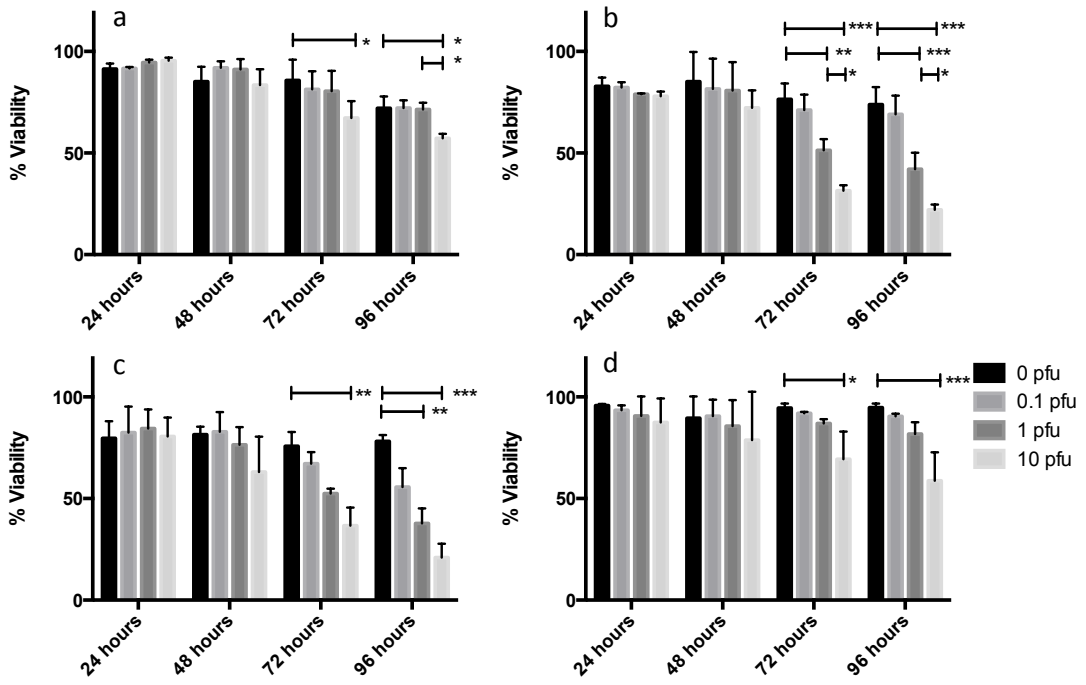

Figure 3-2. Susceptibility of CRC cell lines to JX-594-mediated death by Live/Dead® assay

CRC cell lines a) HCT116 b) LoVo, c) SW480 and d) SW620 were seeded at 2 x 10^5 cells per well in a 6-well plate and infected with JX-594 at concentrations of 0, 0.1, 1 and 10 pfu/cell. Cells were subsequently harvested and stained with a red fluorescent dye (Live/Dead® kit) and fixed. Fluorescence, and hence the viability, of the cells was evaluated by flow cytometry. All experiments were performed in triplicate (N=3) and bars show the mean + SD. * indicate significant reduction in viability; *p<0.05, ** p<0.005, ***p<0.001.

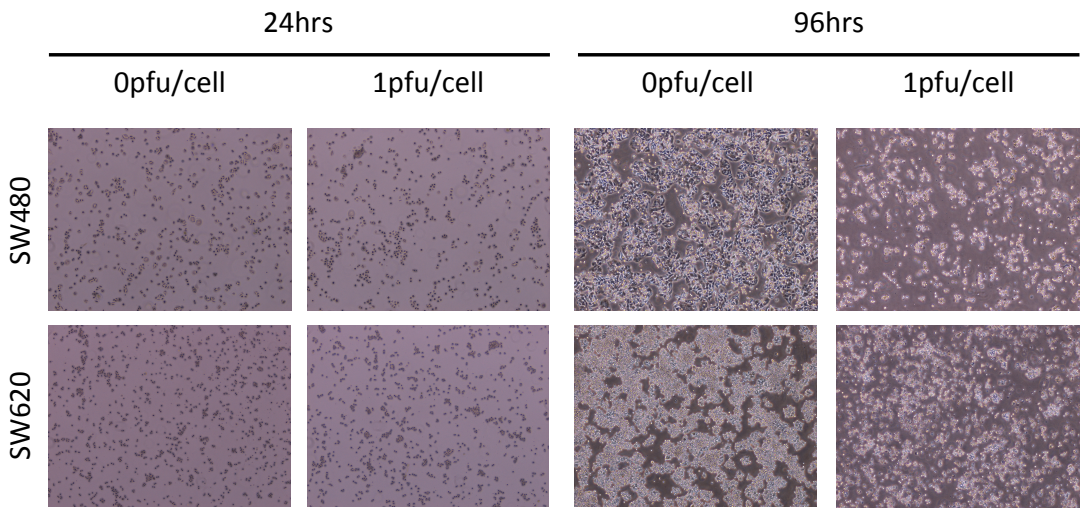

Figure 3-3. JX-594 kills and retards proliferation of CRC cell lines

SW480 and SW620 cells were seeded at 2 x 10^5 cells in a 6-well plate, and were treated with 0pfu and 1pfu/cell JX-594 and photos were taken at 24 and 96 hours at 40x magnification, against white light. SW480s were split at a 1:4 ratio and SW620s at a 1:6 ratio to achieve confluence within 3 days in culture.

3.3 JX-594 Activates Caspase-3 in CRC Cell Lines

To investigate the mechanism by which JX-594 kills CRC cell lines, SW480 and SW620 cells were infected with varying concentrations of JX-594-GM-CSF (0, 0.01, 0.1 and 1 pfu/cell) for 24, 48, 72 and 96 hours, and expression of active Caspase-3 was determined by flow cytometry using an Active Caspase-3 Apoptosis Kit (section 2.8.3). Figure 3-4 demonstrates that an increase in 1) the percentage of cells expressing active caspase-3 (a and c) and 2) the mean fluorescence intensity (b and d) was observed in both cell lines, with an average of 65% of SW480 cells and 35% of SW620 cells expressing active caspase-3 by 96 hours, following treatment with 1 pfu/cell JX-594. Hence, the results indicate that JX-594 induces cell death by activation of caspase-3 and apoptosis mediated pathways. In keeping with the susceptibility to viral killing, SW480 cells expressed more active caspase-3, and hence higher levels of apoptosis.

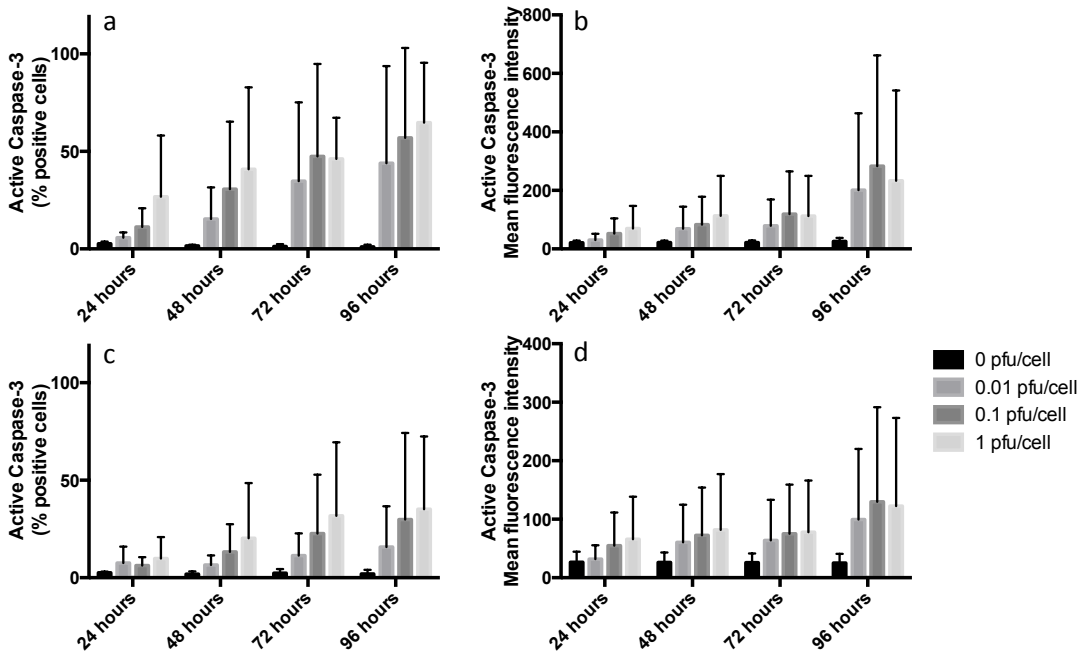

Figure 3-4. JX-594 activates Caspase-3 in CRC cell lines

SW480 (a and b) and SW620 (c and d) CRC cell lines were seeded at 2 x 10^5 in 6-well plates and treated with JX-594 at 0, 0.01, 0.1, and 1 pfu/cell for 24, 48, 72 and 96 hours. Cells were harvested and active caspase-3 production measured using a PE-conjugated Active Caspase-3 Apoptosis Kit and flow cytometry. All experiments were performed in triplicate (N=3) and error bars show the mean + SD. Data is expressed as % cells expressing active caspase-3 (a and c) and mean fluorescence intensity (b and d) of PE anti-caspase-3 fluorophore as detected by flow cytometry.

3.4 Vaccinia replicates effectively in tumour cell lines

3.4.1 JX-594 replication demonstrated by plaque assay

To examine viral replication, SW480 and SW620 CRC cell lines were infected with 0.1 pfu/cell and 1 pfu/cell JX-594. Initially, samples were harvested at four time points post infection (24, 48, 72 and 96 hours) and fold increase in viral replication over time as demonstrated by plaque assay is shown in Figure 3-5. JX-594 replicated in SW480 and SW620, with an increased replication efficiency in the more susceptible cell line, SW480, compared to the more rapidly diving cell line, SW620. Increased replication was seen in the samples infected with 0.1 pfu/cell compared with 1 pfu/cell. A time-dependant increase in viral replication was observed with 0.1 pfu. In contrast, a reduction in fold replication at 96 hours was observed in samples infected with 1 pfu/cell. As the most efficient fold-replication was noted to be following infection with 0.1pfu/cell of JX-594, the remainder of experiments (total N=5) were performed in these conditions. As depicted in figure 3-6, these data confirm an improved replication efficiency in the SW480 cells (mean 216-fold), compared to SW620 (150-fold) correlating with the increased cytotoxicity observed in SW480 cells.

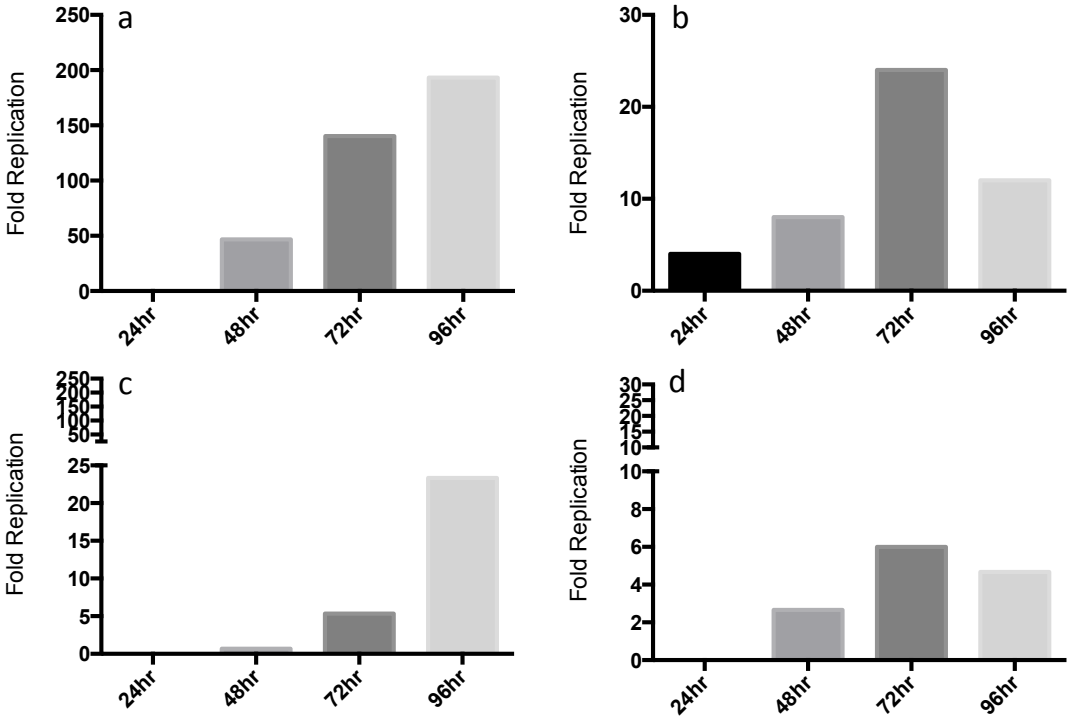

Figure 3-5 JX-594 Replication in SW480 and SW620 cells at 1 and 0.1pfu/cell

2 x 10^5 SW480 (a and b) and SW620 (c and d) cells were adhered onto a 6-well plate with tissue culture medium. 0.1 pfu/cell (a and c) or 1 pfu/cell (b and d) of JX-594 was added and cells and supernatant harvested at specified time points, and frozen, and subjected to 3 rounds of freeze/thaw. A plaque assay was used to asses fold replication. Figure shows the results of a single experiment.

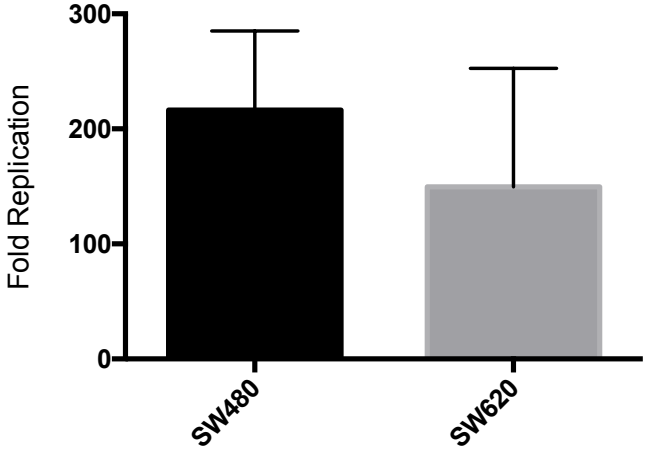

Figure 3-6 JX-594 replication at 0.1pfu/cell at 72 hours

SW480 and SW620 cell lines were infected with JX594 at 0.1 pfu/cell for 72 hours. Cells and supernatant were harvested and subjected to 3 rounds of freeze/thaw. Plaque assay was used to determine virus concentration and hence fold replication compared with input virus. Data is presented as mean fold replication + SD.

3.4.2 Enhanced surface expression of EGFR in SW480 cells may explain enhanced replication

Amongst a plethora of yet-to-be fully-characterised proteins, the vaccinia genome encodes for VGF, which is an EGF analogue. The early-phase production of VGF from JX-594 will bind to EGFR and enhance the environment of the cell for vaccinia replication. To examine the potential mechanisms behind enhanced JX-594 replication in SW480 cells, the surface expression of EGFR was determined. 2 x 10^5 SW480 and SW620 cells were maintained in culture medium up to 96 hours and harvested and incubated with an EGFR-PE antibody for 20 minutes. Figure 3-7 shows that EGFR is expressed on the surface of SW480 cells, but not SW620 cells. Hence, in SW480 cells it is possible that VGF binding to EGFR may facilitate increased JX-594 replication in these cells.

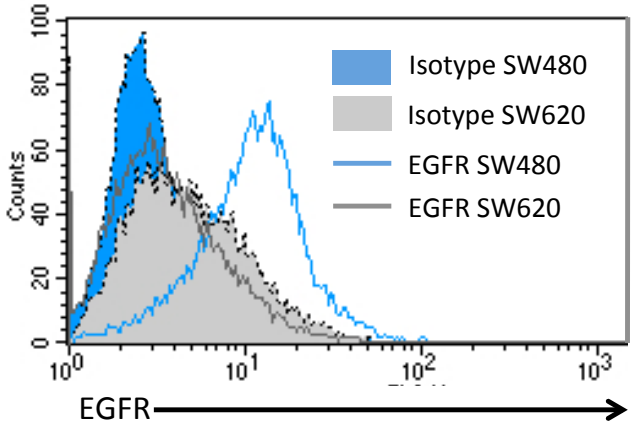

Figure 3-7. EGFR expression in SW480 and SW620 cells

2 x 10^5 SW480 and SW620 cells were cultured in 6-well plates for 96 hours in culture medium. Cells were harvested and surface expression of EGFR determined by flow cytometry using an EGFR-PE antibody.

3.4.3 JX-594 replication demonstrated by Green Fluorescent Protein (GFP) expression

The insertion of GFP into the disrupted TK locus of the vaccinia genome may be exploited to examine the potential replication efficiency of the virus. GFP is expressed under the control of an early/late promoter, hence small quantities of GFP may be transcribed as the virus enters the cell and takes over the cell machinery, and further transcription may take place at the late stage of viral replication. In order to further examine and understand JX-594 replication, SW480 and SW620 cells were treated with varying concentrations of JX-594-GFP; 0, 0.01, 0.1 and 1 pfu/cell for 24 - 96 hours. At specified time points, cells were harvested and fixed in 1% PFA, and GFP expression examined by flow cytometry (FITC). A viral dose- and time-dependant increase in GFP production was seen as shown in figure 3-8. Flow cytometry reveals earlier GFP expression in SW480, which is similar to the findings of the plaque assay where, following 1 pfu/cell JX-594 infection, plaques were visible at 24 hours in the SW480 samples (figure 3-5 b), and only at 48 hours in the SW620 samples (figure 3-5 d). In both cell lines, following 72 hours infection with JX-594-GFP, the % cells positive for GFP expression plateaued, and thus figures 3-8 c) and d) depict a comparison of both cells lines at 72 hours p.i. There is an increase in the mean fluorescence and hence the quantity of GFP protein expression in SW480 cells (significant increase at 1 pfu/cell treatment) compared to SW620 cells, potentially inferring an increased number of replicating viral particles.

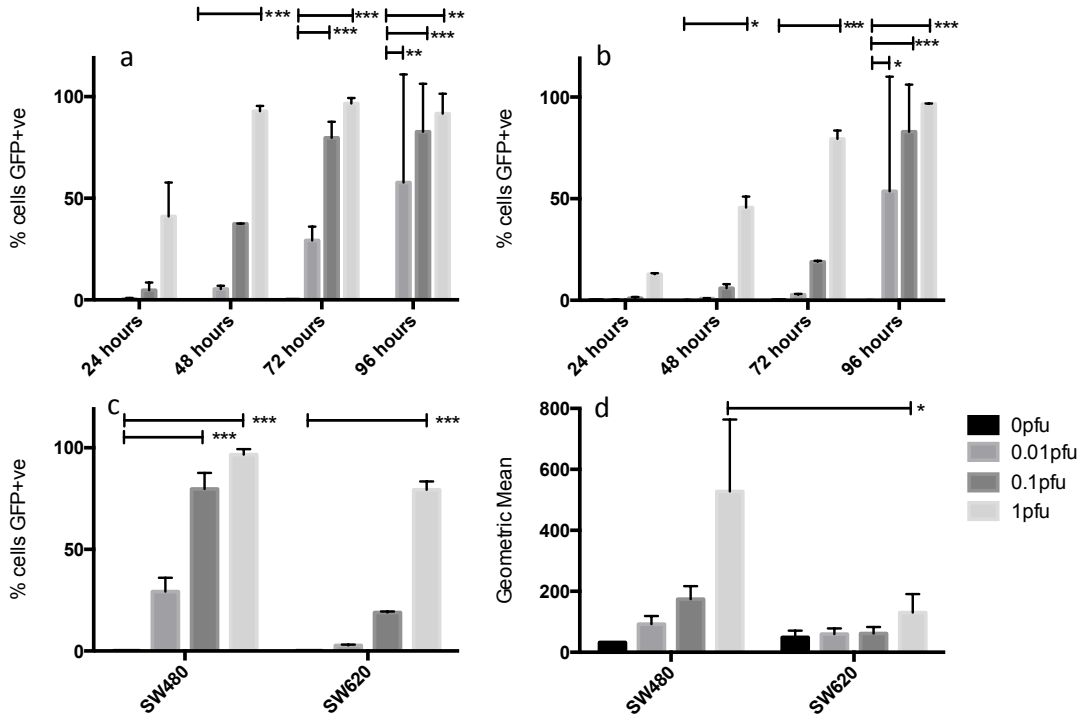

Figure 3-8 JX-594 replication in CRC cell lines as demonstrated by GFP expression

Figure demonstrates an increase in GFP expression as % cells expressing GFP (a, b and c) and the geometric mean of the fluorescence intensity (d) in SW480 (a) and SW620 cells (b). For comparison, GFP expression as % positive cells (c) and geometric mean (d) at 72 hours in both cell lines is plotted. 2 x 10^5 cells were adhered onto a 6-well plate in 2ml of medium and infected with JX-594-GFP and cells harvested, pelleted and fixed with 1% PFA at specified time points. The fluorescence intensity (FITC) was determined by FACS analysis. All experiments were performed in triplicate (N=3) and bars show the mean + SD. * indicate significant increase in viability; *p<0.05, **p<0.01, ***p<0.0001

3.4.4 GFP demonstration by confocal laser scanning microscopy

CLSM allows further demonstration of the replication ability of JX-594 as inferred by GFP production. Figure 3-9 shows GFP production in SW480 (a) and SW620 (b) CRC cell lines respectively. This further demonstrates the difference in replication due to the quantity of green fluorescence in the cells in the photographed field. At both 24 and 48 hours p.i., increased GFP expression is seen in the SW480 cells (figure 4-4 a) as compared to SW620 (figure 4-4 b). By 72 hours (SW480) and 96 hours (SW620) the images also show the resulting death of the tumour cells. The substantial increase in GFP fluorescence between 48 and 72 hours is in keeping with the replication cycle of the virus as detailed in section 1.3, and is the point in which viral progeny will escape from the lysed cell and begin to infect surrounding cells.

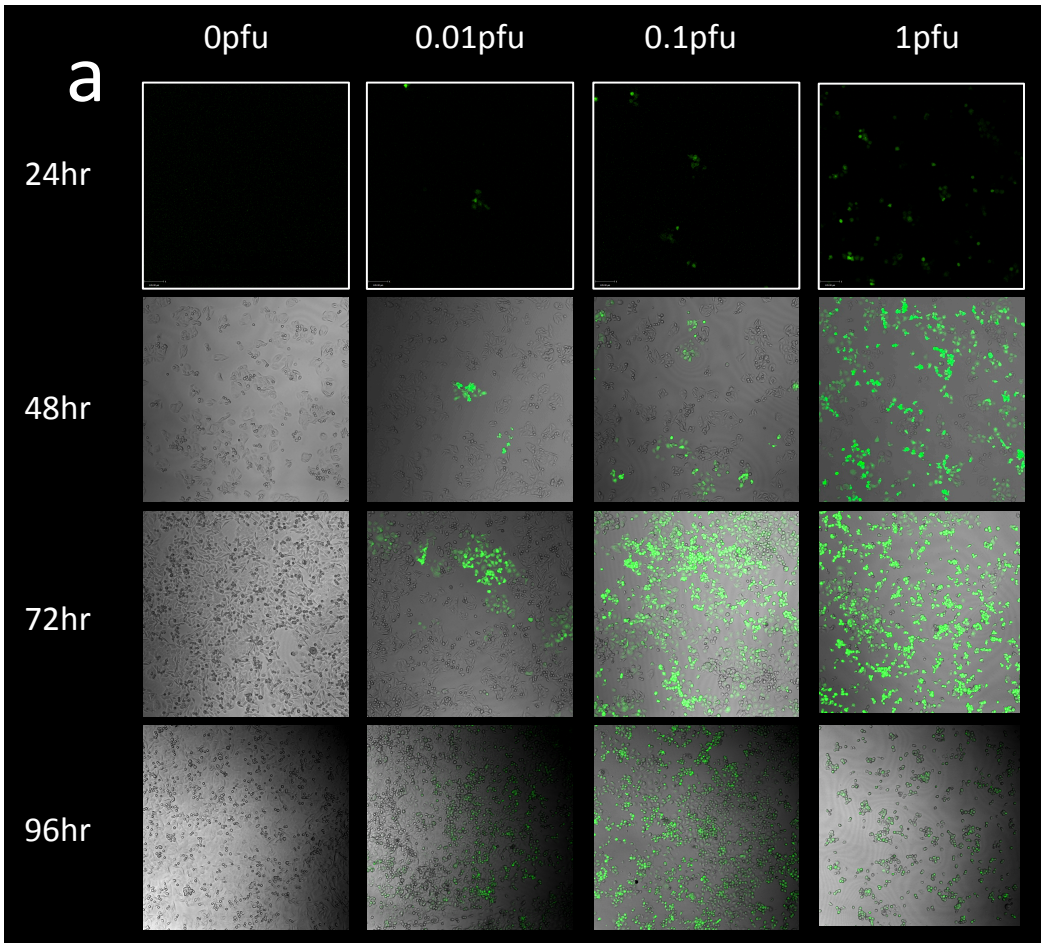
a
0pfu
0.01pfu
0.1pfu
1pfu
24hr
48hr
72hr
96hr

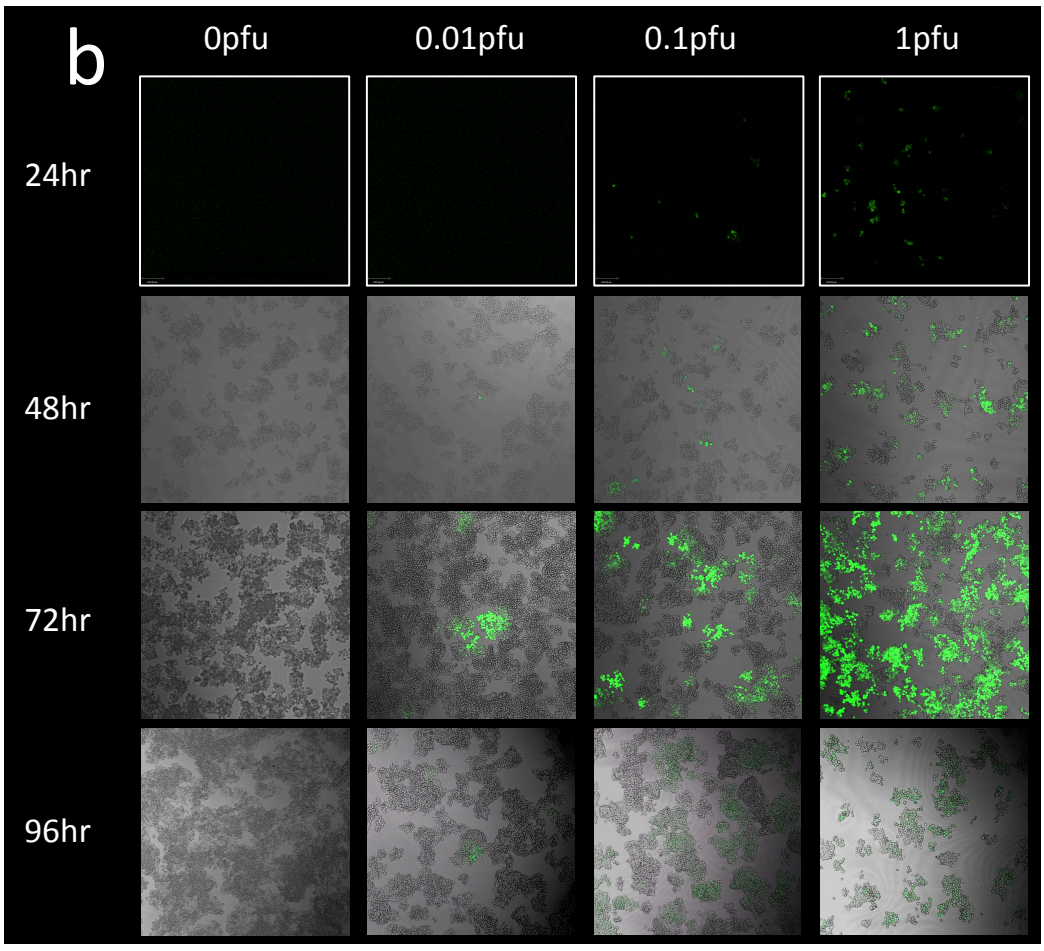
b
0pfu
0.01pfu
0.1pfu
1pfu
24hr
48hr
72hr
96hr

Figure 3-9. CLSM images showing GFP expression by JX-594-GFP replicating in SW620 CRC cell line

(Figure on previous page) 2 x 10^5 SW480 and SW620 cells were adhered onto a 6-well plate and infected with JX-594-GFP at 0, 0.01, 0.1 and 1 pfu/cell. At specified time points, growth medium was removed and cells were fixed in 1% PFA and photographed using confocal laser scanning microscopy with dual phase to depict tumour cells and GFP.

3.5 The induction of an inflammatory tumour microenvironment by JX-594; cytokine and chemokine profiles.

Once the ability of JX-594 to kill CRC cell lines by apoptosis had been determined, the induction of virally-expressed and other chemokines and cytokines by infected tumour cells was investigated. GM-CSF is cytokine that stimulates stem cells to produce granulocytes (neutrophils, eosinophils, and basophils) and monocytes. It also serves as a chemotactic cytokine (chemokine), attracting immune cells. HCT116, LoVo, SW480 and SW620 CRC cell lines were infected with varying concentrations of JX-594-GM-CSF, at concentrations of 0, 0.01, 0.1, 1 and 10 pfu/cell for 24, 48, 72 and 96 hours. At specified time points, cell-free supernatant was collected and expression of GM-CSF from virally-infected cell lines was determined by ELISA. GM-CSF was expressed in a dose/time responsive manner (see Figure 3-10), with significant increase from untreated controls by 48 hours p.i. in all four cell lines. At 72 hours, similar quantities of GM-CSF were detected in all four cell lines (~2000 pg/ml). By 96 hours p.i., there was a reduction in GM-CSF production at 10 pfu/cell JX-594, with a significant decrease in GM-CSF production following treatment with 10 pfu/cell JX-594 compared to 0.01 pfu/cell (SW480) and 0.1 pfu/cell (HCT116).

Vascular endothelial growth factor (VEGF) is a signal protein produced by cells that stimulates the growth of new vessels (vasculogenesis) and the propagation of existing vessels (angiogenesis), and is expressed early in the progression of colorectal cancer [160]. The faster growing HCT116 and SW620 cell lines produced higher levels of VEGF in culture by 96 hours (untreated control); 1395 pg/ml and 1249 pg/ml respectively. Figure 3-11 illustrates that JX-594 treatment induced a significant down-regulation of VEGF production from all four cell lines following 96 hours of treatment.

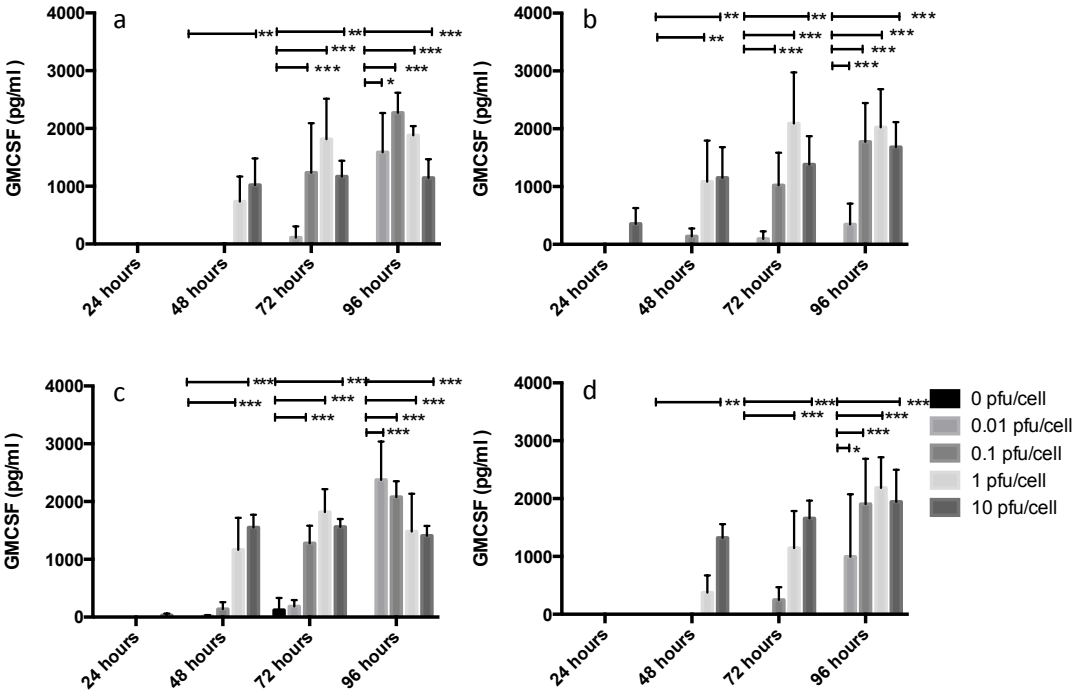

Figure 3-10. GM-CSF production in CRC cell lines treated with JX-594

CRC cell lines, HCT116 (a), LOVO (b), SW480 (c) and SW620 (d) were seeded at 2 x 10^5 in 6-well plates and treated with JX-594 at 0, 0.01, 0.1, 1 and 10 pfu/cell for 24, 48, 72 and 96 hours. Supernatant was collected and GM-CSF production measured by ELISA. All experiments were performed in triplicate (N=3) and bars show the mean + SD. * indicate significant increase/decrease in GM-CSF; *p<0.05, ** p<0.001, ***p<0.0001 (only relevant statistics bars are included).

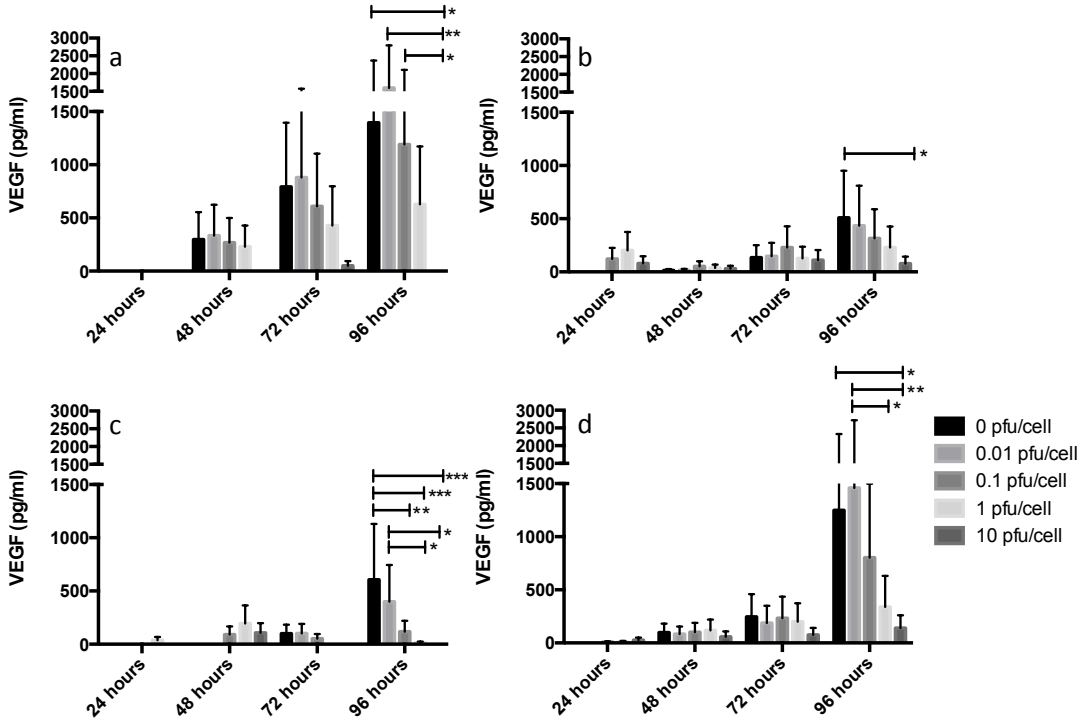

Figure 3-11. VEGF production in CRC cell lines treated with JX-594

CRC cell lines, HCT116 (a), LOVO (b), SW480 (c) and SW620 (d) were seeded at 2 x 10^5 in 6-well plates and treated with JX-594 at 0, 0.01, 0.1, 1 and 10 pfu/cell for 24, 48, 72 and 96 hours. Supernatants were collected and VEGF production determined by ELISA. All experiments were performed in triplicate (N=3) and bars show the mean + SD. * indicate significant decrease in VEGF levels; *p<0.05, ** p<0.01, ***p<0.005.

To assess the induction of a pro-inflammatory tumour micro-environment, IL-6, IL-8, IL-10, CCL5, IFNα, IFNβ and IL-28β production by JX594-infected CRC cell lines was investigated. IL-6 is a pro-inflammatory cytokine and IL-10 is considered to be immunosuppressive, as it inhibits synthesis of pro-inflammatory cytokines, immune priming and T-cell proliferation [161]. IL-6 was produced from all four CRC cell lines, with no significant increase/decrease with time in the untreated controls. There was a general increase in IL-6 in the supernatants of all four CRC cell lines following treatment with JX-594 (data not shown), a finding which was more pronounced in the HCT116 and SW480 cell lines; however, a statistically significant increase was only evident in these cell lines following treatment with 10 pfu/cell of JX-594 for 48 hours.

IL-10 was produced by all four CRC cell lines in the absence of JX-594, with a general increase seen in the LoVo, SW480 and SW620 cell lines with time (see Figure 3-12 for SW480 and SW620 data). Only the SW480 cell line showed a significant increase in IL-10 production in culture with time in the untreated cells, and there was a significant decrease with JX-594 treatment compared to untreated control at 72 hours p.i. (vs 1 and 10 pfu/cell) and 96 hours p.i. (vs 0.01, 0.1, 1 and 10 pfu/cell). In the SW620 cell line, JX-594 treatment only induced significant reduction in IL-10 in the supernatant following 96 hours of treatment (0 vs 10 pfu/cell).

CCL5 (Regulated on Activation, Normal T Cell Expressed and Secreted; RANTES) is chemotactic for T cells, eosinophils, and basophils, and recruits these leukocytes into inflammatory sites; it also induces the proliferation and activation of certain NK cells. There was no dose/time response observed following JX-594 treatment of all four CRC cell lines with JX-594 (data not shown). Similarly to CCL5, there was no

observed dose/time response in the production of IFNα, IFNβ, or IL-28β from CRC cell lines following treatment with JX-594 (data not shown). IFNα and IFNβ are type I interferons and IL-28β is a type III interferon; these are all involved in the immune defence against viruses. As type I interferons may be produced early in response to viral infection, supernatants were also collected at 6 hours p.i., but again no induction of interferons by JX-594 was seen (see table 3-2).

JX-594 treatment of the four CRC cell lines resulted in a variable IL-8 response (see figure 3-13). In the more aggressive cell lines, HCT and SW620, there was an increase in IL-8 production in the supernantant of the untreated cells with time, and after 96 hours of treatment, there was a dose-dependant decrease in IL-8, which was only significant in HCT116 cells (0 vs 10 pfu/cell and 0.01 vs 10 pfu/cell). The converse was true for the LoVo cell line – after 96 hours of JX-594 treatment, there was a significant increase in IL-8 production with up to a dose of 1 pfu/cell, following which there was a significant decrease with 10 pfu/cell treatment.

Overall, JX-594 treatment of CRC was observed to result in a pro-inflammatory and anti-angiogenic tumour microenvironments, with an increase in GM-CSF and IL-6 and a decrease in IL-10 and VEGF (see table 3-2 for data summary).

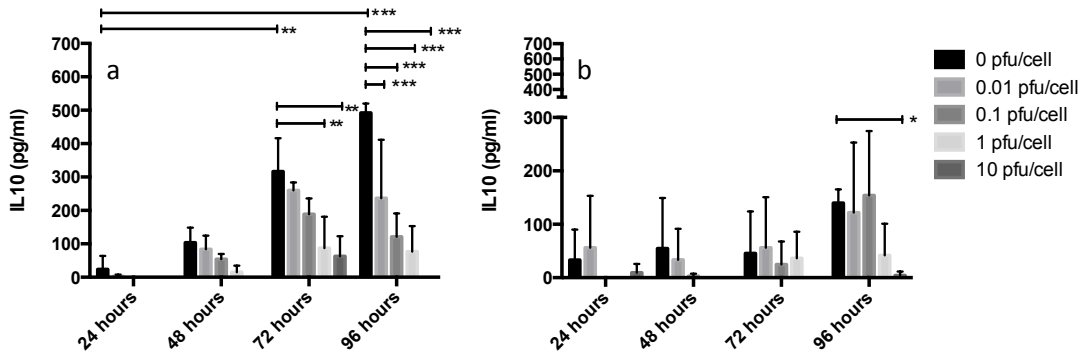

Figure 3-12. IL-10 production in CRC cell lines treated with JX-594

CRC cell lines, SW480 (a) and SW620 (b) were seeded at 2 x 10^5 in 6-well plates and treated with JX-594 at 0, 0.01, 0.1, and 1 pfu/cell for 24, 48, 72 and 96 hours. Supernatant was collected and IL-10 production measured by ELISA. All experiments were performed in triplicate (N=3) and bars show the mean + SD. * indicate significant increase/decrease in IL-10 production; *p<0.05, ** p<0.005, ***p<0.0001.

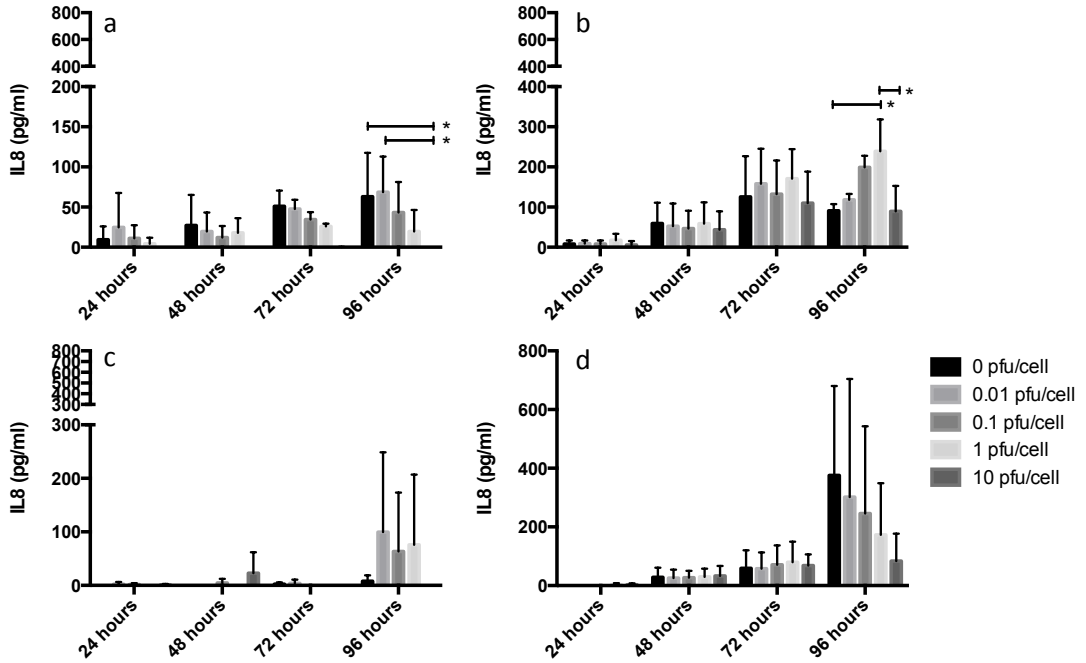

Figure 3-13. IL-8 production in CRC cell lines treated with JX-594

CRC cell lines, HCT (a), LOVO (b), SW480 (c) and SW620 (d) were seeded at 2 x 10^5 in 6-well plates and treated with JX-594 at 0, 0.01, 0.1, and 1 pfu/cell for 24, 48, 72 and 96 hours. Supernatants were collected and IL-8 production measured by ELISA. All experiments were performed in triplicate (N=3) and bars show the mean + SD. * indicate significant increase/decrease in IL-8 production (p<0.05)

	Effect upon infection of CRC cell lines with JX-594	
	Early (< 48 hours)	Late (48 – 96 hours)
GM-CSF	↑*	↑* (dose dependant decrease at 96 hours)
VEGF	↔	↓*
IL-6	↑*	↑
IL-8	↔	↓(HCT, SW620) ↑(LoVo)
IL-10	↓ (SW480, SW620)	↓*(SW480, SW620)
IL-28	↔	↔
CCL5 (RANTES)	↔	↔
IFNα[¶]	↔	-
IFNβ[¶]	↔	-

Table 3-2. Summary of cytokine and chemokine profile following treatment of CRC cell lines with JX594

Table summarises the overall cytokine profile of CRC cell lines infected with JX-594. All experiments were carried out in triplicate.

* Significant ($p<0.05$)

[¶] Supernatant also collected at 6 hours

3.6 Discussion

In the development of an anti-cancer therapy, the primary outcome is that of direct tumour cell lysis. The results displayed in this chapter demonstrate the ability of JX-594 to kill tumour cell lines. There was an observed variability in the growth patterns and sensitivity of the CRC cell lines investigated; both HCT116 and SW620 cell lines were observed to grow more rapidly in culture compared to LoVo and SW480 cell lines, and were less susceptible to viral killing. This is particularly interesting in the context of the SW480 and SW620 cell lines, which are derived from the same patient (51-yr old Caucasian male); SW480 from the primary tumour and SW620 from a secondary lymph node metastatic deposit. Interestingly, there were observed differences in cell viability using the MTT and Live/Dead® assay, which assess different mechanisms of the loss of cell viability; loss of metabolic activity by the MTT assay and loss of cell membrane integrity (presumably, at the point of viral exit from the cell) by the Live/Dead® assay. Both cell lines were found to significantly lose membrane integrity by 72 hours (Live/Dead® assay) which conforms with the life cycle and host-cell interaction of JX-594; however, the slower proliferating cell line (SW480) demonstrated a significant reduction in metabolic activity (MTT) by 48 hours, which was earlier than the faster growing SW620 cell line, which had significant reduction in viability by 72 hours only. The likely explanation of this difference is that in the SW620 cell line, the non-virally infected cells proliferate faster, maintaining a larger number of viable cells with preserved metabolism, leading to a higher metabolic activity of the cell population as a whole.

Similar results have been published in the literature. Lun *et al*. showed that JX-594 was effective against killing of malignant glioma cell lines, with about 10% viability in four out of five cell lines by 72 hours at an MOI of 10 [162]. In addition to this, they also demonstrated greater efficacy and broader spectrum of activity of JX-594

versus other oncolytic viruses such as VSV and Reovirus. Heo *et al*. demonstrated JX-594 mediated killing in HCC cell lines HepG2, SNU423, SNU475, SNU449, and PLC/PRF/5 [134]. Similarly, and more recently, Parato *et al*. demonstrated effective JX-594 mediated killing against a wide panel of tumour cell lines; colorectal, ovarian, kidney, breast, brain, prostate, non-small cell lung cancers, melanoma and leukaemia. They reported ED50 (the initial virus MOI to achieve 50% cell killing compared to untreated control) after 72 hours of treatment in SW620 and HCT116 cell lines to be approximately 1 pfu/cell for both. This is marginally higher than the levels of killing presented in this chapter. In the same study, they also demonstrated killing of tumour initiating cells (TICs) of colorectal and lung origin [163]. This is a significant finding, as TICs are notorious for resistance to many conventional cancer therapies [164].

As discussed in section 3.3, the activation of caspase-3 following JX-594 infection demonstrates that JX-594 promotes apoptosis. Caspases are involved in the transduction of a 'kill' signal, and ultimately in the destruction of various cellular protein targets [165]. Liskova *et al*. used a WR vaccinia strain to infect HeLa G (human cervical carcinoma) and BSC-40 (African green monkey kidney cells). Using a cell-based flow cytometric assay, they showed a activation of caspase-2, 3 and 4 in both cell lines after JX-594 treatment, which was inhibited following treatment with a pan-caspase inhibitor (Z-VAD) [166]. However, they also argue that, although vaccinia can initiate the apoptotic program, apoptosis was not completed and switched into necrosis, as there was no observed vaccinia-induced cleavage of poly ADP-ribose polymerase (PARP), another classical hallmark of apoptosis [167]. The loss of membrane integrity as demonstrated by the Live/Dead® assay, may suggest the development of necrosis, however, *in vitro*, apoptotic cells will proceed to 'late apoptosis', alternatively referred to as 'secondary necrosis'. Although activation of the executioner caspase-3 was evident,

the mechanism of viral exit from the cell following replication by exocytosis or membrane disruption [168] suggests a double-pronged attack by JX-594 (apoptosis and necrosis), which is important in the initiation of an inflammatory reaction. *In vivo*, apoptotic cells would not release their cellular constituents into the surrounding interstitial tissue as they are quickly phagocytosed by surrounding immune cells [169]. In contrast, the disruption of the membrane by viral exit may result in shedding of danger signals, and tumour associated antigens which can bolster an adaptive anti-tumour immune response.

The cytotoxic effects of other oncolytic viruses against CRC cell lines have been studied *in vitro*. Kooby *et al*. demonstrated cell survival ranging between 10 - 75% after 96 hours of treatment with G207, a multi-mutated herpes virus, against a panel of 5 CRC cell lines; C18, C29, C85, C86 and HCT8 [170]. Using a vesicular stomatitis virus (M51R), Stewart *et al*. demonstrated 20% viability of HCT116 cells following 48 hours of treatment at an MOI of 1, and in LoVo cells, 80% viability [171]. Adair *et al*. demonstrated reovirus induced cytotoxicity in a panel of four CRC cell lines; LoVo, LS174T, SW480 and SW620, and showed significant death compared to untreated control following 24 hours treatment with 1 pfu/cell. By 72 hours, >80% killing was evident in SW480 and Lovo cell lines, and 40% death in SW620 [172]. Thus, in comparison to other OVs, JX-594 may have a slower, steadier cytotoxicity rather than a rapidly-ablative tumour cell destruction as demonstrated by these studies.

The slower JX-594-mediated cytotoxicity detailed in this chapter may have beneficial consequences. It allows time for the induction of an inflammatory process and immunogenic activation of the tumour microenvironment, allowing for induction of therapeutically beneficial cytokines, some of which may be chemo-attractant to

immune effector cells. The steady tumour killing induced by JX-594 is particularly beneficial in the context of virally-encoded proteins such as GM-CSF. The results in section 3.4 show that maximal GM-CSF production occurred at 96 hours, and this decreased at higher doses of virus, when less viable cells were available for viral replication and hence cytokine production. Hence, a slower death may allow for greater production of replication-dependant virally-encoded proteins, further supporting JX-594 as a vector for optimal therapy.

The differences in susceptibility of the SW480 and SW620 cell lines may be explained by the ability of JX-594 to replicate within these tumour cell lines. Plaque assays have shown replication to be more efficient in the SW480 cell line. This may be explained by the difference in tumour cell biology of SW480 and SW620 affecting the ability of JX-594 to either infect or replicate within these tumour cells. The finding of surface EGFR expression on SW480 cells may explain the susceptibility of this cell line to viral killing and replication. This variable expression of EGFR has also been published by Dahan *et al*.; no EGFR expression was detected in SW620 cells, while SW480 cells showed an EGFR-positive expression by immunoblot. However, both cell lines are K-Ras mutant [173]. Parato *et al*. have demonstrated that killing of lung and colon tumour initiating cell lines by JX-594 (JX-594-GFP+/β-gal−) is dependant on replicative ability, which is in turn dependent on EGFR/Ras/MAPK (mitogen-activated protein kinase) pathway signalling. SW620 and HCT116 CRC cell lines (both K-Ras mutant) were pre-treated for 2 hours with U0126, an inhibitor specific for extracellular signal-regulated kinase (ERK) (a MAPK that is rapidly phosporylated following EGFR activation) prior to treatment with 0.1pfu/cell, and they found U0126 inhibited JX-594-GFP+/β-gal− replication [163]. Langammer *et al*. have also demonstrated that an EGFR inhibitor, Gefitinib (Iressa), can impair poxvirus spreading [174]. Thus, EGFR expression by tumour cells may make them more susceptible to JX-594 treatment, and enhancing the EGFR

pathway may augment replication of JX-594, which is mechanistically important, as direct JX-594 mediated killing is dependant on replication.

Exploiting the GFP early/late promoter gene in JX-594-GFP provides an adjunct to the plaque assay in demonstrating and understanding replication of JX-594 in CRC cell lines. In the plaque assay technique, no plaque-forming viral progeny were present in the *in vitro* samples by 24 hours, but flow cytometry and CLSM of CRC cell lines revealed GFP expression at 24 hours, in keeping with the recognition that the early steps of vaccinia replication have already begun at this stage [175]. The finding of early GFP expression with no demonstrable replication is explained by the temporal fashion of the expression of the vaccinia genome; immediately after entry into the host cell, mRNA is synthesised by enzymes packed within the virus core. Hence, early-phase genomic expression occurs independently of replication and is not prevented by either inhibitors of protein or DNA synthesis. Late genes are not expressed until after DNA replication has begun [176]. The surge in GFP expression at 72 hours correlates with the plaque assay findings, and it may be that at this stage the virus is undergoing the final stages of replication. The EEV form of the virus has been synthesised, exiting the cell to infect nearby tumour cells, and beginning early phase replication in these infected neighbouring cells.

The results described in this chapter demonstrate an induction of several cytokines during JX-594 mediated tumour cell killing. The bystander immune effect of cytokines such as IL-6, IL-8 and IL-10 is still debatable, as most cytokines that promote inflammation may also support tumour proliferation. IL-6 is secreted by T cells and macrophages in response to IL-1 and TNF-β, and functions to stimulate an immune response. IL-6 has been shown to enhance the generation of CTL [177], up-regulate intracellular adhesion molecule 1 (ICAM-1) on endothelial cells

and both attract monocytes and skew them towards macrophage differentiation [178]. IL-6 has also been shown to be important in oncolytic virus treatment; *in vivo* blocking of IL-6 in a CRC (CT26) syngeneic BALB/c mouse model led to a reduced anti-tumour response by Sendai virus (anti-T_{Reg} mediated) [179]. On the other hand, IL-6 has been implicated in the aetiology of some cancers [180] and in an *in vitro* model, knockdown of IL-6, genetic ablation of the *IL-6* gene, or treatment with a neutralizing IL-6 antibody was shown to retard Ras-driven tumorigenesis [181]. More recently, IL-6 has been found to promote prostate tumorigenesis and progression through autocrine cross-activation of insulin-like type I growth factor receptor (IGF-IR) [182].

The effects of IL-8 are mediated through the binding of IL-8 to two cell-surface G protein–coupled receptors, CXCR1 and CXCR2, and the expression of IL-8 receptors on cancer cells, endothelial cells, neutrophils, and tumour-associated macrophages suggests that the secretion of IL-8 from cancer cells may have a profound effect on the tumour microenvironment. IL-8 secreted from tumour cells may enhance the proliferation and survival of cancer cells through autocrine signalling pathways, and may activate endothelial cells in the tumour vasculature to promote angiogenesis, which in turn will induce a chemotactic infiltration of neutrophils into the tumour site. IL-8 can induce tumour-associated macrophages to secrete additional growth factors, which further affect the tumour microenvironment to increase the rate of tumour cell proliferation and invasion [183]. In more clinically relevant translations models, IL-8 signalling has also been shown to attenuate TRAIL- and chemotherapy-induced apoptosis in prostate cancer cells [184] but promotes tumour growth, metastasis, chemoresistance and angiogenesis *in vitro* and *in vivo* in colon cancer cell line models [185]; it also promotes tumour growth of HeLa cells overexpressing oncogenic Ras [186].

A variety of tumor cells secrete IL-10, which is generally considered an anti-inflammatory cytokine as it inhibits immune priming and NK cell activity. It down-regulates the expression of Th1 cytokines, MHC class II antigens, and co-stimulatory molecules on macrophages, and is capable of inhibiting synthesis of pro-inflammatory cytokines such as IFN-γ, IL-2, TNFα and GM-CSF expressed by immune cells [187]. However, some studies have also revealed that IL-10 may have the pleotropic ability to stimulate anti-tumour innate and adaptive immunity [188]. In addition, IL-10 can favour tumor growth *in vitro* by stimulating cell proliferation and inhibiting cell apoptosis [189], and high systemic levels of IL-10 correlate with poor survival of some cancer patients. This is not clinically conclusive, as this may just be due to the tumour grade and the converse has also been demonstrated [188, 190]. The results displayed here show that in some cell lines *in vitro*, JX-594 treatment decreases levels of IL-10 in the tumour microenvironment, which may have potentially beneficial effects on innate and adaptive immunity, and potentially, tumour proliferation.

VEGF stimulates vasculogenesis and angiogenesis, and VEGF expression in tumours correlates with invasiveness, vascular density, metastasis, recurrence, and prognosis. Anti-VEGF therapy (bevacizumab, a monoclonal antibody to VEGF) has been used in the treatment of metastatic CRC, non–small cell lung cancer (NSCLC), metastatic renal cell carcinoma (RCC) and glioblastoma (GBM). Bevacizumab has been shown to be promising and safe in the neo-adjuvant treatment of metastatic CRC in phase II trials [191] and effective in phase III trials in recurrent ovarian cancer [192], but not in adjuvant phase III trials [193]. The results in this chapter demonstrate a decrease in VEGF following JX-594 treatment, which otherwise increased over time in untreated cells. Breitbach *et al*. have demonstrated that VEGF treatment of human dermal endothelial cells (HDMECs) resulted in an increase in JX-594 output following 72 hours of treatment. This was

due to downstream signalling resulting in an increase in TK following VEGFR phosphorylation. Hence colorectal tumours, which produce high levels of VEGF, serve as a favourable targets for JX-594 therapy. Breitbach *et al*. have also demonstrated the anti-angiogenic properties of JX-594 *in vivo*. In mouse models, diffuse endothelial cell infection of subcutaneous 4T1 (breast cancer) tumours was demonstrated, with a concurrent reduction in tumour perfusion [194]. HCC is a hypervascular and VEGF-rich tumor type, and a phase I trial demonstrated dose-dependent endothelial cell infection and transgene expression of JX-594 (in multiple tumour types) [134]. Moreover, in a phase II clinical trial treating 18 patients, higher-dose JX-594 treatment was shown to disrupt tumour perfusion (5/8 patients), with no evident toxicity to normal blood vessels [194]. Liu *et al*. have also previously demonstrated reduction in serum VEGF following JX-594 treatment [76].

The coupled response described in this chapter of the reduction in VEGF and IL-10 is an interesting observation. Liu *et al*. observed that IL-10 was significantly co-expressed with VEGF using an *in vitro* model of epithelial ovarian cancer. VEGF was found to interfere with DC maturation, and consequently the immature DCs secreted high levels of IL-10 in the tumour microenvironment, which induced T_{reg} generation without antigen presentation in DCs [195].

Type I IFNs serve as an important part of the host's anti-viral defence. The antiviral effect of IFNs is potent and rapid; IFNs are released almost instantly upon viral infection and then bind to receptors to activate signal transducer and activator of transcription (STAT) complexes, triggering expression of a series of IFN-responsive genes such as PKR, which convert cells to an antiviral state. Infection of CRC cell lines with JX-594 resulted in no measurable IFNα or IFNβ (see table 3-2). The large vaccinia genome codes for several immune evation proteins, with the B18R

proteins being important members of the virus's arsenal against host anti-virus mechanisms. They act as decoy receptors to block the activity of type I IFNs from various species, inhibiting them from binding their cognate receptors and triggering an anti-viral response. The lack of measureable IFNs following JX-594 infection of CRC cell lines in these experiments may be explained by early expression of B18R, which may prevent detection of IFNs *in vitro*, even at 6 hours.

The role of inflammation in cancer remains a matter for debate. Chronic inflammation and thus genotoxic stress can induce cancer initiation, and cancer promotion and progression by inducing cellular proliferation and enhancing angiogenesis and tissue invasion. A such, the development of HCC is related to the chronic inflammatory response generated by Hepatitis B and C viruses [196]. Inhibition of chronic inflammation with long-term use of anti-inflammatory drugs has a protective effect in patients with pre-malignant disease [197], as has been demonstrated in colorectal cancer, with a moderate chemopreventive effect of aspirin on adenomas in the large bowel [198]. However, intravesical BCG is effective in the treatment of superficial bladder cancer, and promotes inflammation at the site of disease, with an increase in detectable urinary IL-1, IL-2, IL-6, IL-8, IL-10, IL-12, IL-18, IFNγ, macrophage colony stimulating factor, and TNF-α [52]. The induction of pro-inflammatory cytokines and the diminished anti-inflammatory cytokine activity induced by JX-594 treatment may have beneficial effects, particularly when coupled with the lytic activity of the virus. OVs, combined with targeting of cytokine signalling pathways, may have important implications in halting disease progression and attenuating tumour resistance to other chemotherapeutic and biological agents. The expression of virally-encoded GM-CSF provides further support for the importance of therapeutic inflammation in virotherapy, which will function to enhance innate immunity and subsequent anti-tumour memory (discussed in chapter 5).

This chapter describes the potential benefit of tumour cell killing following JX-594 treatment; however it's advantage over other conventional therapies may be related to its tumour-specificity. Work addressing this aspect of JX-594 therapy is shown in the following chapter.

Chapter 4

Results: JX-594 preferentially replicates in tumour cells *ex vivo*

4 JX-594 preferentially replicates in tumour cells *ex vivo*

4.1 Introduction

One particularly favourable characteristic of oncolytic viruses in their application as an emerging therapeutic modality is their selectivity for replication within cancerous cells. The resulting viral progeny when released from a cell consequently infect neighbouring cells, resulting in a rapid spread throughout a solid tumour. The insertion of genes of interest into the VV-*TK* locus also makes it a favourable candidate for gene therapy, selectively expressing potentially therapeutic genes in the tumour environment. The previous chapter has demonstrated viral replication in CRC cell lines; however, this does not address the issues of viral penetration into tumour tissue and tumour-specificity. Hence, an *ex vivo* system was developed, where surgically resected CRLM tumour and normal liver were infected with JX-594 expressing GFP.

4.2 JX-594 replicates in liver tumour, but not in matched normal liver tissue

4.2.1 Tumour specific transgene (GFP) expression in precision-cut tissue slices

The findings in chapter 3 so far have shown competent viral replication in tumour cell lines, which only presumably translate *in vivo*. In order to address this, and to demonstrate the difference between replication in liver tumour and normal tissue, a novel *ex vivo* system was used. Directly from the operating theatre, freshly resected liver tumour and matched normal tissue was sliced using a precision-cutting microtone (see section 2-13). In order to demonstrate tumour-specific replication,

JX-594-encoded GFP expression in the tissue slices was determined by confocal microscopy. GFP is under the control of a synthetic early/late promoter, thus its expression is in two phases – early, as the virus takes over the cell, and late, as the virus prepares for escape from the cell. Figure 4-1a shows the expression of GFP in tumour slices, but not in matched normal liver tissue slices. Although this illustrated the tumour-specificity of viral protein expression, the images were difficult to capture on confocal microscopy, due to the lack of a well defined focal point. Hence, a nuclear counterstain (DAPI) was then used (figure 4-1b), which enabled acquisition of higher quality images.

Tumour specific replication was further demonstrated using tissue from a benign liver tumour, focal nodular hyperplasia (FNH). In figure 4-2, there was no GFP expression in the normal liver, nor the liver tumour (FNH). Hence, JX-594 appears to require malignant cells in order to efficiently replicate.

As seen in figure 4-1 and 4-2, the observation of ‘speckles’ of green signal in the normal liver tissue was noted, and although this was likely to be due to autofluorescence, it was later investigated (see section 4.2.3).

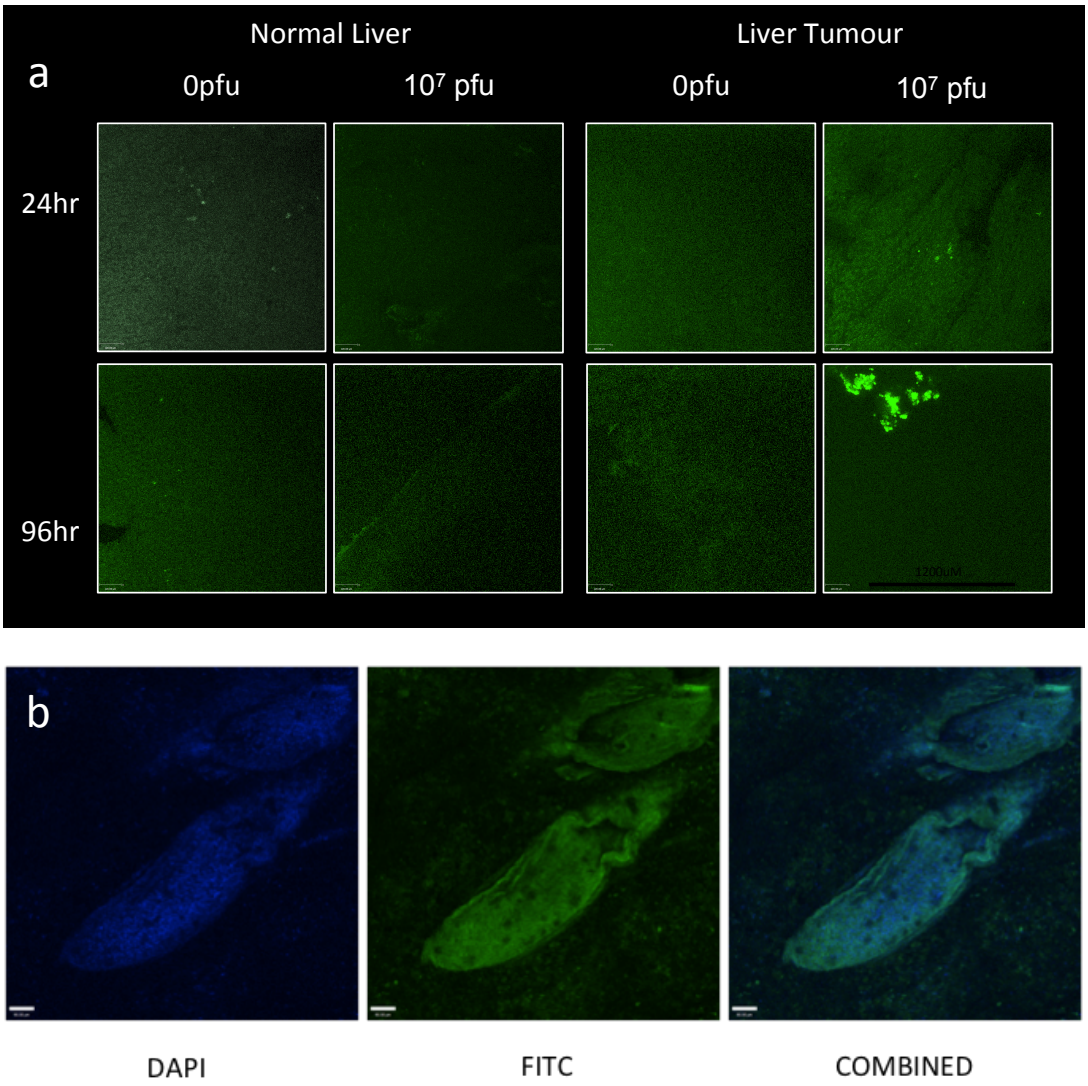

Figure 4-1. CLSM images of precision cut tumour slices and tissue slices and modification of protocol.

Freshly resected liver tumour and match normal tissue were collected directly from the operating theatre and embedded in agar. Using a precision-cut microtone, sections of tissue 250 µm in thickness were created, maintained in 'fresh tissue culture medium' for 96 hours, and infected with 0 and 10^7 pfu. Images were taken using the Nikon A1 confocal laser scanning microscope at 10x magnification. Figure a) shows the expression of GFP in the precision cut slices of CRLM but not matched normal liver tissue from the same patient. Figure b) depicts the addition of DAPI nuclear counterstain to the protocol. By selecting filters that only allow specific fluorescent wavelengths to pass through, images of nucleic acid staining (DAPI) and inherent tissue GFP fluorescence (FITC) can be detected in separate images, or combined.

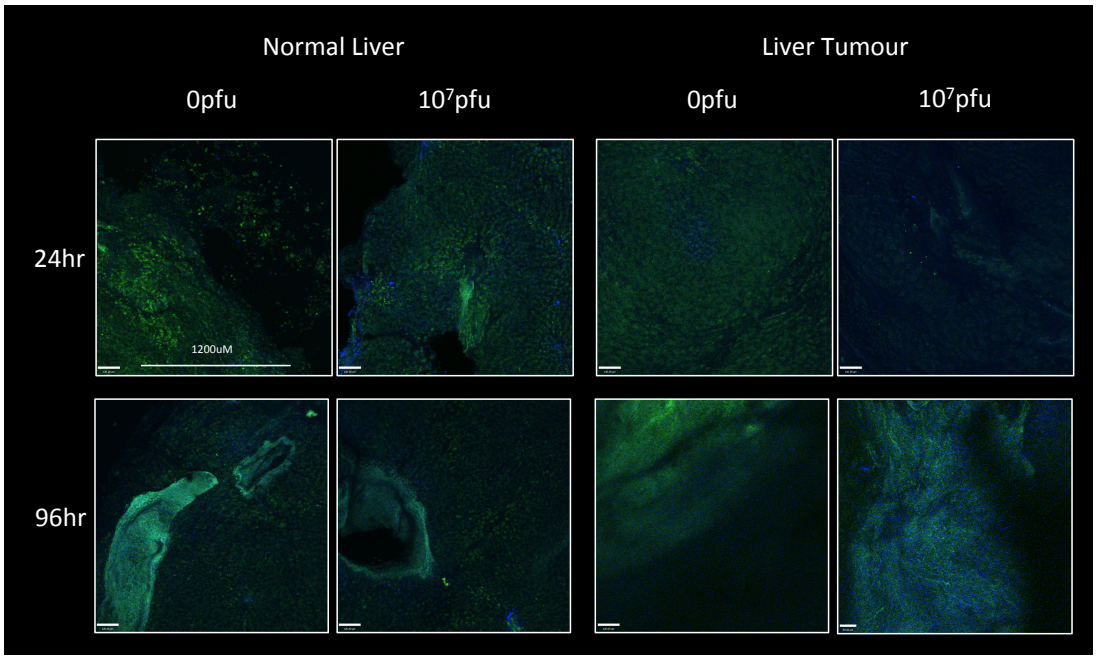

Figure 4-2. No GFP expression in benign liver tumour

Freshly resected liver tumour (FNH) and match normal tissue were collected directly form the operating theatre and embedded in agar. Using a precision-cut microtone, sections of tissue 250 µm in thickness were created, maintained in 'fresh tissue culture medium' for 96 hours, and infected with 0 and 10^7 pfu. Immediately prior to CFLM, tissue slices were stained with DAPI for 45 minutes and washed, and re-fixed in 1%PFA. Images were taken using the Nikon A1 confocal laser scanning microscope. There was no GFP expression in either the normal tissue or FNH.

4.2.2 Tissue Cores; optimising methodology

The production of thin (250 μm thickness) tissue slices proved to be very time consuming, and the process of agar embedding prior to slicing caused some tissue damage and potentially compromised sterility - hence the tissue core method was adopted for all future experiments. Cylinders of liver and CRLM tumour tissue were created using a Tru-cut® biopsy needle to produce small sections/cylinders of tissue that can be grown in media for 96 hours. Firstly, it had to be determined that the cores maintained viability for the entire course of the assay. In order to do this, tissue cores were maintained in media, and alamer blue dye was added to the wells containing either normal liver or tumour core, and the fluorescence of the metabolised product (resorufin) determined as described in section 2.13. This assay was performed in two conditions; firstly using the same cores for the entire duration of the experiment (three 5mm cores per well) with fresh media replenished at each time point up to 120 hours (figure 4-3 a). In the second condition (figure 4-3 b and c), separate cores were set up for each time point, and thus by 96 hours, the cores had no replenishing of media, which mimicked the experimental conditions applied to all future experiments. In both systems, the normal tissue maintained similar levels of metabolic activity up to 120 hours, whilst the tumour tissue did lose some activity by 96 hours in culture, which is likely to be due to the higher metabolic demand of the tumour cells.

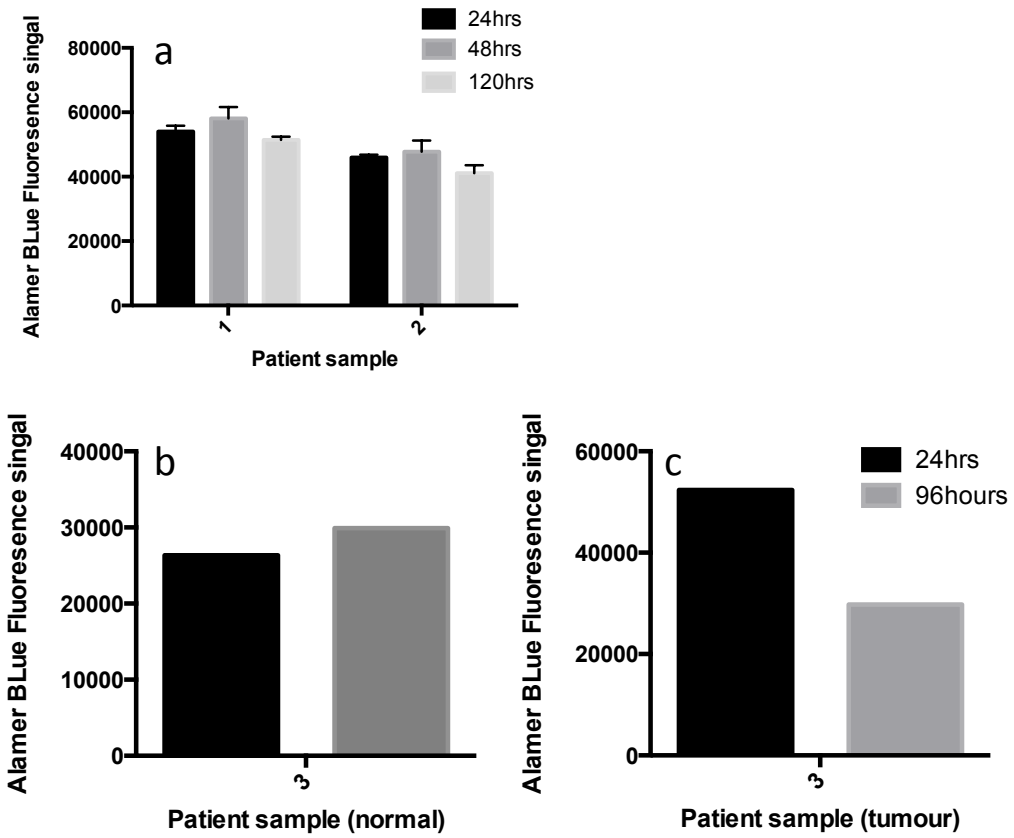

Figure 4-3. Tissue viability using Alamer Blue

Three cores of tissue per well in 'fresh tissue medium' was set up to test the viability of liver tissue and CRLM when maintained in culture. 25 µL of Alamer Blue dye was added to each well, and left to incubate for 1 hour at 37^{o}C, media collected and fluorescence measured using a fluorescence plate reader. In figure a the same three cores were used for each time point, with fresh media replenished after alamer blue analysis. Figure a) shows the fluorescence signal in normal liver tissue cores from two separate patient samples, taken from opposite ends of the excised tissue mass, and data presented is the mean reading from cores taken from opposite ends of the tissue mass in two patients. In figures b (normal liver) and c (CRLM tumour), three cores per well were maintained in the same media for up to 96 hours, with a different well at each time point (N=1). The detection of similar levels of fluorescence over time indicates the maintenance of tissue metabolic activity and thus viability.

4.2.3 Normal liver tissue expresses high auto-fluorescence

Normal liver exhibits high background fluorescence, due to the fatty deposits which auto-fluoresce. In order to establish that the green signal seen in normal liver is due to auto-fluorescence and not due to GFP expression, a viral construct that does not express GFP was used (JX-594-YFP). Tissue cores from normal liver were treated with both JX-594-YFP and JX-594-GFP and the resulting fluorescence signals were similar for both (see Figure 4-4); hence, these 'speckles' can be regarded as non-specific background auto-fluorescence.

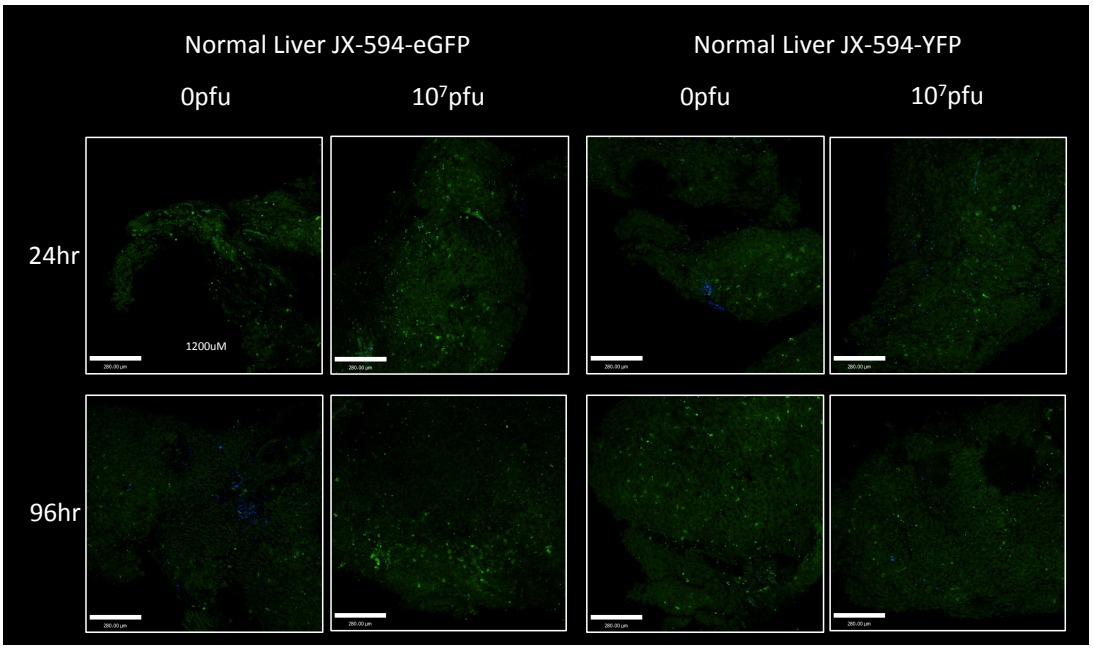

Figure 4-4. Confocal microscopy for auto-fluorescence of tissue cores treated with JX-594.

Freshly-resected liver tissue from a single patient was collected immediately following resection and cylindrical cores of 5mm x 1mm were made using a Tru-Cut® biopsy needle, and cultured in 'fresh tissue culture medium' infected with JX-594-GFP and JX-594-YFP at either 0 and 10^7 pfu. At specified time points, supernatant was collected and tissue fixed in 1% PFA. Immediately prior to CFLM, tissue cores were stained with DAPI for 45 minutes and washed, and re-fixed in 1% PFA. Images were taken using the Nikon A1 confocal laser scanning microscope.

4.2.4 Tumour specific transgene (GFP) expression in tissue cores

Once it had been established that the viability of the tissue cores would be adequate to support viral infection, and that the green signal in the normal liver tissue was non-specific autofluorescence, the finalised protocol was performed in a total of 10 samples of CRLM tissue, each with matched normal liver. Cores were treated with JX-594-GFP for up to 96 hours in culture. Similar to the findings in the precision cut tissue slice system (figure 4-1), treatment of the liver tumour tissue cores with JX-594-GFP, resulted in an increase in GFP expression, which was not seen in the matched normal liver (figure 4-5 and 4-6). In 9 out of 10 CRLM samples, tumour-specific GFP expression was observed, and in the majority of cases, there was a pronounced increase in GFP expression between 48 and 72 hours, with maximal expression by 96 hours (see Appendix A for all 10 cases and table 4-1). There was an observed difference in the intensity of the GFP signal in various samples (as seen in 2 representative patients, figures 4-5 and 4-6), and this was subjectively quantified as displayed in table 4-1. In some cases (sample 4 and 8), there was a high GFP signal early at 24 hours, in comparison to the other tissue samples.

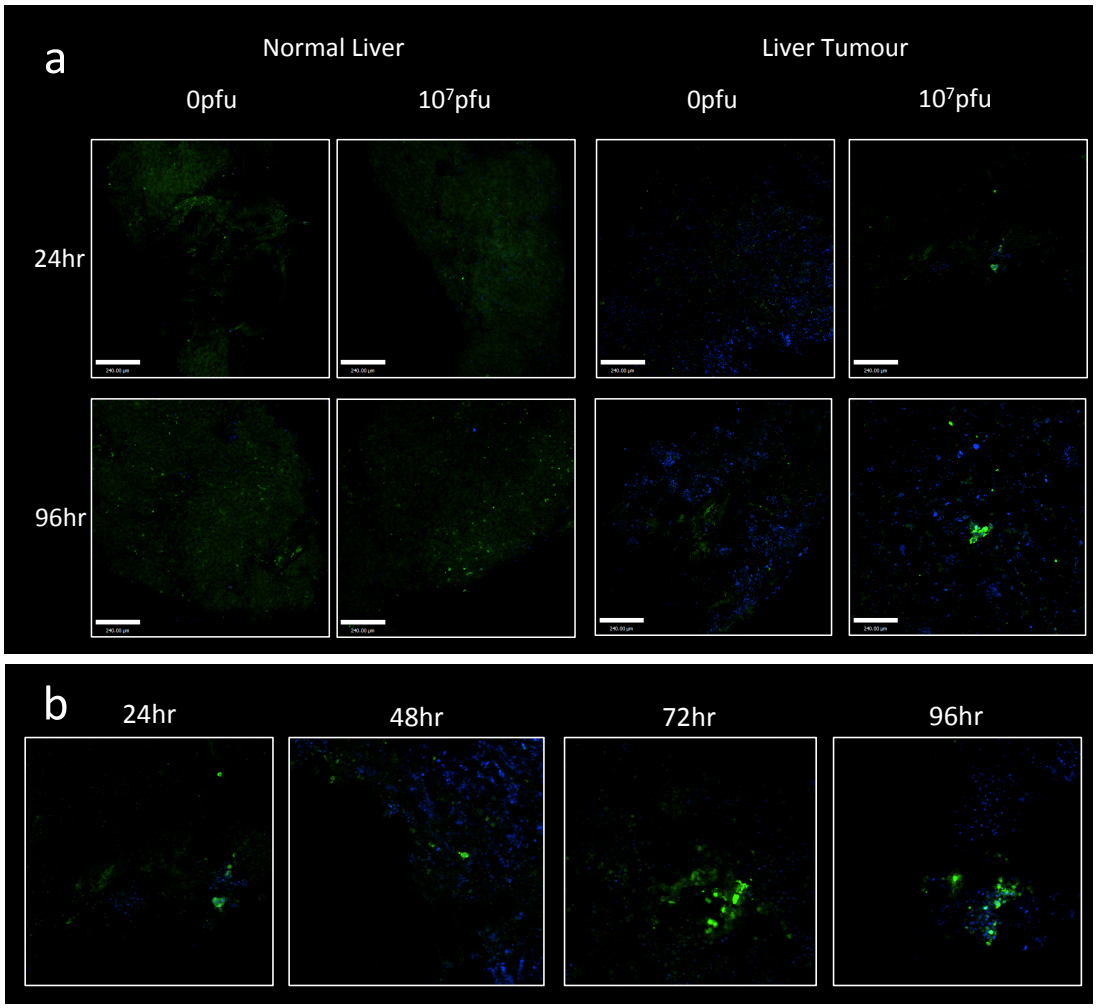

Figure 4-5. GFP expression in CRLM tumour cores – example 1

Freshly-resected liver tumour and matched normal tissue were collected immediately following resection and cylindrical cores of 5mm x 1mm were made using a Tru-Cut® biopsy needle, and cultured in 'fresh tissue culture medium' infected with JX-594-GFP at either 0 or 10^7 pfu (figure a). At specified time points, supernatant was collected and tissue fixed in 1% PFA. Immediately prior to CFLM, tissue cores were stained with DAPI for 45 minutes and washed, and re-fixed in 1%PFA. Images were taken using the Nikon A1 confocal laser scanning microscope. Figure b) shows the progression of GFP signal intensity in cores treated with 10^7 pfu JX-594-GFP.

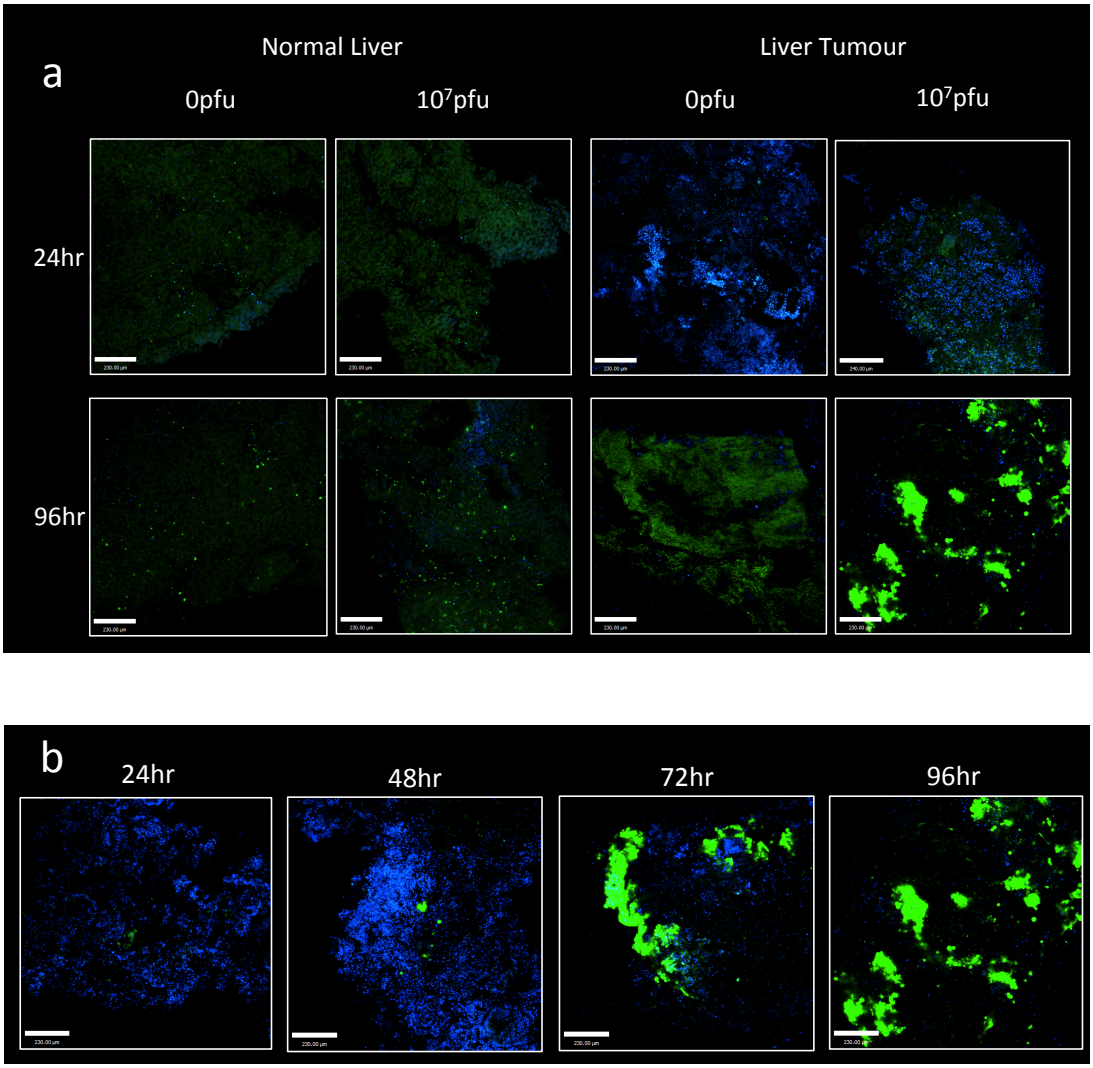

Figure 4-6. GFP expression in CRLM tumour cores – example 2

Freshly-resected liver tumour and matched normal tissue were collected immediately following resection and cylindrical cores of 5mm x 1mm were made using a Tru-Cut® biopsy needle, and cultured in 'fresh tissue culture medium' infected with JX-594-GFP at either 0 or 10^7 pfu (figure a). At specified time points, supernatant was collected and tissue fixed in 1% PFA. Immediately prior to CFLM, tissue cores were stained with DAPI for 45 minutes and washed, and re-fixed in 1%PFA. Images were taken using the Nikon A1 confocal laser scanning microscope. Figure b) shows the progression of GFP signal intensity in cores treated with 10^7 pfu JX-594-GFP.

Patient Demographics		Colorectal Liver Metastasis		Normal Liver	
Details	Age	GFP 24 hr	GFP 96 hr	GFP 24 hr	GFP 96 hr
GH	72	↑	↑↑↑	↔	↔
RC	66	↑	↑↑	↔	↔
TC	48	↑	↑↑	↔	↔
LF	77	↑↑	↑	↔	↔
JC	57	↔	↔	↔	↔
RP	69	↑	↑↑	↔	↔
JM	64	↑	↑↑	↔	↔
AM	78	↑↑	↑↑	↔	↔
MI	84	↔	↑	↔	↔
AB	53	↑	↑↑↑	↔	↔

Table 4-1 Summary of GFP expression in patient samples

A total of 10 patients with CRLM were recruited for sample collection. Matched normal and tumour tissue was available from all patients. The level of GFP expression by confocal microscopy at 24 hours and 96 hours was quantified subjectively.

4.2.5 GM-CSF expression in tissue cores treated with JX-594

Genes encoding GFP and GM-CSF are within the same (disrupted *TK*) locus, and under the control of an early/late promoter. Hence, expression of both transgenes should be evident simultaneously, and GM-CSF expression would be expected to be higher in tumour tissue. At specific time points, when the tissue cores were transferred into 1% PFA for confocal microscopy, the supernatant was collected and stored for future ELISA. Figure 4-7 shows that GM-CSF in the tissue culture medium was found to increase significantly with viral treatment compared to untreated control by 48 hours in both normal and tumour tissue, and to a similar extent in both (around 200 pg/ml, $p<0.05$). However, after 48 hours, the levels of GM-CSF remained unchanged in the supernatant of the normal liver tissue cores, with no significant difference between treated (10^7 pfu) and untreated cores and between cores treated with 10^7 pfu at 24 and 72 p.i. In the liver tumour, there continued to be a significant increase in GM-CSF in treated (10^7 pfu) vs untreated cores at 72 and 96 hours, and there was a significant increase in GM-CSF from 24 to 72 hours p.i. following treatment with 10^7 pfu. Although the average readings showed an overall increase in GM-CSF in the tumour vs normal tissue, there was a variable response evident in each experiment, particularly at 24 hours p.i. (figure 4-7 c). By 96 hours p.i. (figure 4-7 d), most tumour cores had a higher level of GM-CSF expression compared to normal liver tissue.

In order to determine if the objective increase in GM-CSF correlated with subjective GFP expression, a single value of the increase in GM-CSF ($^{\Delta}$GM-CSF) from the baseline was calculated as: $GM\text{-}CSF_{max} - GM\text{-}CSF_{0pfu}$, where $GM\text{-}CSF_{max}$ is the maximal GM-CSF production at that particular time point and $GM\text{-}CSF_{0pfu}$ is the GM-CSF production from the untreated 'control' core. Although there was some coupling of GFP expression with increased GM-CSF expression (see table 4-2), the subjective grading of GFP expression by confocal microscopy did not significantly

correlate with the objective GM-CSF expression by ELISA (p>0.05, Spearman's rank correlation).

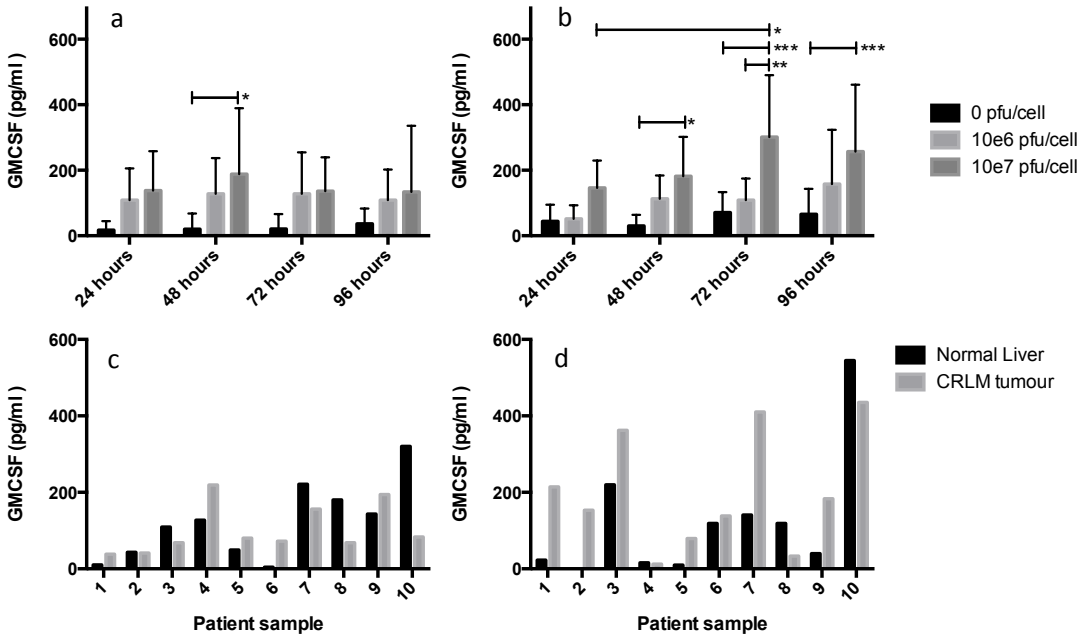

Figure 4-7. GM-CSF production from tissue

Freshly-resected normal liver tissue (a) and matched liver tumour (b) were collected immediately following resection; cylindrical cores of 5mm x 1mm were made using a Tru-Cut® biopsy needle, and cultured in 'fresh tissue culture medium' infected with JX-594-GFP at either 0, 10^6 or 10^7 pfu. At specified time points, supernatant was collected and GM-CSF production measured by ELISA. Figure c) and d) show individual patient results at 24 and 96 hours respectively. Experiments were performed in decuplicate (N=10); *p<0.05, **p<0.005, ***p<0.001.

Patient Demographics		Colorectal Liver Metastasis				Normal Liver	
Details	**Age**	**GFP 24 hr**	**GFP 96 hr**	**$^{\Delta}$GM-CSF 24 hr (pg/ml)**	**$^{\Delta}$GM-CSF 96 hr (pg/ml)**	**$^{\Delta}$GM-CSF 24 hr (pg/ml)**	**$^{\Delta}$GM-CSF 96 hr (pg/ml)**
GH	72	↑	↑↑↑	38	214	10	22
RC	66	↑	↑↑	41	153	43	0
TC	48	↑	↑↑	68	362	109	219
LF	77	↑↑	↑	219	12	127	15
JC	57	←→	←→	80	79	49	9
RP	69	↑	↑↑	72	138	4	118
JM	64	↑	↑↑	156	410	221	140
AM	78	↑↑	↑↑	68	33	180	118
MI	84	←→	↑	194	183	143	39
AB	53	↑	↑↑↑	83	435	320	544
			Average	102	202	121	122

Table 4-2 Summary of findings in patient samples

A total of 10 patients were recruited for sample collection. Matched normal and tumour tissue was available from all patients. The level of GFP expression by confocal microscopy was quantified subjectively and the increase in GM-CSF was quantified objectively by ELISA. $^{\Delta}$GM-CSF = GM-CSF$_{max}$ – GM-CSF$_{0pfu}$, where GM-CSF$_{max}$ is the maximal GM-CSF production at that time-point and GM-CSF0$_{pfu}$ is the production of GM-CSF in the untreated core.

4.3 Infection of tissue cores with JX-595 does not result in a generalised inflammatory response

The ability of JX-594 to induce a pro-inflammatory tumour microenvironment was described in chapter 3 using *in vitro* studies. In order to examine the effect in an *ex vivo* model, tissue cores were treated with 0, 10^6 and 10^7 pfu JX-594 for 24 to 96 hours and the supernatants collected at specified time intervals for the cytokine/chemokine profile to be studied by ELISA. Following the findings of *in vitro* experiments, GM-CSF, VEGF, IL-6, IL-8 and IL-10 were studied, along with IFNα, IFNγ and TNFα. The dose/time response in GM-CSF has been described in section 4.2. VEGF is known to be produced from CRC, and this finding was confirmed in the tumour tissue cores expressing higher levels than normal liver. However, there was no reduction in VEGF production as seen with the CRC cell lines (Figure 4-8). There was no consistent dose/time response after viral treatment in any of the other cytokines studied, aside from IL-10, which showed an increased production with escalating virus doses. This was only significantly increased in tumour cores at 24 hours p.i., but not at later time points (data not shown). Production of IL-6 and IL-8 from the cores did not show any response to viral infection, and were produced maximally within the first 24 hours, and reduced thereafter (data not shown). There was no difference in IL-6 and IL-8 production in liver tumour and normal liver samples. No consistently detectable IFNα, IFNγ and TNFα was found by ELISA (data not shown). Table 4-2 summarises the changes in cytokines in response to JX-594 treatment of tissue cores.

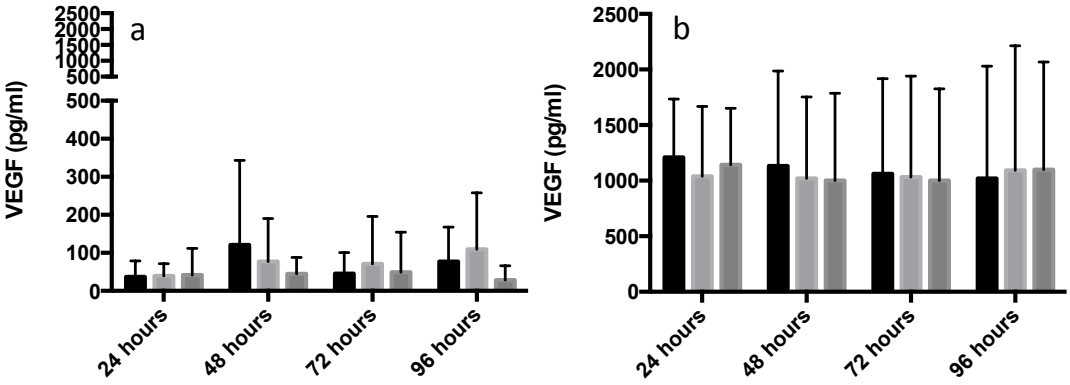

Figure 4-8. VEGF production in tissue cores treated with JX-594

Freshly-resected normal liver tissue (a) and matched liver tumour (b) were collected immediately following resection; cylindrical cores of 5mm x 1mm were made using a Tru-Cut® biopsy needle, and cultured in 'fresh tissue culture medium' infected with JX-594-GFP at either 0, 10^6 or 10^7 pfu. At specified time points, supernatant was collected and VEGF production measured by ELISA. Experiments were performed in decuplicate (N=10).

	Effect upon infection of *ex vivo* 'tissue cores' with JX-594	
	Tumour	Normal
GM-CSF	↑* (at all time points)	↑* (at 48 hours only)
VEGF	↔	↔
IL-6	↔	↔
IL-8	↔	↔
IL-10	↔	↔
IFNα	↔	↔
IFNγ	↔	↔
TNFα	↔	↔

Table 4-3. Summary of cytokine and chemokine profile following *ex vivo* treatment of CRLM tumour and normal liver 'tissue cores' with JX594

Table summarises the overall cytokine profile of CRLM tumour and normal liver 'tissue cores' infected with JX-594. Experiments were carried out in triplicate in all circumstances.

* Significant ($p<0.05$)

4.4 Discussion

There are several mechanisms that contribute to the tumour-selectivity of vaccinia replication (see Figure 1-3). The knockout of the *TK* gene results in the virus being replication-competent only in cells of high TK environment, as is characteristic of many cancer cells [199]. The activation of the EGFR/Ras/MAPK signal pathway which is inherent in most cancer cells also aids JX-594 replication, and the induction of JX-594 replication results in positive feedback due to the further activation of this pathway by VGF, which is an EGF-analogue. VGF binds onto EGFR on the cell surface, activating downstream pathways which further enhance the cell's environment for vaccinia replication. The inhibition of the anti-viral interferon response by another vaccinia-encoded protein, B18R, results in further enhancement of replication by binding IFN receptors on the tumour cell surface. Indeed, these mechanisms are all tumour specific, and make vaccinia an attractive platform for anti-tumour therapy. This is by no means an exhaustive list of the favourable characteristics of JX-594, and due to the large genome, there is scope for many gene therapy approaches to be investigated to further increase the efficiency of this agent.

In chapter 3, replication in tumour cells was demonstrated by the plaque assay technique and by utilising GFP transgene. Plaque assays demonstrated increased replication by 72 hours p.i. which was supported by GFP expression by confocal microscopy in cell lines treated with JX-594-GFP. Indeed, these findings are supported by the *ex vivo* system, where the surge in GFP and significant increase in GM-CSF occurs between 48 and 72 hours. It is evident that the replication efficiency within the patient cohort is understandably variable, which may be due to several factors. The biology of the tumour cells will be different, as will the composition of the tissue core; some may have more immune cells and some may

have more necrotic debris rather than viable tumour. It is difficult to standardise for this, although this would not affect the primary aim; to determine tumour-specific replication. Indeed, information about the tumour biology may be useful, particularly with EGFR expression, and this should be addressed in future studies.

Genes encoding both GM-CSF and GFP are inserted into the *TK* locus, and are both under the control of an early/late promoter; however, there was no significant correlation in the expression of these transgenes in the *ex vivo* system. At 48 hours p.i., there was little GFP seen in the majority of the JX-594 infected *ex-vivo* tumour tissue and none in the normal liver, but there was a significant increase in GM-CSF in both tumour and normal liver cores in response to virus. Hence the GM-CSF produced at this stage is likely to be from immune cells, hepatocytes and colorectal tumour cells in response to JX-594 infection, rather than being solely translated from the JX-594 genome. By 72 hours p.i. however, GM-CSF expression continued to exhibit a dose-time dependant increase in tumour cores, but not in normal liver cores, and there was a concomitant surge in GFP expression between 48 and 72 hours, in keeping with the *in vitro* findings. This would suggest that after 48 hours, late-phase JX-594 replication occurs in tumour tissue, but not in normal liver tissue. These findings of potential non-concomitant expression of GM-CSF and GFP, which are both driven by early/late promoters, may also lead one to question the efficacy of the two early/late promoters; GM-CSF driven by a synthetic promoter inserted into the *TK* gene locus and GFP by the p 7.5 early/late promoter, although the methodology required to investigate this is beyond the scope of this work.

The preferential expression of GFP in tumour cells has been described in both *ex vivo* and *in vivo* systems in the literature, and the results displayed in this chapter are in keeping with published findings [136, 163]. Parato *et al*. described tumour-

specific JX-594-derived GFP expression in *ex vivo* lung, colon, endometrial and renal cancers, with a 100-fold increase in viral amplification in colonic tumour vs normal colonic mucosa. Kirn *et al*. demonstrated similar tumour specificity in a similar *ex vivo* model. They collected fresh human colonic and liver tumour and adjacent normal tissue specimens which were sliced into approximately $2mm^3$ pieces. These were placed on a medium-soaked Surgifoam sponge and vaccinia (WR backbone, $B18R^{-ve}$ and TK $gene^{-ve}$) encoding GFP was then added directly to the specimen (at 1×10^7 pfu) for 2 hours at 37 ^{0}C; the tissue specimen was then covered in media. At 48 hours, tumour-specific GFP was detected using fluorescence microscopy [100]. The literature only reports small numbers of these *ex vivo* systems, and not all tumour biopsies were accompanied by matched normal tissue, which has been addressed in our study. This *ex vivo* system addresses a few of the potential drawbacks of *in vitro* methodology. Although human cancer-derived cell lines are the most widely used models to study the biology of cancer and for testing of new therapies, their use has been continuously questioned. Prolonged cell culture is more likely to induce secondary genomic changes. The immortalisation of these cell lines make them different in their biology to *in vivo* tumours, and they are not subject in normal culture conditions to other biological stresses such as hypoxia and nutrition depletion, and have no tumour architecture or 3D structure. This has been addressed to some extent - and the development of standardised protocols for authentication of cell lines and the establishment of the National Cancer Institute 60 (NCI-60) panel has helped to standardise findings between research groups [200]. The use of an *ex vivo* system, as described here, maintains tumour architecture and also allows for the interactions between the various cell types in the tumour, although this is obviously not dynamic and responsive to physiological stresses as it would be *in vivo*. Although the results displayed in the last two chapters display parallels between *in vitro* and *ex vivo* JX-594 gene expression, there are stark differences in the cytokine and chemokine

profiles, which may be explained by enhanced replicative ability of JX-594 *in vitro* and the potential lack of tumour proliferation in *ex vivo* samples. Also, there may be restricted access to the tumour cells themselves in 3D models versus 2D *in vitro* models, due to penetration of the virus into a solid block of tissue; also, other cells may 'mop up' the virus. The immunosuppressive environment of tumours is well documented, and inherent immunosuppressive cytokines and cell populations may inhibit the cytokine response as seen *in vitro*.

The major finding described herein of tumour-specific JX-594 transgene expression may be exploited not only in cancer therapy, but potentially in diagnostics, particularly in the ever-growing recognition of the role of sentinel lymph node excision during cancer surgery. Using an animal foot pad model of melanoma metastasis, and IT injection of a replication competent HSV virus (NV1023), Brader *et al*. demonstrated 100% trafficking of virus to positron emission tomography (PET)-positive draining (popliteal and inguinal) lymph nodes [201]. Similarly in an *in vivo* model of breast cancer lymphatic metastasis in mice, IT injection of NV1066 resulted in transit of viruses to draining axillary lymph nodes, which could be measured by *in vivo* fluorescent imaging with a sensitivity of 80% and a specificity of 96% [202]. Oncolytic viruses have been shown to not only penetrate into, but also to kill, lymph nodes metastases, as published using vaccinia virus in an orthotopic mouse model of metastatic triple negative breast cancer. Following IT injection, GLV-1h153 (Vaccinia, Lister strain, expresses GFP) could be tracked in metastatic lymph nodes after 48 hours, and following 5 weeks of treatment, all harvested lymph nodes showed no evidence of metastatic cells [126].

The findings presented in this chapter demonstrating preferential replication of JX-594 in tumour tissues makes it an ideal candidate for anti-tumour therapy. It limits toxicity and allows for targeted gene-therapy by manipulation of the viral genome. The expression of GM-CSF leads to potentially interesting consequences within the tumour micro-environment, with activation of innate immune effector cells aiding not only direct tumour lysis, but also the development of subsequent adaptive anti-tumour memory via antigen presentation. Work investigating these questions is presented in the following chapter.

Chapter 5

Results: Activation of Innate Immunity

5 Activation of Innate Immunity

5.1 Introduction

Because this chapter focuses on the activation of innate anti-tumour immunity by JX-594, a wider introduction to the innate immune system is given here. Since Virchow's description of the infiltration of leukocytes into tumours in the 1860s [203] the role of inflammation and the immune system in cancer has remained a controversial subject. It is becoming increasingly recognised that the immune system will play an important role in tumour progression and there is overwhelming evidence that immunity against transformed cells can develop to protect the host from cancer development [204]. Both the innate and adaptive immune systems will play a role in cancer cell recognition and destruction, and this chapter will concentrate on the role of innate anti-tumour immunity.

5.1.1 The innate immune system

The innate immune system is an evolutionarily primitive mechanism and induces a response that remains unchanged irrespective of the frequency of exposure to the pathogenic antigen. Recognition between 'self' and 'anti-self' forms the first trigger of induction of this innate immune response and the cellular components responsible are phagocytes (macrophages, neutrophils, and dendritic cells), cells that release inflammatory mediators (mast cells, eosinophils, basophils) and natural killer cells [13].

5.1.1.1 Natural Killer Cells

NK cells were first isolated in mice [205, 206], are defined as $CD3^{-ve}CD56^{+ve}$ lymphocytes and constitute approximately 10-20% of PBMCs. NK cells have evolved to recognize and kill abnormal (infected and malignant) host cells [207]. They are 'educated' early in their development in the bone marrow to distinguish between 'self' and 'anti-self' [208]. They can be sub-classified as $CD56^{bright}$ and $CD56^{dim}$ NK cells, with distinct activity. $CD56^{dim}$ NK cells exist predominantly in the blood and sites of inflammation and are highly cytotoxic, whilst $CD56^{bright}$ NK cells make up the majority of lymph node NK cells, have little cytotoxic activity, and have a more immunoregulatory function, rapidly producing cytokines and chemokines [209].

5.1.1.2 NK cell activation: receptor expression

NK cells possess Fc (Fragment, crystallizable) receptors that bind IgG (eg FcγRIII / CD16). Thus, IgG-coated target cells are recognised and killed by a process called antibody-dependant cellular cytotoxicity (ADCC). $CD56^{dim}$ NK cells also display another recognition system which consists of killer-activating and killer-inhibiting receptors. These receptors detect molecules on the target cell surface and a 'kill' signal is then issued, which can be negated by an 'anti-kill' signal. Following infection or malignant transformation, cells lose expression of MHC class I molecules on their surface, and hence lose an inhibitory signal, causing activation of NK cell mediated killing. NK cell recognition of target cells is a balance between activatory (NKp30, NKp44, NKp46, NKG2D, DNAM-1, CD16) and inhibitory (killer-cell immunoglobulin like receptors -KIR) signalling. DNAM-1 (DNAX accessory molecule-1) and NKG2D (NK group 2 member D) are major NK cell activating receptors, which transduce activating signals after binding their ligands CD155, CD112 and major histocompatibility complex class I-related chains A and B (MICA/B) [210].

5.1.1.3 NK cell activation: cytokine response

Innate responses involve soluble factors as well as the cellular component, and NK cells respond to signals from other immune cells, including dendritic cells, macrophages, and pathogen-infected tissue cells (see table 5-1). This signalling is mediated by the release of cytokines, which can activate NK cells, including type-I interferons (IFNα/β), IL-2, IL-10, IL-12, IL-15, and IL-18. NK cells also secrete cytokines that can activate immune responses, such as IFNγ, TNFα, GM-CSF and IL-13 [209, 211]. NK-derived IFNγ can stimulate DCs, inducing the production of IL-12 activating T-cell 'helper' functions [208]. Helper T-cell may be classified into either Th1 and Th2, and secrete cytokines with differing roles. Th1-type cytokines, such as IFNγ, initiate a proinflammatory response responsible for killing intracellular parasites and for perpetuating autoimmune responses. However, excessive proinflammatory responses can lead to uncontrolled inflammation and thus Th2-type cytokines (IL-4, IL-5,IL-10, IL-13) function to counteract this. Table 5-1 shows a summary of the cytokines investigated during this work, with a brief summary of the source and function of these cytokines.

Table 5-1. Investigated cytokines involved in the innate immune system

Cytokine	Source	Function
IL-2	Th1 T-cells	Activation of lymphocytes, NK cells and macrophages
IL-6	Th2 T-cells and macrophages	Activation of lymphocytes, differentiation of B cells, stimulating production of acute-phase proteins
IL-8	T-cells and macrophages	Chemotaxis of neutrophils, basophils, DCs and T cells
IL-10	Monocytes and Lymphocytes	Inhibiting synthesis of pro-inflammatory cytokines
TNFα	Macrophages, NK cells, T-cells, B-cells, and Mast cells	Promotion of inflammation
GM-CSF	T-cells, macrophages, NK cells, and B-cells	Promotion of the growth of granulocytes and macrophages
IFNα IFNβ	Virally infected cells, NK cells, B-cells and T-cells, pDCs (maximal IFNα), macrophages, fibroblasts, endothelial cells, osteoblasts	Innate immune response against viral infection Resistance to virus
IFNγ	NK and NK-T cells, Th1 T-cells, $CD8^{+ve}$ CTLs	Innate and adaptive immunity against viral and intracellular bacterial infections Tumor control Activation of macrophages and inhibition of Th2 T-cells

5.1.1.4 NK cell degranulation and perforin-mediated killing

Activated NK cells can be recognised by the expression of CD69 [212]. Upon activation, NK cells produce cytokines and cytotoxic granules containing perforin and granzyme (see figure 5-1). Perforin is a pore-forming molecule that enables granzymes to enter target cells. Granzymes are serine proteases which can induce apoptosis by cleaving caspase II [14, 213]. This process of release of antimicrobial cytotoxic molecules from secretory vesicles is referred to as 'degranulation' and 'degranulated' cells may be characterized by the expression of cellular antigens CD107a/b.

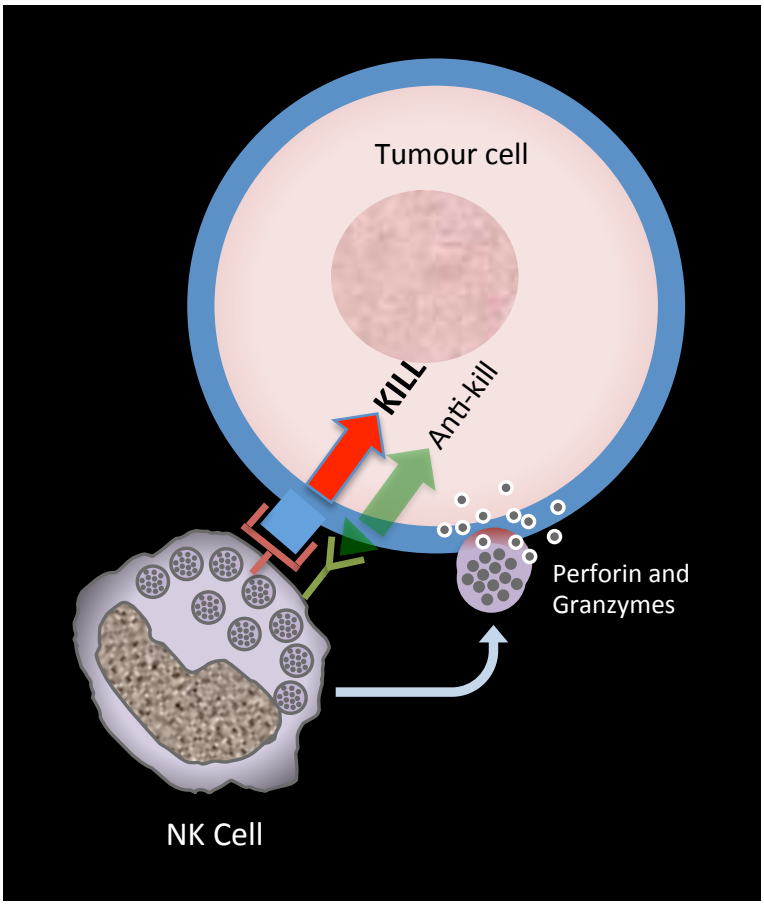

Figure 5-1. NK cell activity

Tumour cells can, for example, lose MHC-I expression, and hence a 'Kill' signal is initiated, which leads to the release of cytolytic granzymes, which are packaged within endosomes in the NK cell cytoplasm. The release of perforin enzymes causes the tumour cell membrane to fuse with the endosome, and releases granzymes into the tumour cell, resulting in death by apoptosis.

5.1.2 Dendritic Cells

Dendritic cells (DCs) are antigen presenting cells (APC), that are a key component of the innate immune system. DCs are derived from bone marrow progenitor cells, and exist in the mature (mDC) and immature (iDC) state [214]. iDCs constantly survey the surrounding environment, and usually become activated at the site of pathogenic entry (by 'danger signals') utilising pattern recognition receptors (PRR) such as the toll-like receptors (TLR). GM-CSF leads to recruitment and maturation of DCs, and thus improves antigen presentation by DC [215]. This is important in the context of oncolytic virotherapy, and the transfection of GM-CSF into several OVs such as HSV, MV and VV (including JX-594) has resulted in improved anti-tumour immune responses [216]. Upon activation, DCs migrate to the draining lymph node, activating lymphocytes by presenting processed antigens via major-histocompatibility-complex molecules.

DCs form a group of antigen presenting cells (APCs) known as 'professional' APCs, which efficiently internalise an antigen, either by phagocytosis or by receptor-mediated endocytosis, and display these antigens complexed with major histocompatibility complex (MHC) on their surfaces. T-cells are unable to recognise 'free' antigen, but can recognize these complexes, leading to initiation of an adaptive response.

5.1.3 Cross-talk

NK cells and DCs play a synergistic role in the anti-tumour immune response. Direct tumour cytotoxicity of NK cells can release TAAs into the tumour micro-environment, along with inflammatory cytokines and danger signals, thereby

activating DCs, including through IFN-γ and TNF-α dependant mechanisms. Reciprocally, DCs can activate NK cells through cytokines such as IL-12 and IFNα. [15] [217]. Cell-to-cell interactions play an important role in NK cell activation, and it has been demonstrated that contact-dependent interactions (using eg trans-well separation) between activated human NK cells and immature DCs provide a "control switch" for the immune system [217] [218].

5.1.4 Liver-specific lymphocytes

The immunological environment within the human liver is unique; it receives constant antigenic stimuli from gut-derived antigens, which does not result in inflammation. Up to 30–50% of all human hepatic lymphocytes are NK cells, which are preferentially located in the hepatic sinusoids [219]. Kuppfer cells, unique to the liver, secrete chemokines CCL2, CCL3 (MIP1α) and CXC-chemokine ligand 10 (CXCL10), which attract NK cells into the liver [220]. However, Kuppfer cells have been shown to secrete high levels of IL-10 in response to gut-derived LPS, which can lead to decreased NK cell activation [219]. Tu *et al*. used a novel method to isolate lymphocytes from the liver, by perfusion of living donor liver lobes prior to transplantation (n=5). They found that the healthy human liver was a site of intense immunological activity, with activated lymphocytes compared to those from peripheral blood in the same donors. There were increased numbers of NK cells, which were in a higher state of activation (CD69; 80% vs 7% in PBMCs) and increased numbers of $CD56^{+ve}$, $CD4^{+ve}$ and $CD8^{+ve}$ T cells [221].

The clinicopathological significance of tumor-infiltrating lymphocytes (TILs) is well recognised [222, 223] but typically, NK cells are found in only small numbers in advanced human neoplasms. In patients with multiple liver metastases from gastric and colonic primaries, fewer intratumoural $CD56^{+ve}$ cells were detected compared

to those with single metastases, and a reduced number of intrahepatic $CD56^{+ve}$ cells was observed in patients with metastases compared to those without [224]. Hence, this suggests that low NK cell numbers could result in the 'escape' of metastatic malignant cells from immune control within the liver. Within most human tumours, the phenotype of NK cells is immunosuppressive, with an overexpression of inhibitory receptors such as NKG2A, and an underexpression of activating receptors such as CD16, NKG2D, NKG2C and NKp30 [225].

5.1.5 Oncolytic viruses to activate innate anti-tumour immunity

OVs may present an immunological 'trigger' to activate innate immune cells, particularly in the tumour microenvironment, where replication of OVs is most prolific. It has been demonstrated that iv VV therapy following colorectal cancer resection in humans resulted in enhanced NK cell function [226]. This chapter investigated the ability of JX-594 to activate human NK cells *in vitro*.

5.2 Phenotypic analysis of NK cells

In order to select the NK cell population during flow cytometric analysis, the lymphocyte population is selected (or 'gated') using a forward –scatter (FSC) (cell mass) vs side-scatter (SSC) (cell density/granularity) box-plot. This relies on pattern recognition of known cellular properties to 'gate' around the population of interest. This 'gate' is applied onto a CD3 (PerCP) / CD56 (PE) histogram and NK cells are defined as the $CD3^{-ve}CD56^{+ve}$ cell population. The gating strategy is shown in Figure 5-2, with the 'R4' gate selecting the lymphocyte population. The significance of the R1, R2 and R3 gates will be discussed later.

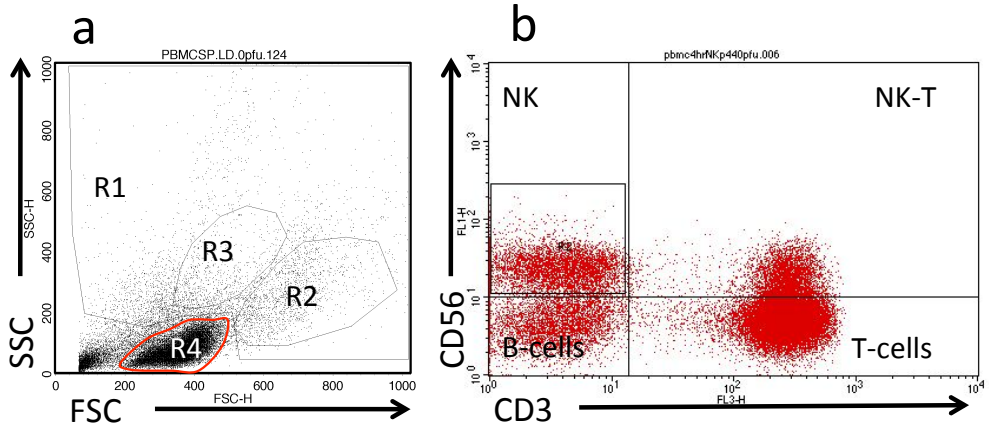

Figure 5-2. Selection of sub-population of immune cells within PBMCs

Figure shows a box plot of Forward Scatter (FSC) versus side-scatter (SSC) (a). The gating strategy for all experiments is shown here. R1; all non-lymphocyte population, mainly consisting of monocytes, R2; All viable Monoctyes, R3; population shift following activation of monocytes with JX-594, R4; lymphocytes. In Figure 5-2 b, The R4 lymphocyte population has been selected and box-plot of CD3 vs CD56 obtained. The NK cell population can be selected as the CD3-ve and CD56+ve population.

5.3 JX-594 treatment of PBMCs leads to activation of NK cells

In order to determine the effect of JX-594 on immune cells, first fresh whole blood was collected from healthy donors and patients undergoing resection for CRLM. PBMCs were isolated by density gradient centrifugation, treated *in vitro* with JX-594-GM-CSF for 24 hours and flow cytometry used to determine the percentage of NK cells expressing CD69. Whole PBMCs were used, rather than isolated NK cells, as this is more comparable to the clinical scenario *in vivo*. Figure 5-3 shows the upregulation of CD69 in NK cells from healthy donors, and there is a significant increase in % of NK cells expressing CD69 compared to untreated controls following treatment with 0.1 pfu/cell JX-594-GM-CSF (15% vs 36%) or 1 pfu/cell JX-594-GM-CSF (15% vs 34%). There was a marginally better overall response following treatment at 0.1 pfu/cell ($p<0.01$ vs untreated control) and treatment at 1 pfu/cell ($p<0.05$ vs untreated control). The response following JX-594-GM-CSF treatment compared well to that following treatment with Reovirus (42% CD69 expressing NK cells), which is known to be highly immunogenic. To determine whether a similar response was observed in patients with metastatic colorectal cancer, PBMCs from patients were also treated with JX-594 and a similar pattern of CD69 upregulation was observed (figure 5-4); however the response did not reach significance compared to untreated control (13%, 33% and 33% for 0 pfu/cell, 0.1 pfu/cell and 1 pfu/cell respectively, $p>0.05$ in all cases). Again, the response remained similar to that of Reovirus treated PBMCs (30%). In both healthy donors (figure 5-3b) and patients (figure 5-4b), there was a viariable response, with some non-responders.

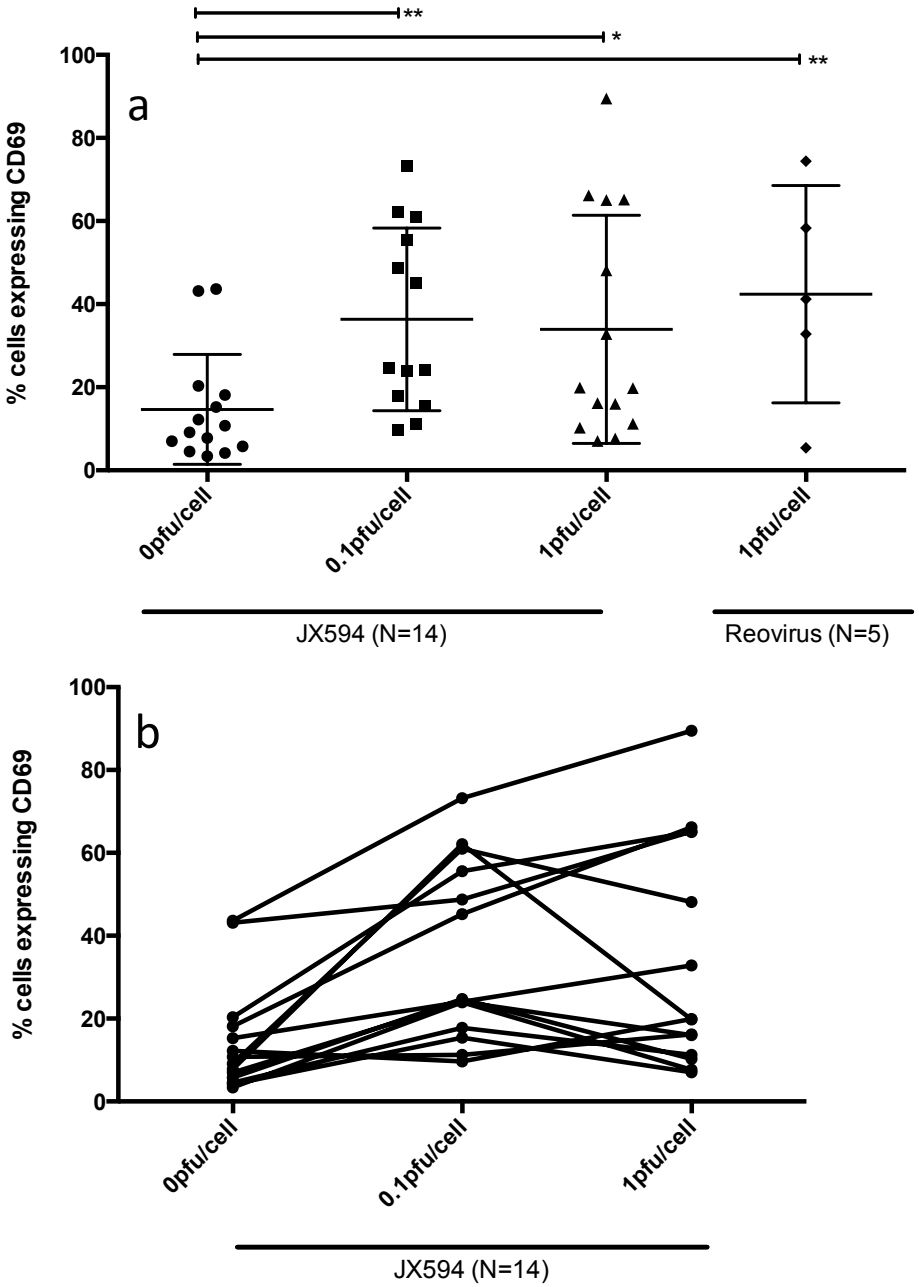

Figure 5-3. Treatment of whole healthy-donor-derived PBMCs with JX-594 *in vitro* results in NK cell activation as demonstrated by CD69 upregulation

Fresh whole blood was sampled from healthy donors, PBMCs were isolated by centrifugation over lymphoprep gradient and PBMCs treated with JX-594 at 0, 0.1 and 1 pfu/cell and Reovirus at 1 pfu/cell (positive control). The percentage of cells expressing CD69 was demonstrated by flow cytometry. Experiments were carried out between N=3 and N=14 and bars show the mean +/- SD * indicate significant reduction in viability; *p<0.05, **p<0.01.

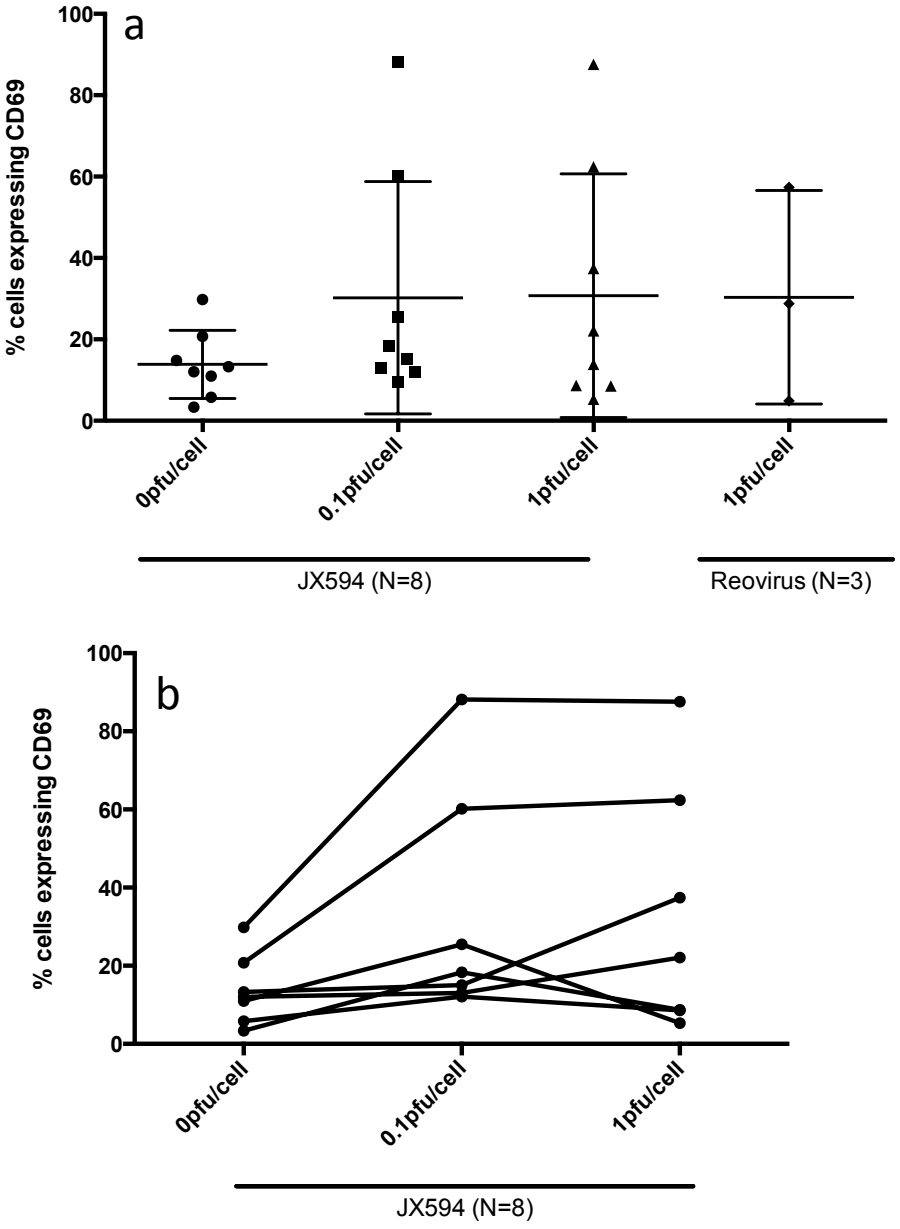

Figure 5-4. Treatment of whole patient-derived PBMCs with JX-594 *in vitro* results in NK cell activation as demonstrated by CD69 upregulation

Fresh whole blood was sampled from patients undergoing liver resection for CRLM, PBMCs were isolated by centrifugation over lymphoprep gradient and PBMCs treated with JX-594 at 0, 0.1 and 1 pfu/cell and Reovirus at 1 pfu/cell (positive control). The percentage of cells expressing CD69 was demonstrated by flow cytometry. Experiments were carried out between N=3 and N=8 and bars show the mean +/- SD.

5.4 JX-594 treatment does not lead to upregulation of activatory receptors on NK cells

NK cells express activatory receptors, which when bound to ligands on potential target cells, can result in activation of the NK cells. Up-regulation of these activatory markers may lead to more potent NK cell cytotoxiocity, if the targets express appropriate ligands.

Figure 5-5 shows that the majority of NK cells (>75%) from healthy donors (figure 5-5 a and c) and patients with CRLM (figure 5-5 b and d) expressed NKG2D and DNAM. There was no significant increase in percentage of cells expressing these markers or the staining mean fluorescence intensity (data not shown) following treatment with JX-594. Potentially, there is a marginal decrease in NKG2D expression on NK cells from patients; however, the small number of samples (N=3) makes this difficult to confirm. Figure 5-6 shows that the majority of NK cells expressed the receptors NKp30 and NKp46, but not NKp44. There was no significant increase in percentage of cells expressing these markers or the mean fluorescence intensity (data not shown) following treatment with JX-594. There was a marginally decreased expression of NKp46 on NK cells from patients, although this was only in a single experiment .

Thus, although there was an increase in surface CD69 expression on NK cells (and hence activation) following JX-594 treatment, there was no change in NK receptor expression.

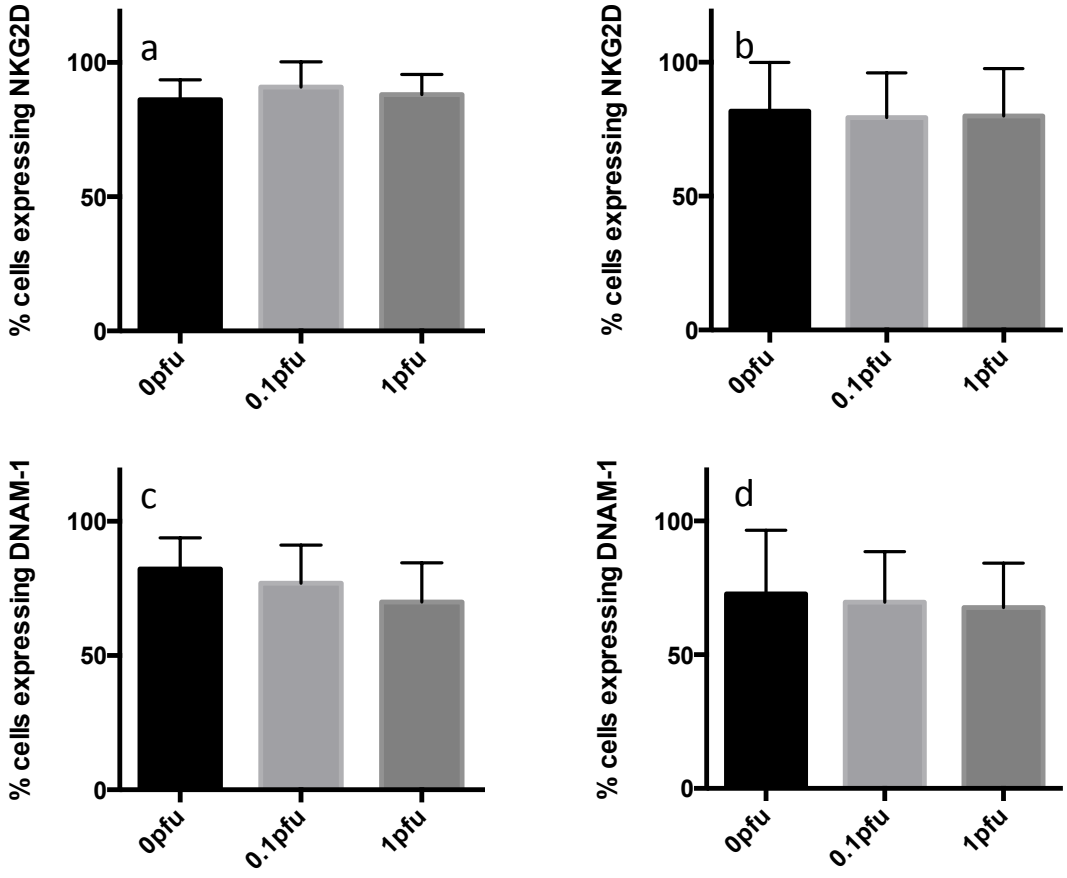

Figure 5-5. JX-594 treatment *in vitro* does not upregulate activatory receptors NKG2D and DNAM-1 on NK cells

Fresh whole blood was sampled from healthy volunteers (a and c) and patients undergoing liver resection for CRLM (b and d). PBMCs were isolated by centrifugation over lymphoprep gradient and treated with JX-594 at 0, 0.1 and 1 pfu/cell. The percentages of cells expressing the activatory receptors NKG2D and DNAM-1 were determined by flow cytometry. Experiments were carried out in triplicate (N=3 donors) and bars show the mean + SD.

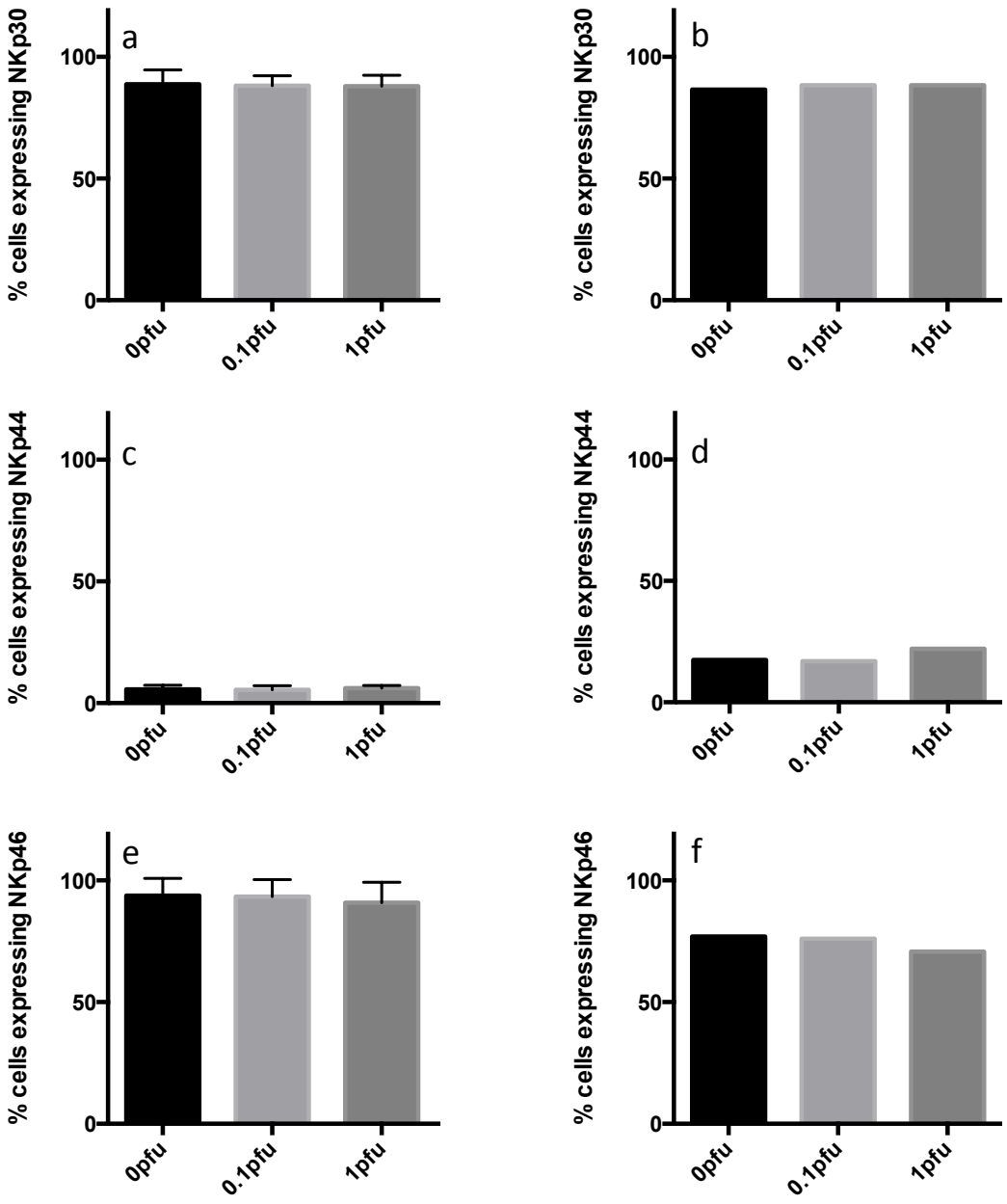

Figure 5-6. JX-594 treatment *in vitro* does not upregulate activatory receptors NKp30, NKp44 and NKp46 on NK cells

Fresh whole blood was sampled from healthy volunteers (a, c and e) and patients undergoing liver resection for CRLM (b, d and f). PBMCs were isolated by centrifugation over lymphoprep gradient and treated with JX-594 at 0, 0.1 and 1 pfu/cell. The percentages of cells expressing the activatory receptors NKp33, NKp44 and NKp46 were determined by flow cytometry. Experiments were carried out in triplicate (N=3) for healthy donors and a single experiment for patient sample (N=1) and bars show the mean + SD.

5.5 JX-594-treatment of PBMCs stimulates NK cell degranulation in response to CRC cell targets

NK-cell mediated killing requires the release of granules, a process known as degranulation, which can be characterised *in vitro* by the expression of surface CD107. PBMCs from healthy donors and patients undergoing resection for CRLM were treated overnight with JX-594-GM-CSF. JX-594-GM-CSF treated PBMCs and untreated controls were co-cultured with near-confluent CRC cells (SW480 and SW620) and K562 cells, which served as a positive control (see section 2.12.1). Figure 5-7a) shows that untreated NK cells degranulated appropriately against K562 targets (42%), which responded positively (up to 56%, non-significant) to JX-594 treatment. In figure 5-7b), PBMCs from healthy donors exhibited small increase in percentage of cell degranulating in response to JX-594 treatment without exposure to any CRC targets (12% following treatment with 1 pfu/cell JX-594). When exposed to SW480 and SW620 targets, untreated NK cells from both healthy donors and patients showed increased degranulation compared to no-target controls. When PBMCs from healthy donors were treated with 0.1 pfu/cell JX-594, NK cells from healthy donors degranulated against SW480 and SW620 targets, although there was no significant difference with virus (30% against SW480 and 38% SW620, $p>0.05$ vs untreated control in both cases). However, following treatment with 1 pfu/cell JX-594, there was a significant increase in percentage of NK cells degranulating against SW480 cells, but not SW620 cells. Significantly, NK cells from patients treated with JX-594 exhibited a greater response than those from healthy donors (figure 5-7 c). There was a significant increase in percentage of NK cells degranulating against SW480 targets with 0.1 pfu/cell treatment (51%, $p<0.005$) and 1 pfu/cell treatment (42%, $p<0.05$), and against SW620 targets with 0.1 pfu/cell treatment (50%, $p<0.005$) and 1 pfu/cell treatment (42%%, $p<0.01$).

Hence, these experiments show that JX-594 treatment may enhance NK cell degranulation against CRC tumour cells in patients.

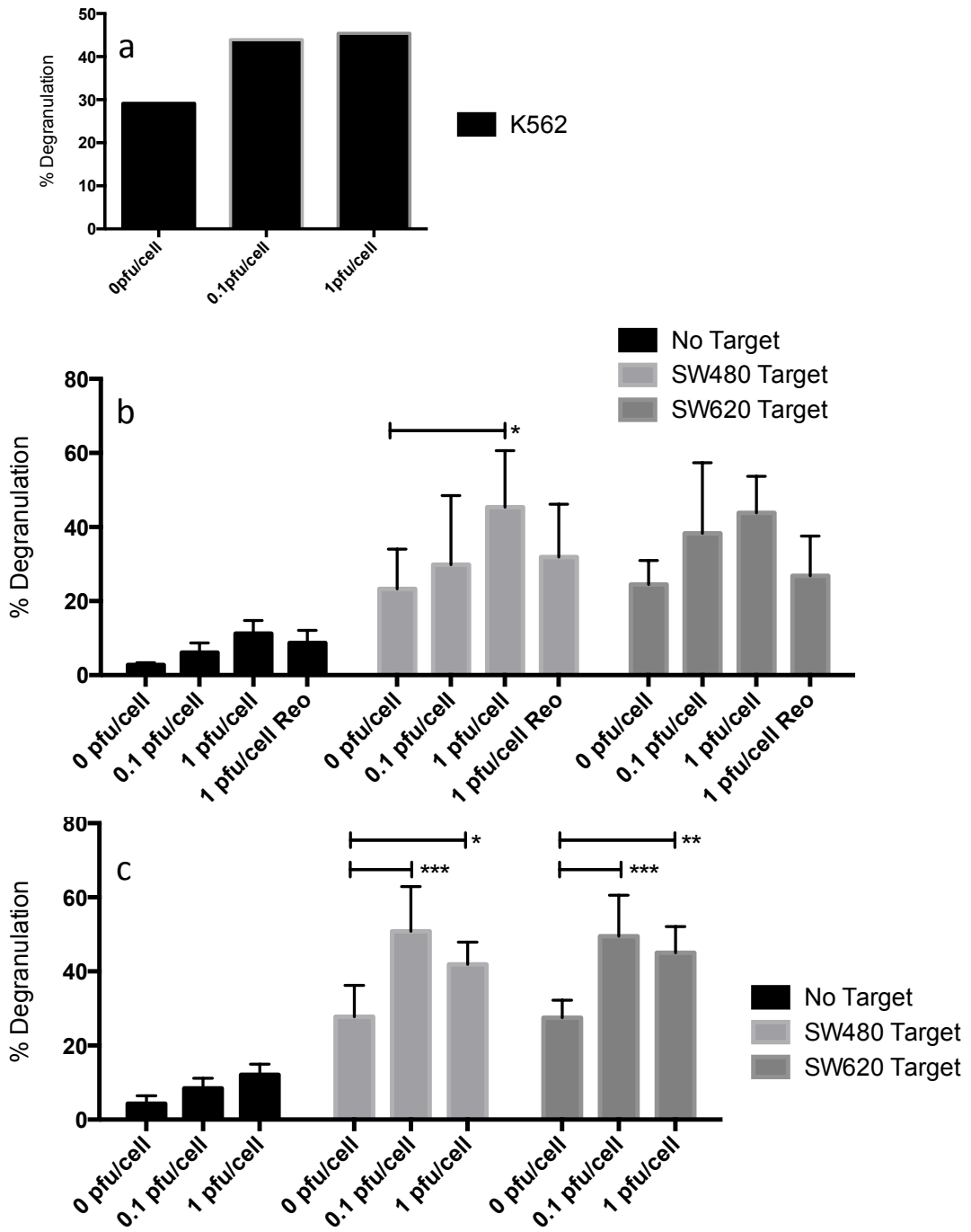

Figure 5-7. JX-594-treatment increases NK cell degranulation against CRC targets.

Fresh whole blood was sampled from healthy volunteers (a and b) and patients undergoing liver resection for CRLM (c). PBMCs were isolated by centrifugation over lymphoprep gradient, treated overnight with JX-594 at 0, 0.1 and 1 pfu/cell and in some cases Reovirus at 1 pfu/cell (as a potential positive control), and co-cultured for 4 hours with SW480 and SW620 cell lines at an effector: target ratio of 10:1 (b and c) with K562 targets as a positive control (a). CD107a/b expression was measured by flow cytometry within the gated NK cells. Experiments were carried out in triplicate (N=3 donors) and bars show the mean + SD. * indicate significant reduction in viability; *$p<0.05$, **$p<0.01$, **$p<0.005$.

5.6 JX-594-treatment of PBMCs activates NK cells to kill CRC cell targets, which is perforin/granzyme mediated.

In order to determine if activated NK cells were able to kill tumour targets, and furthermore, to investigate the mechanism of killing, ^{51}Cr-release assays were utilised (see section 2.12.2). PBMCs from healthy volunteers were treated overnight with JX-594 at 0, 0.1 and 1 pfu/cell. Near confluent CRC cell lines (SW480 and SW620) were labelled with ^{51}Cr, and co-cultured with PBMCs at various effector:target ratios. Figure 5-8a) shows that at all effector/target ratios, PBMCs were cytotoxic against SW480 cells, and increased killing was seen at higher effector:target ratios and after treatment with JX-594. For example, at an effector to target ratio of 100:1, PBMCs treated with 0.1 pfu/cell JX-594-GM-CSF killed 44% of SW480 cells vs 24% in the untreated control ($p<0.0001$). A similar response was evident against SW620 cells; at a ratio of 100:1, cells treated with 0.1 pfu/cell JX-594-GM-CSF killed 40% of SW480 cells vs 23% in the untreated control ($p<0.01$). At all effector:target ratios, against both SW480 and SW620 targets, a higher treatment dose of 1 pfu/cell did not result in a significant increase in killing compared to untreated control; at 100:1 effector:target ratio, 24% vs 30% against SW480 cells, and 23% vs 30% against SW620 cells. In order to determine if the mechanism of killing was perforin/granzyme mediated, the assay was repeated in the presence of ethylene glycol tetraacetic acid (EGTA) (N=2), a calcium chelator which blocks perforin-mediated killing (figure 5-8 c and d). EGTA blocked all killing from PBMCs irrespective of JX-594 treatment (at all effector:target ratios, but only data for 100:1 shown). A similar increase in PBMC-mediated killing was observed after JX-594 treatment in these experiments in the absence of EGTA. Hence, JX-594 treatment can increase PBMC-mediated killing of CRC cells, which is mediated by perforin/granzyme. These findings, along with results of degranulation

experiments, support the role of NK cells in the JX-594 activated killing of CRC cell targets.

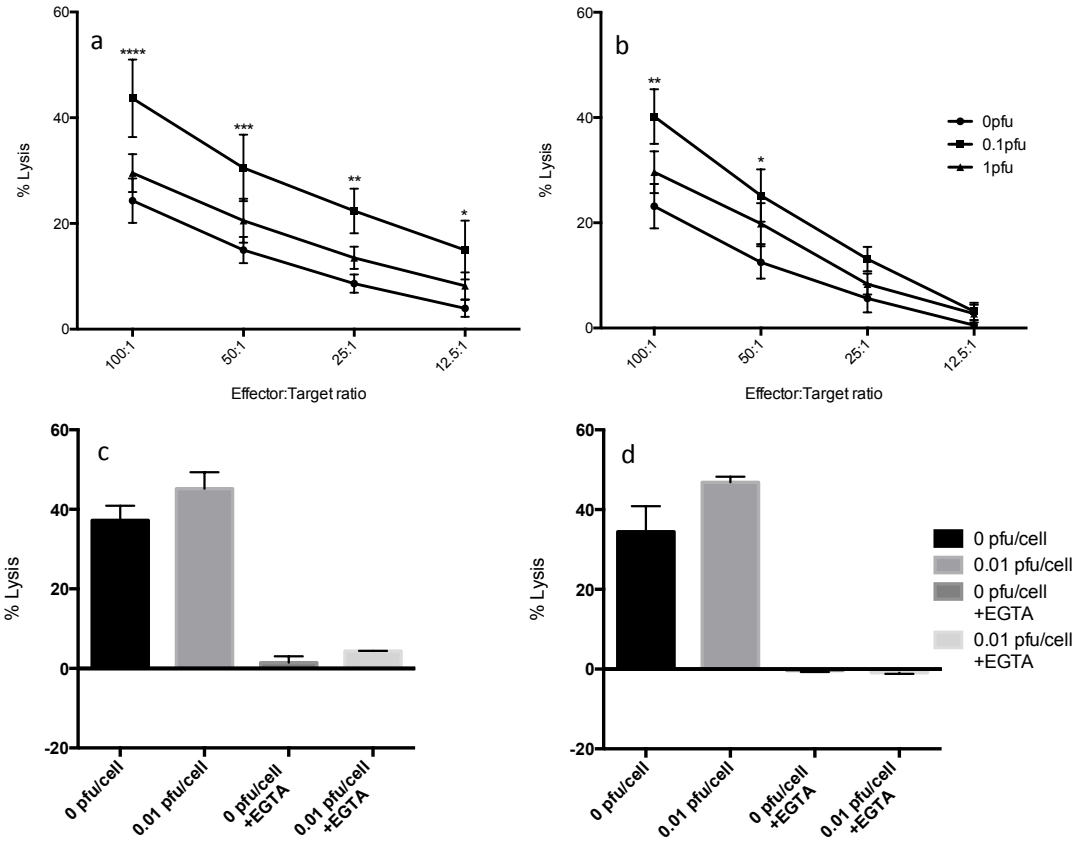

Figure 5-8. JX-594-treated PBMCs kill CRC targets, in a perforin/granzyme dependant process.

PBMCs were isolated from healthy volunteers, treated overnight with JX-594 at 0, 0.1 and 1 pfu/cell, and co-cultured at various effector:target ratios for 4 hours with SW480 (a and c) and SW620 (b and d) cell lines which had been labelled with ^{51}Cr (N=3). Chromium release from labelled CRC cells was measured to determine PBMC-mediated CRC cell killing. The assay was repeated in the presence of EGTA (c and d, N=2) to block perforin-mediated killing; data is shown at 100:1 effector:target ratio only. * indicate significant reduction in viability compared to untreated controls; * $p<0.05$, ** $p<0.01$, ***$p<0.005$, ****$p<0.0001$.

5.7 PBMCs/Lymphocytes do not support JX-594 replication

The most commonly utilised route for delivery of JX-594 in the most recent trials is intravenous delivery. The results detailed in this chapter so far suggest that JX-594 may be beneficial in activating innate anti-tumour immunity. However, before suggesting this finding contributes to the therapeutic potential of JX-594, it was important to elucidate if the virus was capable of infecting and replicating within these immune effector cells. PBMCs were isolated from 5 healthy donors and treated with 0, 0.1 and 1 pfu/cell JX-594-GFP (N=2) or JX-594-GM-CSF (N=3) for 24 and 48 hours. PBMCs treated with JX-594-GM-CSF were subjected to three cycles of freeze/thaw (cells and supernatant) to lyse the cells and release cell-associated virus, and a plaque assay performed to examine replication; none was found (data not shown). In addition, PBMCs treated with JX-594-GFP were fixed in 1% PFA and GFP expression in gated lymphocytes determined by flow cytometry. Figure 5-9 shows that JX-594-derived GFP was expressed in less than 2% of lymphocytes, suggesting that JX-594 does not exhibit any significant replication within lymphocytes, and possibly only early phase transcription/translation in a small number of cells.

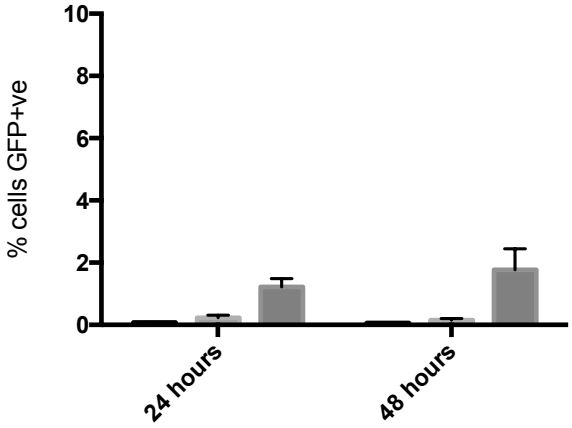

Figure 5-9. JX-594 does not replicate in gated lymphocytes

PBMCs were isolated from healthy volunteers and treated with JX-594 at 0, 0.1 and 1 pfu/cell for 24 and 48 hours. PBMCs were harvested and gated lymphocytes analysed by flow cytometry (N=2) to examine the expression of virally-derived GFP.

5.8 JX-594 treatment of PBMCs does not significantly decrease viability

The lack of replicative ability of JX-594 within lymphocytes is important for its promotion as an intravenous agent; however, it must also be demonstrated that there is no toxicity to PBMCs. To address this, PBMCs from three healthy donors were treated with 0, 0.1 and 1 pfu/cell JX-594- GM-CSF for 24, 48 and 72 hours, and cell viability was determined using a Live/dead® PE-conjugated dye and flow cytometry (figure 5-10). There was a small decrease in viability in untreated cells over time (99% to 83%) as expected, but importantly, no increased loss in viability of lymphocytes was observed after treatment with JX-594.

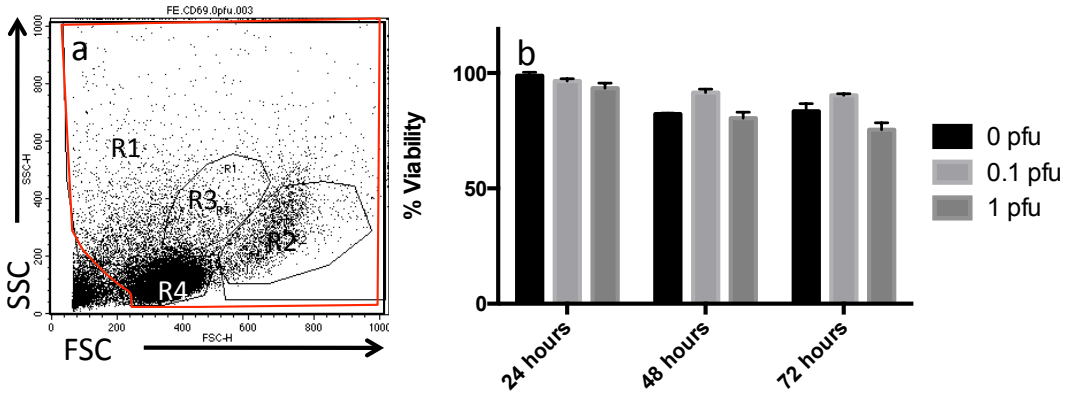

Figure 5-10. Viability of PBMCs following *in vitro* treatment with JX-594

PBMCs from healthy volunteers were treated with JX-594 at 0, 0.1 and 1 pfu/cell for 24, 48 and 72 hours. The entire cell population was selected (a) and cell viability of R4 lymphocytes was evaluated by Live/Dead® method (b). Data is presented as the mean +SD of N=3.

5.9 CD14+ve monocytes are required for JX-594 mediated activation of NK cells

Based on the understanding of 'cross-talk' between various sub-populations within PBMCs, we next investigated whether the activation of NK cells was dependant on other PBMC cell populations. PBMCs from seven healthy volunteers and three patients undergoing resection for CRLM were isolated. Using magnetic beads, NK cells and $CD14^{-ve}$ PBMCs were isolated by negative selection (NK cells) and $CD14^{+ve}$ cells removed by positive selection (see figure 5-11). In all five donors, the three populations of cells (whole PBMCs, purified NK cells and $CD14^{-ve}$ PMBCs) were treated with JX-594-GM-CSF at 0 pfu/cell, 0.1 pfu/cell and 1 pfu/cell for 24 hours and CD69 expression determined by flow cytometry. A reovirus positive control was used in experiments with whole PBMCs only, due to the small number of $CD14^{-ve}$ PBMCs and NK cells collected during the isolation procedure.

Figure 5-12 shows that $CD14^{+ve}$ monocytes are required for activation of NK cells within PBMCs. Histograms a) and b) show that after removing the $CD14^{+ve}$ population (figure 5-12 b), there was no upregulation in CD69 expression on NK cells following JX-594 treatment; interestingly reovirus treatment still resulted in NK cell activation. In healthy donors (figure 5-12 c – e), the percentage of NK cells expressing CD69 within whole PBMCs increased from 6% to 33% following treatment of whole PBMCs with 0.1 pfu/cell JX-594-GM-CSF ($p<0.05$). In purified NK cells and $CD14^{-ve}$ PBMCs there was no appreciable increase in CD69 following treatment (NK cells; 3% to 8%, $CD14^{-ve}$ cells; 4% to 6%). In patients, a similar finding was observed, with an upregulation of NK cell CD69 expression in whole PBMCs following treatment with 0.1 pfu/cell JX-594-GM-CSF (7% vs 18%, $p>0.05$) but not with purified NK cells (13% vs 13%) or $CD14^{-ve}$ PBMCs (3% vs 3%).

Figure 5-13 shows that JX-594 treatment of whole PBMCs not only resulted in CD69 upregulation on NK cells, but also downregulated CD14 expression on monocytes (R1 gate). There was a significant decrease in the percentage of PBMCs expressing CD14 following treatment with 1 pfu/cell compared to untreated PBMCs (38% vs 6%, $p<0.005$). A similar downregulation of CD14 was not evident following 1 pfu/cell Reovirus treatment. This CD14 downregulation was also evident following treatment of whole PBMCs from patients with CRLM, although the difference between untreated PBMCs and those treated with 1 pfu/cell JX-594 did not reach significance (18% vs 2%). The results thus indicate that JX-594 and Reovirus both activate NK cells, but via different mechanisms, with $CD14^{+ve}$ monocytes playing a significant role in the context of JX-594 treatment.

Little is known about the interaction of PBMCs with oncolytic viruses, particularly with regards to the findings illustrated in figures 5-13 and 5-14 - the requirement of $CD14^{+ve}$ monocytes within a whole PBMC population for JX-594-driven innate immune activation. Here we demonstrate that JX-594 requires $CD14^{+ve}$ monocytes to activate NK cells, and that this interaction is associated with loss of monocyte CD14 expression.

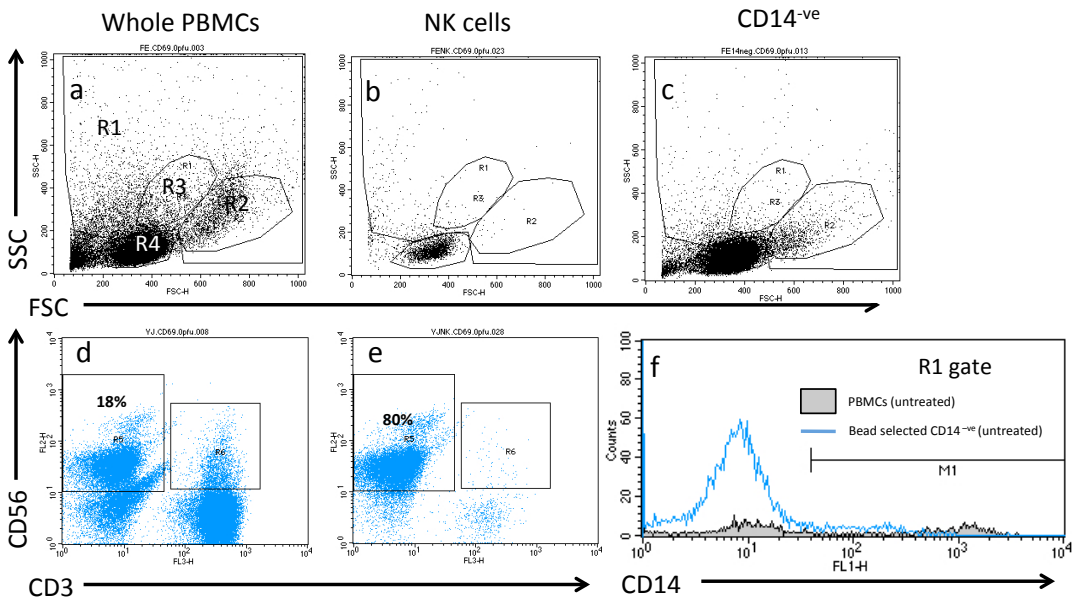

Figure 5-11. Bead purification of NK cells and CD14^{-ve} cells

Figure shows representative images of the outcome of the bead purification of whole PBMCs (a and d) to isolate NK cells (b and e) and CD14^{-ve} PBMCs (c and f). The NK cell (CD3^{-ve}CD56^{+ve}) isolation protocol resulted in 80% purity as depicted by the box-plots b) and e), with a reduction in density of the R4-gated lymphocyte population (b), due to the loss of the CD3^{+ve} and CD56^{-ve} populations (e). The selection of the CD14^{-ve} population is depicted by plot c) and histogram f), which shows the loss of the CD14^{+ve} population in gate R1.

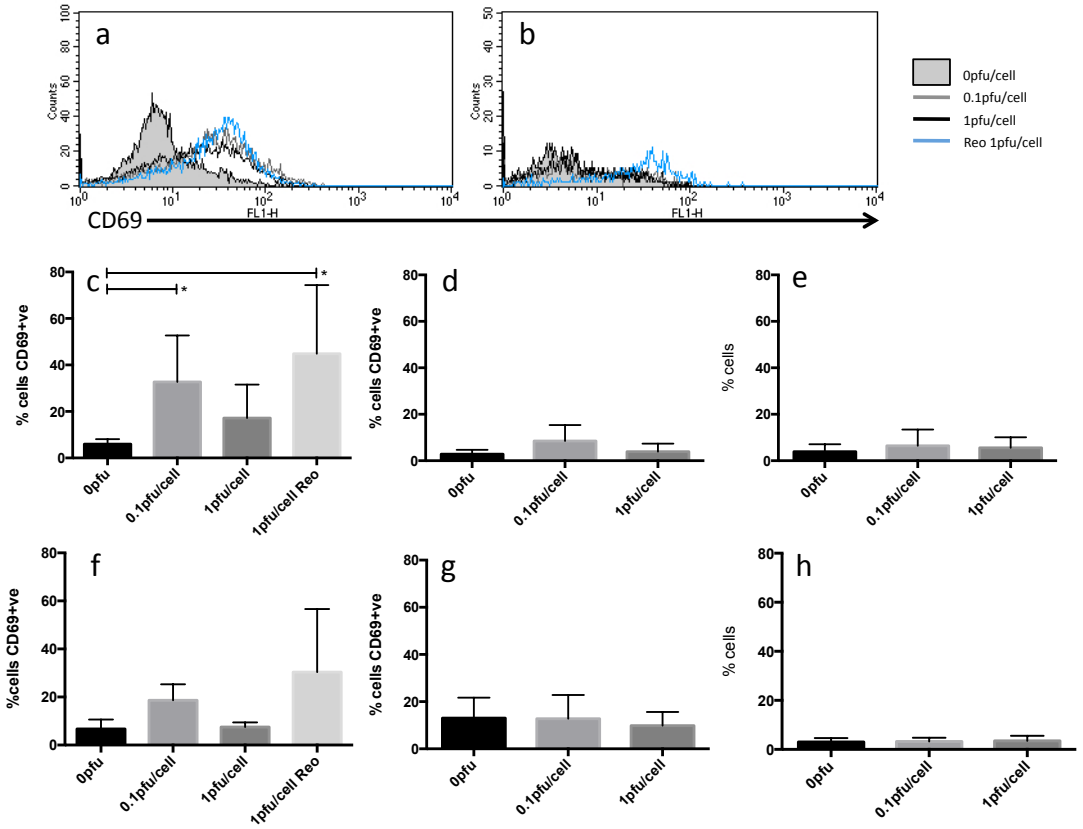

Figure 5-12, CD14+ve monocytes are required for JX-594 mediated activation of NK cells within whole PBMCs

Fresh whole blood was sampled from healthy donors (a - e) and patients undergoing liver resection for metastatic CRC (f - h), and PBMCs were isolated by centrifugation over lymphoprep gradient; cell populations were separated using magnetic beads. Whole PBMCs (a, c and f), purified NK cells (d and g) and $CD14^{-ve}$ PBMCs (b, e and h) were treated with JX-594 at 0, 0.1 and 1 pfu/cell and, where indicated, Reovirus at 1 pfu/cell for 24 hours. Surface expression of CD69 was quantified by flow cytometry and data expressed as a histogram of CD69 expression (a, b; representative histogram from a single patient) and % cells expressing CD69 (c – h). Experiments were carried out in 7 healthy donors and 3 patients and data is presented as the mean +SD. * signifies significant difference, $p<0.05$.

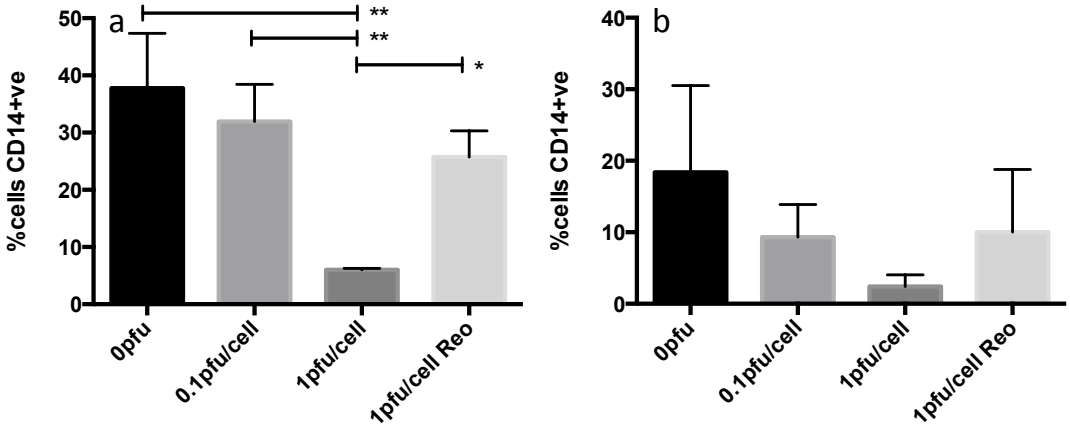

Figure 5-13. Monocytes downregulate CD14 expression in response to JX-594 infection *in vitro*

PBMCs from healthy donors (a) and patients undergoing liver resection for metastatic CRC (b) were treated with JX-594 at 0, 0.1 and 1 pfu/cell and Reovirus at 1 pfu/cell for 24 hours. Percentage of cells in gate R1 expressing surface CD14 was quantified by flow cytometry. Experiments were carried out in quintuplicate (N=5) data is presented as the mean +SD. * signifies significant difference; * $p<0.05$, ** $P<0.01$.

5.10 JX-594 treatment of PBMCs results in a 'shift' of the monocyte population, but not death

During flow cytometric analysis, in addition to the finding of a downregulation of CD14 expression, a ' left shift' in the FCS vs SSC dot-plots of the apparent monocyte population was observed following JX-594 treatment, with some of the monocytes becoming smaller (↓FSC) and more granular (↑SSC). Hence, a careful gating strategy was developed to identify these sub-populations for future analyses (figure 5-14 a - d). Firstly, it was important to determine whether this change in size and granularity was due to a change in morphology, or cell death. A Live/Dead® assay and Active-Caspase 3 assay kit were used to determine PBMC death by flow cytometry. Histogram 5-14 e) shows that in the R1 gate, there was a small population of cells that were dead, although this did not increase significantly following JX-594 treatment (figure 5-14 f). Importantly, in gate R3 ('shifted' monocyte population) there were <10% dead cells, and this did not change with JX-594 treatment. Figure 5-14 g) shows that no more than 2% of cells were positive for active caspase-3, and hence there was no appreciable JX-594-induced apoptosis.

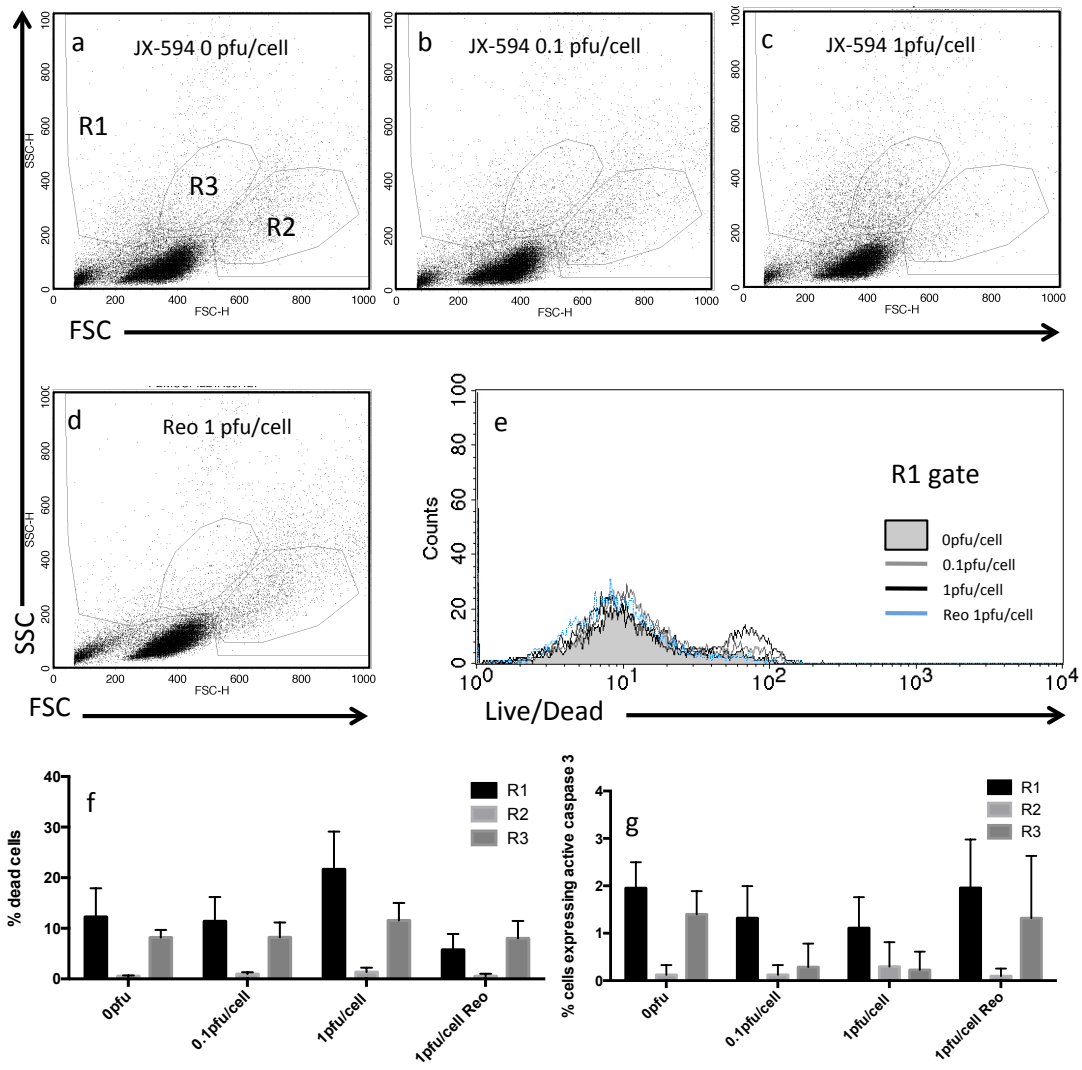

Figure 5-14. JX-594 treatment results in a 'shift' in the apparent monocyte population, and the emerging cell population is viable.

PBMCs from healthy volunteers were isolated and treated with JX-594 at 0, 0.1 and 1 pfu/cell and Reovirus at 1 pfu/cell (comparision) for 24 hours. During flow cytometry, the gating strategy R2 and R3 (a – d) was used to separate the shifting cell population (R2 ➔R3) following JX-594 treatment, and R1, the whole monocyte population. Viability of PBMCs was analysed by Live/Dead® assay (e; representative histogram, f; summary bar chart) and Active-Caspase 3 assay kit (g). Experiments were performed in 3 donors and bars show the mean + SD.

5.11 JX-594 treatment of PBMCs results in differentiation of monocytes towards an antigen presenting phenotype

Once it had been established that the 'shifted' monocyte population of cells were not dead, the phenotype of these cells was characterised. PBMCs were isolated from three healthy donors and three patients undergoing resection for CRLM and treated for 24 hours with JX-594 at 0, 0.1 and 1 pfu/cell JX-594, and 1 pfu/cell Reovirus, harvested, and expression of CD14/CD11c/CD86/ClassIIDR/CD80 determined by flow cytometry. Figures 5-15 to 5-20 show that monocytes treated with JX-594 differentiated towards an antigen-presenting phenotype. In figure 5-15, in the population of interest (R3 gate), there is an emergence of $CD11c^{+ve}$ cells in all three healthy donors (figure 5-15, b - d) following JX-594 treatment, but not Reovirus treatment. Although analyzing the cells within the R3 gate specifically studies the population of interest, it does not give any information on the dynamic shift of cells from gates R2 to R3; hence for all future analyses depicted in figures 5-16 to 5-20, the cells within the whole non-lymphocyte R1 gate were anaylsed and all dot plots divided into quadrants based on CD14 expression and the expression of the investigated APC markers (CD11c/CD86/ClassIIDR/CD80). Figures 5-16 to 5-19 show representative data for a single experiment, whilst figure 5-20 shows summary data. Figures 5-16 (representative donor), appendix C and figure 5-20 a) show that JX-594 treatment shifted monocytes towards a $CD14^{-ve}$ $CD11c^{+ve}$ phenotype, with an average increase from 37% (untreated) to 71% (1 pfu/cell) ($p<0.005$) in $CD14^{-ve}CD11c^{+ve}$ cells, a finding that was not observed following Reovirus treatment ($p<0.001$). A similar finding was observed in patients' monocytes (figure 5-20 b), with an increase in $CD14^{-ve}CD11c^{+ve}$ cells from 26% to 49% ($p>0.05$), which was again significantly different to Reovirus. In figure 5-17, appendix C and figure 5-20 c) and d) the shift towards a $CD14^{-ve}CD86^{+ve}$ phenotype following JX-594 treatment was demonstrated, with an average increase from 40%

(untreated) to 73% (1 pfu/cell) $CD14^{-ve}CD86^{+ve}$ cells ($p<0.0001$). This was also observed in patients' monocytes (figure 5-20 d) (27% to 50%, $p>0.05$). Figure 5-18, appendix C and figure 5-20 e) and f), show the shift towards a $CD14^{-ve}ClassIIDR^{+ve}$ phenotype following JX-594 treatment, with an average increase from 46% (untreated) to 80% ($p<0.0001$). Similarly, in patients' monocytes (figure 5-20 f), there was a moderate increase in $CD14^{-ve}ClassIIDR^{+ve}$ phenotype following 1 pfu/cell JX-594 treatment (49% to 68%, $p>0.05$). There was no appreciable upreguation of CD80 on JX-594-treated monocytes (figure 5-19, figure 5-20 g and h, and appendix C).

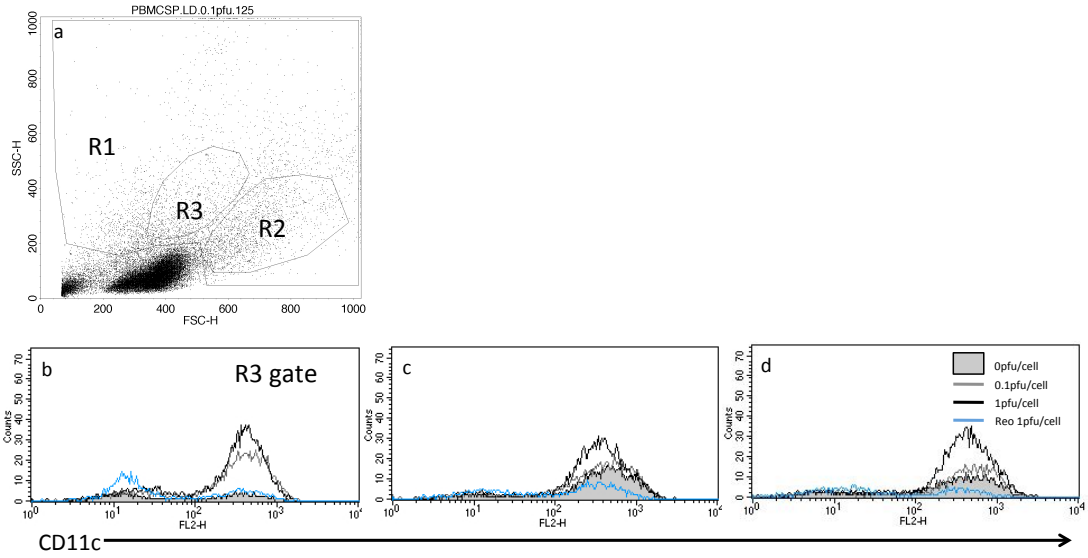

Figure 5-15. Emergence of CD11c+ve cells in R3 gate following JX-594 treatment

PBMCs were isolated from three healthy donors (histograms b-d, each in a separate donor) and treated with 0, 0.1 and 1 pfu/cell JX-594, and 1 pfu/cell Reovirus control. Figure (a) is a representative dot plot showing the gating strategy. The upregulation of CD11c as an indicator of APC phenotype was measured by flow cytometry. Histograms b – d are gated on the 'shifted' R3 population.

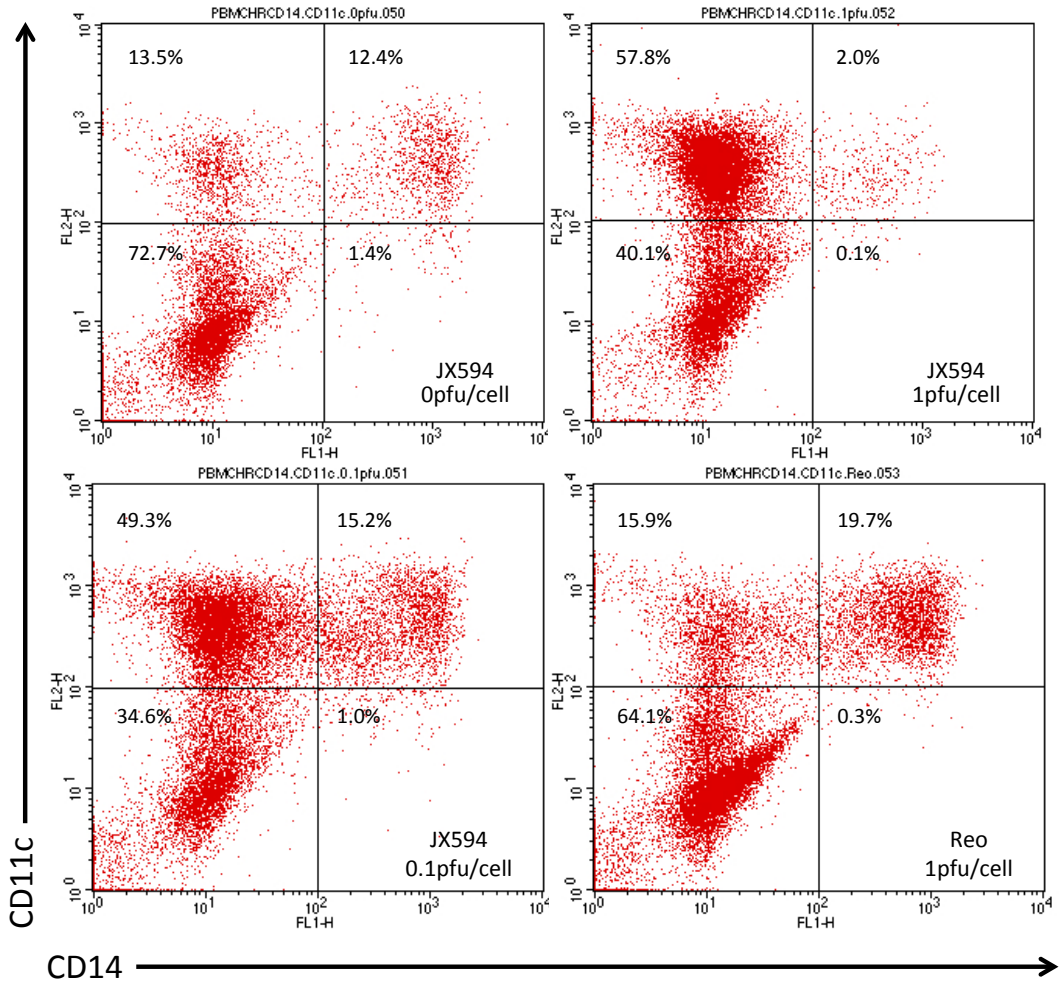

Figure 5-16. JX-594 treatment of PBMCs alters monocyte phenotype, resulting in a new population of $CD14^{-}/CD11c^{+}$ cells

PBMCs from three healthy donors were treated with JX-594 at 0, 0.1 and 1 pfu/cell and Reovirus at 1 pfu/cell (comparison) for 24 hours. PBMCs were harvested and CD14 and CD11c expression determined by flow cytometry of the non-lymphocyte population. Box plots are representative from one of three independent experiments, and % cells in each quadrant are indicated.

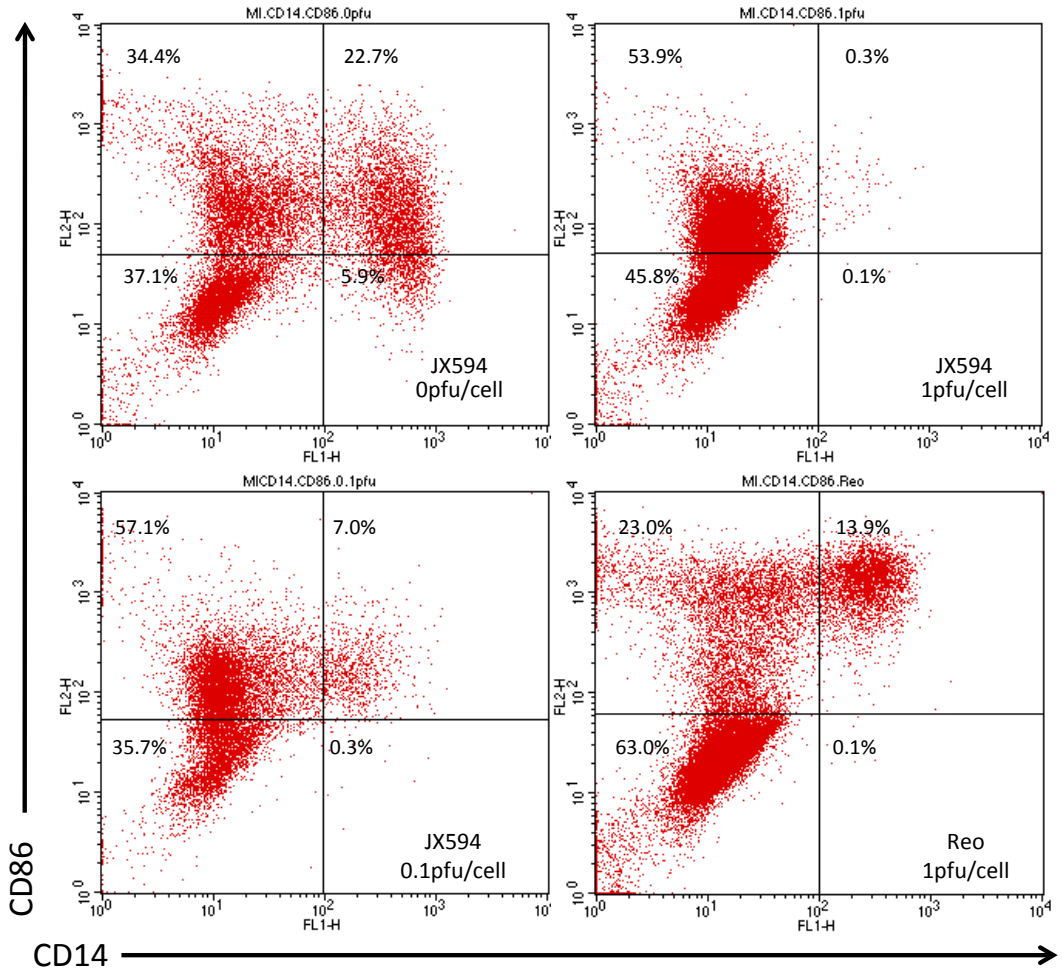

Figure 5-17. JX-594 treatment of PBMC alters monocyte phenotype, resulting in a new population of $CD14^{-}/CD86^{+}$ cells

PBMCs from three healthy donors were treated with JX-594 at 0, 0.1 and 1 pfu/cell and Reovirus at 1 pfu/cell (comparison) for 24 hours. PBMCs were harvested and CD14 and CD86 expression determined by flow cytometry. Box plots are representative from one of three independent experiments, and % cells in each quadrant are indicated.

.

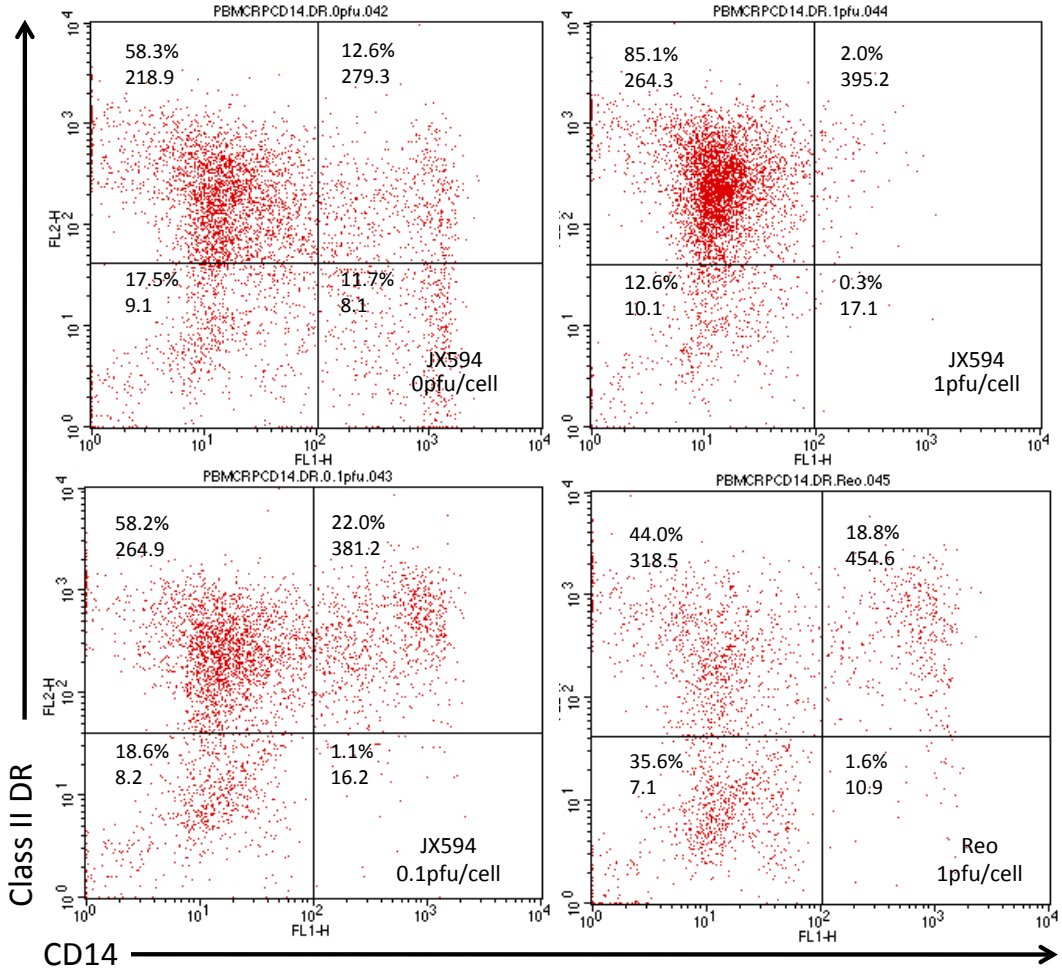

Figure 5-18. JX-594 treatment of PBMC alters monocyte phenotype, resulting in a new population of CD14$^-$/ClassIIDR$^+$ cells

PBMCs from three healthy donors were treated with JX-594 at 0, 0.1 and 1 pfu/cell and Reovirus at 1 pfu/cell (comparison) for 24 hours. PBMCs were harvested and CD14 and ClassIIDR expression determined by flow cytometry. Box plots are representative from one of three independent experiments, and % cells in each quadrant are indicated.

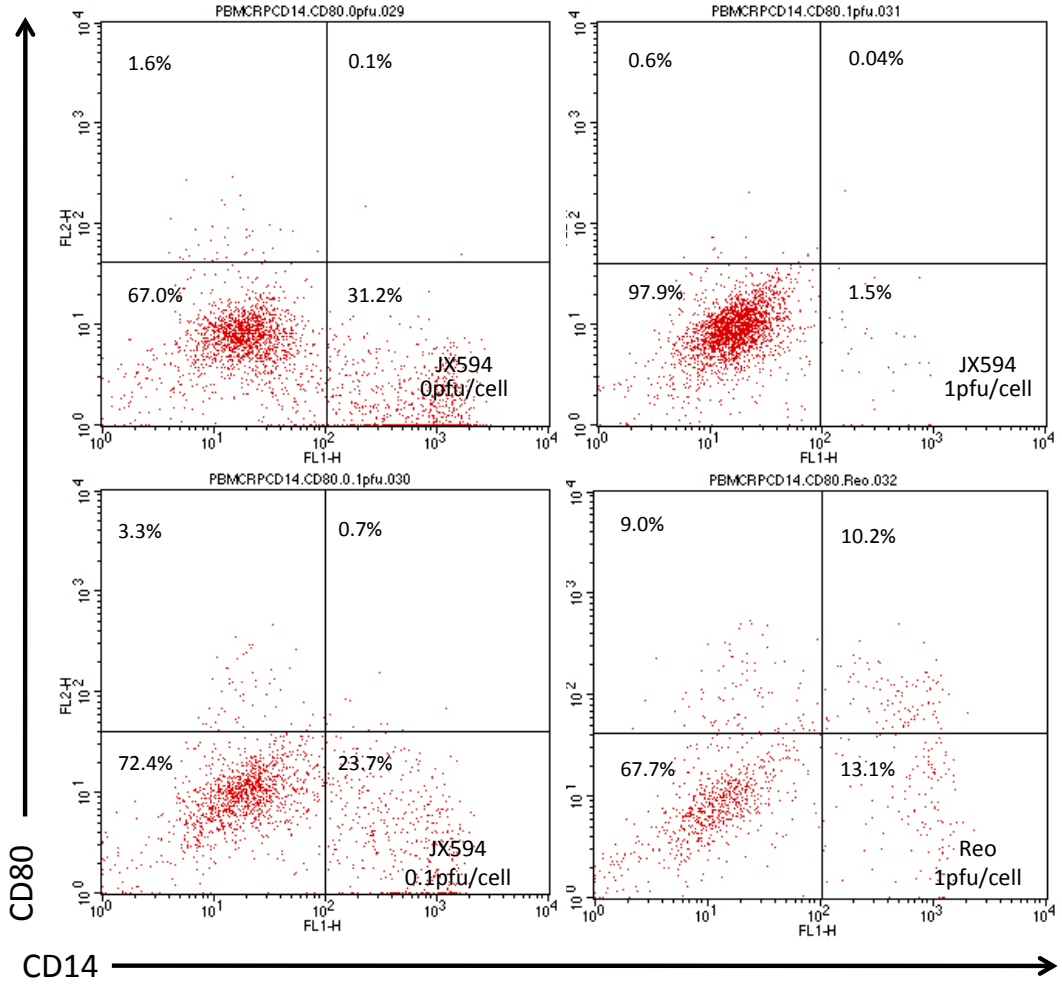

Figure 5-19. JX-594 treatment of PBMC does not alter monocyte phenotype towards $CD14^{-}/CD80^{+}$ cells

PBMCs from three healthy donors were treated with JX-594 at 0, 0.1 and 1 pfu/cell and Reovirus at 1 pfu/cell (comparision) for 24 hours. PBMCs were harvested and CD14 and CD80 expression determined by flow cytometry. Box plots are representative from one of three independent experiments, and % cells in each quadrant are indicated.

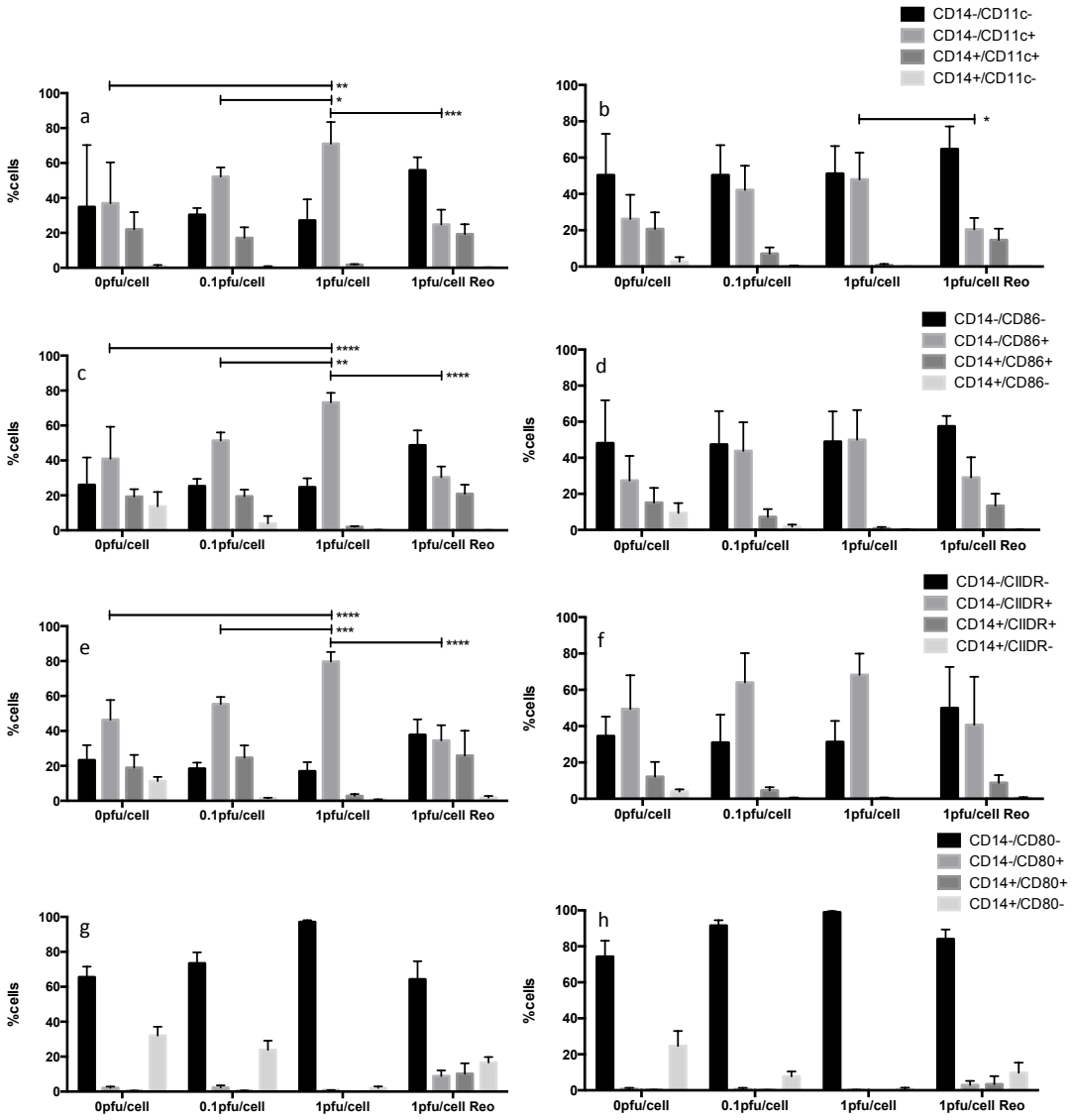

Figure 5-20. JX-594 treatment of PBMC alters monocyte phenotype, resulting in a new population antigen presenting-like cells

PBMCs were isolated from healthy donors (a, c, e, g) and patients with CRLM (b, d, f, h) and treated with JX-594 at 0, 0.1 and 1 pfu/cell, and Reovirus at 1 pfu/cell (comparison) for 24 hours. PBMCs were harvested and CD14 and CD11c/CD86/ClassIIDR/CD80 expression on non-lymphocyte R1-gated cells determined by flow cytometry. Experiments were carried out in triplicate (N=3) and bars show the mean +SD * indicate significant upregulation of antigen; *p<0.05, **p<0.01, ***p<0.0005, ****p<0.0001.

5.12 JX-594 infects and begins early phase replication in monocytes

The demonstration of a change in phenotype of monocytes may potentially be due to JX-594 infection and potentially replication within monocytes. It has been shown in section 5.7 that JX-594 does not replicate within PBMCs (by plaque assay) or lymphocytes (by GFP expression). In a similar fashion, PBMCs from three healthy donors were treated with JX-594-GFP and GFP expression in the monocyte population (figure 5-21a, gate R1) determined by flow cytometry. Figure 5-21 shows that there was an upregulation in GFP production in monocytes following treatment with escalating doses of JX-594-GFP. After 24 hours (figure 5-21c), 75% of the monocytes in the R2 gate treated with JX-594-GFP expressed GFP, and after 48 hours (figure 5-21c) this dropped to 18%, with the majority (69%) of the shifted monocytes in the R3 gate now expressing GFP.

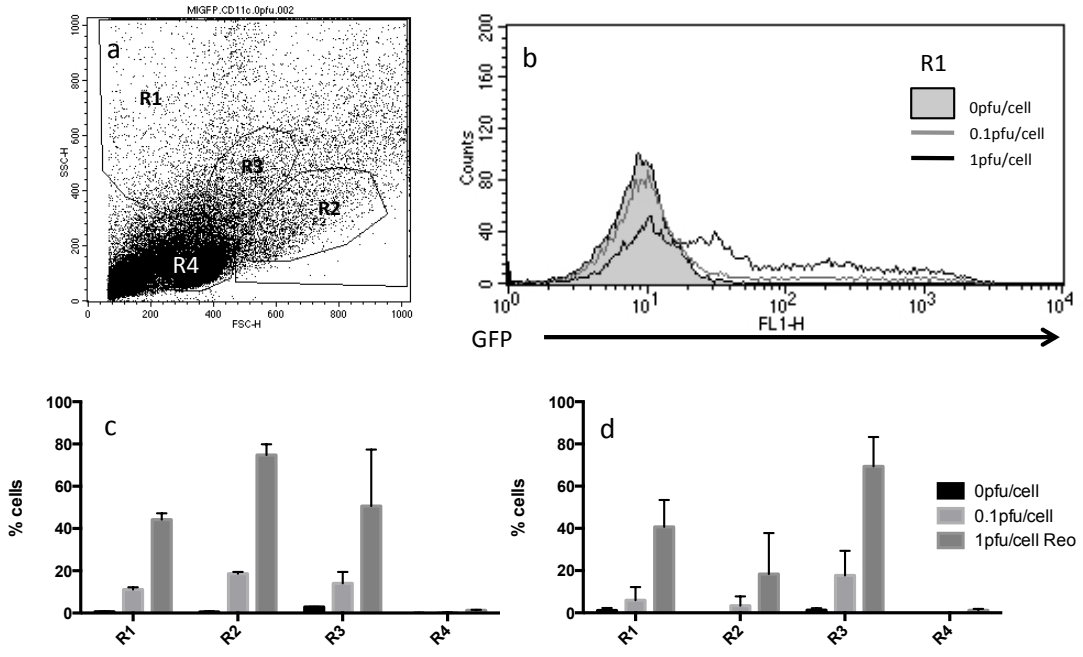

Figure 5-21. JX-594 will infect and begin early-phase replication in monocytes

PBMCs were isolated from healthy donors and treated with JX-594-GFP at 0, 0.1 and 1 pfu/cell for 24 hours. PBMCs were harvested and GFP expression (FITC) determined by flow cytometry. Experiments were carried out in duplicate (N=2). Figures (a) and (b) show representative dot plot and histogram respectively. Figures (c) and (d) show summary data at 24 hours and 48 hours respectively.

5.13 Cytokine profile of PBMCs treated with JX-594

After demonstrating that JX-594 can activate NK cells within whole PBMCs, it was then determined if this activation was associated with an inflammatory cytokine response. Fresh blood was obtained from up to ten healthy donors and ten patients undergoing resection for CRLM by venepuncture, PBMCs isolated by density gradient centrifugation, and treated with 0, 0.1 and 1 pfu/cell JX-594-GM-CSF for 24 (N=10) and 48 hours (N=3). Cell-free supernatant was collected and production of GM-CSF, IFNα, IFNβ, IFNγ, TNFα, IL2, IL-8, IL-10, RANTES and IL29 determined by ELISA. Figure 5-22 shows the upregulation of GM-CSF and IFNα following 24 hours JX-594 treatment with PBMCs from healthy donors and patients. In healthy donors, compared to the untreated control, after 24 hours of treatment with 1 pfu/cell JX-594-GM-CSF, there was an increase in GM-CSF (12 pg/ml vs 63 pg/ml) and IFNα (18 pg/ml vs 173 pg/ml), although these did not reach statistical significance. Compared to reovirus, JX-594 treatment of PBMCs for 24 hours led to a greater response in the production of GM-CSF (63 pg/ml vs 16 pg/ml, $p>0.05$) but not IFNα (173 pg/ml vs 1106 pg/ml, $p<0.05$).

In PBMCs from patients with CRLM (Figure 5-22b and d) treated with 1 pfu/cell JX-594-GM-CSF for 24 hours, there was a significant increase in GM-CSF (9 pg/ml vs 86 pg/ml, $p<0.05$) but not IFNα (23 pg/ml vs 678 pg/ml, $p>0.05$).

There was an upward trend in the production of IL-2 and IL-8 in both healthy donors' and patients' PBMCs following JX-594 treatment (data not shown), but there was no consistent trend in production of any of the other cytokines studied; IFNγ, TNFα, IL-10, RANTES, IL29 and IFNβ (see table 5-2 for summary).

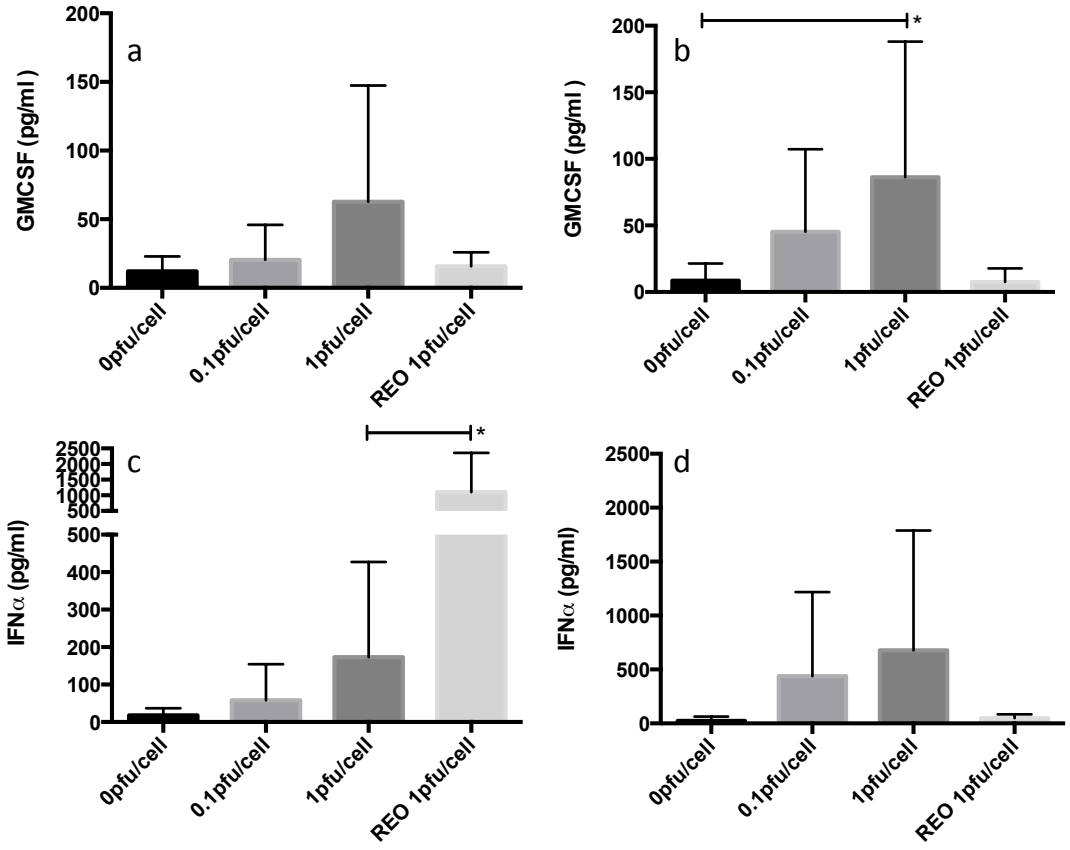

Figure 5-22. GM-CSF and IFNα production following *in vitro* JX-594 infection of PBMCs

PBMCs from healthy volunteers (a, c) and patients with CRLM (b and d) were treated with JX-594 at 0, 0.1 and 1 pfu/cell and Reovirus at 1 pfu/cell (positive control) for 24 hours. Supernatant was collected and cytokine expression quantified by ELISA. Experiments were and bars show the mean + SD. * indicates significant increase in cytokine production; *p<0.05.

5.14 Monocytes are required for modulation of an inflammatory response

To further investigate the role of $CD14^{+ve}$ monocytes in NK cell activation, PBMCs from three healthy volunteers were sampled and NK cells and $CD14^{-ve}$ cells were isolated by negative selection, and $CD14^{+ve}$ cells removed by positive selection, to obtain $CD14^{-ve}$ PBMCs. (see figure 5-11). In all three donors, the four populations of cells (whole PBMCs, purified NK cells, $CD14^{-ve}$ cells and $CD14^{+ve}$ cells) were treated with 0 pfu/cell, 0.1 pfu/cell and 1 pfu/cell of JX-594-GM-CSF for 24 hours and cell-free supernatant was collected and inflammatory cytokines (GM-CSF, IFNα and IL8) analysed by ELISA. Data for whole PBMCs and $CD14^{-ve}$ cells is displayed in figure 5-23. There was no difference in production of GM-CSF in the four cell populations. In contrast, whole PBMCs were required for IFNα production, and removal of $CD14^{+ve}$ PBMCs inhibited IFNα production in response to JX-594. IL-8 was produced in high quantities from $CD14^{+ve}$ monocytes, either pure or within whole PBMCs; similar findings were observed in experiments with patient blood (see table 5-2).

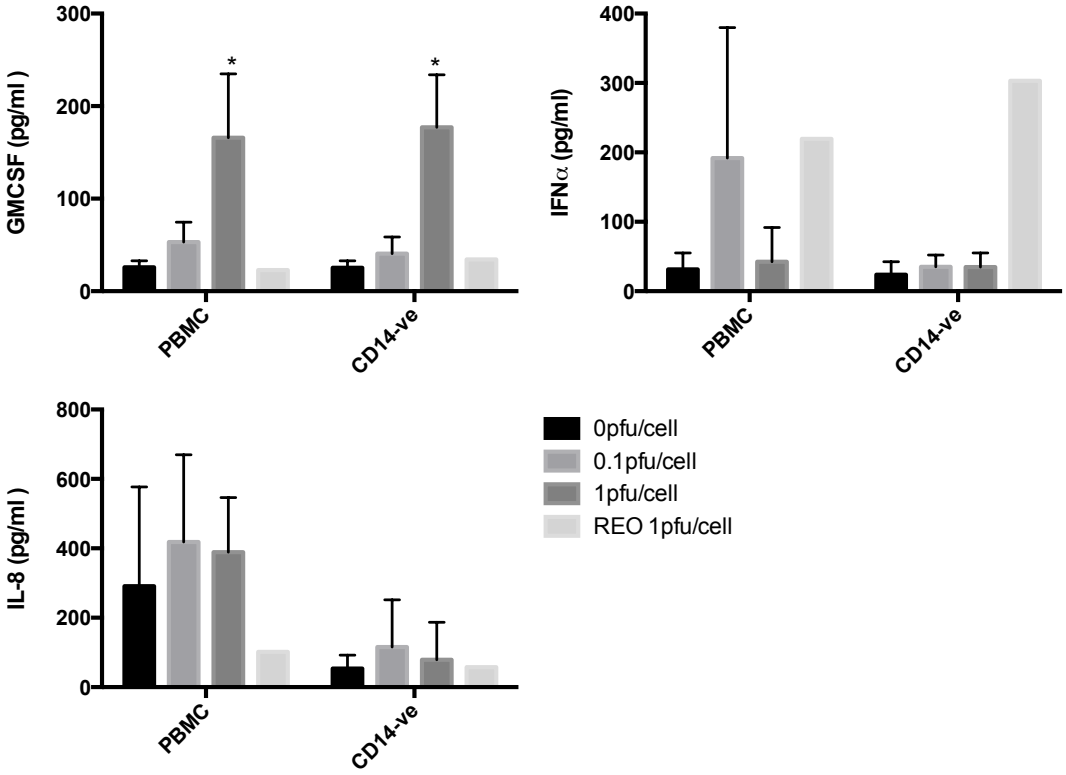

Figure 5-23. CD14^{+ve} Monocytes potentiate an inflammatory reaction from PBMCs treated with JX-594 *in vitro.*

Fresh whole blood was sampled from healthy donors, PBMCs were isolated by centrifugation over lymphoprep gradient, and cell populations separated using magnetic beads. Whole PBMCs and CD14^{-ve} cells were treated with JX-594 at 0, 0.1 and 1 pfu/cell for 24 hours. Supernatant was collected and levels of cytokine determines by ELISA. Experiments were carried out in triplicate (N=3) and bars show the mean + SD * $p<0.05$.

	Healthy Donors				Patients			
	PBMC	NK cells	$CD14^{-ve}$	$CD14^{+ve}$	PBMCs	NK	$CD14^{-}$	$CD14^{+ve}$
GM-CSF (24)	↑	↑	↑	↑	↑	↑	↑	↑
GM-CSF (48)	↔	-	-	-	-	-	-	-
IFNα (24)	↑	↔	↔	↑	↑	↔	-	-
IFNα (48)	↔	-	-	-	-	-	-	-
IL-8 (24)	↑↑	↑	↑	↑↑	↑↑	↑	↑	↑↑
IL-8 (48)	↑	-	-	-	↔	-	-	-
IFNγ (24)	↔	↔	-	-	↔	↔	-	-
IFNγ (48)	↔	-	-	-	↔	-	-	-
TNFα (24)	↔	-	-	-	↔	-	-	-
TNFα (48)	↔	-	-	-	↔	-	-	-
IL-10 (24)	↔	-	-	-	↔	-	-	-
IL-10 (48)	↔	-	-	-	-	-	-	-
RANTES (24)	↔	-	-	-	↔	-	-	-
RANTES (48)	↔	-	-	-	-	-	-	-
IL2 (24)	↑	-	-	-	-	-	-	-
IL2 (48)	↑	-	-	-	-	-	-	-
IL29 (24)	↓	-	-	-	↑	-	-	-
IL29 (48)	↔	-	-	-	-	-	-	-
IFNβ (24)	↔	-	-	-	-	-	-	-
IFNβ (48)	↔	-	-	-	-	-	-	-

Table 5-2. Summary of cytokine profile following *in vitro* treatment of components of PBMCs with JX-594

Fresh whole blood was sampled from healthy volunteers, PBMCs were isolated by centrifugation over lymphoprep gradient and treated with JX-594 at 0, 0.1 and 1 pfu/cell for 24 and 48 hours. Supernatant was collected and cytokine expression quantified by ELISA. Experiments were carried out in 8 to 10 donors for samples at 24 hours, and 3 donors for samples at 48 hours.

5.15 Liver and Tumour derived NK cells are not activated by JX-594 *in vitro*

The liver is a highly vascular structure, and peripherally-activated NK cells following intravenous therapy are likely to infiltrate into the liver. However, it also important to investigate the effect of JX-594 on liver- and tumour- derived mononuclear cells (LMCs and TMCs respectively), particularly if intratumoural or transarterial delivered therapy is to be considered. Fresh surgical specimens immediately following resection were processed as detailed in section 2.13 and 2.14. LMCs and TMCs were isolated by centrifugation over lymphoprep gradient, and labelled with CD3-PerCP and CD56-PE antibodies and analysed by flow cytometry. Isolation of LMCs and TMCs was initially performed with collagenase to aide dissociation of the tissue, which eased the process of passing the liver tissue through a 70 μm cell strainer. However, the resulting single cell suspension had excessive cellular debris. In addition, the liver tissue was also processed via lymphoprep gradient centrifugation, and although some hepatocyte- and tumour- bound mononuclear cells were lost in this process, a purer population was achieved (see figure 5-24); therefore, all future liver and tumour mononuclear cell isolation experiments were performed using this protocol.

Figures 5-24 and 5-25 depict the gating strategy for LMCs and TMCs, and illustrates the difficulty in attaining pure and viable cell populations. Figure 5-25 b) shows that the normal liver is NK cell-rich (close to 30%, compared to 10% in peripheral blood), but the CRLM tumour deposit has fewer NK cells (8%).

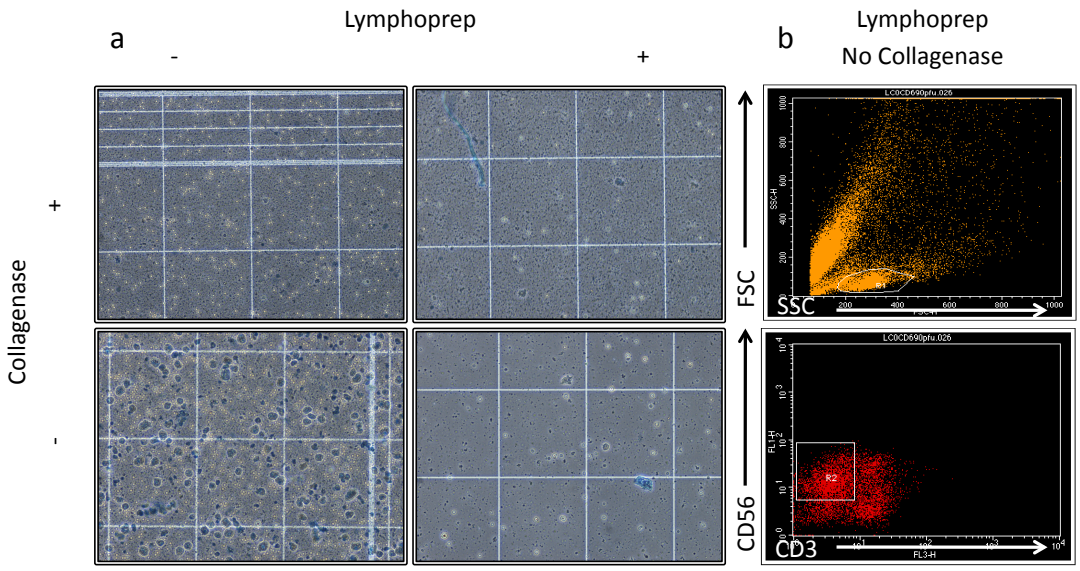

Figure 5-24. Analysis of LMC and TMC isolation protocol

Photomicrographs of the resulting single cell suspension when the LMC and TMC isolation protocol was performed with and without collagenase and lymphoprep gradient centrifuge is depicted in figure a). The optimised conditions (with lymphoprep, without collagenase) was selected based on the appearance of mononuclear cells and lack of cellular debris. Figure b) shows the flow cytometric analysis of immune mononuclear cells isolated without collagenase and with lymphoprep, and demonstrates the presence of $CD3^{-ve}CD56^{+ve}$ NK cells (see section 2.14).

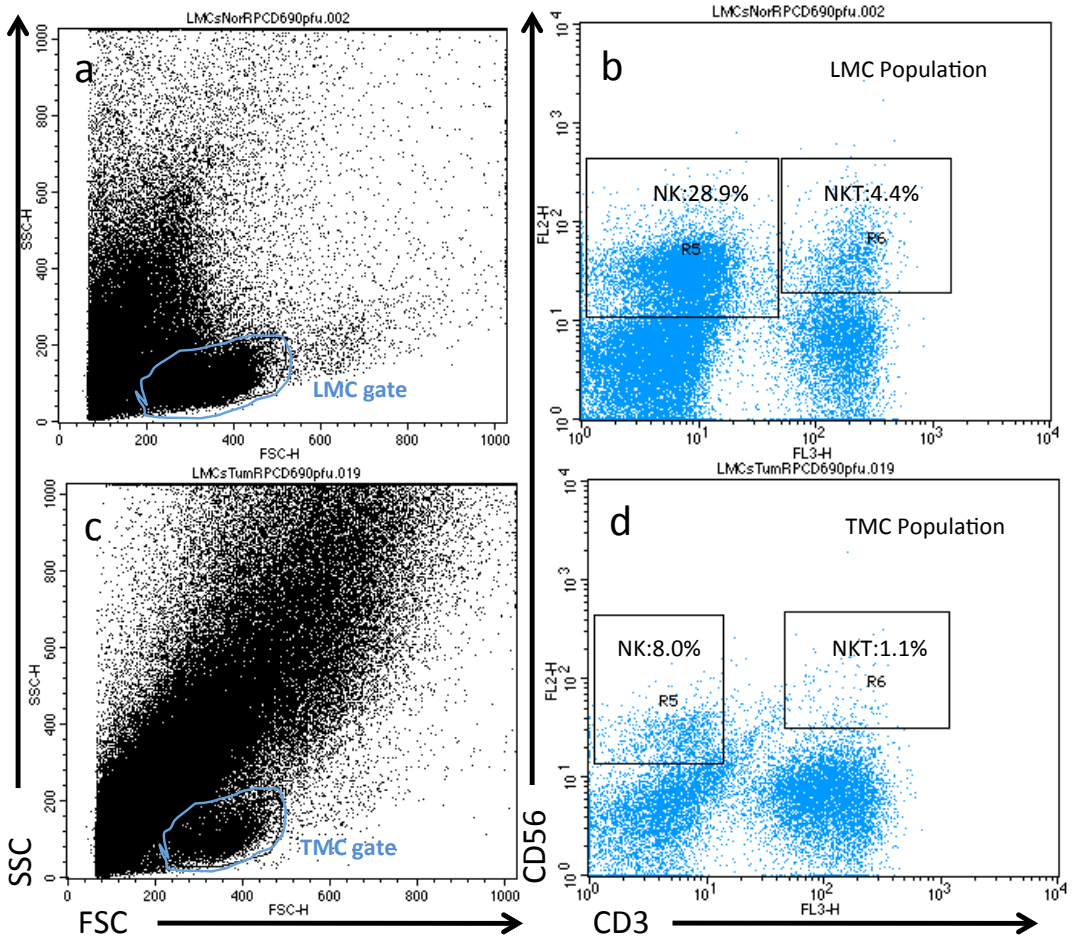

Figure 5-25. Depleted levels of NK cells in CRLM compared to normal liver

Fresh surgical specimens immediately following resection were processed as detailed in section 2.6. Liver- (a, b) and Tumour- (c, d) mononuclear cells were isolated by centrifugation over lymphoprep gradient, and labelled with CD3-PerP and CD56-PE antibodies and analysed by flow cytometry. Figures (a) and (c) show FSc vs SSc and illustrate the lymphocyte population and figure (b) and (d) show identification of $CD56^{+ve}CD3^{-ve}$ NK cells within the LMC and TMC gate.

In figure 5-26, representative histograms (figure 5-26, a – c) and summary bar charts (figure 5-26, d – f) depict that NK cells from peripheral blood, but not normal liver or tumour could be activated by JX-594. Following Reovirus treatment, however, compared to untreated control, NK cells from normal liver (14% to 56% CD69 positive) and from CRLM tumour (28% to 60% CD69 positive) could be activated. This positive control with Reovirus was only performed in one patient due to availability of adequate quantities of LMCs and TMCs. It has been demonstrated earlier in this chapter that activation of NK cells in peripheral blood is associated with a downregulation of CD14 on monocytes, hence the % of $CD14^{+ve}$ cells in LMCs and TMCs was determined. In these patient samples, PBMCs had approximately 20% $CD14^{+ve}$ monocytes (figure 5-26, g and j) which was downregulated in response to JX-594 treatment. Within the liver, there was a higher percentage of $CD14^{+ve}$ cells, which did not show appreciable downregulation in response to JX-594 treatment, whilst in liver tumour, there were hardly any $CD14^{+ve}$ cells at all (<1%), and these did not respond to JX-594 treatment.

The inflammatory cytokine production (GM-CSF, IFNα and IL-8) associated with JX-594 treatment of LMCs and TMCs was investigated (figure 5-27). Following 24 hours in culture, cell-free supernatant was collected and cytokine profile studied by ELISA. GM-CSF production was significantly higher following treatment of PBMCs, LMCs and TMCs with 1 pfu/cell JX-594. IFNα was only produced in small quantities in these samples (data not shown). IL-8 was produced in high quantities by both LMCs and TMCs, which decreased moderately in response to JX-594 treatment.

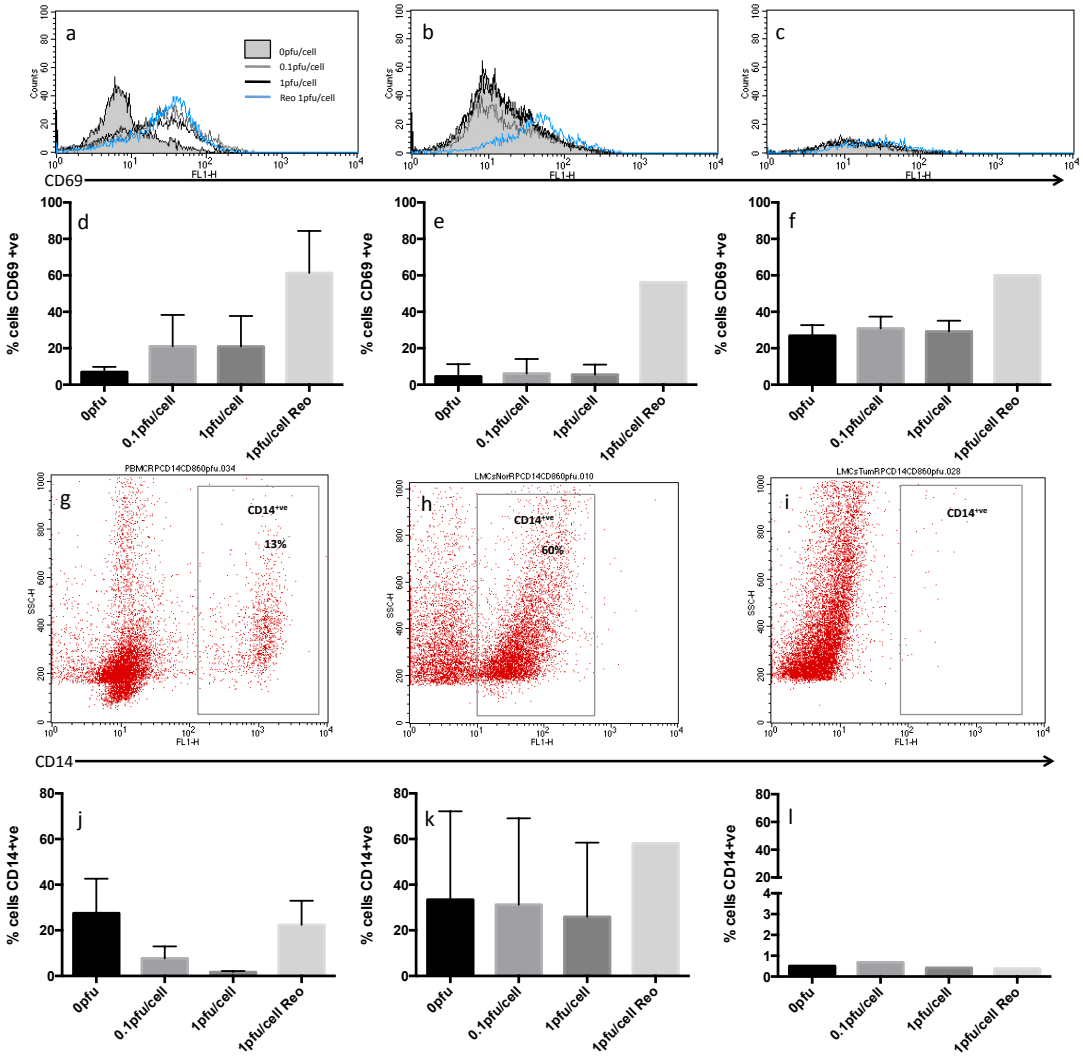

Figure 5-26. Liver- and CRC tumour-derived NK cells are not activated by JX-594.

PBMCs were isolated from patients undergoing liver resection for metastatic CRC, and LMCs and TMCs isolated from fresh surgical specimens immediately following resection. PBMCs (a, d, g and j), LMCs (b, e, h and k) and TMCs (c, f, i and l) were treated with JX-594-GM-CSF at 0, 0.1 and 1 pfu/cell for 24 hours, and cell surface expression of CD14 and CD69 quantified by flow cytometry. Figures (a), (b) and (c) show representative histograms of CD69 expression on $CD56^{+ve}CD3^{-ve}$ NK cells, and figures (d), (e) and (f) show summary bar charts of CD69 expression on $CD56^{+ve}CD3^{-ve}$ NK cells; experiments were carried out in triplicate (N=3) and bars show the mean+SD. Figures (g), (h) and (i) show CD14 expression in the non-lymphocyte population. Figures (j), (k) and (l) show the summary bar charts of CD14 expression on the non-lymphocyte population; experiments were carried out in triplicate (N=3) for PMBCs and LMCs, and N=1 for TMCs, and bars show the mean+SD.

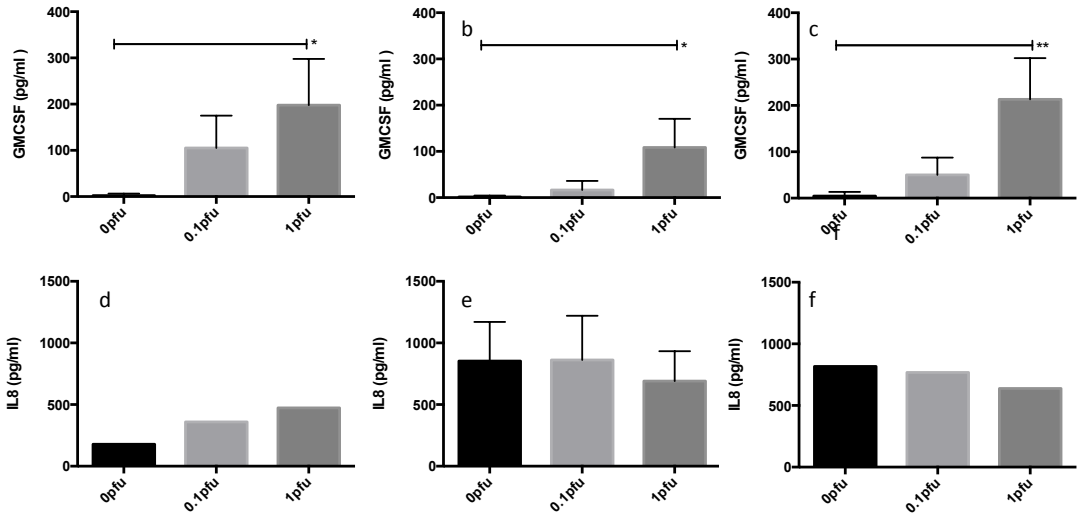

Figure 5-27. Cytokine profile of LMCs and TMCs following JX-594 treatment

Fresh whole blood was sampled from patients undergoing liver resection for metastatic CRC and PBMCs (a and d) were isolated by centrifugation over lymphoprep gradient. Fresh surgical specimens were obtained from the same patients immediately following resection and were processed as detailed in section 2.6, and LMCs (b and e) and TMCs (c and f) were isolated by centrifugation over lymphoprep gradient. PBMCs, LMCs and TMCs were cultured for 24 hours +/- JX-594 and supernatant collected and cytokine production determined by ELISA; (GM-CSF N=3, IL8, N= 1 to 2). Bars show the mean + SD where indicated. * indicates significant increase in cytokine production; *$p<0.05$ **$p<0.005$.

5.16 Discussion

The theory that the immune system can regulate tumourigenesis has been the subject of debate for over a century, and has gained more understanding as our knowledge of the immune system has developed. Burnett and Thomas' Immunosurveillance theory emerged, hailing adaptive immunity as the key player in preventing cancer development. This theory soon lost favour, with the demonstration of similar incidence of spontaneous and carcinogen-induced cancer in immunocompetent and nude mice with partial immunodeficiency, and an increased incidence of tumourigenesis in mice that lacked NK cells. The immuno-editing and danger hypothesis soon became more accepted, and it is now accepted that an inflammatory microenvironment is a component of many tumours, and can facilitate both tumour growth and control. The previously described theory of immunosurveillance and its initial criticism lends itself as an important supportive argument for the role of NK cells. Further work has defined that in both immunocompetent and immunodeficient mice, IFNγ [32, 227, 228] and perforin [229-232] activities can (in various reports, independently) control tumor initiation, growth, and metastasis.

The function of NK cells is determined by a balance between activating and inhibitory signals; hence before implicating NK cells as potential immunotherapy effectors against CRC, it must first be elucidated whether CRC cells display immunogenicity by expressing NK-activating receptor ligands. Zhang *et al*. have demonstrated a higher expression of CD155, CD112 and MHC class I chain-related (MIC) molecules (MICA/B) ligands in colon carcinoma tissues, and functional blocking of these ligands led to significant inhibition of NK cell cytotoxicity. Similar to findings in this chapter, they also observed reduced expression of DNAM-1 and NKG2D in NK cells of colon cancer patients compared to healthy donors, which

was explained by their finding of higher serum concentrations of sCD155 and sMICA/B (soluble ligands to NK cell surface activatory receptor proteins, which are secreted or shed from malignant cells) in CRC patients compared to healthy donors; sCD155 and sMICA/B may down-regulate DNAM-1 and NKG2D on NK cells [210]. Doubrovina *et al*. also showed that circulating sMIC in CRC cancer patients deactivates NK cell immunity by down-modulating NKG2D, and only $NKG2D^{+ve}$ NK cells were tumouricidal *in vitro* [233]. Thus CRC, despite immune evasion strategies, is a potentially immunogenic tumour, and lends itself as a target for NK cell-mediated killing. Results in this chapter demonstrate that NK cells from both healthy donors and patients with metastatic CRC can be activated by JX-594, demonstrated by the upregulation of CD69 on the surface of NK cells within JX-594-treated PBMCs, which is an established activatory marker for NK cells [234]. The lack of significant upregulation compared to untreated control in patients may be partly explained by the lower numbers of subjects investigated, but also by the small number of patients who responded weakly to JX-594. These patients may have suppressed innate immunity due to the systemic consequence of malignancy, which may include over-expression and shedding of some of the soluble ligands as described above.

A similar upregulation following JX-594 treatment as observed with CD69, was not seen with the activatory receptors NKG2D, DNAM-1, NKp30, NKp44 and NKp46. It is possible that there may be another undefined receptor and ligand pair that may have been upregulated following JX-594 treatment, which was not investigated in the experimental protocol. This is supported by the findings of Bhat *et al*., who showed that blocking NKp30, 44 and 46 in combination, and NKG2D and DNAM-1 alone, inhibited the NK cell-mediated killing of pancreatic ductal adenocarcinoma cells, which was overcome by infection of the target cells with an oncolytic

parvovirus (H-1PV); this suggested that parvovirus may induce additional NK cell ligands on pancreatic ductal adenocarcinoma cells [235].

Along with the activation of NK cells, the results in this chapter demonstrate that JX-594 treated NK cells can degranulate and kill CRC cell targets by perforin/granzyme mediated cytotoxicity. A high level of degranulation was seen with NK cells in response to presentation to K562 cells (which express ligand for NKp30 [236]). Interestingly, although CD69 upregulation was greater in healthy donors compared to patients with CRLM, NK cells from patients exhibited greater degranulation; less virus was required for maximal degranulation, and degranulation was significant against the cell line more resistant to direct virus toxicity (SW620). In cytotoxicity studies, maximal killing was seen following treatment with 0.1 pfu/cell JX-594. Following 1 pfu/cell treatment, the response diminished, perhaps indicating that at this dose, although there is no demonstrated toxicity towards PBMCs, JX-594 may result in 'defective' NK cells which, although they can degranulate, do not kill efficiently - this is important to note when considering the optimal dose for trial therapy. There has been little published in the literature examining the activation of NK cells from patients with metastatic CRC by JX-594 *in vitro,* and the mechanistic findings detailed in this chapter are novel; hence few comparisons can be made with the published literature. During intravenous delivery of JX-594 in clinical trials, JX-594 has been found in the circulation shortly after IV or IT administration, with a second peak following a period of *in vivo* replication [77]. As JX-594 will be exposed to blood cells, it is important to determine whether blood cells become infected by JX-594. The results presented here suggest that JX-594 will not infect or kill lymphocytes, and that lymphocytes attracted to sites of viral replication and tumour cell destruction will not themselves be destroyed. Similarly, Parato *et al*. have also shown that PBMCs are resistant to JX-594 replication (virus-driven βgal activity), and are not susceptible to infection even in an activated state [163]. Breitbach *et al*.

have shown that NAbs were only detectable in 6/22 patients receiving IV JX-594 and that there was no correlation between NAb titres and JX-594 replication, safety or antitumour activity [101].

The requirement for $CD14^{+ve}$ cells for JX-594 activation of NK cells is a novel finding, although the described reduction in total number of $CD14^{+ve}$ cells following JX-594 treatment *in vitro* has been described in the literature [237]. This CD14-dependant NK activation is not a phenomenon observed in reovirus-treated PBMCs, thus inferring a different mechanism of immune activation in these two OVs. $CD14^{+ve}$ monocytes may be the first to take up JX-594, leading to a cascade of events, including cell-to-cell interaction and cytokine production.

The cytokine profile of PBMCs treated with JX-594 *in vitro* has been illustrated for the first time. JX-594 treatment leads to production of GM-CSF and IFNα, and to a lesser extent, IL-2 and IL-8. Interestingly, there was a viral dose-dependant expression of GM-CSF from PBMCs, and no demonstrable replication, with an initial increase at 24 hours in GM-CSF and IL-8 production which diminished at 48 hours p.i. Taken together, these results lead us to postulate that GM-CSF was produced by immune cells in reaction to the initial viral exposure, or due to early-phase replication of the virus which occurs independently of host-cell machinery. Support for the former comes from the demonstration of similar levels of GM-CSF production from isolated sub-populations of PBMCs; whole PBMCs, NK cells, $CD14^{-ve}$ cells and $CD14^{+ve}$ cells. The lack of IFNα production in $CD14^{-ve}$ PBMCs following JX-594 treatment and the lack of CD69 upregulation on NK cells, furthers our mechanistic understanding of innate immune activation by JX-594. However, further experiments, including transwell assays are required to further characterise this phenomenon. Although similar *in vitro* cytokine profiles have not been

published in the literature, cytokine profiles have been studied following *in vivo* therapy; Breitbach *et al*. treated 22 patients with IV JX-594 and evaluated the cytokine profile. IFNγ, TNFα and IL-6 increased acutely in a dose-dependent manner (peak at 8 h and resolution at day 4). Levels of IL-10 were found to increase later, on days 4–8 [136]. The *in vitro* studies described in this chapter do not match this published *in vivo* cytokine profile, although they were only performed to a maximum of 48 hours.

It is evident from the results discussed in this chapter that JX-594 will first infect monocytes and begin early-phase replication (with no new viral progeny, as demonstrated by plaque assay experiments). The lack of any demonstrated killing despite virally-expressed GFP within monocytes demonstrates the ability of PBMCs to prevent this highly-lytic virus from hijacking host cell machinery. These infected monocytes down-regulate CD14 expression, and attain an APC phenotype. The presentation of antigens by APCs is necessary for the induction of a memory T-cell response to a particular antigen. APCs include DCs, macrophages and B-cells, and activated APCs may be identified by the upregulation of CD86, CD11c and ClassIIDR [237, 238].

It is interesting to note that, compared to untreated control, the increase in a $CD14^{-ve}/CD11c^{+ve}/CD86^{+ve}/ClassIIDR^{+ve}$ phenotype in patient-derived monocytes was not significant; this corresponded with a lack of significant increase in CD69 in NK cells from patients following JX-594 treatment. Hence, understanding the interaction of JX-594 with monocytes, and potentiating this, may be the key to enhancing immune-mediated anti-tumour outcomes following IV-delivered JX-594 therapy.

There is little in the literature describing this phenomenon of virus-induced monocytes shift towards APC. Hou *et al*. have described this shift to APC phenotype with several viruses, including Influenza A virus, VSV, and VV. They found that 18 hours of virus treatment induced monocytes to differentiate into $CD16^{-ve}CD83^{+ve}$ mature dendritic cells, which did not require cell division (γ-irradiation on monocytes did not affect the conversion), but did require viral gene expression in the case of IAV [237]. We can only postulate that JX-594 induces a similar conversion of monocytes to DCs, but confirming this would require further studies to determine the exact identity of these cells. Future studies could involve treating isolated monocytes with JX-594 and incubating with NK cells, and trans-well experiments, to further characterised the 'cross-talk' involved in NK-cell activation by JX-594.

Another interesting finding is that of high numbers of $CD14^{+ve}$ cells in the liver, which do not downregulate CD14 in response to JX-594 treatment. Although many of these may be macrophages/monocytes which do not respond to JX-594 in the same way as peripheral $CD14^{+ve}$ cells, some of these may be hepatocytes or Kupffer cells, both of which can express CD14 [239, 240]. Thus, the inability of JX-594 to activate liver-derived NK cells may be due to the lack of an appropriate $CD14^{+ve}$ cell response. Similarly in the CRC tumour deposit from the liver, no $CD14^{+ve}$ cells were isolated, and concurrently, tumour-derived NK cells could not be activated by JX-594. The more general significance of $CD14^{+ve}$ immune cells has been reported in the literature; Kinouchi *et al*. have shown that infiltration of $CD14^{+ve}$ macrophages at the invasive front indicated a favourable prognosis in patients with metastatic CRC [241]. These findings are important in the context of understanding how to potentiate the effectiveness of JX-594 therapy, and future trials may need to evaluate the $CD14^{+ve}$ population. Future work examining chemo-attraction of

$CD14^{+ve}$ cells into the tumour environment, or even direct $CD14^{+ve}$ cell injection into tumours, may be worth considering.

In addition to the lack of JX-594-responsive NK cells from the liver, the results in this chapter have demonstrated a reduction in the percentage of NK cells in tumour compared to normal liver and peripheral blood. However, the majority of these NK cells are in a higher state of activation ($CD69^{+ve}$). This has been reported in the literature, with increased CD69, HLA-DR, and NKp44 expression [242] on NK cells derived from liver tumours. In the same study, liver-derived NK cells from patients with hepatic malignancy were less cytolytic compared to their peripheral counterparts, and were found to express less CD16 compared to peripheral NK cells (50% vs 90% of NK cells expressing CD16). The activation of NK cells is important in the context of metastatic CRC and it has been shown that metastatic spread of colorectal cancer is associated with decreased NK-cell activity, with overexpression of inhibitory receptors and defective expression of activatory receptors, and fewer NK cells in the tumour compared to normal tissue [225, 243]. It has been suggested that during surgery, manipulation of the affected organ may lead to tumour cell emboli, and NK cell clearance is a vital preventative mechanism against metastatic deposition. However, post-operative physiological stress can also lead to immune suppression. Tai *et al*. showed that in mice, perioperative administration of oncolytic parapoxvirus ovis (ORFV) and vaccinia virus reversed surgical stress-induced NK cell suppression, which correlated with a reduction in the postoperative formation of metastases. This was also demonstrated in human studies following pre-operative oncolytic vaccinia virus administration [226].

Oncolytic viruses can be designed to maximise ‘good’ inflammation to promote immune-mediated anti-tumour therapy alongside direct tumour cell killing. Hence,

compared to current conventional treatments, oncolytic virotherapy may have the particular benefit of providing disease control via activation of an innate response which may in turn induce an long-term adaptive T-cell memory response to keep tumours in check. The results presented in this chapter further our mechanistic understanding of the action of JX-594 and present another attractive anti-tumour characteristic of JX-594 - the potential to induce effective antigen presentation of a tumour antigen for adaptive anti-tumour immune priming.

6 Conclusion and future work

JX-594 is a double-stranded, enveloped, lytic DNA virus with a large capacity for foreign DNA. It is easy to manipulate genetically, has rapid replication and spread, it is motile, does not integrate into host DNA, and it is safe in animal models and primates [244]. JX-594 is highly immunogenic and produces a strong anti-tumour cytotoxic T-Lymphocyte (CTL) response [245]. The tumour-specificity of JX-594 is achieved by deletion of the *TK* gene, rendering it incapable of replication in TK-deficient (normal) cells; the insertion of *GM-CSF* into the *TK* locus enhances its immunogenicity. Despite the use of this OV in phase I and early phase II trials, there is little in the literature about the mechanism by which the virus functions, particularly the immunogenic actions of the virus. The work detailed in this thesis investigates the consequences of JX-594 treatment on CRC and PBMCs, and the mechanisms by which it achieves its anti-tumour outcome.

The results displayed in the thesis demonstrate the ability of JX-594 to kill CRC tumour cells *in vitro* and replicate whilst doing so, inducing an inflammatory tumour microenvironment in its wake. Through the use of MTT and Live/Dead® assays, the loss of metabolic activity and viability of CRC cell lines *in vitro* is demonstrated, which is more pronounced in cells with increased surface EGFR expression. In all cell lines, the cytolytic effects of JX-594 became more pronounced following a 72-hour incubation period, demonstrating that the virus initiates a ‘slow-kill’ of the CRC cell lines treated. Through the demonstration of an increased expression of active caspase-3, it is elucidated that the mechanism of CRC cell-killing is in part due to activation of the apoptotic pathway, with the more susceptible cell lines also displaying a higher quantity of active caspase-3. Alongside the killing, it is evident that JX-594 can replicate within these CRC cell lines, as demonstrated by the

plaque assay technique and the expression of a virally-encoded protein; GFP, with increased replication in the more susceptible cell lines. The use of confocal microscopic determination of GFP expression on cell lines demonstrated the bi-phasic replication of JX-594, with a clear burst of transgene products after 48 hours infection.

In addition to the tumour-specific cytotoxicity and replicative ability of JX-594, there are also inflammatory changes induced within the tumour microenvironment. The encoded GM-CSF is expressed with a dose-time response following treatment of CRC cell lines with JX-594 up to 72 hours, following which there is reduction in GM-CSF expression due to death of the tumour cells by 96 hours. At this late stage of the assay, there is also a reduction in the quantity of VEGF expression with increased treatment doses of the virus. A pro-inflammatory microenvironment following JX-594 treatment is achieved not only by the expression of GM-CSF, but also by upregulation of IL-6 and downregulation of Il-10, however there was no discernible upregulation of IL-28, RANTES, IFNα or IFNβ. The slower death of the cell lines induced by JX-594 compared to other OVs may be beneficial in the context of the induction of a pro-inflammatory environment particularly for encoded replication-dependant proteins such as GM-CSF.

In order to verify the *in vitro* findings in more clinically relevant model, an *ex vivo* system is adopted. Fresh liver tissue from CRLM and adjacent normal liver is collected immediately following resection, from which ‘cores’ of tissue are made and maintained in culture for up to 96 hours (n=10). Tumor-specific replication is shown by the preferential expression of GFP in JX-594-GFP-treated CRLM cores, but not in cores of normal liver. Similarly, the expression of GM-CSF in CRLM cores continues to increase after 48 hours, in keeping with the *in vitro* findings of a bi-

phasic burst of transgene expression, whereas in normal liver this is not the case. Unlike in the *in vitro* system, treatment of CRLM cores with JX-594 is not associated with a generalised inflammatory response.

The description of the generation of a pro-inflammatory tumour microenvironment as a beneficial characteristic of JX-594 is a controversial one, as there remains a debate as to the role of inflammation in cancer. JX-594 can influence the cells of the immune system both locally and peripherally. The tumour-specific expression of GM-CSF will attract immune cells into the tumour tissue where they will be exposed to the virus and the melee of cytokines and TAAs following viral-mediate cell death. As the favoured route of administration of the virus is via intravenous infusion, the virus will also be in contact with immune cells peripherally. NK cells remain the only immune cell type whose presence within the tumour microenvironment has not been shrouded with the controversy of the pro- and anti-tumourgenic debate. Hence, the influence of JX-594 treatment on NK cell activity is the focus of this thesis' investigation into the immunogenicity of JX-594. It is demonstrated that JX-594 treatment of PBMCs *in vitro* leads to an activation of NK cells as demonstrated by an increase in CD69 expression on the NK cell surface, and an increased de-granulation against tumour cell lines. These activated and de-granulated NK cells are also shown to cytotoxic against CRC cell line targets, as determined by ^{51}Cr-release assays, which also reveal the mechanism of killing to be perforin/granzyme mediated. Importantly, it is also demonstrated that JX-594 is not cytotoxic against PBMCs *in vitro*, and JX-594 will not replicate in PBMCs. There is little cytokine activity observed following JX-594 treatment of PBMCS; with a dose-dependant increase in GM-CSF and a modest increase in IFNα.

Mechanistically, it is revealed here that JX-594 requires $CD14^{+ve}$ monocytes in order to activate NK cells; when these are removed by bead selection, then JX-594 treatment of the remaining (non-$CD14^{+ve}$) population results in no CD69 upregulation on NK cells. It is also shown that JX-594 will preferentially infect monocytes, and begin early-phase replication, without killing. In addition to the upregulation of CD69 on NK cells in a whole PBMC population, JX-594 treatment also results in a downregulation of CD14 expression on the non-lymphocyte population, resulting in a shift of these cells to a smaller, more granular phenotype. Following flow cytometric analysis, this new shifted cell population is characterized as a $CD14^{-ve}$/ $CD86^{+ve}$/ClassIIDR^{+ve}/$CD11c^{+ve}$ APC-like phenotype. This observation is particularly important when considering the long-term implications of JX-594 therapy and the potential generation of a memory response against new tumour burden, as these new APC-like cells have the potential to induce effective antigen presentation of a tumour antigen, resulting in adaptive anti-tumour immune priming. This may, however, be reliant on the infiltration of peripherally-activated immune cells into the tumour, as NK cells derived from within the normal liver and the CRLM did not show the same activatory response when treated with JX-594, with no associated downregulation of CD14 expression.

Future work should be focused on further examining this proposed mechanism of immune cell activation further, and determining the exact mechanism by which $CD14^{+ve}$ cells can influence innate immune activation; through cell-to-cell contact or cytokine messaging. It is clear that the presence of $CD14^{+ve}$ cells is required for JX-594-mediated NK cell activation, but more cytokine analysis is required, including intra-cellular IFNs and GM-CSF analysis, and trans-well assays. It would also be interesting to characterize the response of nodal mononuclear cells/NK cells/monocytes to JX-594 treatment. The lack of an activatory response on NK cells within LMCs and TMCs needs further clarification, along with if/how this can

be overcome, and further analyses of the potential shift towards APC in monocytes from LMCs. The tissue core model developed here has potential for further refinement and may also be used to determine JX-594-induced killing of CRLM tumour cells, and sparing of normal liver cells.

Ultimately, the effects of JX-594 *in vivo* needs to be investigated; either though an animal model or a human trial, to confirm the *in vitro* and *ex vivo* findings of this thesis. This needs to be performed in subjects with not only disseminated disease (as in the majority of the trials performed so far), but also in early disease, as this would provide more information on particularly the immune-mediated effects of JX-594 on cancer cells that have not undergone excessive transformation and thus escaped from immune surveillance. A proposal for a functionally significant animal model would ideally involve an animal model with CRC and time-dependant liver metastasis, injecting the primary colorectal tumour with JX-594 along with IV infusion. This presents a multitude of possibilities for analysis: the treated and untreated animals can be compared for survival and generation of liver metastases; following sacrifice, colonic tissue can be analysed for tumour-specific replication, death and immune response; nodal tissue can be gathered for analysis of nodal infiltration of JX-594 and the presence of TAA-specific APCs; and liver tissue can be analysed for JX-594 infiltration into any developing metastatic tumours.

The field of oncolytic virotherapy is promising, and holds potential to develop into a novel adjunct to current therapeutic modalities. It is not the intention of this thesis to suggest that it is a magic bullet, but rather that it does provide a new modality for therapy that may provide further treatment options for patients and clinicians.

7 Bibliography

1. *Mortality Statistics: Deaths registered in 2009, England and Wales* O.f.N. Statistics, Editor 2010, National Statistics: London.
2. Statistics, O.f.N., *Cancer Statistics Registrations, England (Series MB1)*, 2012.
3. *CancerStats Key Facts: colorectal cancer*, 2009, Cancer Research UK.
4. Berri, R.N. and E.K. Abdalla, *Curable metastatic colorectal cancer: recommended paradigms.* Current oncology reports, 2009. **11**(3): p. 200-8.
5. Primrose, J.N., *Surgery for colorectal liver metastases.* British journal of cancer, 2010. **102**(9): p. 1313-8.
6. Choti, M.A., et al., *Trends in long-term survival following liver resection for hepatic colorectal metastases.* Annals of surgery, 2002. **235**(6): p. 759-66.
7. Nordlinger, B., et al., *Does chemotherapy prior to liver resection increase the potential for cure in patients with metastatic colorectal cancer? A report from the European Colorectal Metastases Treatment Group.* European journal of cancer, 2007. **43**(14): p. 2037-45.
8. *Liver Cancer statistics*. 2012 12/01/2013]; Available from: http://www.cancerresearchuk.org/cancer-info/cancerstats/types/liver/uk-liver-cancer-statistics.
9. Scheffner, M., et al., *The HPV-16 E6 and E6-AP complex functions as a ubiquitin-protein ligase in the ubiquitination of p53.* Cell, 1993. **75**(3): p. 495-505.
10. Hanahan, D. and R.A. Weinberg, *Hallmarks of cancer: the next generation.* Cell, 2011. **144**(5): p. 646-74.
11. Hanahan, D. and R.A. Weinberg, *The hallmarks of cancer.* Cell, 2000. **100**(1): p. 57-70.
12. Valdespino-Gomez, V.M. and V.E. Valdespino-Castillo, *[Non-classical cellular and molecular deficits in cancer development].* Gac Med Mex, 2010. **146**(3): p. 185-98.
13. Medzhitov, R., *Recognition of microorganisms and activation of the immune response.* Nature, 2007. **449**(7164): p. 819-26.
14. Delves, P.J. and I.M. Roitt, *The immune system. First of two parts.* The New England journal of medicine, 2000. **343**(1): p. 37-49.
15. Kalinski, P., et al., *Natural killer-dendritic cell cross-talk in cancer immunotherapy.* Expert opinion on biological therapy, 2005. **5**(10): p. 1303-15.
16. Bagshawe, K.D., *Radioimmunoassay and saturation analysis. Tumor-associated antigens.* British medical bulletin, 1974. **30**(1): p. 68-73.
17. Gold, P. and S.O. Freedman, *Demonstration of Tumor-Specific Antigens in Human Colonic Carcinomata by Immunological Tolerance and Absorption Techniques.* The Journal of experimental medicine, 1965. **121**: p. 439-62.

18. Liu, W., et al., *Evaluation of tumour-associated antigen (TAA) miniarray in immunodiagnosis of colon cancer.* Scandinavian journal of immunology, 2009. **69**(1): p. 57-63.
19. Babel, I., et al., *Identification of tumor-associated autoantigens for the diagnosis of colorectal cancer in serum using high density protein microarrays.* Molecular & cellular proteomics : MCP, 2009. **8**(10): p. 2382-95.
20. Kuniyasu, H., et al., *Induction of angiogenesis by hyperplastic colonic mucosa adjacent to colon cancer.* The American journal of pathology, 2000. **157**(5): p. 1523-35.
21. Ishigami, S.I., et al., *Predictive value of vascular endothelial growth factor (VEGF) in metastasis and prognosis of human colorectal cancer.* British journal of cancer, 1998. **78**(10): p. 1379-84.
22. Diaz-Rubio, E., et al., *First-line XELOX plus bevacizumab followed by XELOX plus bevacizumab or single-agent bevacizumab as maintenance therapy in patients with metastatic colorectal cancer: the phase III MACRO TTD study.* The oncologist, 2012. **17**(1): p. 15-25.
23. Petrelli, F. and S. Barni, *Resectability and outcome with anti-EGFR agents in patients with KRAS wild-type colorectal liver-limited metastases: a meta-analysis.* International journal of colorectal disease, 2012.
24. Cany, J., et al., *A transgenic mouse with beta-Galactosidase as a fetal liver self-antigen for immunotherapy studies.* Journal of hepatology, 2007. **47**(3): p. 396-403.
25. Butterfield, L.H., et al., *A phase I/II trial testing immunization of hepatocellular carcinoma patients with dendritic cells pulsed with four alpha-fetoprotein peptides.* Clinical cancer research : an official journal of the American Association for Cancer Research, 2006. **12**(9): p. 2817-25.
26. Tran, L., et al., *The immunogenicity of the tumor-associated antigen alpha-fetoprotein is enhanced by a fusion with a transmembrane domain.* J Biomed Biotechnol, 2012. **2012**: p. 878657.
27. Matzinger, P., *Tolerance, danger, and the extended family.* Annual review of immunology, 1994. **12**: p. 991-1045.
28. Zhang, Q., et al., *Circulating mitochondrial DAMPs cause inflammatory responses to injury.* Nature, 2010. **464**(7285): p. 104-7.
29. Thompson, A.J. and S.A. Locarnini, *Toll-like receptors, RIG-I-like RNA helicases and the antiviral innate immune response.* Immunol Cell Biol, 2007. **85**(6): p. 435-45.
30. Burnet, M., *Cancer: a biological approach. III. Viruses associated with neoplastic conditions. IV. Practical applications.* British medical journal, 1957. **1**(5023): p. 841-7.
31. Stutman, O., *Tumor development after 3-methylcholanthrene in immunologically deficient athymic-nude mice.* Science, 1974. **183**(4124): p. 534-6.
32. Shankaran, V., et al., *IFNgamma and lymphocytes prevent primary tumour development and shape tumour immunogenicity.* Nature, 2001. **410**(6832): p. 1107-11.
33. Dunn, G.P., L.J. Old, and R.D. Schreiber, *The immunobiology of cancer immunosurveillance and immunoediting.* Immunity, 2004. **21**(2): p. 137-48.

34. Dunn, G.P., et al., *Cancer immunoediting: from immunosurveillance to tumor escape.* Nature immunology, 2002. **3**(11): p. 991-8.
35. MacKie, R.M., R. Reid, and B. Junor, *Fatal melanoma transferred in a donated kidney 16 years after melanoma surgery.* The New England journal of medicine, 2003. **348**(6): p. 567-8.
36. Bubenik, J., *MHC class I down-regulation: tumour escape from immune surveillance? (review).* International journal of oncology, 2004. **25**(2): p. 487-91.
37. Brennan, A.J., et al., *Perforin deficiency and susceptibility to cancer.* Cell death and differentiation, 2010. **17**(4): p. 607-15.
38. French, L.E. and J. Tschopp, *Protein-based therapeutic approaches targeting death receptors.* Cell death and differentiation, 2003. **10**(1): p. 117-23.
39. Bennett, M.W., et al., *The Fas counterattack in vivo: apoptotic depletion of tumor-infiltrating lymphocytes associated with Fas ligand expression by human esophageal carcinoma.* Journal of immunology, 1998. **160**(11): p. 5669-75.
40. Mann, B., et al., *FasL is more frequently expressed in liver metastases of colorectal cancer than in matched primary carcinomas.* British journal of cancer, 1999. **79**(7-8): p. 1262-9.
41. Salih, H.R., S. Holdenrieder, and A. Steinle, *Soluble NKG2D ligands: prevalence, release, and functional impact.* Frontiers in bioscience : a journal and virtual library, 2008. **13**: p. 3448-56.
42. Ochsenbein, A.F., et al., *Immune surveillance against a solid tumor fails because of immunological ignorance.* Proceedings of the National Academy of Sciences of the United States of America, 1999. **96**(5): p. 2233-8.
43. Mapara, M.Y. and M. Sykes, *Tolerance and cancer: mechanisms of tumor evasion and strategies for breaking tolerance.* Journal of clinical oncology : official journal of the American Society of Clinical Oncology, 2004. **22**(6): p. 1136-51.
44. Fahey, J.L., *Cancer in the immunosuppressed patient.* Annals of internal medicine, 1971. **75**(2): p. 310-2.
45. Penn, I. and T.E. Starzl, *Proceedings: The effect of immunosuppression on cancer.* Proceedings. National Cancer Conference, 1972. **7**: p. 425-36.
46. Grivennikov, S.I., F.R. Greten, and M. Karin, *Immunity, inflammation, and cancer.* Cell, 2010. **140**(6): p. 883-99.
47. Park, E.J., et al., *Dietary and genetic obesity promote liver inflammation and tumorigenesis by enhancing IL-6 and TNF expression.* Cell, 2010. **140**(2): p. 197-208.
48. Dvorak, H.F., *Tumors: wounds that do not heal. Similarities between tumor stroma generation and wound healing.* The New England journal of medicine, 1986. **315**(26): p. 1650-9.
49. Apetoh, L., et al., *The interaction between HMGB1 and TLR4 dictates the outcome of anticancer chemotherapy and radiotherapy.* Immunological reviews, 2007. **220**: p. 47-59.
50. Dougan, M. and G. Dranoff, *Immune therapy for cancer.* Annual review of immunology, 2009. **27**: p. 83-117.
51. Coley, W.B., *II. Contribution to the Knowledge of Sarcoma.* Annals of surgery, 1891. **14**(3): p. 199-220.

52. Hoption Cann, S.A., J.P. van Netten, and C. van Netten, *Dr William Coley and tumour regression: a place in history or in the future.* Postgrad Med J, 2003. **79**(938): p. 672-80.
53. Hasday, J.D., K.D. Fairchild, and C. Shanholtz, *The role of fever in the infected host.* Microbes Infect, 2000. **2**(15): p. 1891-904.
54. Alexandroff, A.B., et al., *Recent advances in bacillus Calmette-Guerin immunotherapy in bladder cancer.* Immunotherapy, 2010. **2**(4): p. 551-60.
55. Topalian, S.L., G.J. Weiner, and D.M. Pardoll, *Cancer immunotherapy comes of age.* Journal of clinical oncology : official journal of the American Society of Clinical Oncology, 2011. **29**(36): p. 4828-36.
56. Roentgen, W.C., *[On a new kind of ray (first report)].* Munchener medizinische Wochenschrift, 1959. **101**: p. 1237-9.
57. Farber, S. and L.K. Diamond, *Temporary remissions in acute leukemia in children produced by folic acid antagonist, 4-aminopteroyl-glutamic acid.* N Engl J Med, 1948. **238**(23): p. 787-93.
58. Garber, K., *China approves world's first oncolytic virus therapy for cancer treatment.* J Natl Cancer Inst, 2006. **98**(5): p. 298-300.
59. Kelly, E. and S.J. Russell, *History of oncolytic viruses: genesis to genetic engineering.* Mol Ther, 2007. **15**(4): p. 651-9.
60. Ring, C.J., *Cytolytic viruses as potential anti-cancer agents.* The Journal of general virology, 2002. **83**(Pt 3): p. 491-502.
61. Dock, G., *The influence of complicating diseases upon leukaemia.* American Journal of the Medical Sciences, 1904. **127**: p. 563-592.
62. Hoster, H.A., R.P. Zanes, Jr., and E. Von Haam, *Studies in Hodgkin's syndrome; the association of viral hepatitis and Hodgkin's disease; a preliminary report.* Cancer Res, 1949. **9**(8): p. 473-80.
63. Taylor, A.W., *Effects of glandular fever infection in acute leukaemia.* Br Med J, 1953. **1**(4810): p. 589-93.
64. Asada, T., *Treatment of human cancer with mumps virus.* Cancer, 1974. **34**(6): p. 1907-28.
65. Heise, C., et al., *ONYX-015, an E1B gene-attenuated adenovirus, causes tumor-specific cytolysis and antitumoral efficacy that can be augmented by standard chemotherapeutic agents.* Nat Med, 1997. **3**(6): p. 639-45.
66. Bell, J.C., B. Lichty, and D. Stojdl, *Getting oncolytic virus therapies off the ground.* Cancer Cell, 2003. **4**(1): p. 7-11.
67. Parato, K.A., et al., *Recent progress in the battle between oncolytic viruses and tumours.* Nat Rev Cancer, 2005. **5**(12): p. 965-76.
68. Thorne, S.H., T. Hermiston, and D. Kirn, *Oncolytic virotherapy: approaches to tumor targeting and enhancing antitumor effects.* Semin Oncol, 2005. **32**(6): p. 537-48.
69. Kirn, D., R.L. Martuza, and J. Zwiebel, *Replication-selective virotherapy for cancer: Biological principles, risk management and future directions.* Nat Med, 2001. **7**(7): p. 781-7.
70. Stojdl, D.F., et al., *Exploiting tumor-specific defects in the interferon pathway with a previously unknown oncolytic virus.* Nat Med, 2000. **6**(7): p. 821-5.
71. Hermiston, T.W. and D.H. Kirn, *Genetically based therapeutics for cancer: similarities and contrasts with traditional drug discovery and development.* Mol Ther, 2005. **11**(4): p. 496-507.

72. Kim, J.H., et al., *Systemic armed oncolytic and immunologic therapy for cancer with JX-594, a targeted poxvirus expressing GM-CSF.* Mol Ther, 2006. **14**(3): p. 361-70.
73. McCart, J.A., et al., *Systemic cancer therapy with a tumor-selective vaccinia virus mutant lacking thymidine kinase and vaccinia growth factor genes.* Cancer Res, 2001. **61**(24): p. 8751-7.
74. Thorne, S.H., et al., *Rational strain selection and engineering creates a broad-spectrum, systemically effective oncolytic poxvirus, JX-963.* J Clin Invest, 2007. **117**(11): p. 3350-8.
75. Guo, Z.S., et al., *The enhanced tumor selectivity of an oncolytic vaccinia lacking the host range and antiapoptosis genes SPI-1 and SPI-2.* Cancer Res, 2005. **65**(21): p. 9991-8.
76. Liu, T.C., et al., *The targeted oncolytic poxvirus JX-594 demonstrates antitumoral, antivascular, and anti-HBV activities in patients with hepatocellular carcinoma.* Mol Ther, 2008. **16**(9): p. 1637-42.
77. Park, B.H., et al., *Use of a targeted oncolytic poxvirus, JX-594, in patients with refractory primary or metastatic liver cancer: a phase I trial.* Lancet Oncol, 2008. **9**(6): p. 533-42.
78. Buller, R.M. and G.J. Palumbo, *Poxvirus pathogenesis.* Microbiol Rev, 1991. **55**(1): p. 80-122.
79. Fenner, F., *The Eradication of Smallpox.* Impact of Science on Society, 1988. **38**(2): p. 147-158.
80. Temple, R., *The Genius of China: 3,000 Years of Science, Discovery and Invention.*1986, New York: Simon and Schuster, Inc.
81. Atkinson, W., *Epidemiology and Prevention of Vaccine-Preventable Diseases (The Pink Book)*. 9th ed2005, Washinton DC: Public Health Foundation.
82. Schmidt, F.I., C.K. Bleck, and J. Mercer, *Poxvirus host cell entry.* Curr Opin Virol, 2012. **2**(1): p. 20-7.
83. Kato, S.E., et al., *Temperature-sensitive mutants in the vaccinia virus 4b virion structural protein assemble malformed, transcriptionally inactive intracellular mature virions.* Virology, 2004. **330**(1): p. 127-46.
84. Smith, G.L., A. Vanderplasschen, and M. Law, *The formation and function of extracellular enveloped vaccinia virus.* The Journal of general virology, 2002. **83**(Pt 12): p. 2915-31.
85. Kirn, D.H. and S.H. Thorne, *Targeted and armed oncolytic poxviruses: a novel multi-mechanistic therapeutic class for cancer.* Nat Rev Cancer, 2009. **9**(1): p. 64-71.
86. Bengali, Z., A.C. Townsley, and B. Moss, *Vaccinia virus strain differences in cell attachment and entry.* Virology, 2009. **389**(1-2): p. 132-40.
87. Moss, B., *Poxvirus entry and membrane fusion.* Virology, 2006. **344**(1): p. 48-54.
88. Everts, B. and H.G. van der Poel, *Replication-selective oncolytic viruses in the treatment of cancer.* Cancer Gene Ther, 2005. **12**(2): p. 141-61.
89. Katsafanas, G.C. and B. Moss, *Vaccinia virus intermediate stage transcription is complemented by Ras-GTPase-activating protein SH3 domain-binding protein (G3BP) and cytoplasmic activation/proliferation-associated protein (p137) individually or as a heterodimer.* J Biol Chem, 2004. **279**(50): p. 52210-7.

90. Buller, R.M., et al., *Cell proliferative response to vaccinia virus is mediated by VGF.* Virology, 1988. **164**(1): p. 182-92.
91. McCart, J.A., et al., *Systemic cancer therapy with a tumor-selective vaccinia virus mutant lacking thymidine kinase and vaccinia growth factor genes.* Cancer research, 2001. **61**(24): p. 8751-7.
92. Wali, A. and D.S. Strayer, *Infection with vaccinia virus alters regulation of cell cycle progression.* DNA Cell Biol, 1999. **18**(11): p. 837-43.
93. Vanderplasschen, A., et al., *Extracellular enveloped vaccinia virus is resistant to complement because of incorporation of host complement control proteins into its envelope.* Proc Natl Acad Sci U S A, 1998. **95**(13): p. 7544-9.
94. Ichikawa, T. and E.A. Chiocca, *Comparative analyses of transgene delivery and expression in tumors inoculated with a replication-conditional or -defective viral vector.* Cancer Res, 2001. **61**(14): p. 5336-9.
95. Guo, Z.S., S.H. Thorne, and D.L. Bartlett, *Oncolytic virotherapy: molecular targets in tumor-selective replication and carrier cell-mediated delivery of oncolytic viruses.* Biochim Biophys Acta, 2008. **1785**(2): p. 217-31.
96. Smith, G.L. and B. Moss, *Infectious poxvirus vectors have capacity for at least 25 000 base pairs of foreign DNA.* Gene, 1983. **25**(1): p. 21-8.
97. Yang, S., et al., *A new recombinant vaccinia with targeted deletion of three viral genes: its safety and efficacy as an oncolytic virus.* Gene Ther, 2007. **14**(8): p. 638-47.
98. Colamonici, O.R., et al., *Vaccinia virus B18R gene encodes a type I interferon-binding protein that blocks interferon alpha transmembrane signaling.* J Biol Chem, 1995. **270**(27): p. 15974-8.
99. Hodge, J.W., et al., *A triad of costimulatory molecules synergize to amplify T-cell activation.* Cancer Res, 1999. **59**(22): p. 5800-7.
100. Kirn, D.H., et al., *Targeting of interferon-beta to produce a specific, multi-mechanistic oncolytic vaccinia virus.* PLoS Med, 2007. **4**(12): p. e353.
101. Breitbach, C.J., et al., *Targeted inflammation during oncolytic virus therapy severely compromises tumor blood flow.* Mol Ther, 2007. **15**(9): p. 1686-93.
102. Weibel, S., et al., *Viral-mediated oncolysis is the most critical factor in the late-phase of the tumor regression process upon vaccinia virus infection.* BMC Cancer, 2011. **11**: p. 68.
103. Lusky, M., et al., *Oncolytic vaccinia virus: a silver bullet?* Expert Rev Vaccines, 2010. **9**(12): p. 1353-6.
104. Mackett, M., G.L. Smith, and B. Moss, *General method for production and selection of infectious vaccinia virus recombinants expressing foreign genes.* J Virol, 1984. **49**(3): p. 857-64.
105. Hengstschlager, M., et al., *Different regulation of thymidine kinase during the cell cycle of normal versus DNA tumor virus-transformed cells.* J Biol Chem, 1994. **269**(19): p. 13836-42.
106. Mastrangelo, M.J., et al., *Intratumoral recombinant GM-CSF-encoding virus as gene therapy in patients with cutaneous melanoma.* Cancer gene therapy, 1999. **6**(5): p. 409-22.

107. Savage, C.R., Jr., T. Inagami, and S. Cohen, *The primary structure of epidermal growth factor.* J Biol Chem, 1972. **247**(23): p. 7612-21.
108. Gregory, H., *Isolation and structure of urogastrone and its relationship to epidermal growth factor.* Nature, 1975. **257**(5524): p. 325-7.
109. Buller, R.M., et al., *Deletion of the vaccinia virus growth factor gene reduces virus virulence.* J Virol, 1988. **62**(3): p. 866-74.
110. Buller, R.M., et al., *Decreased virulence of recombinant vaccinia virus expression vectors is associated with a thymidine kinase-negative phenotype.* Nature, 1985. **317**(6040): p. 813-5.
111. Lun, X.Q., et al., *Efficacy of systemically administered oncolytic vaccinia virotherapy for malignant gliomas is enhanced by combination therapy with rapamycin or cyclophosphamide.* Clinical cancer research : an official journal of the American Association for Cancer Research, 2009. **15**(8): p. 2777-88.
112. Acres, B., et al., *Directed cytokine expression in tumour cells in vivo using recombinant vaccinia virus.* Ther Immunol, 1994. **1**(1): p. 17-23.
113. Li, J., et al., *Chemokine Expression From Oncolytic Vaccinia Virus Enhances Vaccine Therapies of Cancer.* Mol Ther, 2011.
114. Lee, J.H., et al., *Oncolytic and immunostimulatory efficacy of a targeted oncolytic poxvirus expressing human GM-CSF following intravenous administration in a rabbit tumor model.* Cancer Gene Ther, 2010. **17**(2): p. 73-9.
115. Fu, X., et al., *Incorporation of the B18R gene of vaccinia virus into an oncolytic herpes simplex virus improves antitumor activity.* Mol Ther, 2012. **20**(10): p. 1871-81.
116. Kirn, D.H., et al., *Targeting of interferon-beta to produce a specific, multi-mechanistic oncolytic vaccinia virus.* PLoS medicine, 2007. **4**(12): p. e353.
117. Gnant, M.F., et al., *Systemic administration of a recombinant vaccinia virus expressing the cytosine deaminase gene and subsequent treatment with 5-fluorocytosine leads to tumor-specific gene expression and prolongation of survival in mice.* Cancer Res, 1999. **59**(14): p. 3396-403.
118. Chalikonda, S., et al., *Oncolytic virotherapy for ovarian carcinomatosis using a replication-selective vaccinia virus armed with a yeast cytosine deaminase gene.* Cancer Gene Ther, 2008. **15**(2): p. 115-25.
119. Foloppe, J., et al., *Targeted delivery of a suicide gene to human colorectal tumors by a conditionally replicating vaccinia virus.* Gene Ther, 2008. **15**(20): p. 1361-71.
120. Wallack, M.K., S.D. Scoggin, and M. Sivanandham, *Active specific immunotherapy with vaccinia melanoma oncolysate.* Mt Sinai J Med, 1992. **59**(3): p. 227-33.
121. Wallack, M.K., et al., *Surgical adjuvant active specific immunotherapy for patients with stage III melanoma: the final analysis of data from a phase III, randomized, double-blind, multicenter vaccinia melanoma oncolysate trial.* J Am Coll Surg, 1998. **187**(1): p. 69-77; discussion 77-9.
122. Kim, E.M., et al., *Overview analysis of adjuvant therapies for melanoma--a special reference to results from vaccinia melanoma oncolysate adjuvant therapy trials.* Surg Oncol, 2001. **10**(1-2): p. 53-9.

123. Hersey, P., et al., *Adjuvant immunotherapy of patients with high-risk melanoma using vaccinia viral lysates of melanoma: results of a randomized trial.* J Clin Oncol, 2002. **20**(20): p. 4181-90.
124. Tanaka, N., M. Sivanandham, and M.K. Wallack, *Immunotherapy of a vaccinia colon oncolysate prepared with interleukin-2 gene-encoded vaccinia virus and interferon-alpha increases the survival of mice bearing syngeneic colon adenocarcinoma.* J Immunother Emphasis Tumor Immunol, 1994. **16**(4): p. 283-93.
125. He, S., et al., *Effective oncolytic vaccinia therapy for human sarcomas.* The Journal of surgical research, 2012. **175**(2): p. e53-60.
126. Gholami, S., et al., *Vaccinia virus GLV-1h153 is effective in treating and preventing metastatic triple-negative breast cancer.* Annals of surgery, 2012. **256**(3): p. 437-45.
127. Correale, P., et al., *Generation of human cytolytic T lymphocyte lines directed against prostate-specific antigen (PSA) employing a PSA oligoepitope peptide.* J Immunol, 1998. **161**(6): p. 3186-94.
128. Gulley, J., et al., *Phase I study of a vaccine using recombinant vaccinia virus expressing PSA (rV-PSA) in patients with metastatic androgen-independent prostate cancer.* Prostate, 2002. **53**(2): p. 109-17.
129. Arlen, P.M., et al., *Clinical safety of a viral vector based prostate cancer vaccine strategy.* J Urol, 2007. **178**(4 Pt 1): p. 1515-20.
130. Kantoff, P.W., et al., *Overall survival analysis of a phase II randomized controlled trial of a Poxviral-based PSA-targeted immunotherapy in metastatic castration-resistant prostate cancer.* J Clin Oncol, 2010. **28**(7): p. 1099-105.
131. Amato, R.J. and M. Stepankiw, *Clinical Efficacy of TroVax in the Treatment of Progressive Castration-resistant Prostate Cancer.* Clinical Medicine Insights. Oncology, 2012. **6**: p. 67-73.
132. Harrop, R., et al., *Vaccination of colorectal cancer patients with modified vaccinia Ankara delivering the tumor antigen 5T4 (TroVax) induces immune responses which correlate with disease control: a phase I/II trial.* Clinical cancer research : an official journal of the American Association for Cancer Research, 2006. **12**(11 Pt 1): p. 3416-24.
133. Hwang, T.H., et al., *A mechanistic proof-of-concept clinical trial with JX-594, a targeted multi-mechanistic oncolytic poxvirus, in patients with metastatic melanoma.* Molecular therapy : the journal of the American Society of Gene Therapy, 2011. **19**(10): p. 1913-22.
134. Heo, J., et al., *Sequential therapy with JX-594, a targeted oncolytic poxvirus, followed by sorafenib in hepatocellular carcinoma: preclinical and clinical demonstration of combination efficacy.* Molecular therapy : the journal of the American Society of Gene Therapy, 2011. **19**(6): p. 1170-9.
135. Heo, J., et al., *Randomized dose-finding clinical trial of oncolytic immunotherapeutic vaccinia JX-594 in liver cancer.* Nat Med, 2013.
136. Breitbach, C.J., et al., *Intravenous delivery of a multi-mechanistic cancer-targeted oncolytic poxvirus in humans.* Nature, 2011. **477**(7362): p. 99-102.

137. Boozari, B., et al., *Antitumoural immunity by virus-mediated immunogenic apoptosis inhibits metastatic growth of hepatocellular carcinoma.* Gut, 2010. **59**(10): p. 1416-26.
138. Nelson, C.B., et al., *An outbreak of conjunctivitis due to Newcastle disease virus (NDV) occurring in poultry workers.* American journal of public health and the nation's health, 1952. **42**(6): p. 672-8.
139. Alkassar, M., et al., *The combined effects of oncolytic reovirus plus Newcastle disease virus and reovirus plus parvovirus on U87 and U373 cells in vitro and in vivo.* Journal of neuro-oncology, 2011. **104**(3): p. 715-27.
140. Pecora, A.L., et al., *Phase I trial of intravenous administration of PV701, an oncolytic virus, in patients with advanced solid cancers.* Journal of clinical oncology : official journal of the American Society of Clinical Oncology, 2002. **20**(9): p. 2251-66.
141. Laurie, S.A., et al., *A phase 1 clinical study of intravenous administration of PV701, an oncolytic virus, using two-step desensitization.* Clinical cancer research : an official journal of the American Association for Cancer Research, 2006. **12**(8): p. 2555-62.
142. Lorence, R.M., et al., *Phase 1 clinical experience using intravenous administration of PV701, an oncolytic Newcastle disease virus.* Current cancer drug targets, 2007. **7**(2): p. 157-67.
143. Hastie, E. and V.Z. Grdzelishvili, *Vesicular stomatitis virus as a flexible platform for oncolytic virotherapy against cancer.* The Journal of general virology, 2012. **93**(Pt 12): p. 2529-45.
144. Senzer, N.N., et al., *Phase II clinical trial of a granulocyte-macrophage colony-stimulating factor-encoding, second-generation oncolytic herpesvirus in patients with unresectable metastatic melanoma.* Journal of clinical oncology : official journal of the American Society of Clinical Oncology, 2009. **27**(34): p. 5763-71.
145. Nakamura, T. and S.J. Russell, *Oncolytic measles viruses for cancer therapy.* Expert opinion on biological therapy, 2004. **4**(10): p. 1685-92.
146. Galanis, E., et al., *Phase I trial of intraperitoneal administration of an oncolytic measles virus strain engineered to express carcinoembryonic antigen for recurrent ovarian cancer.* Cancer research, 2010. **70**(3): p. 875-82.
147. Donnelly, O.G., et al., *Recent clinical experience with oncolytic viruses.* Curr Pharm Biotechnol, 2012. **13**(9): p. 1834-41.
148. Adair, R.A., et al., *Cell carriage, delivery, and selective replication of an oncolytic virus in tumor in patients.* Science translational medicine, 2012. **4**(138): p. 138ra77.
149. Doehn, C., et al., *Drug evaluation: Therion's rV-PSA-TRICOM + rF-PSA-TRICOM prime-boost prostate cancer vaccine.* Curr Opin Mol Ther, 2007. **9**(2): p. 183-9.
150. Jager, E., et al., *Recombinant vaccinia/fowlpox NY-ESO-1 vaccines induce both humoral and cellular NY-ESO-1-specific immune responses in cancer patients.* Proc Natl Acad Sci U S A, 2006. **103**(39): p. 14453-8.
151. Rochlitz, C., et al., *Phase I immunotherapy with a modified vaccinia virus (MVA) expressing human MUC1 as antigen-specific*

immunotherapy in patients with MUC1-positive advanced cancer. J Gene Med, 2003. **5**(8): p. 690-9.
152. Garrido, F., et al., *Implications for immunosurveillance of altered HLA class I phenotypes in human tumours.* Immunology today, 1997. **18**(2): p. 89-95.
153. Power, A.T. and J.C. Bell, *Taming the Trojan horse: optimizing dynamic carrier cell/oncolytic virus systems for cancer biotherapy.* Gene therapy, 2008. **15**(10): p. 772-9.
154. Merrick, *Cell Culture Guide. Teaching and Learning for new students.* 2008.
155. Radcliff, G. and M.J. Jaroszeski, *Basics of flow cytometry.* Methods in molecular biology, 1998. **91**: p. 1-24.
156. Mosmann, T., *Rapid colorimetric assay for cellular growth and survival: application to proliferation and cytotoxicity assays.* Journal of immunological methods, 1983. **65**(1-2): p. 55-63.
157. Dulbecco, R. and M. Vogt, *Some problems of animal virology as studied by the plaque technique.* Cold Spring Harbor symposia on quantitative biology, 1953. **18**: p. 273-9.
158. Al-Nasiry, S., et al., *The use of Alamar Blue assay for quantitative analysis of viability, migration and invasion of choriocarcinoma cells.* Human reproduction, 2007. **22**(5): p. 1304-9.
159. Diallo, J.S., et al., *Ex vivo infection of live tissue with oncolytic viruses.* Journal of visualized experiments : JoVE, 2011(52).
160. Ferrara, N., H.P. Gerber, and J. LeCouter, *The biology of VEGF and its receptors.* Nat Med, 2003. **9**(6): p. 669-76.
161. Taga, K. and G. Tosato, *IL-10 inhibits human T cell proliferation and IL-2 production.* J Immunol, 1992. **148**(4): p. 1143-8.
162. Lun, X., et al., *Efficacy and safety/toxicity study of recombinant vaccinia virus JX-594 in two immunocompetent animal models of glioma.* Molecular therapy : the journal of the American Society of Gene Therapy, 2010. **18**(11): p. 1927-36.
163. Parato, K.A., et al., *The Oncolytic Poxvirus JX-594 Selectively Replicates in and Destroys Cancer Cells Driven by Genetic Pathways Commonly Activated in Cancers.* Molecular therapy : the journal of the American Society of Gene Therapy, 2012. **20**(4): p. 749-58.
164. Zhou, B.B., et al., *Tumour-initiating cells: challenges and opportunities for anticancer drug discovery.* Nature reviews. Drug discovery, 2009. **8**(10): p. 806-23.
165. Fischer, U., R.U. Janicke, and K. Schulze-Osthoff, *Many cuts to ruin: a comprehensive update of caspase substrates.* Cell death and differentiation, 2003. **10**(1): p. 76-100.
166. Liskova, J., et al., *Apoptosis and necrosis in vaccinia virus-infected HeLa G and BSC-40 cells.* Virus research, 2011. **160**(1-2): p. 40-50.
167. Kalbacova, M., et al., *Lytic infection with vaccinia virus activates caspases in a Bcl-2-inhibitable manner.* Virus research, 2008. **135**(1): p. 53-63.
168. Smith, G.L. and M. Law, *The exit of vaccinia virus from infected cells.* Virus research, 2004. **106**(2): p. 189-97.
169. Elmore, S., *Apoptosis: a review of programmed cell death.* Toxicol Pathol, 2007. **35**(4): p. 495-516.

170. Kooby, D.A., et al., *Oncolytic viral therapy for human colorectal cancer and liver metastases using a multi-mutated herpes simplex virus type-1 (G207).* FASEB journal : official publication of the Federation of American Societies for Experimental Biology, 1999. **13**(11): p. 1325-34.
171. Stewart, J.H.t., et al., *Vesicular stomatitis virus as a treatment for colorectal cancer.* Cancer gene therapy, 2011. **18**(12): p. 837-49.
172. Adair, R.A., et al., *Cytotoxic and immune-mediated killing of human colorectal cancer by reovirus-loaded blood and liver mononuclear cells.* Int J Cancer, 2012.
173. Dahan, L., et al., *Modulation of cellular redox state underlies antagonism between oxaliplatin and cetuximab in human colorectal cancer cell lines.* British journal of pharmacology, 2009. **158**(2): p. 610-20.
174. Langhammer, S., et al., *Inhibition of poxvirus spreading by the anti-tumor drug Gefitinib (Iressa).* Antiviral Res, 2011. **89**(1): p. 64-70.
175. Joklik, W.K. and Y. Becker, *The Replication and Coating of Vaccinia DNA.* Journal of molecular biology, 1964. **10**: p. 452-74.
176. Cochran, M.A., C. Puckett, and B. Moss, *In vitro mutagenesis of the promoter region for a vaccinia virus gene: evidence for tandem early and late regulatory signals.* J Virol, 1985. **54**(1): p. 30-7.
177. Ming, J.E., R.M. Steinman, and A. Granelli-Piperno, *IL-6 enhances the generation of cytolytic T lymphocytes in the allogeneic mixed leucocyte reaction.* Clin Exp Immunol, 1992. **89**(1): p. 148-53.
178. Scheller, J., et al., *The pro- and anti-inflammatory properties of the cytokine interleukin-6.* Biochim Biophys Acta, 2011. **1813**(5): p. 878-88.
179. Kurooka, M. and Y. Kaneda, *Inactivated Sendai virus particles eradicate tumors by inducing immune responses through blocking regulatory T cells.* Cancer Res, 2007. **67**(1): p. 227-36.
180. Trikha, M., et al., *Targeted anti-interleukin-6 monoclonal antibody therapy for cancer: a review of the rationale and clinical evidence.* Clinical cancer research : an official journal of the American Association for Cancer Research, 2003. **9**(13): p. 4653-65.
181. Ancrile, B., K.H. Lim, and C.M. Counter, *Oncogenic Ras-induced secretion of IL6 is required for tumorigenesis.* Genes & development, 2007. **21**(14): p. 1714-9.
182. Rojas, A., et al., *IL-6 promotes prostate tumorigenesis and progression through autocrine cross-activation of IGF-IR.* Oncogene, 2011. **30**(20): p. 2345-55.
183. Waugh, D.J. and C. Wilson, *The interleukin-8 pathway in cancer.* Clinical cancer research : an official journal of the American Association for Cancer Research, 2008. **14**(21): p. 6735-41.
184. Wilson, C., et al., *Interleukin-8 signaling attenuates TRAIL- and chemotherapy-induced apoptosis through transcriptional regulation of c-FLIP in prostate cancer cells.* Mol Cancer Ther, 2008. **7**(9): p. 2649-61.
185. Ning, Y., et al., *Interleukin-8 is associated with proliferation, migration, angiogenesis and chemosensitivity in vitro and in vivo in colon cancer cell line models.* Int J Cancer, 2011. **128**(9): p. 2038-49.

186. Sparmann, A. and D. Bar-Sagi, *Ras-induced interleukin-8 expression plays a critical role in tumor growth and angiogenesis.* Cancer Cell, 2004. **6**(5): p. 447-58.
187. Pestka, S., et al., *Interleukin-10 and related cytokines and receptors.* Annual review of immunology, 2004. **22**: p. 929-79.
188. Mocellin, S., F.M. Marincola, and H.A. Young, *Interleukin-10 and the immune response against cancer: a counterpoint.* Journal of leukocyte biology, 2005. **78**(5): p. 1043-51.
189. Alas, S., C. Emmanouilides, and B. Bonavida, *Inhibition of interleukin 10 by rituximab results in down-regulation of bcl-2 and sensitization of B-cell non-Hodgkin's lymphoma to apoptosis.* Clinical cancer research : an official journal of the American Association for Cancer Research, 2001. **7**(3): p. 709-23.
190. Bohlen, H., et al., *Poor clinical outcome of patients with Hodgkin's disease and elevated interleukin-10 serum levels. Clinical significance of interleukin-10 serum levels for Hodgkin's disease.* Ann Hematol, 2000. **79**(3): p. 110-3.
191. Kabbinavar, F., et al., *Phase II, randomized trial comparing bevacizumab plus fluorouracil (FU)/leucovorin (LV) with FU/LV alone in patients with metastatic colorectal cancer.* J Clin Oncol, 2003. **21**(1): p. 60-5.
192. Gonzalez Martin, A., et al., *Bevacizumab as front-line treatment for newly diagnosed epithelial cancer.* Expert Rev Anticancer Ther, 2013. **13**(2): p. 123-9.
193. de Gramont, A., et al., *Bevacizumab plus oxaliplatin-based chemotherapy as adjuvant treatment for colon cancer (AVANT): a phase 3 randomised controlled trial.* Lancet Oncol, 2012. **13**(12): p. 1225-33.
194. Breitbach, C.J., et al., *Oncolytic Vaccinia Virus Disrupts Tumor-Associated Vasculature in Humans.* Cancer Res, 2013.
195. Liu, C.Z., et al., *Overexpression and immunosuppressive functions of transforming growth factor 1, vascular endothelial growth factor and interleukin-10 in epithelial ovarian cancer.* Chin J Cancer Res, 2012. **24**(2): p. 130-7.
196. Matsuzaki, K., et al., *Chronic inflammation associated with hepatitis C virus infection perturbs hepatic transforming growth factor beta signaling, promoting cirrhosis and hepatocellular carcinoma.* Hepatology, 2007. **46**(1): p. 48-57.
197. Ulrich, C.M., J. Bigler, and J.D. Potter, *Non-steroidal anti-inflammatory drugs for cancer prevention: promise, perils and pharmacogenetics.* Nature reviews. Cancer, 2006. **6**(2): p. 130-40.
198. Baron, J.A., et al., *A randomized trial of aspirin to prevent colorectal adenomas.* The New England journal of medicine, 2003. **348**(10): p. 891-9.
199. Hengstschlager, M., M. Pfeilstocker, and E. Wawra, *Thymidine kinase expression. A marker for malignant cells.* Advances in experimental medicine and biology, 1998. **431**: p. 455-60.
200. Gillet, J.P., S. Varma, and M.M. Gottesman, *The Clinical Relevance of Cancer Cell Lines.* J Natl Cancer Inst, 2013.

201. Brader, P., et al., *Imaging of lymph node micrometastases using an oncolytic herpes virus and [F]FEAU PET.* PloS one, 2009. **4**(3): p. e4789.
202. Eisenberg, D.P., et al., *Real-time intraoperative detection of breast cancer axillary lymph node metastases using a green fluorescent protein-expressing herpes virus.* Annals of surgery, 2006. **243**(6): p. 824-30; discussion 830-2.
203. Balkwill, F. and A. Mantovani, *Inflammation and cancer: back to Virchow?* Lancet, 2001. **357**(9255): p. 539-45.
204. Vesely, M.D., et al., *Natural innate and adaptive immunity to cancer.* Annual review of immunology, 2011. **29**: p. 235-71.
205. Kiessling, R., E. Klein, and H. Wigzell, *"Natural" killer cells in the mouse. I. Cytotoxic cells with specificity for mouse Moloney leukemia cells. Specificity and distribution according to genotype.* European journal of immunology, 1975. **5**(2): p. 112-7.
206. Kiessling, R., et al., *"Natural" killer cells in the mouse. II. Cytotoxic cells with specificity for mouse Moloney leukemia cells. Characteristics of the killer cell.* European journal of immunology, 1975. **5**(2): p. 117-21.
207. Biron, C.A., et al., *Natural killer cells in antiviral defense: function and regulation by innate cytokines.* Annual review of immunology, 1999. **17**: p. 189-220.
208. Held, W., et al., *The function of natural killer cells: education, reminders and some good memories.* Current opinion in immunology, 2011. **23**(2): p. 228-33.
209. Cooper, M.A. and M.A. Caligiuri, *Isolation and characterization of human natural killer cell subsets.* Current protocols in immunology / edited by John E. Coligan ... [et al.], 2004. **Chapter 7**: p. Unit 7 34.
210. Zhang, Z., et al., *Identification and functional analysis of ligands for natural killer cell activating receptors in colon carcinoma.* The Tohoku journal of experimental medicine, 2012. **226**(1): p. 59-68.
211. Fauriat, C., et al., *Regulation of human NK-cell cytokine and chemokine production by target cell recognition.* Blood, 2010. **115**(11): p. 2167-76.
212. Cambiaggi, C., et al., *Constitutive expression of CD69 in interspecies T-cell hybrids and locus assignment to human chromosome 12.* Immunogenetics, 1992. **36**(2): p. 117-20.
213. Hesslein, D.G. and L.L. Lanier, *Transcriptional control of natural killer cell development and function.* Advances in immunology, 2011. **109**: p. 45-85.
214. Steinman, R.M., *The dendritic cell system and its role in immunogenicity.* Annual review of immunology, 1991. **9**: p. 271-96.
215. Chang, D.Z., et al., *Granulocyte-macrophage colony stimulating factor: an adjuvant for cancer vaccines.* Hematology, 2004. **9**(3): p. 207-15.
216. Prestwich, R.J., et al., *The case of oncolytic viruses versus the immune system: waiting on the judgment of Solomon.* Human gene therapy, 2009. **20**(10): p. 1119-32.
217. Fernandez, N.C., et al., *Dendritic cells directly trigger NK cell functions: cross-talk relevant in innate anti-tumor immune responses in vivo.* Nature medicine, 1999. **5**(4): p. 405-11.

218. Piccioli, D., et al., *Contact-dependent stimulation and inhibition of dendritic cells by natural killer cells.* The Journal of experimental medicine, 2002. **195**(3): p. 335-41.
219. Krueger, P.D., et al., *Regulation of NK cell repertoire and function in the liver.* Crit Rev Immunol, 2011. **31**(1): p. 43-52.
220. Lassen, M.G., et al., *Intrahepatic IL-10 maintains NKG2A+Ly49- liver NK cells in a functionally hyporesponsive state.* J Immunol, 2010. **184**(5): p. 2693-701.
221. Tu, Z., et al., *The activation state of human intrahepatic lymphocytes.* Clin Exp Immunol, 2007. **149**(1): p. 186-93.
222. Naito, Y., et al., *CD8+ T cells infiltrated within cancer cell nests as a prognostic factor in human colorectal cancer.* Cancer Res, 1998. **58**(16): p. 3491-4.
223. Sato, E., et al., *Intraepithelial CD8+ tumor-infiltrating lymphocytes and a high CD8+/regulatory T cell ratio are associated with favorable prognosis in ovarian cancer.* Proc Natl Acad Sci U S A, 2005. **102**(51): p. 18538-43.
224. Gulubova, M., et al., *Decrease in intrahepatic CD56+ lymphocytes in gastric and colorectal cancer patients with liver metastases.* APMIS, 2009. **117**(12): p. 870-9.
225. Levy, E.M., M.P. Roberti, and J. Mordoh, *Natural killer cells in human cancer: from biological functions to clinical applications.* J Biomed Biotechnol, 2011. **2011**: p. 676198.
226. Tai, L.H., et al., *Preventing postoperative metastatic disease by inhibiting surgery-induced dysfunction in natural killer cells.* Cancer Res, 2013. **73**(1): p. 97-107.
227. Dighe, A.S., et al., *Enhanced in vivo growth and resistance to rejection of tumor cells expressing dominant negative IFN gamma receptors.* Immunity, 1994. **1**(6): p. 447-56.
228. Street, S.E., et al., *Suppression of lymphoma and epithelial malignancies effected by interferon gamma.* The Journal of experimental medicine, 2002. **196**(1): p. 129-34.
229. Darcy, P.K., et al., *Redirected perforin-dependent lysis of colon carcinoma by ex vivo genetically engineered CTL.* Journal of immunology, 2000. **164**(7): p. 3705-12.
230. Smyth, M.J., et al., *Differential tumor surveillance by natural killer (NK) and NKT cells.* The Journal of experimental medicine, 2000. **191**(4): p. 661-8.
231. Smyth, M.J., et al., *Perforin-mediated cytotoxicity is critical for surveillance of spontaneous lymphoma.* The Journal of experimental medicine, 2000. **192**(5): p. 755-60.
232. Street, S.E., E. Cretney, and M.J. Smyth, *Perforin and interferon-gamma activities independently control tumor initiation, growth, and metastasis.* Blood, 2001. **97**(1): p. 192-7.
233. Doubrovina, E.S., et al., *Evasion from NK cell immunity by MHC class I chain-related molecules expressing colon adenocarcinoma.* Journal of immunology, 2003. **171**(12): p. 6891-9.
234. Testi, R., et al., *The CD69 receptor: a multipurpose cell-surface trigger for hematopoietic cells.* Immunology today, 1994. **15**(10): p. 479-83.

235. Bhat, R., et al., *Enhancement of NK cell antitumor responses using an oncolytic parvovirus.* Int J Cancer, 2011. **128**(4): p. 908-19.
236. Veuillen, C., et al., *Primary B-CLL Resistance to NK Cell Cytotoxicity can be Overcome In Vitro and In Vivo by Priming NK Cells and Monoclonal Antibody Therapy.* Journal of clinical immunology, 2012.
237. Hou, W., et al., *Viral infection triggers rapid differentiation of human blood monocytes into dendritic cells.* Blood, 2012. **119**(13): p. 3128-31.
238. Baravalle, G., et al., *Ubiquitination of CD86 is a key mechanism in regulating antigen presentation by dendritic cells.* J Immunol, 2011. **187**(6): p. 2966-73.
239. Matsuura, K., et al., *Upregulation of mouse CD14 expression in Kupffer cells by lipopolysaccharide.* The Journal of experimental medicine, 1994. **179**(5): p. 1671-6.
240. Su, G.L., et al., *CD14 expression and production by human hepatocytes.* Journal of hepatology, 1999. **31**(3): p. 435-42.
241. Kinouchi, M., et al., *Infiltration of CD14-positive macrophages at the invasive front indicates a favorable prognosis in colorectal cancer patients with lymph node metastasis.* Hepatogastroenterology, 2011. **58**(106): p. 352-8.
242. Burt, B.M., et al., *The lytic potential of human liver NK cells is restricted by their limited expression of inhibitory killer Ig-like receptors.* J Immunol, 2009. **183**(3): p. 1789-96.
243. Zamai, L., et al., *NK cells and cancer.* J Immunol, 2007. **178**(7): p. 4011-6.
244. Hodge, J.W., et al., *A recombinant vaccinia virus expressing human prostate-specific antigen (PSA): safety and immunogenicity in a non-human primate.* Int J Cancer, 1995. **63**(2): p. 231-7.
245. Miller, J.D., et al., *Human effector and memory CD8+ T cell responses to smallpox and yellow fever vaccines.* Immunity, 2008. **28**(5): p. 710-22.
246. Leibovitz, A., et al., *Classification of human colorectal adenocarcinoma cell lines.* Cancer research, 1976. **36**(12): p. 4562-9.
247. Drewinko, B., et al., *Establishment of a human carcinoembryonic antigen-producing colon adenocarcinoma cell line.* Cancer Res, 1976. **36**(2 Pt 1): p. 467-75.
248. Drewinko, B., et al., *Further biologic characteristics of a human carcinoembryonic antigen-producing colon carcinoma cell line.* J Natl Cancer Inst, 1978. **61**(1): p. 75-83.
249. Leibovitz, A., et al., *Classification of human colorectal adenocarcinoma cell lines.* Cancer Res, 1976. **36**(12): p. 4562-9.

8 List of Abbreviations

5-FC	5-Fluorocytosine
5-FU	5-Fluorouracil
ADCC	Antibody-Dependent Cell-Mediated Cytotoxicity
AFP	Alpha-Feto Protein
AIDS	Aquired Immuno-Deficiancy syndrome
ANOVA	Analysis Of Variants
APC	Atigen Presenting Cell
ATP	Adenosine tTri-phosphate
BCG	Bacillus Calmette-Guerin
CD	Cluster of Differentiation
CDC	Complement-Dependant Cytotoxicity
CEA	Carcino-Embryogenic Antigen
CEV	Cell-associated Enveloped Virus
CIK	Cytokine-Induced Killer cells
CLSM	Confocal Laser Scanning Microscopy
CMC	Carboxymethylecellulose
CRC	Colorectal Carcinoma
CRLM	Colorectal Liver Metastases
CT	Computed Tomography
CTL	Cyto-toxic T Lymphocyte
DAMP	Damage-Associated Molecular Patterns
DC	Dendritic Cells
DFI	Disease Free Interval
DMEM	Dulbecco's Modified Eagle Medium
DMSO	Dimethyl Sulphoxide
DNA	Deoxyribonucleic acid
EBV	Epstein-Barr Virus
EDTA	Ethylenediaminetetraacetic acid
EEV	Extra-cellular Enveloped Virus
EGF	Epidermal Growth Factor
EGFR	Epidermal Growth Factor Recepter
EGTA	Ethylene Glycol Tetraacetic Acid
ELISA	Enzyme Linked Immunoabsorbent Assay

FACS	Fluorescence Activated Cell Sorting
FCS	Foetal Calf serum
FITC	Fluorescein Isothiocyanate
FNH	Focal Nodular Hyperplasia
FSC	Forward scatter
GAG	Glucosaminoglycans
GFP	Green Fluorescent Protein
GMCSF	Granulocyte-Macrophage Colony Stimulating Factor
HBSS	Hanks' Buffered Salt Solution
HBV	Hepatitis B Virus
HCC	Hepatocellular Carcinoma
HCV	Hepatitis C Virus
HLA	Human Leukocyte Antigen
HPV	Human Papiloma Virus
HSV	Herpes Simplex Virus
HTLV	Human T-cell Leukemia Virus Type I
HU	Hounsefield Units
ICAM	Intracellular Adhesion Molecule
IDO	Indolemine Dioxygenase
IEV	Intracellular Enveloped Virus
IFN	Interferon
IGF	Insulin-like Growth Factor
IL	Interleukin
IMV	Intracellular Mature Virus
IT	Intra-tumoural
ITR	Inverted Terminal Repeats
IV	Intra-venous
Kras	Kirsten rat sarcoma
LIVP	Lister strain from the Institute of Viral Preparations
LMC	Liver Mononuclear Cells
LPS	Lipopolysaccharide
LV	Leocovorin
MACS	Magnetic-Activated Cell Sorting
MAPK	Mitogen-Activated Protein Kinase
MHC	Major Histocompatibility
MOI	Multiplicity of Infection
MTD	Maximum Tolerated Dose

MTT	Microculture Tetrazolium Test
MV	Measles Virus
MVA	Modified Vaccinia virus Ankara
NAb	Neutralising Antibodies
NDV	Newcastle Disease Virus
NK	Natural Killer
NSCLC	Non-Small Cell Lung Cancer
OS	Overall Survival
OV	Oncolytic Virus
p.i.	Post-infection
PAMP	Pathogen-Associated Molecular Patterns
PARP	Poly ADP-Ribose Polymerase
PBMC	Peripheral Blood Mononuncleocytes
PBS	Phosphate Buffered Saline
PET-CT	Positron Emission Tomography -CT
PFA	Paraformaldehyde
PFU	Plaque-forming units
PKR	Protein Kinase R
PRR	Pattern Recognition Receptors
PSA	Prostate-specific antigen
RANTES	Regulated upon Activation, Normal T-cell Expressed and Secreted
RB	Retinoblastoma protein
RECIST	Response Evaluation Criteria in Solid Tumors
RNA	Ribosenucleic Acid
RPMI	Roswell Park Memorial Institute
RT	Room Temperature
SD	Standard Deviation
SEM	Standard Error of the Mean
SIRS	Systemic Inflammatory Response Syndrome
SSC	Side scatter
TAA	Tumour Associated Antigens
TGF	Transforming Growth Factor
Th1	T helper 1
TILs	Tumour Infiltrating Lymphocytes
TK	Thymidine Kinase
TLR	Toll-Like Receptor

TMC	Tumour Mononuclear Cells
TRAIL	Tumour necrosis factor-Related Apoptosis-Inducing Ligand
TSA	Trichostatin
UK	United Kingdom
UPR	Unfolded Protein Response
USA	United States of America
UVB	Ultraviolet B
VCO	Vaccinia Colon Oncolysate
VEGF	Vascular Endothelial Growth Factor
VGF	Vaccinia Growth Factor
VMCL	Vaccinia Melanoma Cell Lysate
VMO	Vaccinia Melanoma Oncolysate
VSV	Vesicular Stomatitis Virus
VV	Vaccinia Virus
WCC	White Cell Count
WR	Western Reserve
WT	Wild Type
YFP	Yellow-Fluorescent Protein

9 Appendix A. Details of cell lines

HCT116: Epithelial cell line derived from adult male. Microsatelite unstable, near diploid and tumorigenic in mice [246].

LoVo: Epithelial cell line derived from adult male, colon (from metastatic site: colon); grade IV; Dukes' type C [247]. Microsatelite unstable, near diploid and tumourigenic in nude mice [248].

SW480: Epithelial cell line derived from 51 year old Caucasian male with colorectal adenocarcinoma Duke's B. Near diploid, and is tumorigenic in Mice [246].

SW620: Epithelial cell line derived from 51-yr old Caucasian male (as above, SW480) with Duke's C colorectal adenocarcinoma. Hyperdiploid, and tumorigenic [249].

K562: human chronic myeloid leukaemia. These are easily killed by natural killer (NK) cells as they lack the MHC complex required to inhibit NK activity.

Vero: These originate from isolated kidney epithelial cells extracted from an African green monkey. They are interferon-deficient; unlike normal mammalian cells, they do not secrete type 1 interferons when infected by viruses.

10 Appendix B: GFP expression in 'Tissue Cores

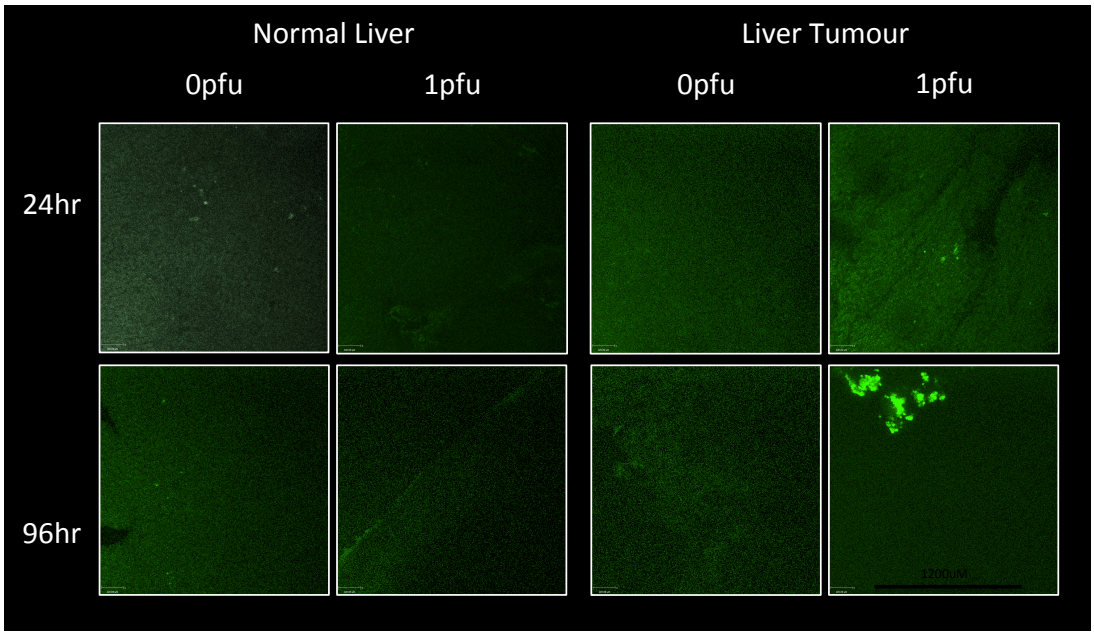

Figure 10-1. Tumour specific transgene (GFP) expression. CRLM, N=1

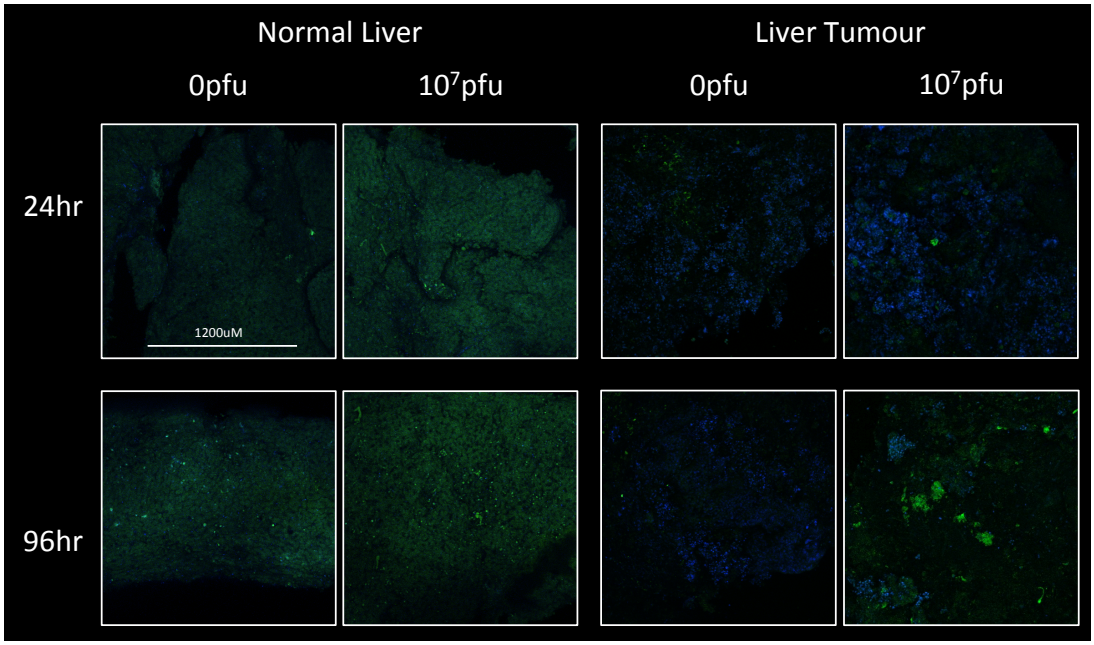

Figure 10-2. Tumour specific transgene (GFP) expression. CRLM, N=2

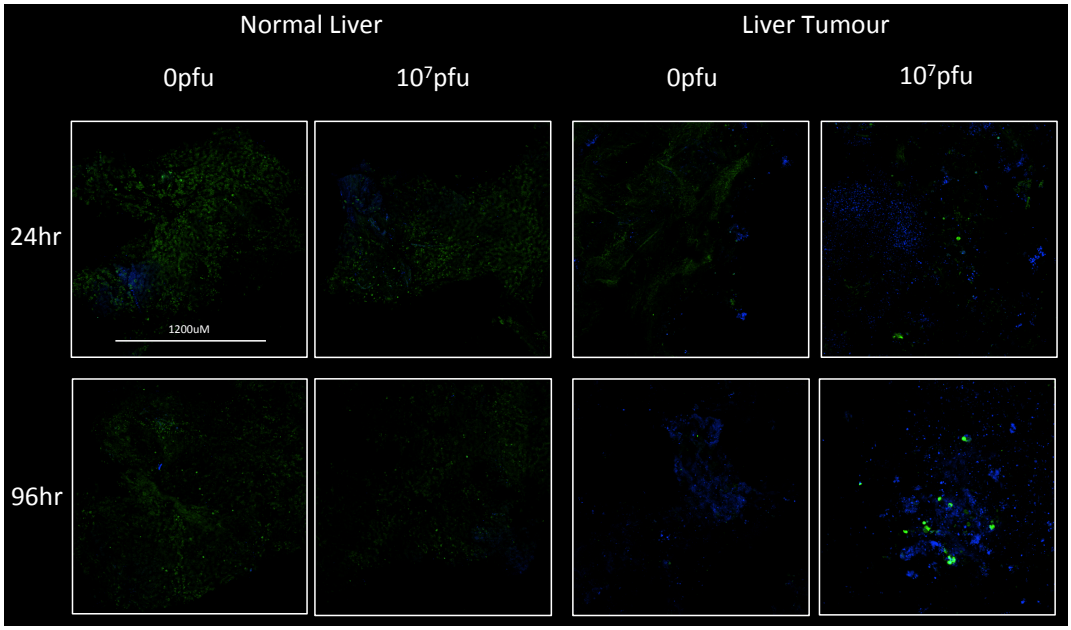

Figure 10-3. Tumour specific transgene (GFP) expression. CRLM, N=3

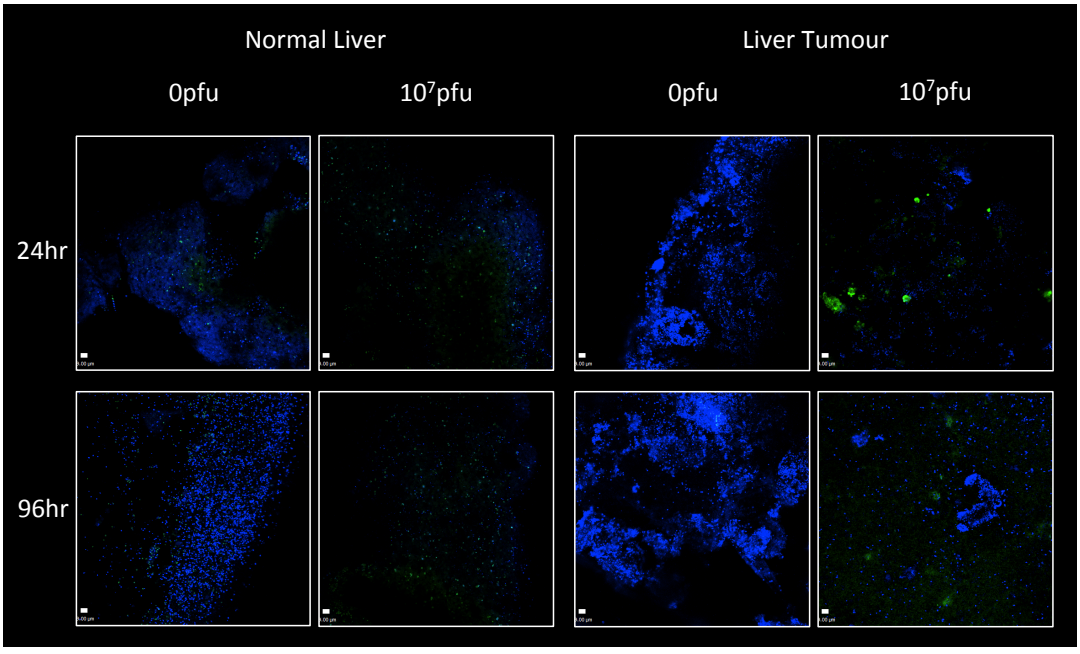

Figure 10-4. Tumour specific transgene (GFP) expression. CRLM, N=4

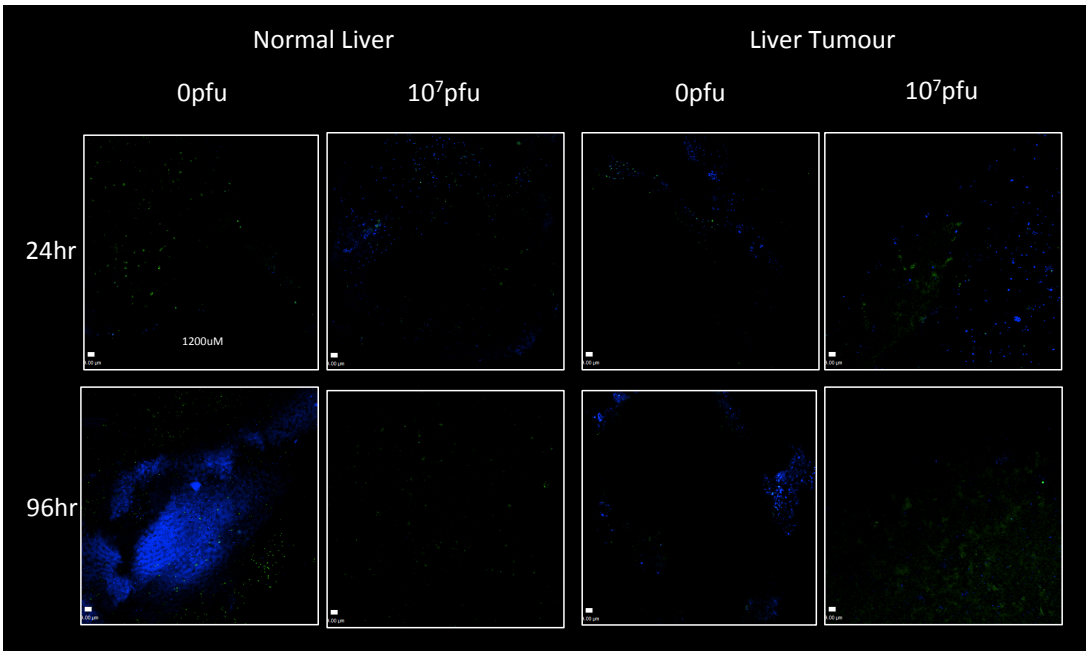

Figure 10-5. Tumour specific transgene (GFP) expression. CRLM, N=5

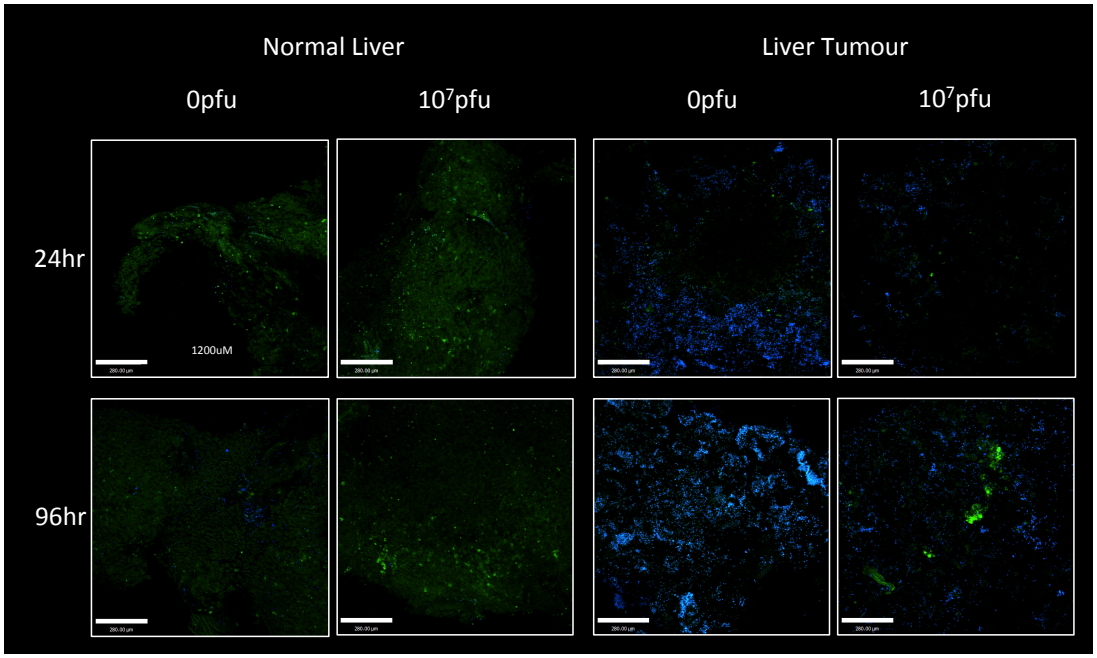

Figure 10-6. Tumour specific transgene (GFP) expression. CRLM, N=6

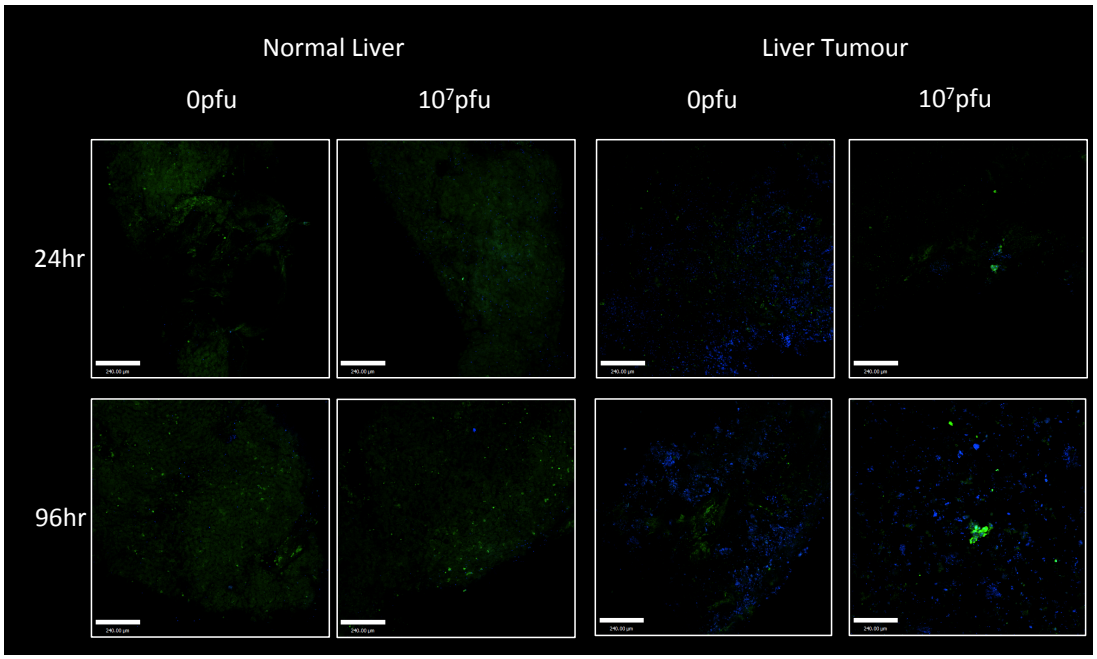

Figure 10-7. Tumour specific transgene (GFP) expression. CRLM, N=7

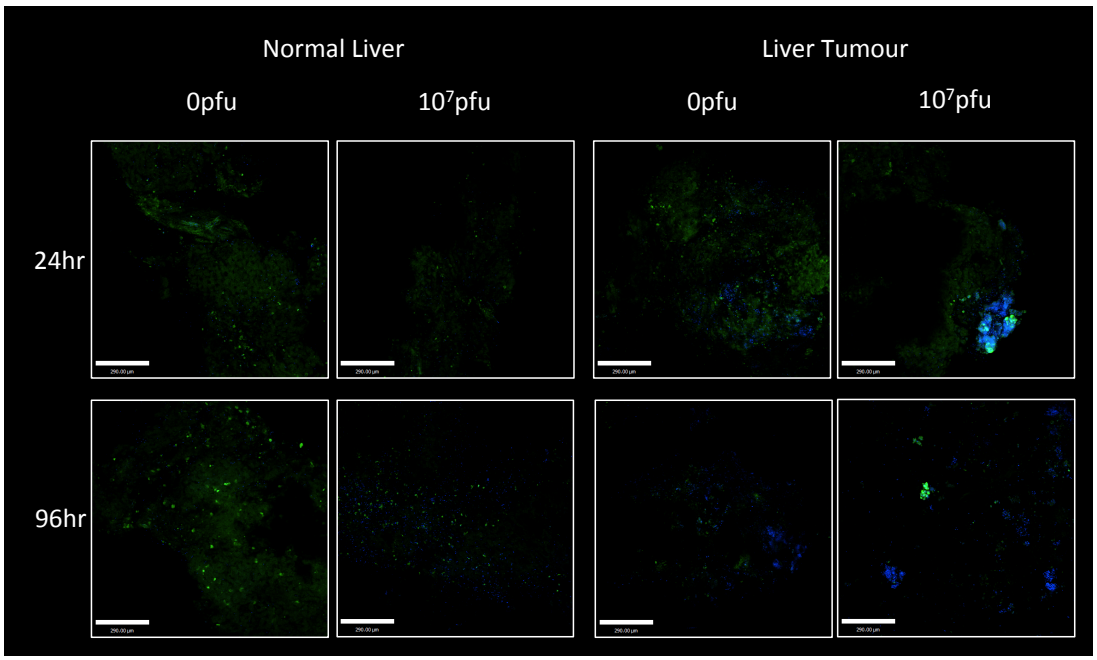

Figure 10-8. Tumour specific transgene (GFP) expression. CRLM, N=8

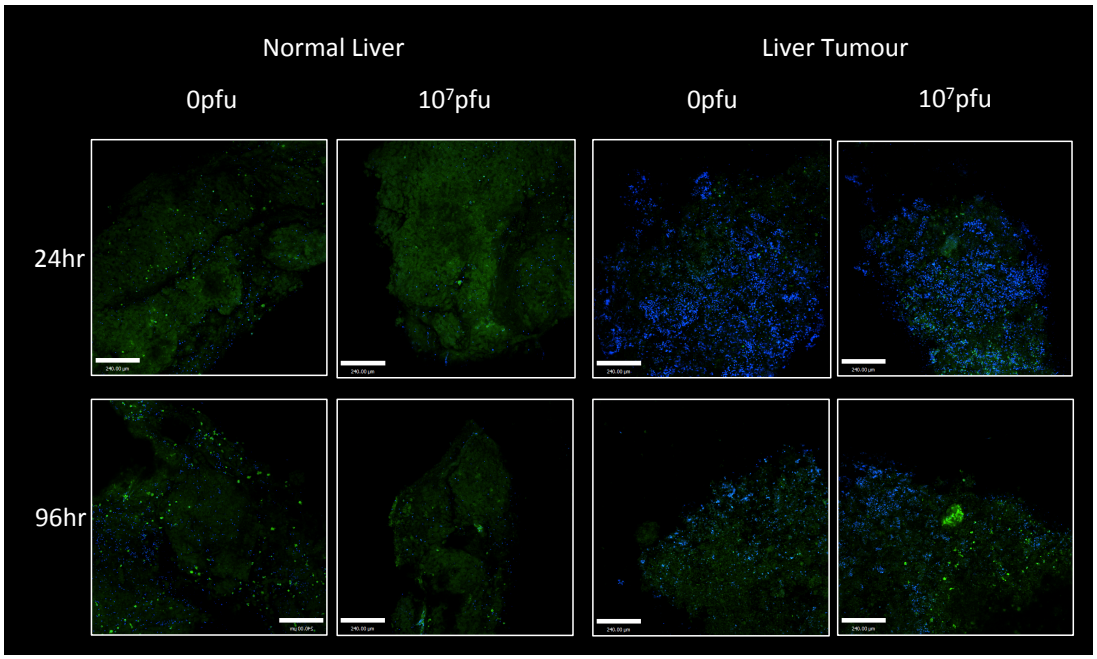

Figure 10-9. Tumour specific transgene (GFP) expression. CRLM, N=9

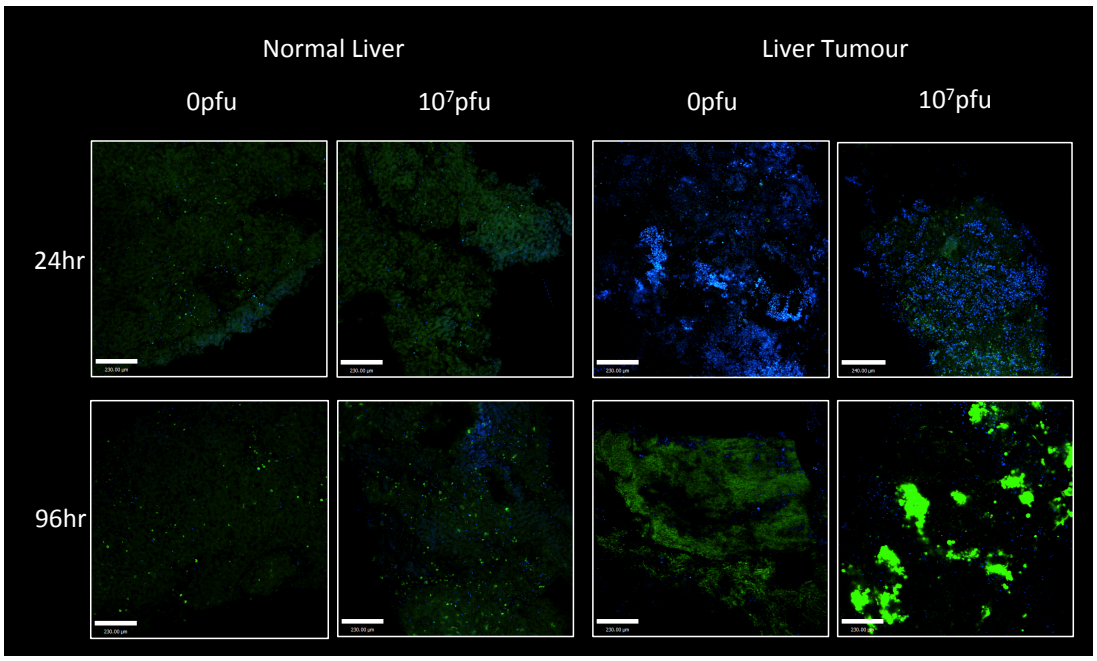

Figure 10-10. Tumour specific transgene (GFP) expression. CRLM, N=10

11 Appendix C: Upregulation of CD86, CD11c and ClassIIDR following JX-59 infection *in vitro*

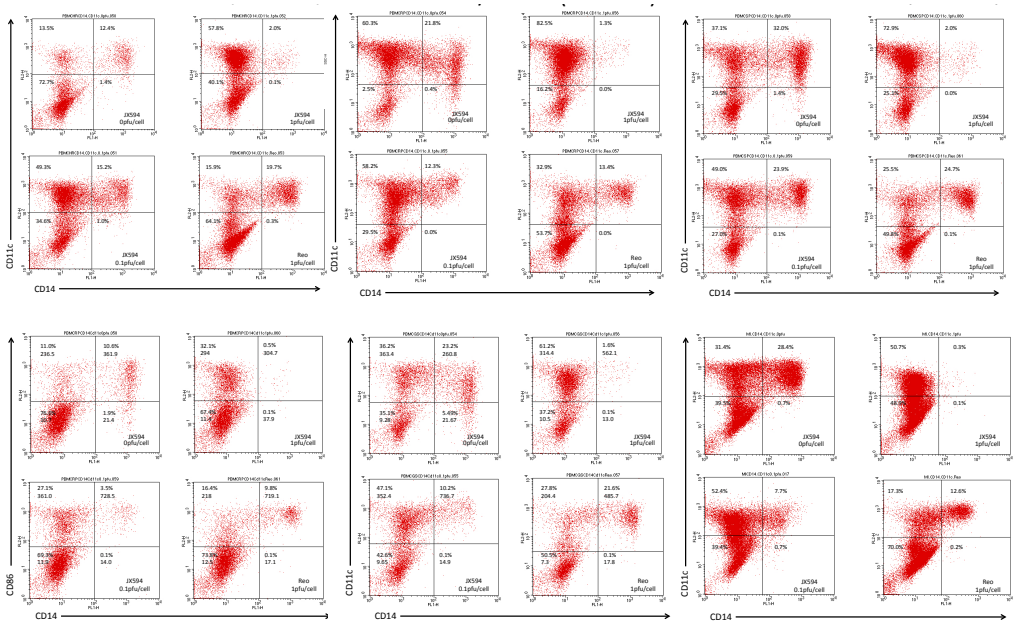

Figure 11-1. Upregulation of $CD14^{+ve}CD11c^{+ve}$ phenotype following JX-594 treatment in three healthy donors

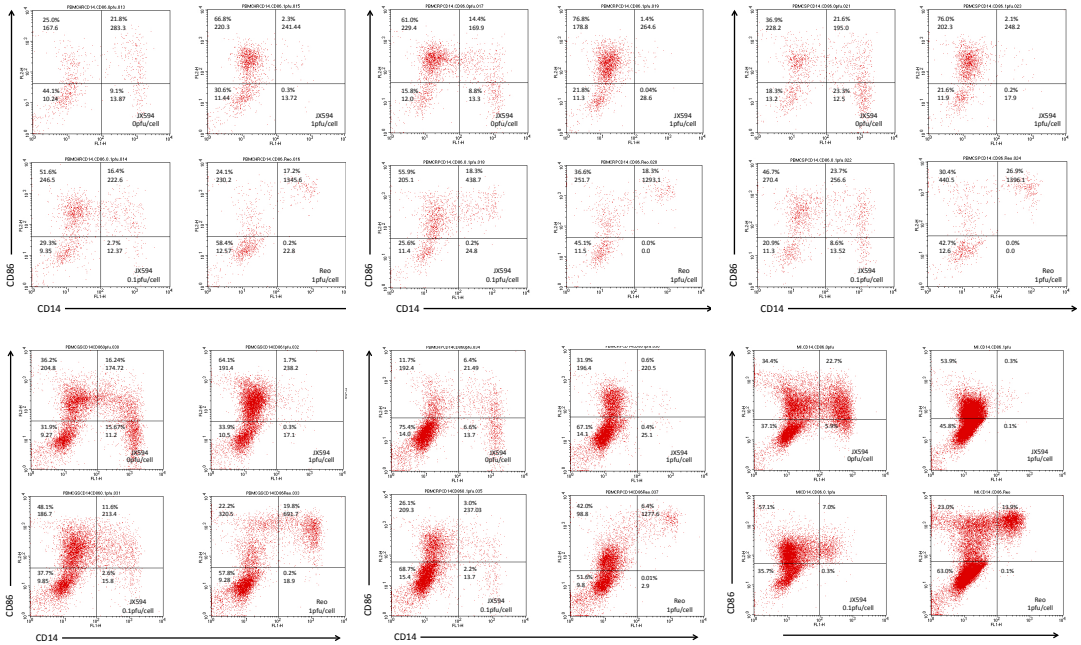

Figure 11-2. Upregulation of $CD14^{+ve}CD86^{+ve}$ phenotype following JX-594 treatment in three healthy donors

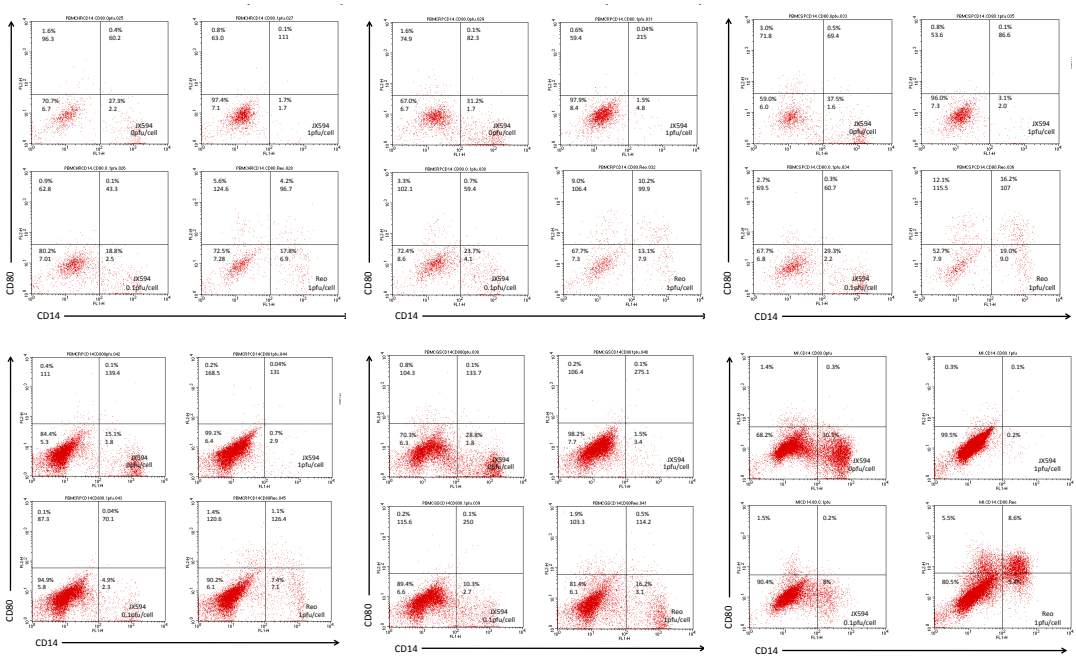

Figure 11-3. No upregulation of $CD14^{+ve}CD80^{+ve}$ phenotype following JX-594 treatment in three healthy donors

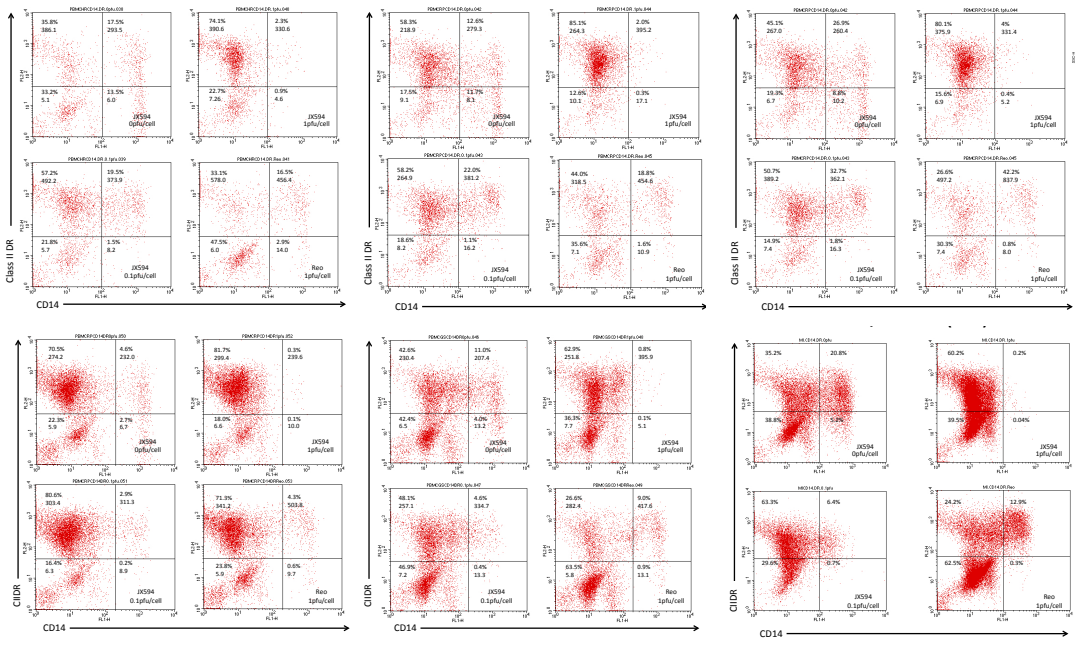

Figure 11-4. Upregulation of $CD14^{+ve}CIIDR^{+ve}$ phenotype following JX-594 treatment in three healthy donors

12 List of Suppliers

AbD Serotec	Endeavour House, Langford Business Park, Langford Lane, Kidlington, Oxon, OX5 1GE, UK
Adams Healthcare	Lotherton Way Garfotch, Leeds, West Yorkshire, LS25 2JY
Alere Ltd.	Alere Limited, Pepper Road, Hazel Grove, Stockport, Cheshire, SK7 5BW, UK
Alpha Laboratories Ltd.	40 Parham Drive, Eastleigh, Hampshire, SO50 4NU, UK
ATCC	Queens Road , Teddington, Middlesex, TW11 0LY , UK
AXIS Shield	Axis-Shield PoC AS, Kjelsåsveien 161, P.O. Box 6863 Rodeløkka, NO-0504, Oslo, Norway
BD Biosciences	The Danby Building, Edmund Halley Road, Oxford Science Park, Oxford, OX4 4DQ, UK
BD Falcon	Supplied by Scientific Laboratory Supplies
Care Fusion	Eurosurgical, Merrow Business Park, Surrey, Guildford, GU4 7WA, UK
Corning Costar	Distributed by Sigma Aldrich Ltd.
Dako	Distributed by Alere Ltd.

Dupont	Windham Road, Chilton Industrial Estate, SUDBURY, Suffolk, CO10 2XD, UK.
Fisher Scientific UK Ltd.	Bishop Meadow Road, Loughborough, Leicestershire, LE11 5RG, UK.
Gibco	Supplied by Life technologies Ltd.
Grant Instruments	Grant Instruments (Cambridge) Ltd, Shepreth, Cambridgeshire, SG8 6GB, UK.
Greiner Bio-One Ltd.	Brunel Way, Stroudwater Business Park, GL10 3SX, UK
Invitrogen	Supplied by Life Technologies
Life Technologies Ltd	3 Fountain Drive, Inchinnan Business Park, Paisley PA4 9RF, UK
Lorne Laboratories	Lorne Laboratories Limited Unit 1 Danehill Cutbush Park Industrial Estate Lower Earley Reading RG6 4UT
Mabtech	Box 1233, SE-131 28 Nacka Strand, Sweden
Miltenyi Biotec Ltd.	Almac House, Church Lane, Bisley, Surrey, GU24 9DR, UK
Molecular Devices UK	Unit 660 665, Eskdale Road, Wokingham, Berkshire, RG41 5TS, UK
NIKON	5-21, Katsushima 1-chome, Shinagawa-ku, Tokyo 140-0012, Japan

NHS Supplies	Valley Point Valley Drive, Rugby , Warwickshire CV21 1TN, UK
NuAire Inc.	2100 Fernbrook Lane N Plymouth, MN 55447, USA
Nunc®	Distributed by Fisher Scientific
PBL Interferon source	131 Ethel Rd West, Suite 6, Piscataway, NJ 08854, USA.
Perkin Elmer	Kelvin Close, Birchwood Science Park, Risley, Warrington, Cheshire WA3 7PB, UK
Pharmingen	See BD Biosciences
R & D Systems Europe Ltd.	19 Barton Lane, Abingdon Science Park, Abingdon,OX14 3NB, UK
Sanyo	Sanyo Gallenkamp Plc., Monarch Way, Belton Park, Loughborough, LE11 5XG, UK
Sigma-Aldrich Ltd.	Sigma Chemical Company, Fancy Road, Poole, Dorset, BH17 7NH, UK
Swann-Morton	Supplied by NHS Supplies
Thermo Fisher Scientific	Unit 5, The Ringway Centre, Edison Rd., Basingstoke, Hampshire, RG21 6YH, UK
Weber Scientific	2732 Kuser Road, Hamilton, NJ 08691, USA